Synthesis of multicyclic peptides via CLiPS and oxime ligations

Streefkerk, D.E.

Publication date
2021
Document Version
Final published version
License
Other

Link to publication

Citation for published version (APA):
Streefkerk, D. E. (2021). *Synthesis of multicyclic peptides via CLiPS and oxime ligations*.
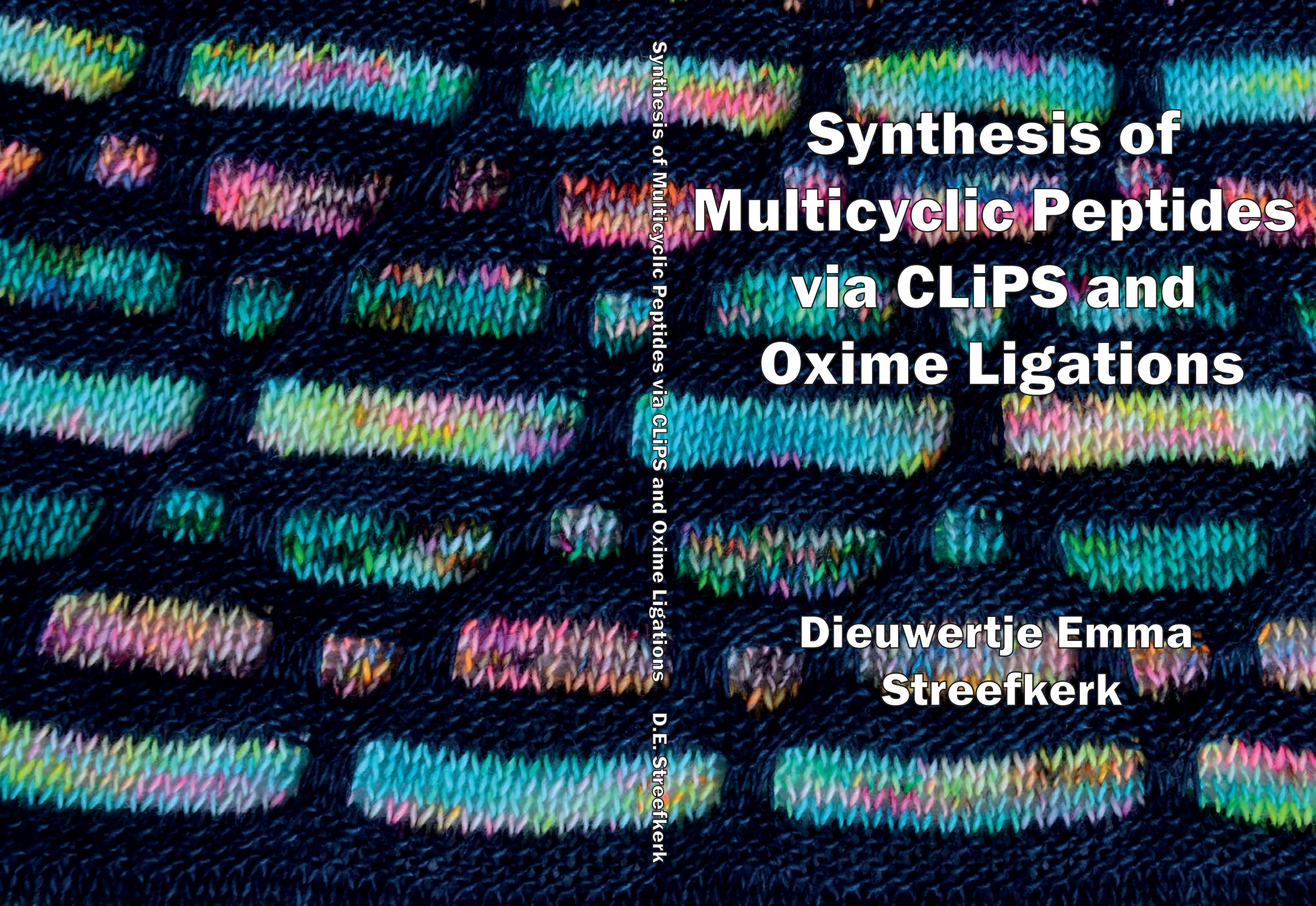
Synthesis of Multicyclic Peptides via CLiPS and Oxime Ligations

Dieuwertje Emma Streefkerk

Lieve pap en mam,

Ik doet het ook voor jou hoor, Nel!

'Hoe kan je dit lezen, nergens plaatjes'

'Je kan ook je verbeelding gebruiken'

- Uit Disney's Belle en het Beest (1991) -

Synthesis of Multicyclic Peptides via CLiPS and Oxime Ligations

ACADEMISCH PROEFSCHRIFT

ter verkrijging van de graad van doctor
aan de Universiteit van Amsterdam
op gezag van de Rector Magnificus
prof. dr. ir. K.I.J. Maex
ten overstaan van een door het College voor Promoties ingestelde commissie,
in het openbaar te verdedigen in de Agnietenkapel
op dinsdag 16 februari 2021, te 12.00 uur

door Dieuwertje Emma Streefkerk
geboren te Blaricum

Table of Contents

Chapter 1:

General Introduction

1 Introduction

In our efforts to combat diseases, humanity has often turned to Nature for inspiration. Among Nature's most versatile molecules are the amino acids, and these can be regarded as one of the main building blocks of life. Combined, the twenty canonical amino acids are the small gears in proteins that together fulfill a plethora of functions. As the building blocks of enzymes, they catalyze reactions, while as antibodies they are responsible for recognizing external threats and triggering the immune response. These large peptide structures are famed for their exceptional selectivity, and interest in these so called 'biologics' for therapeutical purposes has grown tremendously since the 1990's.[1]

Monoclonal antibodies (mAbs) are a prime example of such biologics, and many have been developed for the treatment of cancers. Trastuzumab, better known under the brand name Herceptin®, is used for the treatment of breast cancers that are HER2 (receptor) positive.[2] Its mode of action is by binding to the HER2 receptor, which slows down cell proliferation, and treatment is often supplemented with classical chemotherapy.[3,4] Herceptin® is part of the World Health Organization's list of essential medicines.[5] Infliximab is another example of a mAb used in the treatment of autoimmune diseases, such as Crohn's disease, rheumatoid arthritis and psoriasis.[6] It binds to TNF-α, a cytokine which is part of the autoimmune response reaction, thereby blocking its binding to the receptor.[7–9]

While biologics exhibit high selectivities and affinities, the production of antibodies is often challenging, laborious and expensive. Moreover, administering mAbs often requires specialist care as they suffer from low stability and oral inavailability. Hence, the pharmaceutical market is still dominated by small molecules, which adhere to the Lipinski's rule of five.[6,10] However, the space between small molecules and large biologics has been less explored. In the natural world, a wide variety of compounds that bridge this gap can be found. They possess the high selectivity found for biologics, while being rather small in size, adhering more to the Lipinski's rule. For example, in bacteria, small peptides are highly modified and subsequently used as chemical warfare agents in the defense against other bacteria. These smaller peptides have gained attention as potent antibacterial agents.[11,12] Indeed, many peptide-based antibiotics, such as Vancomycin, Daptomycin etc. are of bacterial origin.

Antimicrobial peptides come from many sources.[13] Peptidic natural products can usually be classified as non-ribosomally produced peptides (NRPs) and ribosomally produced post-translationally modified peptides (RiPPs). Both pathways also allow peptide macrocyclization.[12] Macrocyclization is a powerful method to ensure the stability of a peptide, which in turn also aids in binding events. Therefore, the interest into cyclized, constrained peptides has surged in drug discovery research.

In this introduction, we explore the world of naturally occurring, biologically active (multi)cyclic peptides, from monocyclic to hexacyclic peptides. Additionally, we focus on methods to synthesize these classes of compounds. As highlighted before, research into the topic is booming, and we will therefore particularly highlight scaffold-assisted synthesis of multicyclic peptides. Within these boundaries, we focus on two types of reactions: reactions involving cysteine sulfhydryl nucleophiles and the oxime ligation click reaction. These reactions are of importance for our research interest, which is the scaffold-assisted synthesis of multicyclic peptides via CLiPS and oxime ligation reactions.

1.1 Monocyclic Peptides

One of the key features of the aforementioned classes of compounds, such as biologics and antimicrobial peptides, is their well-defined three-dimensional structure, which is essential for the function they fulfill. The conformation of these large structures is usually stabilized by intramolecular hydrogen bonding and other non-covalent interactions, or

covalent connections such as disulfide bridges. Smaller peptides often need more elaborate strategies for constraining their conformation, such as macrocyclization, which is common for bacterially synthesized antibiotic peptides.

In solution, linear peptides exist in many different conformations. This means that binding of linear peptides to specific targets is not necessarily favorable, due to entropic factors. By constraining the peptide, a favored conformation of the peptide may be stabilized and locked, enabling a specific biological function. In addition, constrained peptides are metabolically more stable compared to their linear counterparts, as they are less susceptible to proteolytic cleavage from peptidases.[14]

There are many methods for constraining a peptide, with macrocyclization being the most common. There are roughly four strategies of macrocyclization: head-to-tail (C-terminus to N-terminus), head-to-side chain, side-chain-to-tail or side-chain-to-side-chain (Figure 1.1).[15] For natural peptides, cyclization reactions are catalyzed by specific enzymes. As cyclic peptides have many advantages, a plethora of different chemical methods have been developed to achieve their macrocyclization.
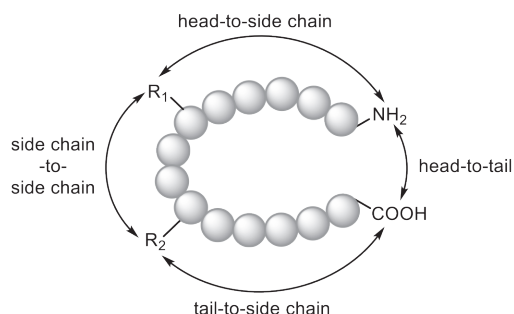
Figure 1.1: The four different options by which a linear peptide can be cyclized.

The natural peptide antibiotic Daptomycin (Figure 1.2) is an example of a monocyclic peptide which is cyclized in a tail-to-side-chain manner. A mid-chain threonine residue is connected to the C-terminal acid via an ester bond. The monocyclic lipopeptide is a potent antibiotic against Gram-positive bacteria. Its mode of action has been extensively studied by Silverman and coworkers, and one of Daptomycin's mode of action is the disruption of the bacterial cell membrane.[16]
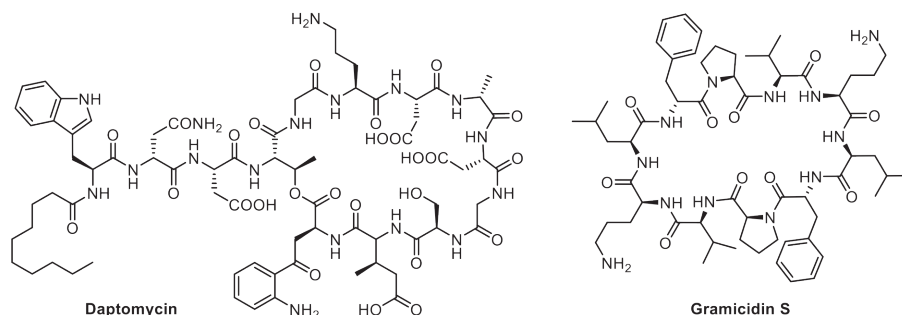
Figure 1.2: structures of Daptomycin and Gramicidin S.

A prime example of a head-to-tail cyclized natural peptide is Gramicidin S, from *Bacillus Brevis* (Figure 1.2).[17] The cyclic decapeptide is a dimer of two identical pentapeptides, *cyclo*(-VOL*d*FP)$_2$ featuring the non-canonical amino acids ornithine and

D-phenylalanine.[17–19] Therefore, the biosynthesis of this peptide does not involve the ribosome, but is accomplished by multifunctional peptide synthetases 1 and 2.[18] Its chemical synthesis has been a subject of many studies and as such, it is often used as a model compound in synthetic methodology studies.[20–22]

1.1.1 Chemical Methods to Synthesize Monocyclic Peptides

By head-to-tail cyclization via lactamization the C-terminus is activated, after which the free N-terminus serves as a nucleophile. This reaction in itself is not trivial due to, for example, inherent linearity of the peptide structure because the backbone amide bonds have a preference for a transoid-conformation. As a result, the concentration of the productive conformation for cyclization is low, often leading to low yields for cyclization reactions. Inducing a favorable conformation for cyclization can be achieved by including turn-inducing elements, such as prolines, pseudoprolines or *D*-amino acids in the peptide.[23,24] Incorporation of non-canonical N-functionalized amino acids can also favor cyclization and improve peptide properties.[25,26]

Synthetic approaches towards head-to-tail cyclized peptides are often hampered by elaborate approaches using protective groups, and low overall yields.[19,27] When solution-phase chemistry is applied, high dilution, long reaction times, low yields and epimerization are often reported. One of the most important steps is activation of the C-terminus of the peptide chain. Activating agents, such as carbodiimides (DCC, EDC) and peptide coupling reagents (HATU, HBTU, Oxyma and PyBOP) are commercially available and widely applied. However, due to the low rate of difficult macrolactamization reactions, the activated C-terminal amino acid often suffers from epimerization, and many efforts have been undertaken to overcome this side-reaction.[28,29] On-resin cyclization strategies have been successfully applied to the cyclization of hexapeptides and longer ones.[30] For such Solid Phase Peptide Synthesis (SPPS) cyclization strategies, special resins have been developed.[31] However, many of these on-resin strategies focus on cyclization via the side-chain functional groups.[32,33] The most widely applied side-chain cyclization reaction is the formation of a disulfide bond between two cysteines, as this is a common natural structural element and often crucial for activity, for example in the peptide hormone insulin.[34–36]

Perhaps the most limiting factor to prepare macrocyclic peptides is the requirement of side-chain protection to limit side-reactions. The most important protective group free ligation technique is Native Chemical Ligation (NCL), and it is used to ligate large peptide fragments in aqueous solution (Figure 1.3).[37] The C-terminus is activated as a thioester, whereby the sulfhydryl group of the N-terminal cysteine first attacks as the nucleophile, via a trans-thioesterification reaction. The N-terminal amine, now in close proximity, attacks the nearby thioester, and this S-to-N acyl shift yields the thermodynamically favored amide bond connecting the two peptide fragments. Macrocyclization has also been reported with this method to good avail. In many natural peptides, cysteine is not a very common amino acid. Therefore, methods to remove the cysteine sulfhydryl group have been developed, enabling a wider variety of compounds to be synthesized via this method.[38–40] However, C-terminal activation to the thioester is accompanied by the same issues as described for solution phase cyclization, mainly epimerization of the C-terminal amino acid. [41–44]
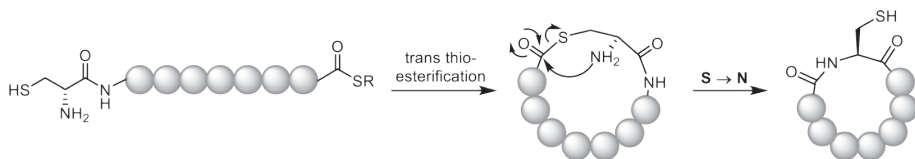

Figure 1.3: Synthesis of a cyclic peptide via Native Chemical Ligation, where the trans-thioesterified product undergoes an S-to-N acyl shift, yielding the ligated peptide.

In recent years, enzymatic head-to-tail cyclization strategies have been gaining attention, thanks to excellent regio- and stereoselectivity. Enzymes such as omniligase-1, butelase and sortase have been successfully applied.[45–50] Omniligase-1 has been applied in the synthesis of various natural products, such as cyclotides.[51,52] For peptide cyclization, the peptide must be equipped with a C-terminal glycolate-ester (Cam-ester), which can easily be obtained using a functionalized resin. During resin cleavage, the Cam-ester is liberated.[46,53] A limitation of enzymatic cyclizations is usually the requirement of an enzyme recognition sequence around the ligation site, requiring specific amino acids. Moreover, cyclization of peptides shorter than 12 amino acids is more difficult using this approach.

Methods to cyclize peptides through side-chain groups have been extensively studied.[54–61] Bi-functional linkers react with functionalities in the peptide side-chains, thereby constraining the peptide as a macrocycle. Commonly known as stapling, this method is often applied to stabilize secondary structures, such as α-helices.[56,60,62–64] Among the reactions that are used for stapling are the so-called click-reactions. Pioneered by Sharpless and co-workers, click reactions are denoted as being fast, high yielding reactions that occur under mild conditions with minimal byproducts.[65] Reactions such as ring closing metathesis,[66–71] thiol-ene addition[60,72–74] and copper-catalyzed azide-alkyne cycloadditions[32,75–82] are valuable methods to staple peptides, but they are beyond the scope of this thesis. Instead, peptide stapling by oxime ligation will be highlighted only.

In oxime ligation, an aldehyde or ketone and an aminooxy group react to form a stable oxime linkage. Oxime ligation belongs to the class of click-reactions and its applications in peptide chemistry have been widely researched.[83,84] Most often, aldehydes are used in favor of ketones, as aldehydes react faster and do not display *E/Z* isomerism of the oxime linkage.[85] Oxime ligation has been used extensively in labelling experiments,[86–91] whereby enhancing the reaction rate through aniline catalysis has been an important part of the work.[92,93] Besides bioconjugation reactions, oxime ligation has found widespread application in constraining peptides.[87,94–104]

As part of their efforts to stabilize α-helices, Horne and co-workers focused their research on aminooxy-group containing peptides, while aldehyde containing linkers were used to staple the peptide (Figure 1.4a).[105] In later work, an intramolecular approach was taken (Figure 1.4b). The peptides therefore also contained masked aldehydes.[63] The 1,2-aminoalcohol motif found in N-terminal serine could be converted to the corresponding glyoxylyl aldehyde by $NaIO_4$-mediated oxidation. Their investigations showed the application of amino acids functionalized for oxime ligation in SPPS and probed further into the dynamics of oxime ligation. Oxime formation was found to be reversible upon addition of a competing aminooxy group. In an effort to increase the structural stability of a peptide by cross-linking, oxime ligation was found to effectively stabilize a peptide conformation. However, compared to a triazole or lactam linkage, the stabilizing effect was slightly less.[62]
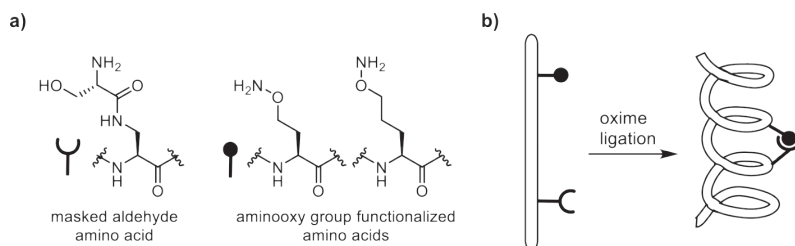

Figure 1.4: a) Amino acids used by Horne and coworkers for intramolecular oxime ligation in peptides. b) α-helix stabilization by intramolecular oxime ligation.

1.2 Higher Order Natural Multicyclic Peptides

Whilst monocyclic peptides have gained attention as potential therapeutics, a plethora of even more complex multicyclic peptidic structures are found in the natural world. In this section, a few (classes of) compounds are highlighted, to showcase the diversity within natural multicyclic peptides.

1.2.1 Bicyclic Peptides

Theonellamides (TNMs) are a family of marine natural products with potent antifungal activity and are isolated from marine invertebrates.[106] Despite extensive efforts to isolate the TNM-binding proteins, the modes of action of these compounds have been heretofore unknown. TNMs have a characteristic bicyclic structure bridged by a histidinoalanine residue, as is shown for TNM-F below in Figure 1.5.
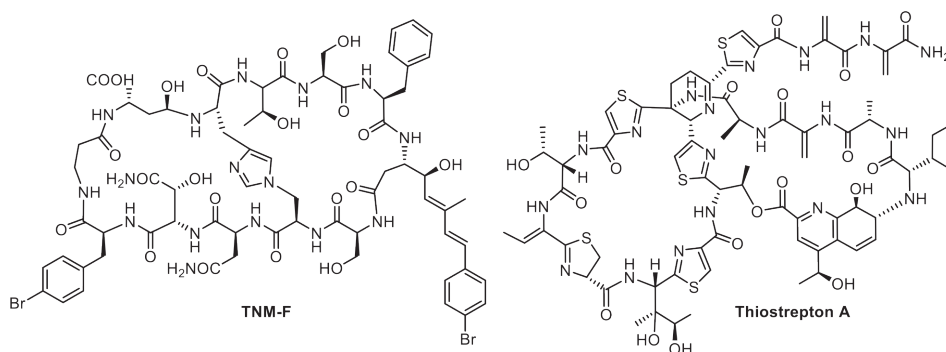

Figure 1.5: Structures of TNM-F and Thiostrepton A

Thiostrepton (Figure 1.5) is considered to be the flagship of thiopeptide antibiotics. It was first isolated from *Streptomyces azureus* in 1954 by Pagano and Weinstein.[107] The structure of thiostrepton is highly complex and the bicyclic peptide includes a 26-membered thiazoline macrocycle and a 27-membered quinaldic acid macrocycle. The core is comprised of a dehydropiperidine ring system, which connects the macrocycles with a thiazole moiety containing the dehydroalanine tail. Its mode of action against Gram-positive bacteria is by inhibiting protein synthesis.[107,108] The total synthesis was completed by Nicolaou and co-workers in 2004.[109–111]

1.2.2 Chemical Synthesis of Bicyclic Peptides

There are many examples of the synthesis of bicyclic peptides that were manufactured via introduction of an intramolecular constraint, such as disulfide bonds,[112,113] isopeptide bonds or unnatural versions, such as ring closing metathesis and copper-catalyzed azide-alkyde cycloaddition, requiring non-canonical amino acids.[114,115]

Because of its importance, we would like to focus on the scaffold-assisted synthesis of bicyclic peptides only. The use of a commercially available trimesic acid as the central scaffold has been explored in the screening against TNFα, a protein that promotes the inflammatory response of our body (Figure 1.6).[113] This protein is linked to many autoimmune diseases as it becomes overexpressed during an inflammation reaction. It can be treated by a TNF inhibitor, usually a monoclonal antibody such as infliximab (Remicade®) or adalimumab (Humira®).[116] For screening against TNFα, peptides were synthesized containing Dap, which was later coupled to the double-protected diallyl trimesic acid scaffold. Removal of the allyl protective groups was followed by a double amidation reaction, yielding the bicyclic peptide. This non-protein inhibitor called

anticachexin C1 was found to be very active against TNFα (K_D value of 0.45 µM) and protects cells from TNFα-induced cell death.

More recently, a bicyclic peptide containing dual functionalities was produced using the same screening methodology (Figure 1.6, right).[117] A sequence showing inhibitory activity (left hand side) was fused with a cell penetrating peptide sequence (right hand side), enhancing the overall function. Library screening was used to find a specific inhibitor against the NEMO-IKKß interaction, which is overexpressed in certain ovarian cancer cell lines. This interaction plays an important role in inducing NF-κB signaling, which controls the transcription of DNA. It was found to be very selective and active against cancer cells with increased NF-κB activities only, while showing minimal activity against normal cells.
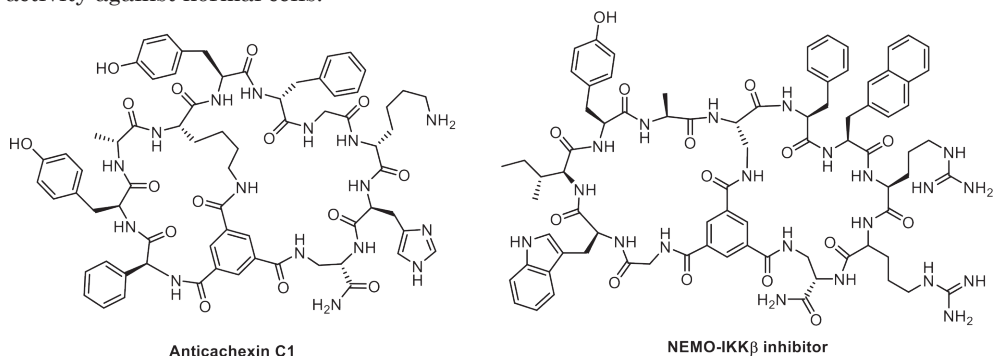

Figure 1.6: Anticachexin C1 and NEMO-IKKβ inhibitor

Chemical Linkage of Peptides onto Scaffolds (CLiPS) is another powerful method to constrain small peptides.[118] This method relies on the presence of multiple cysteines that are transformed into potent thiolate nucleophiles under mildly basic, aqueous conditions. The thiolates thus formed can selectively react with a scaffold equipped with methylene bromide-type electrophiles. When the peptide contains two cysteines, it can be CLiPSed onto a bivalent scaffold (encoded T2), yielding a macrocyclized peptide (Figure 1.7a).[64] The CLiPS reaction can be expanded to bicyclic peptides, by adding another cysteine to the peptide, and another electrophilic functionality to the scaffold (Figure 1.7b). Multiple scaffolds have been developed for such purposes, mainly varying in polarity (Figure 1.7c).[119] The addition of heteroatoms in the scaffolds generally aids solubility of the resulting bicyclic peptide in aqueous solutions, and can sometimes stabilize peptide conformations further through hydrogen bonding.[119,120] Besides the CLiPS reaction being a powerful tool in peptide cyclization, it has also been used in bioconjugation reactions, such as in the synthesis of antibody-drug-conjugates.[121]

One of the main advantages the CLiPS reaction has over other peptide-constraining methods, is the fact that it can use the natural cysteine as the reactive moiety. A key feature of the CLiPS ligation is the use of fully unprotected peptides, as under these reaction conditions no other side-chain functionalities react. Therefore, the common chemical peptide synthesis methods are applicable and special amino acids do not have to be prepared. Moreover, biological synthesis methods are also applicable. Genetically-encoded peptide library screenings methods, that utilize Nature's machinery to generate diversity, yield much higher diversities and therefore the chance of finding a bioactive compound is also much higher. Examples are phage display screening methods, where peptide synthesis is performed by the *E. coli* bacteria. Therefore, CLiPS has a significant advantage over other click-type constraining methods, as these often require non-natural amino acids, which is less desired for genetically encoded library generation. Biosynthetic methods that can process non-canonical amino acids are often highly

specialized, have a higher margin of error and sometimes require re-writing of the biological code when translating peptides.[115,122–124]
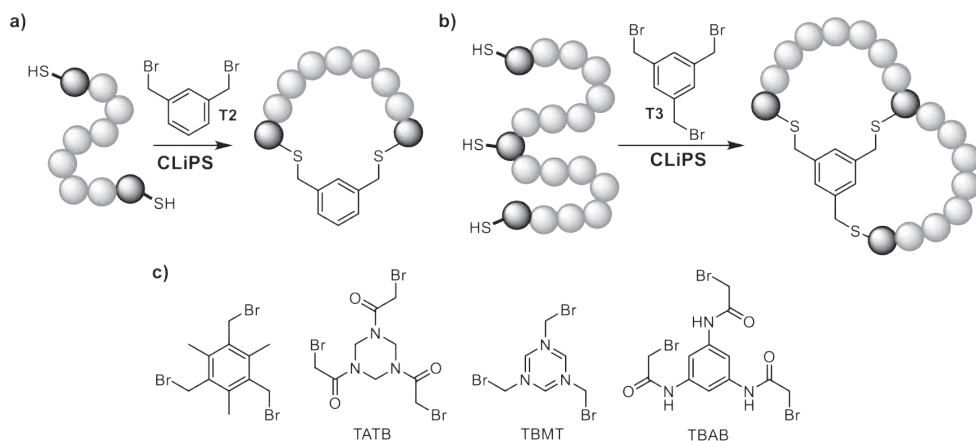
Figure 1.7: The CLiPS reaction to constrain peptides. a) synthesis of a monocyclic peptide using scaffold T2. b) Synthesis of a bicyclic peptide using scaffold T3 (TBMB). c) Examples of other T3-type scaffolds.

The CLiPS reaction has found wide application in phage display technologies and many examples have been published over the years, especially by Heinis, Winter and co-workers. In their seminal 2009 paper, they described the discovery of a new inhibitor for human plasma kallikrein, with a very high binding activity (K_i = 1.5 nM) (Figure 1.8).[125] They applied phage display technology to generate libraries of peptides containing three cysteines. By subsequent reaction with the T3-scaffold TBMB, bicyclic peptide libraries were generated from their linear precursors (Figure 1.8a). A potent inhibitor against human plasma kallikrein was discovered upon screening, which was only active in its bicyclic form (Figure 1.8b).
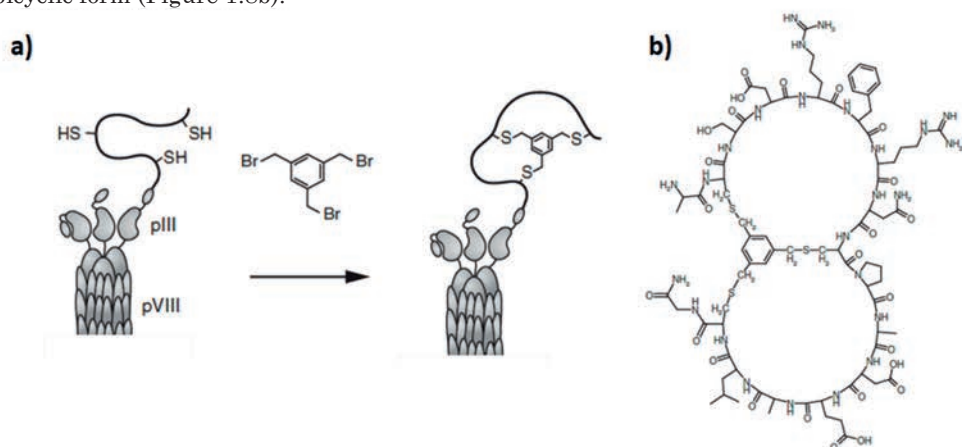
Figure 1.8: a) Phage-encoded library generation and subsequent CLiPS reaction with the T3 scaffold to yield phage-coupled bicyclic CLiPS-peptides. b) Structure of bicyclic inhibitor of plasma kallikrein, isolated by phage display. Image retrieved from the original reference.[125]

Phage display screening of bicyclic peptides has been applied in numerous other studies[126–129] and has been subject of several reviews as well.[130–132] While most studies focus on equally sized peptide loops, combinations of different sizes of peptide loops were more recently investigated.[129] Moreover, introduction of four cysteines in a peptide, combined with using two T2-type scaffolds was used to afford a large variety of structural topologies.[133] As phage display is a very powerful tool used in drug discovery, recent advances have also included the incorporation of non-canonical amino acids[134] and a 'mirror image' phage display screening with all *D*-amino acids.[135]

Unfortunately, the largest number of peptide loops that can be cyclized *selectively* onto one aryl-type scaffold using CLiPS is two, as was explored with T3 scaffolds. Increasing to four connections inevitably leads to the formation of regio-isomers, as the system loses symmetry. This problem will be discussed in-depth at the end of this introduction.

To be able to increase the structural complexity and the number of peptide cycles in a single system, bifunctional scaffolds have been developed in our research group.[136] These bifunctional scaffolds can be utilized to further functionalize the monocyclic peptides formed, via a second orthogonal ligation technique. These bifunctional scaffolds were used to synthesize tricyclic mimics of the discontinuous and conformational β1/β3-loop binding site on hFSH/hCG (Figure 1.9).[104] First, the two peptides β1 and β3 were cyclized via CLiPS onto their scaffolds. Thereafter, the two complementary scaffolds were coupled via oxime ligation, yielding a bicyclic peptide. Final constraining of the bicyclic construct was conducted via disulfide bond formation, yielding the final tricyclic construct. The highly constrained compounds showed much higher activity than those with fewer constraints, illustrating the relation between the correctly constrained 3D structure and activity.
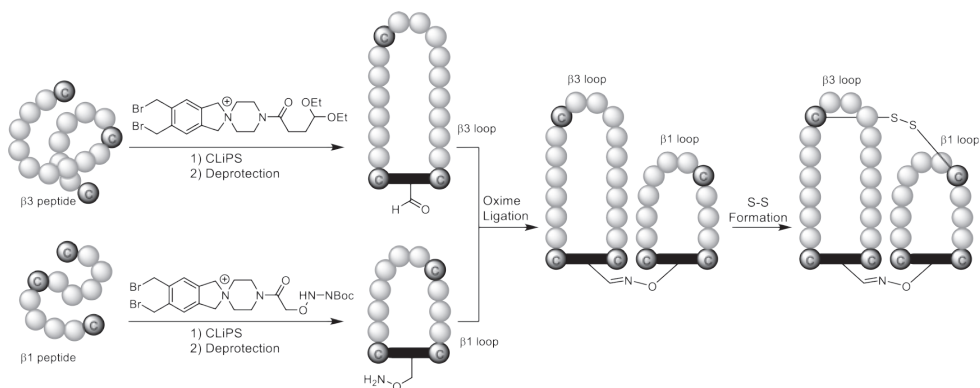
Figure 1.9: Synthesis of the constrained β1/β3-loop binding site on hFSH/hCG, via CLiPS cyclization of monocyclic peptides, followed by joining the scaffolds via intermolecular oxime ligation. Formation of the disulfide bond between the two loops yielded the final mimic.

Another method that utilizes the combination of a CLiPS-type reaction and oxime ligation to synthesize bicyclic peptides was developed by the Dawson group.[137] Instead of a traditional aryl-based CLiPS scaffold, they used 1,3-dichloroacetone (Figure 1.10). After a CLiPS-type reaction to stabilize a peptide helix, the ketone of the linker is available for oxime ligation. They mostly explored intermolecular oxime ligations, but they showed an example of an intramolecular oxime ligation as well (Figure 1.10b). This intramolecular oxime ligation was particularly sluggish, and required the use of an aniline catalyst.[83,92]
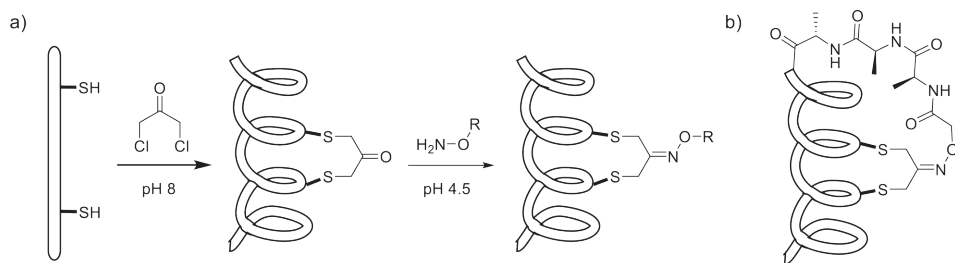
Figure 1.10: Synthesis of bicyclic peptide via CLiPS and oxime ligation. While mostly intermolecular oxime ligation was explored, one example of a bicyclic peptide was shown (b).

1.2.3 Tricyclic Peptides

The glycopeptide antibiotic vancomycin is often referred to as the 'last-resort' antibiotic and is active against Gram-positive bacteria. After its discovery in the 1950s, it was not widely used, as less toxic antibiotics with fewer side-effects, were favored.[138] As oral uptake is quite poor, it is usually administered intravenously. It functions by inhibiting cell wall synthesis in bacteria, thereby inhibiting growth and multiplication.[139] With the insurgence of methicillin-resistant *S. aureus* (MRSA) and penicillin-resistant *Strepto-*

coccus pneumoniae, vancomycin found renewed interest and use during the 1980s. Since then, it has been widely used against infections that are difficult to treat with other antibiotics.[138] As a result, antibiotic resistance has also become more of an issue, threatening the status of 'last resort antibiotic'.

Vancomycin

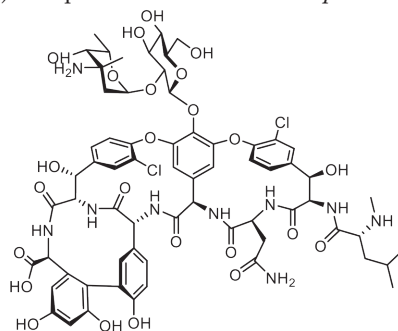Vancomycin features an aromatic core, onto which three peptide loops are wrapped. The same aromatic core is additionally functionalized with a glycan chain. The total synthesis of the vancomycin aglycon was first completed by Evans in 1998,[140] while the full total synthesis - including the disaccharide - was accomplished by Nicolaou one year later.[141]

In the 1990s, a peptide called RP 71955 was discovered in a screening for anti-HIV agents.[142] Isolated from a strain of Streptomyces, secondary metabolite RP 71955 was found to inhibit HIV-replication in cell cultures. It targets the HIV-1 protease, which eventually inhibits HIV-replication.[143] The peptide was found to be a tricyclic 21 amino acid peptide, featuring two disulfide bonds and an isopeptide bond (see Figure 1.11).[144,145] This peptide was later classified as siamycin II, with BMY 29303, NP-06 (FR 901724) belonging to this class as well. They differ only at position 4 (Val or Ile) or 17 (Val or Ile).[142] Together with siamycin I, these peptides belong to a larger class of lasso-peptides.[146] Part of the peptide chain is passed through one of the macrocycles, and the rings are mechanically interlocked. Aside from anti-HIV activity, the lasso peptides are also regarded as intriguing antibacterial peptides, targeting Gram-positive bacteria at Lipid II, inhibiting cell wall synthesis.[146,147] Chemical synthesis of lasso peptides is currently an academic effort only, while genome mining to find new lasso peptides has received widespread attention.[148–150]
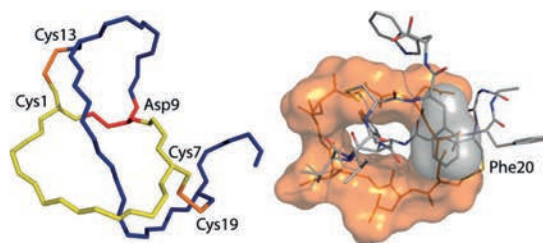
RP 71955

Figure 1.11: Left) Backbone representation of tricyclic lasso-peptide RP 71955, Right) Surface representation of the structure. Image retrieved from the original reference.[146]

The group of Suga applied T3-CLiPS chemistry in combination with a spontaneous intramolecular cyclization of a cysteine onto an N-terminal chloroacetyl group.[124] The methodology to make these fused tricyclic peptides was designed with high throughput screening in mind, and is based on a flexizyme in vitro translation system. Their approach hinges on the selective spontaneous cyclization occurring at one cysteine only. While they indeed report that only one cysteine is capable of this cyclization (as shown in Figure 1.12) it is statistically unlikely that other cysteines in the peptide would not react.
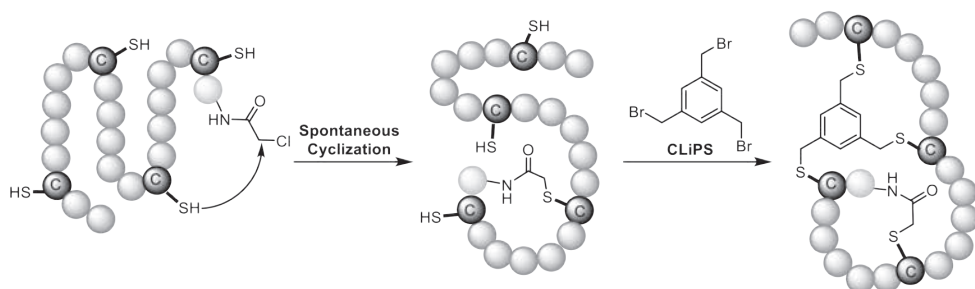
Figure 1.12: Synthesis of a fused tricyclic peptide via spontaneous cyclization onto the N-terminal chloroacetyl group, followed by T3-CLiPS cyclization.

The Ruchala group used scaffold-assisted synthesis of multicyclic peptides in their efforts to synthesize mimics of the iron-regulating hormone hepcidin. Besides their use of T2 and T3 CLiPS scaffolds, they also used a pentaerythritol-derived scaffold (Figure 1.13).[151] This scaffold possesses tetrahedral symmetry (T_d), whereby a single regioisomer of a tricyclic peptide can be obtained only. However, while they reported that products were obtained as single compound, it is most likely they were obtained as a mixture of diastereoisomers due to the tetrahedral configuration of the scaffold in combination with the asymmetry of the peptide.
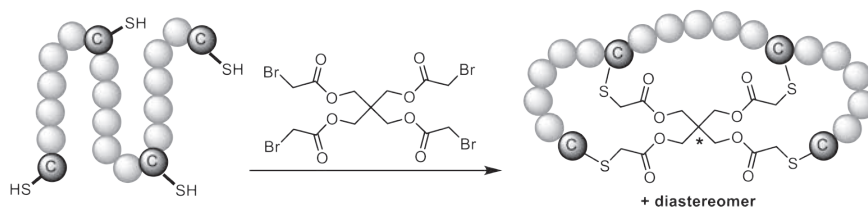
Figure 1.13: Synthesis of a tricyclic peptide using a pentaerythritol-derived scaffold, yielding diastereomeric products.

In their efforts to synthesize tricyclic peptides, the group of Wu applied thiolate/S$_N$Ar (aromatic nucleophilic substitution) reactions.[152] Selectivity depends on two different types of thiolate nucleophiles being i) cysteine and ii) the more sterically congested penicillamine, which therefore have very different reactivities (Figure 1.14). The electron-poor S$_N$Ar-scaffold that was used is 2,3,5,6-tetrafluoroterephthalonitrile (4F-2CN). Cysteine, being the more reactive of the two thiolates, reacts rapidly. After the first thioether bond is formed with cysteine, attack of the second cysteine-derived sulfhydryl group occurs selectively at the para-position of 4F-2CN to give a monocyclic peptide in a regioselective manner. Thereafter, the sterically congested penicillamine sulfhydryl groups reacted to form the tricyclic peptide. As both remaining S$_N$Ar-positions are equally reactive, two regio-isomers can be formed. As such, this strategy reduces the number of possible regio-isomers using a CLiPS-type reaction to only two, instead of the possible six.
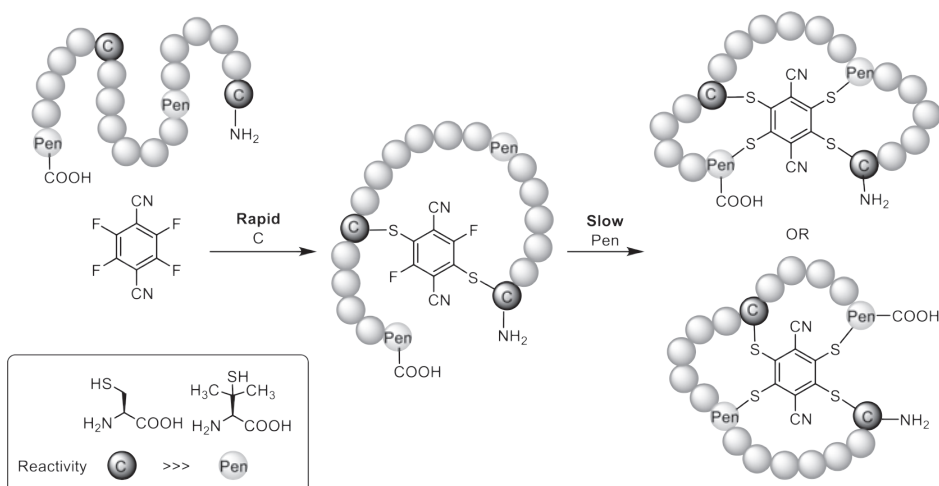
Figure 1.14: Synthesis of tricyclic peptides, using a thiolate/fluoride nucleophilic substitution reaction on the 2,3,5,6-tetrafluoroterephthalonitrile scaffold (4F-2CN). Two different peptide-bound thiolates, cysteine and penicillamine, were used to yield two regioisomeric products.

1.3   Tetra- to Hexacyclic Peptides

1.3.1   Lanthipeptides

A highly diverse class of multicyclic peptides are the ribosomally synthesized lanthipeptides, originating from Gram-positive bacteria.[153–158] Most lanthipeptides show interesting biological activity, generally against other gram-positive bacteria, hence they are often referred to as lanthibiotics. The most important structural element in the lanthipeptide class is the very stable thioether linkage present in the amino acid lanthionine (Lan), which is formed during the cyclization reaction (Figure 1.15).[159,160] Formation of the thioether bond occurs after dehydration of a serine resulting in a dehydroalanine that is subsequently attacked by a nearby cysteine. MeLan, featuring a methyl adjacent to the thioether, is derived from threonine. While Lan can be formed uncatalyzed, MeLan formation is always enzyme-mediated.[161,162]
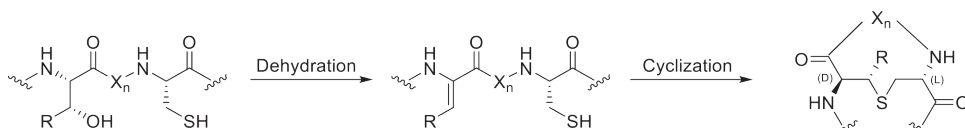
Figure 1.15: Synthesis of the lanthionine thioether bridge, starting with dehydration of serine or threonine (R=H or CH₃ respectively). After formation of dehydroalanine, a nearby cysteine forms the thioether bond, yielding the cyclized peptide Lan (R=H) or MeLan (R=CH₃).

Nisin is the best studied example of all naturally-occurring lanthipeptides (Figure 1.16). This 34-amino acid peptide contains Dha, Dhb, and five thioether linkages, constructing the five macrocyles (A, B, C and the cross-linked D and E rings). Besides its antibiotic properties, resulting in widespread use as a food preservative (E234) in over 80 different countries over 50 years,[163] anti-malarial activity has also been reported.[164]

References to Nisin have a long history. The inhibitory effect of 'a substance' produced by the *Streptococcus Lactis* on the growth of *Lactobacillus Bulgaricus* was first described by Rogers in 1928, making it the first reference to an antibacterial compound.[165,166] This therefore predates Flemings landmark discovery of penicillin in 1929.[167] Whitehead first isolated the antibacterial compound from *St. Lactis* in 1933, and demonstrated the activity towards other bacterial strains.[168] Mattick and coworkers used this compound in the treatment for bacterial infections in mice.[169] The compound was named Nisin, a 'Group N-Inhibitory Substance'. In 1971, the structure was finally elucidated by Gross and Morell.[170] The chemical synthesis of the A and B rings was pioneered by the group of Shiba in 1983 and 1986, respectively, via desulfurization of the disulfide peptide analogues.[39,171,172] They later performed the solution-phase total synthesis via fragment condensation.[173]

The biosynthesis of Nisin and other lanthipeptides have been extensively investigated, particularly by the group of Van der Donk.[174,175] With the discovery of new lanthipeptides, classification started to be based on the gene clusters responsible for the biosynthesis.[176] Particularly the Lan-synthetases have been applied to the synthesis of novel lanthipeptides.[155,163,177–181]
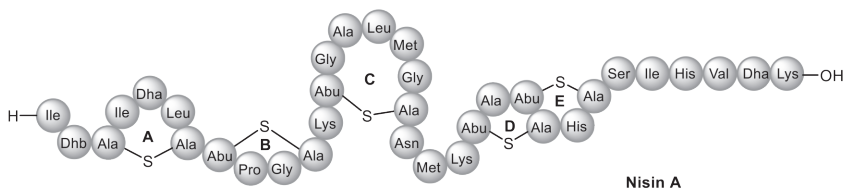
Figure 1.16: Structure of the pentacyclic peptide Nisin.

Chemical synthesis of lanthipeptides has received widespread attention. To date, the total synthesis of natural lanthipeptides Nisin,[173,182] lacticin 3147,[183] lacticin S,[184] and lacticin 481[185] have been completed (selected examples in Figure 1.17). Many other efforts have focused on synthesis of the Lan and/or MeLan structural motif and to synthesize non-natural lantipeptides. However, cyclization of non-natural derivatives is usually very challenging, as the natural peptides have an inherent predisposition for cyclization. Desulfurization strategies of disulfides have been applied in the total synthesis of Nisin, but it is difficult to synthesize the natural Lan with this strategy.[173,182,186] Lan of the correct stereochemistry, equipped with orthogonal protecting groups to incorporate Lan in solid phase peptide synthesis has been achieved by, for example, substitution of β-bromo alanine.[162,185,187,188] However, for the synthesis of novel lanthionines, biochemical engineering is probably the most feasible approach.[189]
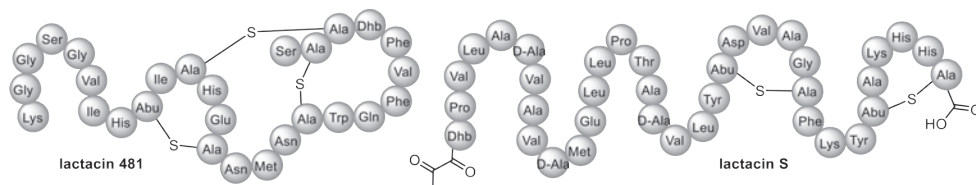
Figure 1.17: Structures of lactacin 481 and lactacin S.

1.4 Aim of This Thesis

There is high interest in small (multi)cyclic peptides as they can bridge the gap between biologics and small molecules. However, in this introduction, we have seen that synthesis of these types of molecules is not trivial. Laborious, costly synthesis with low conversions and little opportunities for diversification have been reported. High throughput library-based syntheses, such as phage display, have limited options for increasing the complexity by adding multicycles. Moreover, structurally complex systems are often burdened by regioselectivity issues, and mixtures of isomers are often obtained. For example, while the synthesis of tricyclic peptides via CLiPS, using 1,2,4,5-tetrabromodurene (T4), would be a natural expansion of the existing chemistry, implementation would result in the formation of a complex mixture of six regio-isomers. This issue is illustrated in Figure 1.18. After connection of the first cysteine, the scaffold loses its symmetry. The other cysteines then react at chemically non-equivalent positions, resulting in the formation of the six depicted isomers.
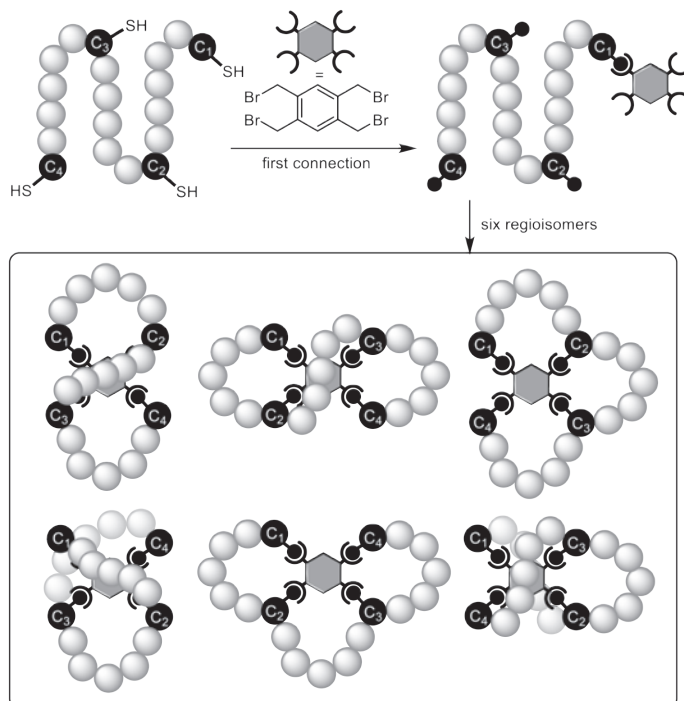
Figure 1.18: Synthesis of tricyclic peptides via CLiPS ligation/cyclization, whereby six possible isomers can form, resulting in a complex product mixture.

In this thesis, the scaffold-assisted synthesis of tri-, tetra- and pentacyclic peptides is explored. Our aim is to establish a one-pot-type procedure to synthesize multicyclic peptides in a facile and easily diversifiable format, which can ideally be made suitable for peptide library synthesis. As the CLiPS reaction is very well-established, this ligation method will be combined with a second, orthogonal ligation. By the sequential nature of this strategy, the number of isomers that can be formed is significantly lowered, preferably to only a single isomer. For this second ligation method, we have chosen oxime ligation. The reaction between an aldehyde or ketone and an aminooxy group (Figure 1.19) has been widely described in peptide chemistry, and has been highlighted in the introduction.[62,63,88,105] Similar to the CLiPS reaction, oxime ligation can occur in aqueous solution at high dilution. However, unlike the CLiPS reaction, oxime ligation occurs only at a slightly acidic pH, with an optimum reactivity at pH 4-5. Therefore, reaction conditions must be made compatible to preferably render a one-pot procedure possible.

When a ketone is used as the electrophile, this could give rise to the formation of *E/Z* isomers of the oxime linkage (Figure 1.19). Although oxime formation is reversible, studies have shown that for trans-oximation, a large excess of the competing reagent is required.[105] However, under physiological conditions oxime linkages are kinetically inert and therefore fully stable. Sofar the oxime ligation reaction has mainly been studied in an intermolecular fashion as opposed to the work described in this thesis, which exclusively involves intramolecular oxime ligations. This shift to intramolecular oxime formation dramatically changes the thermodynamic and kinetic characteristics.
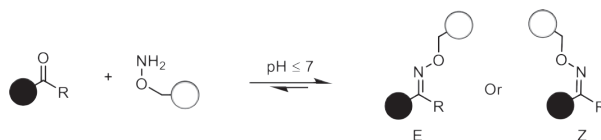
Figure 1.19: Formation of an oxime bond by reaction between an aldehyde or ketone and an aminooxy group. When ketones are used, this can give rise to the formation of E/Z-isomers.

Previous research in our group[104,136] and by others[137] has already established orthogonal compatibility of oxime ligation with the CLiPS reaction. Despite this, the use of various aminooxy or aldehyde-protecting groups were still investigated when comparing different strategies, in order to establish which of these works best in our efforts to synthesize multicyclic peptides. Since oxime ligation takes place between an electrophilic aldehyde or ketone and a nucleophilic aminooxy group, the combination with CLiPS reactivities can be realized via two principally different routes.

In our efforts to synthesize tricyclic peptides, two different strategies were investigated. In **Chapter 2**, the first strategy (strategy 1) will be explored, where the scaffolds contain all electrophiles (arylmethyl bromide and aldehydes or ketones), while the peptides will be equipped with all nucleophiles (thiolates and aminooxy groups). Three novel scaffolds have been developed and were combined with aminooxy-group functionalized peptides, to synthesize tricyclic peptides.

In **Chapter 3**, strategy 2 will be explored, where the electrophiles and nucleophiles will be mixed. The scaffolds will be equipped with electrophilic arylmethyl bromides and nucleophilic aminooxy groups, while the peptides will bear both nucleophilic thiolates and electrophilic aldehydes or ketones. Three novel scaffolds were developed, and combined with peptides bearing two different ketone-functionalized peptides.

Chapter 4 is concerned with the synthesis of tetracyclic peptides, whereby the CLiPS and oxime cyclization ligation reactions are preceded by enzymatic macrolactamization of the peptides. This builds on the chemistry developed in Chapters 2

and 3 and both strategies 1 and 2 will be investigated. **Chapter 5** explores the synthesis of pentacyclic peptides, again via both strategies 1 and 2. Novel phenyl-based scaffolds have been developed. Ultimately, only strategy 2 was fully investigated in the preparation of pentacyclic peptides. Figure 1.20 gives an overview of the topologies explored in this thesis.
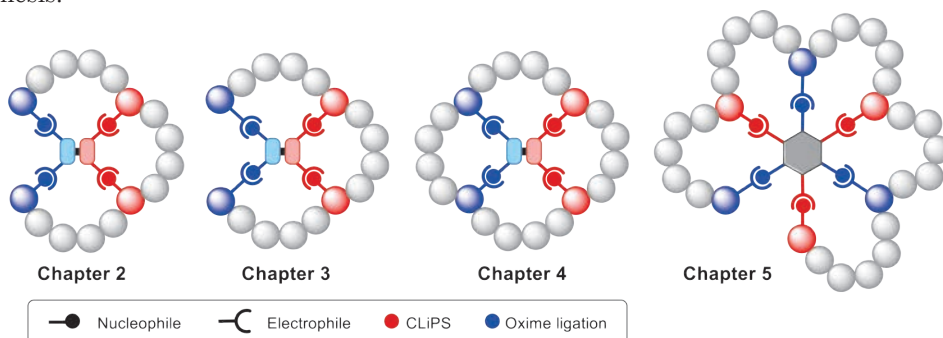
Figure 1.20: Overview of the work in this thesis.

1.5 References

(1) Craik, D. J.; Fairlie, D. P.; Liras, S.; Price, D. *Chem. Biol. Drug Des.* **2013**, *81* (1), 136.

(2) Molina, M. A.; Codony-Servat, J.; Albanell, J.; Rojo, F.; Arribas, J.; Baselga, J. *Cancer Res.* **2001**, *61* (12), 4744 LP.

(3) Hudis, C. A. *N. Engl. J. Med.* **2007**, *357* (1), 39.

(4) Baselga, J.; Cortés, J.; Kim, S.-B.; Im, S.-A.; Hegg, R.; Im, Y.-H.; Roman, L.; Pedrini, J. L.; Pienkowski, T.; Knott, A.; Clark, E.; Benyunes, M. C.; Ross, G.; Swain, S. M. *N. Engl. J. Med.* **2011**, *366* (2), 109.

(5) Organization, W. H. *World Health Organization model list of essential medicines: 21st list 2019*; World Health Organization: Geneva PP - Geneva.

(6) Lipinski, C. A.; Lombardo, F.; Dominy, B. W.; Feeney, P. J. *Adv. Drug Deliv. Rev.* **2001**, *46* (1), 3.

(7) Danese, S.; Sans, M.; Scaldaferri, F.; Sgambato, A.; Rutella, S.; Cittadini, A.; Piqué, J. M.; Panes, J.; Katz, J. A.; Gasbarrini, A.; Fiocchi, C. *J. Immunol.* **2006**, *176* (4), 2617 LP.

(8) Van Deventer, S. J. H. *Gastroenterology* **2001**, *121* (5), 1242.

(9) Weger, W. *Br. J. Pharmacol.* **2010**, *160* (4), 810.

(10) Swinney, D. C.; Anthony, J. *Nat. Rev. Drug Discov.* **2011**, *10* (7), 507.

(11) Liu, W.; Wu, C. *Chinese Chem. Lett.* **2018**, *29* (7), 1063.

(12) Vinogradov, A. A.; Yin, Y.; Suga, H. *J. Am. Chem. Soc.* **2019**, *141* (10), 4167.

(13) Bulet, P.; Stöcklin, R.; Menin, L. *Immunol. Rev.* **2004**, *198* (1), 169.

(14) Conibear, A. C.; Chaousis, S.; Durek, T.; Johan Rosengren, K.; Craik, D. J.; Schroeder, C. I. *Pept. Sci.* **2016**, *106* (1), 89.

(15) White, C. J.; Yudin, A. K. *Nat. Chem.* **2011**, *3*, 509.

(16) Pogliano, J.; Pogliano, N.; Silverman, J. A. *J. Bacteriol.* **2012**, *194* (17), 4494 LP.

(17) Gause, G. F.; Brazhnikova, M. G. *Nature* **1944**, *154* (3918), 703.

(18) Conti, E.; Stachelhaus, T.; Marahiel, M. A.; Brick, P. *EMBO J.* **1997**, *16* (14), 4174.

(19) Davies, J. S. *J. Pept. Sci.* **2003**, *9* (8), 471.

(20) Wadhwani, P.; Afonin, S.; Ieronimo, M.; Buerck, J.; Ulrich, A. S. *J. Org. Chem.* **2006**, *71* (1), 55.

(21) Bu, X.; Wu, X.; Ng, N. L. J.; Mak, C. K.; Qin, C.; Guo, Z. *J. Org. Chem.* **2004**, *69* (8), 2681.

(22) Wu, X.; Bu, X.; Wong, K. M.; Yan, W.; Guo, Z. *Org. Lett.* **2003**, *5* (10), 1749.

(23) Skropeta, D.; Jolliffe, K. A.; Turner, P. *J. Org. Chem.* **2004**, *69* (25), 8804.

(24) Fernandez-Lopez, S.; Kim, H.-S.; Choi, E. C.; Delgado, M.; Granja, J. R.; Khasanov, A.; Kraehenbuehl, K.; Long, G.; Weinberger, D. A.; Wilcoxen, K. M.; Ghadiri, M. R. *Nature* **2001**, *412* (6845), 452.

(25) Dechantsreiter, M. A.; Planker, E.; Mathä, B.; Lohof, E.; Hölzemann, G.; Jonczyk, A.;

Goodman, S. L.; Kessler, H. *J. Med. Chem.* **1999**, *42* (16), 3033.

(26) Chatterjee, J.; Gilon, C.; Hoffman, A.; Kessler, H. *Acc. Chem. Res.* **2008**, *41* (10), 1331.

(27) Thakkar, A.; Trinh, T. B.; Pei, D. *ACS Comb. Sci.* **2013**, *15* (2), 120.

(28) Zhang, Y.; Xu, C.; Lam, H. Y.; Lee, C. L.; Li, X. *Proc. Natl. Acad. Sci.* **2013**, *110* (17), 6657 LP.

(29) Popovic, S.; Bieräugel, H.; Detz, R. J.; Kluwer, A. M.; Koole, J. A. A.; Streefkerk, D. E.; Hiemstra, H.; van Maarseveen, J. H. *Chem. Eur. J.* **2013**, *19* (50), 16934.

(30) Spatola, A. F.; Darlak, K.; Romanovskis, P. *Tetrahedron Lett.* **1996**, *37* (5), 591.

(31) Jensen, K. J.; Alsina, J.; Songster, M. F.; Vágner, J.; Albericio, F.; Barany, G. *J. Am. Chem. Soc.* **1998**, *120* (22), 5441.

(32) Ingale, S.; Dawson, P. E. *Org. Lett.* **2011**, *13* (11), 2822.

(33) Albericio, F.; Hammer, R. P.; García-Echeverría, C.; Molins, M. A.; Chang, J. L.; Munson, M. C.; Pons, M.; Giralt, E.; Barany, G. *Int. J. Pept. Protein Res.* **1991**, *37* (5), 402.

(34) Góngora-Benítez, M.; Tulla-Puche, J.; Albericio, F. *Chem. Rev.* **2014**, *114* (2), 901.

(35) Tam, J. P.; Wu, C. R.; Liu, W.; Zhang, J. W. *J. Am. Chem. Soc.* **1991**, *113* (17), 6657.

(36) Wu, M.; Hancock, R. E. W. *J. Biol. Chem.* **1999**, *274* (1), 29.

(37) Dawson, P. E.; Muir, T. W.; Clark-Lewis, I.; Kent, S. B. *Science (80-.).* **1994**, *266*, 776.

(38) Chen, J.; Wan, Q.; Yuan, Y.; Zhu, J.; Danishefsky, S. J. *Angew. Chemie - Int. Ed.* **2008**, *47* (44), 8521.

(39) Wakamiya, T.; Shimbo, K.; Sano, A.; Fukase, K.; Yasuda, H.; Shiba, T. *Pept. Chem.* **1983**, *20th*, 149.

(40) Thompson, R. E.; Chan, B.; Radom, L.; Jolliffe, K. A.; Payne, R. J. *Angew. Chemie Int. Ed.* **2013**, *52* (37), 9723.

(41) von Eggelkraut-Gottanka, R.; Klose, A.; Beck-Sickinger, A. G.; Beyermann, M. *Tetrahedron Lett.* **2003**, *44* (17), 3551.

(42) Hogenauer, T. J.; Wang, Q.; Sanki, A. K.; Gammon, A. J.; Chu, C. H. L.; Kaneshiro, C. M.; Kajihara, Y.; Michael, K. *Org. Biomol. Chem.* **2007**, *5* (5), 759.

(43) Agrigento, P.; Albericio, F.; Chamoin, S.; Dacquignies, I.; Koc, H.; Eberle, M. *Org. Lett.* **2014**, *16* (15), 3922.

(44) Popovic, S.; Wijsman, L.; Landman, I. R.; Sangster, M. F.; Pastoors, D.; Veldhorst, B. B.; Hiemstra, H.; van Maarseveen, J. H. *Eur. J. Org. Chem.* **2016**, *2016* (3), 443.

(45) Schmidt, M.; Toplak, A.; Quaedflieg, P. J. L. M.; van Maarseveen, J. H.; Nuijens, T. *Drug Discov. Today Technol.* **2017**, *26*, 11.

(46) Schmidt, M.; Toplak, A.; Quaedflieg, P. J. L. M.; Ippel, H.; Richelle, G. J. J.; Hackeng, T. M.; van Maarseveen, J. H.; Nuijens, T. *Adv. Synth. Catal.* **2017**, *359* (12), 2050.

(47) Nguyen, G. K. T.; Kam, A.; Loo, S.; Jansson, A. E.; Pan, L. X.; Tam, J. P. *J. Am. Chem. Soc.* **2015**, *137* (49), 15398.

(48) Wu, Z.; Guo, X.; Guo, Z. *Chem. Commun.* **2011**, *47* (32), 9218.

(49) Jia, X.; Kwon, S.; Wang, C.-I. A.; Huang, Y.-H.; Chan, L. Y.; Tan, C. C.; Rosengren, K. J.; Mulvenna, J. P.; Schroeder, C. I.; Craik, D. J. *J. Biol. Chem.* **2014**, *289* (10), 6627.

(50) Schmidt, M.; Toplak, A.; Quaedflieg, P. J. L. M.; Nuijens, T. *Curr. Opin. Chem. Biol.* **2017**, *38*, 1.

(51) Richelle, G. J. J.; Schmidt, M.; Ippel, H.; Hackeng, T. M.; van Maarseveen, J. H.; Nuijens, T.; Timmerman, P. *ChemBioChem* **2018**, *19* (18), 1934.

(52) Schmidt, M.; Huang, Y.-H.; Texeira de Oliveira, E. F.; Toplak, A.; Wijma, H. J.; Janssen, D. B.; van Maarseveen, J. H.; Craik, D. J.; Nuijens, T. *ChemBioChem* **2019**, *20* (12), 1524.

(53) Nuijens, T.; Toplak, A.; van de Meulenreek, M. B. A. C.; Schmidt, M.; Goldbach, M.; Quaedflieg, P. J. L. M. *Tetrahedron Lett.* **2016**, *57* (32), 3635.

(54) Chang, Y. S.; Graves, B.; Guerlavais, V.; Tovar, C.; Packman, K.; To, K.-H.; Olson, K. A.; Kesavan, K.; Gangurde, P.; Mukherjee, A.; Baker, T.; Darlak, K.; Elkin, C.; Filipovic, Z.; Qureshi, F. Z.; Cai, H.; Berry, P.; Feyfant, E.; Shi, X. E.; Horstick, J.; Annis, D. A.; Manning, A. M.; Fotouhi, N.; Nash, H.; Vassilev, L. T.; Sawyer, T. K. *Proc. Natl. Acad. Sci.* **2013**, *110* (36), E3445 LP.

(55) Ali, A. M.; Atmaj, J.; Van Oosterwijk, N.; Groves, M. R.; Dömling, A. *Comput. Struct. Biotechnol. J.* **2019**, *17*, 263.

(56) Iyer, V. V. *Current Medicinal Chemistry*. 2016, pp 3025–3043.

(57) Walensky, L. D.; Bird, G. H. *J. Med. Chem.* **2014**, *57* (15), 6275.

(58) Tan, Y. S.; Lane, D. P.; Verma, C. S. *Drug Discov. Today* **2016**, *21* (10), 1642.

(59) Cromm, P. M.; Spiegel, J.; Grossmann, T. N. *ACS Chem. Biol.* **2015**, *10* (6), 1362.
(60) Wang, Y.; Chou, D. H. C. *Angew. Chemie - Int. Ed.* **2015**, *54* (37), 10931.
(61) Lau, Y. H.; De Andrade, P.; Wu, Y.; Spring, D. R. *Chem. Soc. Rev.* **2015**, *44* (1), 91.
(62) Haney, C. M.; Werner, H. M.; McKay, J. J.; Horne, W. S. *Org. Biomol. Chem.* **2016**, *14* (24), 5768.
(63) Haney, C. M.; Loch, M. T.; Horne, W. S. *Chem. Commun.* **2011**, *47* (39), 10915.
(64) Fairlie, D. P.; Dantas de Araujo, A. *Biopolymers* **2016**, *106* (6), 843.
(65) Kolb, H. C.; Finn, M. G.; Sharpless, K. B. *Angew. Chemie Int. Ed.* **2001**, *40* (11), 2004.
(66) Piekielna, J.; Perlikowska, R.; Gach, K.; Janecka, A. *Curr. Drug Targets* **2013**, *14* (7), 798.
(67) Islam, M. N.; Islam, M. S.; Hoque, M. A.; Kato, T.; Nishino, N.; Ito, A.; Yoshida, M. *Bioorganic Med. Chem.* **2014**, *22* (15), 3862.
(68) Gleeson, E. C.; Jackson, W. R.; Robinson, A. J. *Tetrahedron Lett.* **2016**, *57* (39), 4325.
(69) Jarvo, E. R.; Copeland, G. T.; Papaioannou, N.; Bonitatebus, P. J.; Miller, S. J. - *J. Am. Chem. Soc.* **1999**, *121* (50), 11638.
(70) Reichwein, J. F.; Versluis, C.; Liskamp, R. M. J. *J. Org. Chem.* **2000**, *65* (19), 6187.
(71) Masuda, S.; Tsuda, S.; Yoshiya, T. *Org. Biomol. Chem.* **2018**, *16* (48), 9364.
(72) Zhao, B.; Zhang, Q.; Li, Z. *J. Pept. Sci.* **2016**, *22* (8), 540.
(73) Aimetti, A. A.; Shoemaker, R. K.; Lin, C.-C.; Anseth, K. S. *Chem. Commun.* **2010**, *46* (23), 4061.
(74) Hoyle, C. E.; Bowman, C. N. *Angew. Chemie Int. Ed.* **2010**, *49* (9), 1540.
(75) Mulder, G. E.; Kruijtzer, J. A. W.; Liskamp, R. M. J. *Chem. Commun.* **2012**, *48* (80), 10007.
(76) Mulder, G. E.; Quarles Van Ufford, H. C.; Van Ameijde, J.; Brouwer, A. J.; Kruijtzer, J. A. W.; Liskamp, R. M. J. *Org. Biomol. Chem.* **2013**, *11* (16), 2676.
(77) Hacker, D. E.; Hoinka, J.; Iqbal, E. S.; Przytycka, T. M.; Hartman, M. C. T. *ACS Chem. Biol.* **2017**, *12* (3), 795.
(78) Stefanucci, A.; Lei, W.; Pieretti, S.; Novellino, E.; Dimmito, M. P.; Marzoli, F.; Streicher, J. M.; Mollica, A. *Sci. Rep.* **2019**, *9* (1), 5771.
(79) Li, H.; Aneja, R.; Chaiken, I. *Molecules* **2013**, *18* (8), 9797.
(80) Jagasia, R.; Holub, J. M.; Bollinger, M.; Kirshenbaum, K.; Finn, M. G. *J. Org. Chem.* **2009**, *74* (8), 2964.
(81) van Maarseveen, J. H.; Horne, W. S.; Ghadiri, M. R. *Org. Lett.* **2005**, *7* (20), 4503.
(82) Bock, V. D.; Perciaccante, R.; Jansen, T. P.; Hiemstra, H.; van Maarseveen, J. H. *Org. Lett.* **2006**, *8* (5), 919.
(83) Agten, S. M.; Dawson, P. E.; Hackeng, T. M. *J. Pept. Sci.* **2016**, *22* (5), 271.
(84) Lang, K.; Chin, J. W. *ACS Chem. Biol.* **2014**, *9* (1), 16.
(85) Guthrie, Q. A. E.; Young, H. A.; Proulx, C. *Chem. Sci.* **2019**, *10* (41), 9506.
(86) Dirksen, A.; Dawson, P. E. *Bioconjug. Chem.* **2008**, *19* (12), 2543.
(87) Tuchscherer, G. *Tetrahedron Lett.* **1993**, *34* (52), 8419.
(88) Ulrich, S.; Boturyn, D.; Marra, A.; Renaudet, O.; Dumy, P. *Chem. – A Eur. J.* **2014**, *20* (1), 34.
(89) Gauthier, M. A.; Klok, H.-A. *Chem. Commun.* **2008**, No. 23, 2591.
(90) Clavé, G.; Boutal, H.; Hoang, A.; Perraut, F.; Volland, H.; Renard, P. Y.; Romieu, A. *Org. Biomol. Chem.* **2008**, *6* (17), 3065.
(91) Viault, G.; Dautrey, S.; Maindron, N.; Hardouin, J.; Renard, P. Y.; Romieu, A. *Org. Biomol. Chem.* **2013**, *11* (16), 2693.
(92) Dirksen, A.; Hackeng, T. M.; Dawson, P. E. *Angew. Chemie - Int. Ed.* **2006**, *45* (45), 7581.
(93) Agten, S. M.; Suylen, D. P. L.; Hackeng, T. M. *Bioconjug. Chem.* **2016**, *27* (1), 42.
(94) Shao, J.; Tam, J. P. *J. Am. Chem. Soc.* **1995**, *117* (14), 3893.
(95) Frost, J. R.; Vitali, F.; Jacob, N. T.; Brown, M. D.; Fasan, R. *ChemBioChem* **2013**, *14* (1), 147.
(96) Nyanguile, O.; Mutter, M.; Tuchscherer, G. *Lett. Pept. Sci.* **1994**, *1* (1), 9.
(97) Cremer, G. A.; Bureaud, N.; Lelièvre, D.; Piller, V.; Piller, F.; Delmas, A. *Chem. - A Eur. J.* **2004**, *10* (24), 6353.
(98) Wahl, F.; Mutter, M. *Tetrahedron Lett.* **1996**, *37* (38), 6861.
(99) Rose, K.; Zeng, W.; Regamey, P. O.; Chernushevich, I. V.; Standing, K. G.; Gaertner, H. F. *Bioconjug. Chem.* **1996**, *7* (5), 552.
(100) Zeng, W.; Ghosh, S.; Macris, M.; Pagnon, J.; Jackson, D. C. *Vaccine* **2001**, *19* (28–29), 3843.
(101) Sohma, Y.; Kent, S. B. H. *J. Am. Chem. Soc.* **2009**, *131* (44), 16313.

(102) Palei, S.; Mootz, H. D. *ChemBioChem* **2016**, *17* (5), 378.

(103) Lamping, M.; Grell, Y.; Geyer, A. *J. Pept. Sci.* **2016**, *22* (4), 228.

(104) Smeenk, L. E. J.; Timmers-Parohi, D.; Benschop, J. J.; Puijk, W. C.; Hiemstra, H.; Van Maarseveen, J. H.; Timmerman, P. *ChemBioChem* **2015**, *16* (1), 91.

(105) Haney, C. M.; Horne, W. S. *J. Pept. Sci.* **2014**, *20* (2), 108.

(106) Nishimura, S.; Arita, Y.; Honda, M.; Iwamoto, K.; Matsuyama, A.; Shirai, A.; Kawasaki, H.; Kakeya, H.; Kobayashi, T.; Matsunaga, S.; Yoshida, M. *Nat. Chem. Biol.* **2010**, *6*, 519.

(107) Donovick, R.; Pagano, J. F.; Stout, H. A.; Weinstein, M. J. *Antibiot. Annu.* **1955**, *3*, 554.

(108) McConkey, G. A.; Rogers, M. J.; McCutchan, T. F. *J. Biol. Chem.* **1997**, *272* (4), 2046.

(109) Nicolaou, K. C.; Safina, B. S.; Zak, M.; Lee, S. H.; Nevalainen, M.; Bella, M.; Estrada, A. A.; Funke, C.; Zécri, F. J.; Bulat, S. *J. Am. Chem. Soc.* **2005**, *127* (31), 11159.

(110) Nicolaou, K. C.; Zak, M.; Safina, B. S.; Estrada, A. A.; Lee, S. H.; Nevalainen, M. *J. Am. Chem. Soc.* **2005**, *127* (31), 11176.

(111) Nicolaou, K. C. *Angew. Chemie Int. Ed.* **2012**, *51* (50), 12414.

(112) Sable, R.; Durek, T.; Taneja, V.; Craik, D. J.; Pallerla, S.; Gauthier, T.; Jois, S. *ACS Chem. Biol.* **2016**, *11* (8), 2366.

(113) Lian, W.; Upadhyaya, P.; Rhodes, C. A.; Liu, Y.; Pei, D. *J. Am. Chem. Soc.* **2013**, *135* (32), 11990.

(114) Ahangarzadeh, S.; Kanafi, M. M.; Hosseinzadeh, S.; Mokhtarzadeh, A.; Barati, M.; Ranjbari, J.; Tayebi, L. *Drug Discov. Today* **2019**, *24* (6), 1311.

(115) Sako, Y.; Morimoto, J.; Murakami, H.; Suga, H. *J. Am. Chem. Soc.* **2008**, *130* (23), 7232.

(116) St. Clair, E. W.; van der Heijde, D. M. F. M.; Smolen, J. S.; Maini, R. N.; Bathon, J. M.; Emery, P.; Keystone, E.; Schiff, M.; Kalden, J. R.; Wang, B.; DeWoody, K.; Weiss, R.; Baker, D.; Group, A.-C. S. of P. R. I. for the T. of R. A. of E. O. S. *Arthritis Rheum.* **2004**, *50* (11), 3432.

(117) Rhodes, C. A.; Dougherty, P. G.; Cooper, J. K.; Qian, Z.; Lindert, S.; Wang, Q.-E.; Pei, D. *J. Am. Chem. Soc.* **2018**, *140* (38), 12102.

(118) Timmerman, P.; Beld, J.; Puijk, W. C.; Meloen, R. H. *ChemBioChem* **2005**, *6* (5), 821.

(119) Chen, S.; Bertoldo, D.; Angelini, A.; Pojer, F.; Heinis, C. *Angew. Chemie - Int. Ed.* **2014**, *53* (6), 1602.

(120) Meuleman, T. J.; Cowton, V. M.; Patel, A. H.; Liskamp, R. M. J. *J. Pept. Sci.* **2020**, *26* (1), e3222.

(121) Ramos-Tomillero, I.; Perez-Chacon, G.; Somovilla-Crespo, B.; Sanchez-Madrid, F.; Domínguez, J. M.; Cuevas, C.; Zapata, J. M.; Rodríguez, H.; Albericio, F. *Bioconjug. Chem.* **2018**, *29* (4), 1199.

(122) Tian, F.; Tsao, M. L.; Schultz, P. G. *J. Am. Chem. Soc.* **2004**, *126* (49), 15962.

(123) Chin, J. W.; Cropp, T. A.; Anderson, J. C.; Mukherji, M.; Zhang, Z.; Schultz, P. G. *Science (80-.).* **2003**, *301* (5635), 964.

(124) Bashiruddin, N. K.; Nagano, M.; Suga, H. *Bioorg. Chem.* **2015**, *61*, 45.

(125) Heinis, C.; Rutherford, T.; Freund, S.; Winter, G. *Nat. Chem. Biol.* **2009**, *5* (7), 502.

(126) Angelini, A.; Cendron, L.; Chen, S.; Touati, J.; Winter, G.; Zanotti, G.; Heinis, C. *ACS Chem. Biol.* **2012**, *7* (5), 817.

(127) Rentero Rebollo, I.; Heinis, C. *Methods* **2013**, *60* (1), 46.

(128) Rhodes, C. A.; Pei, D. *Chem. - A Eur. J.* **2017**, *23* (52), 12690.

(129) Rebollo, I. R.; Angelini, A.; Heinis, C. *Medchemcomm* **2013**, *4* (1), 145.

(130) Heinis, C.; Winter, G. *Next Gener. Ther.* **2015**, *26*, 89.

(131) Bosma, T.; Rink, R.; Moosmeier, M. A.; Moll, G. N. *ChemBioChem* **2019**, *20* (14), 1754.

(132) Sohrabi, C.; Foster, A.; Tavassoli, A. *Nat. Rev. Chem.* **2020**, *4* (2), 90.

(133) Kale, S. S.; Villequey, C.; Kong, X.-D.; Zorzi, A.; Deyle, K.; Heinis, C. *Nat. Chem.* **2018**, *10* (7), 715.

(134) Oller-Salvia, B.; Chin, J. W. *Angew. Chemie Int. Ed.* **2019**, *58* (32), 10844.

(135) Adaligil, E.; Patil, K.; Rodenstein, M.; Kumar, K. *ACS Chem. Biol.* **2019**, *14* (7), 1498.

(136) Smeenk, L. E. J.; Dailly, N.; Hiemstra, H.; Van Maarseveen, J. H.; Timmerman, P. *Org. Lett.* **2012**, *14* (5), 1194.

(137) Assem, N.; Ferreira, D. J.; Wolan, D. W.; Dawson, P. E. *Angew. Chemie Int. Ed.* **2015**, *54* (30), 8665.

(138) Levine, D. P. *Clin. Infect. Dis.* **2006**, *42* (Supplement_1), S5.

(139) Watanakunakorn, C. *J. Antimicrob. Chemother.* **1984**, *14* (suppl_D), 7.

(140) Evans, D. A.; Wood, M. R.; Trotter, B. W.; Richardson, T. I.; Barrow, J. C.; Katz, J. L. *Angew. Chemie Int. Ed.* **1998**, *37* (19), 2700.

(141) Nicolaou, K. C.; Mitchell, H. J.; Jain, N. F.; Winssinger, N.; Hughes, R.; Bando, T. *Angew. Chemie Int. Ed.* **1999**, *38* (1-2), 240.

(142) Helynck, G.; Dubertret, C.; Mayaux, J. F.; Leboul, J. *J. Antibiot. (Tokyo).* **1993**, *46* (11), 1756.

(143) De Clercq, E. *Med. Res. Rev.* **2000**, *20* (5), 323.

(144) Frechet, D.; Guitton, J. D.; Herman, F.; Faucher, D.; Helynck, G.; Monegier du Sorbier, B.; Ridoux, J. P.; James-Surcouf, E.; Vuilhorgne, M. *Biochemistry* **1994**, *33* (1), 42.

(145) Constantine, K. L.; Friedrichs, M. S.; Detlefsen, D.; Nishio, M.; Tsunakawa, M.; Furumai, T.; Ohkuma, H.; Oki, T.; Hill, S.; Bruccoleri, R. E.; Lin, P.-F.; Mueller, L. *J. Biomol. NMR* **1995**, *5* (3), 271.

(146) Hegemann, J. D.; Zimmermann, M.; Xie, X.; Marahiel, M. A. *Acc. Chem. Res.* **2015**, *48* (7), 1909.

(147) Tan, S.; Ludwig, K. C.; Müller, A.; Schneider, T.; Nodwell, J. R. *ACS Chem. Biol.* **2019**, *14* (5), 966.

(148) Maksimov, M. O.; Link, A. J. *J. Ind. Microbiol. Biotechnol.* **2014**, *41* (2), 333.

(149) Maksimov, M. O.; Pan, S. J.; Link, J.A. *Nat. Prod. Rep.* **2012**, *29* (9), 996.

(150) Ziemert, N.; Alanjary, M.; Weber, T. *Nat. Prod. Rep.* **2016**, *33* (8), 988.

(151) Chua, K.; Fung, E.; Micewicz, E. D.; Ganz, T.; Nemeth, E.; Ruchala, P. *Bioorganic Med. Chem. Lett.* **2015**, *25* (21), 4961.

(152) Liu, W.; Zheng, Y.; Kong, X.; Heinis, C.; Zhao, Y.; Wu, C. *Angew. Chemie Int. Ed.* **2017**, *56* (16), 4458.

(153) McAuliffe, O.; Ross, R. P.; Hill, C. *FEMS Microbiol. Rev.* **2001**, *25* (3), 285.

(154) Nagao, J.; Asaduzzaman, S. M.; Aso, Y.; Okuda, K.; Nakayama, J.; Sonomoto, K. *J. Biosci. Bioeng.* **2006**, *102* (3), 139.

(155) Al-Mahrous, M. M.; Upton, M. *Expert Opin. Drug Discov.* **2011**, *6* (2), 155.

(156) Gasson, M. J. *Biotechnol. Ser.* **1995**, *28* (Genetics and Biochemistry of Antibiotic Production), 283.

(157) Bierbaum, G.; Sahl, H. G. *Zentralblatt fur Bakteriol.* **1993**, *278* (1), 1.

(158) Willey, J. M.; Van der Donk, W. A. *Annu. Rev. Microbiol.* **2007**, *61*, 477.

(159) Bierbaum, G.; Brotz, H.; Sahl, H.-G. *BIOspektrum* **1997**, No. Sonderausg., 51.

(160) Shiba, T.; Wakamiya, T.; Fukase, K.; Sano, A.; Shimbo, K.; Ueki, Y. *Biopolymers* **1986**, *25* (Suppl.), S11.

(161) Paul, M.; Van der Donk, W. A. *Mini-Rev. Org. Chem.* **2005**, *2*, 23.

(162) Tabor, A. B. *Org. Biomol. Chem.* **2011**, *9* (22), 7606.

(163) Chatterjee, C.; Paul, M.; Xie, L.; Van der Donk, W.A. *Chem. Rev.* **2005**, *105* (2), 633.

(164) Gross, E.; Morell, J. L. *J. Am. Chem. Soc.* **1967**, *89* (11), 2791.

(165) Rogers, L. A.; Whittier, E. O. *J. Bacteriol.* **1928**, *16*, 211.

(166) Rogers, L. A. *J. Bacteriol.* **1928**, *16*, 321.

(167) Fleming, A. *Br. J. Exp. Pathol.* **1929**, *10*, 226.

(168) Whitehead, H. R. *Biochem. J.* **1933**, 1793.

(169) Mattick, A. T. R.; Hirsch, A.; Berridge, N. J. *The Lancet* **1947**, *250* (6462), 5.

(170) Gross, E.; Morell, J. L. *J. Am. Chem. Soc.* **1971**, *93* (18), 4634.

(171) Wakamiya, T.; Shimbo, K.; Sano, A.; Fukase, K.; Shiba, T. *Bull. Chem. Soc. Jpn.* **1983**, *56* (7), 2044.

(172) Fukase, K.; Wakamiya, T.; Shiba, T.; Shimbo, K.; Sano, A.; Fukase, K.; Shiba, T.; Wakamiya, T.; Shiba, T. *Bull. Chem. Soc. Jpn.* **1983**, *59* (7), 2505.

(173) Fukase, K.; Kitazawa, M.; Sano, A.; Shimbo, K.; Horimoto, S.; Fujita, H.; Kubo, A.; Wakamiya, T.; Shiba, T. *Bull. Chem. Soc. Jpn.* **1992**, *65* (8), 2227.

(174) Yu, Y.; Zhang, Q.; Van Der Donk, W. A. *Protein Sci.* **2013**, *22* (11), 1478.

(175) Repka, L. M.; Chekan, J. R.; Nair, S. K.; Van Der Donk, W. A. *Chem. Rev.* **2017**, *117* (8), 5457.

(176) Dischinger, J.; Chipalu, S.B.; Bierbaum, G. *Int. J. Medical Microbiol.* **2014**, *304* (1), 51.

(177) Chatterjee, C.; Patton, G. C.; Cooper, L.; Paul, M.; van der Donk, W. A. *Chem. Biol.* **2006**, *13* (10), 1109.

(178) Piper, C.; Cotter, P. D.; Ross, R. P.; Hill, C. *Curr. Drug Discov. Rechn.* **2009**, *6*, 1.

(179) Rink, R.; Kluskens, L. D.; Kuipers, A.; Driessen, A. J. M.; Kuipers, O. P.; Moll, G. N. *Biochemistry* **2007**, *46* (45), 13179.
(180) Lubelski, J.; Rink, R.; Khusainov, R.; Moll, G. N.; Kuipers, O. P. *Cell. Mol. Life Sci.* **2008**, *65* (3), 455.
(181) Moll, G.; Kuipers, A.; Rink, R. *Antonie Van Leeuwenhoek* **2010**, *97* (4), 319.
(182) Fukase, K.; Kitazawa, M.; Sano, A.; Shimbo, K.; Fujita, H.; Horimoto, S.; Wakamiya, T.; Shiba, T. *Tetrahedron Lett.* **1988**, *29* (7), 795.
(183) Liu, W.; Chan, A. S. H.; Liu, H.; Cochrane, S. A.; Vederas, J. C. *J. Am. Chem. Soc.* **2011**, *133* (36), 14216.
(184) Ross, A. C.; Liu, H.; Pattabiraman, V. R.; Vederas, J. C. *J. Am. Chem. Soc.* **2010**, *132* (2), 462.
(185) Knerr, P. J.; Van der Donk, W.A. *J. Am. Chem. Soc.* **2013**, *135* (19), 7094.
(186) Harpp, D. N.; Gleason, J. G. *J. Org. Chem.* **1971**, *36* (1), 73.
(187) Martin, N. I. *J. Org. Chem.* **2009**, *74* (2), 946.
(188) Bregant, S.; Tabor, A. B. *J. Org. Chem.* **2005**, *70* (7), 2430.
(189) Ongey, E. L.; Neubauer, P. *Microb. Cell Fact.* **2016**, *15* (1), 97/1.

Chapter 2:

Synthesis of Tricyclic Peptides via Strategy 1:

Aldehyde-Functionalized Scaffolds and Aminooxy Group Functionalized Peptides

2   Introduction

In our endeavors to synthesize tricyclic peptides via a scaffolded approach, we have decided to utilize the well-established CLiPS reaction, in combination with a second, orthogonal, oxime ligation reaction. In order to facilitate the ligation reactions between scaffold and peptide, they had to be equipped with the appropriate mutually reactive moieties.

Over the years, the CLiPS reaction has been optimized thoroughly, utilizing natural cysteines in peptides as the thiolate nucleophile source.[1] While many variations of scaffolds have been developed, they have always been based on a methylene-linked halogen electrophile, for example a benzylic bromide. For oxime ligation, however, there is no such precedent whether the best suited position of the electrophile or nucleophile is on the peptide or the scaffold. Oxime ligation has been described using peptides equipped with aminooxy groups on the side chain, as well as ketone or aldehyde functionalized peptides. This dual directionality of oxime ligation leaves two different strategies to be explored simultaneously.

Firstly, the peptide could be equipped with an aminooxy group, while the scaffold bears the electrophilic aldehyde. Secondly, the peptide could bear the electrophilic ketone or aldehyde, while the scaffold is equipped with the nucleophilic aminooxy group. For this chapter, peptide cyclization-ligation following the first strategy was explored. This strategy is characterized by a separation of the electrophiles and nucleophiles on the two reactive components. This entails 'all nucleophilic' peptides containing both cysteines for the CLiPS reactions and aminooxy groups for oxime ligation. Complimentary are the 'all electrophilic' scaffolds bearing the activated methylene bromide electrophile for the CLiPS reaction and an electrophilic aldehyde for oxime ligation. We have chosen for aldehydes instead of ketones to prevent the formation of the oximes as complex E/Z-mixtures. Due to their high reactivity, the aldehydes in the scaffold were protected as acid-labile acetals.

Earlier work has shown that the formation of regio-isomers in CLiPS cyclizations can be avoided by using symmetrical phenyl-ring centered scaffolds.[1,2] By maintaining the phenyl ring as the core for combined CLiPS/oxime scaffolds, it was synthetically challenging to include all desired reactivities in a symmetrical way. Instead, we have chosen a modular, convergent approach, whereby the parts carrying the two different ligation handles are synthesized separately, and joined in the final stages of scaffold synthesis.

Three scaffolds were designed for this strategy (Figure 2.1). The CLiPS handles were introduced at a phenyl ring as highly reactive benzylic or α-keto methylene bromides. The protected aldehydes for oxime ligation were introduced via bis(2,2-diethoxyethyl)amine as a rigid quaternary ammonium salt (T4-C1) or an amide (T4-C2 and T4-C3). The linkage of the CLiPS-part of the scaffold to the amine handle is a distinguishing feature of the scaffolds. It is noteworthy that the configurationally stable quaternary sp[3]-hybridized nitrogen atom in scaffold T4-C1 is a prochiral center. As a result, this can give rise to the formation of diastereomers, as the scaffold has a top and bottom face which become chemically inequivalent upon reaction with the peptide. Scaffolds T4-C2 and T4-C3 differ from T4-C1 by the presence of a flexible, rotatable amide linker between the CLiPS- and oxime-reactive moieties. This amide linker allows rotational relaxation, thus preventing the formation of structural isomers. Besides this important design feature, the amide group may also provide further stabilization of certain peptide conformations through hydrogen bonding as found earlier by Heinis *et al*.[3]

Scaffolds T4-C2 and T4-C3 mutually differ by the CLiPS-reactive parts, although both T4-C2 and T4-C3 contain the methylene bromides in *meta* orientation. T4-C3 is equipped with a short amide spacer between the aromatic core and the bromoacetamides.
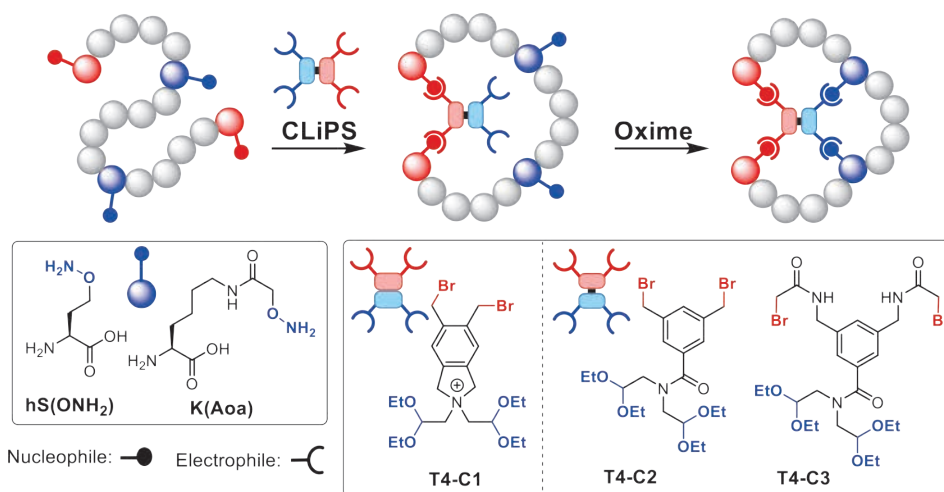
Figure 2.1: Synthesis of tricyclic peptides via CLiPS and oxime ligation via Strategy 1 (top), showing the reaction sequence and amino acids and scaffolds designed.

Cysteines will be installed in the peptides, delivering the nucleophilic sulfhydryl groups for the CLiPS reaction. For oxime ligation, installation of amino acids with an aminooxy group in the peptides is envisioned. For this, a commercially available lysine derivative featuring an aminooxy group in the side chain (K(Aoa)) was chosen. Furthermore, a homo-serine derived, aminooxy group containing amino acid, was selected (hS(ONH$_2$)) that has recently been described by Horne and co-workers.[4]

In this chapter, the synthesis of the scaffolds, aminooxy group functionalized amino acids and their introduction into peptides is described. Subsequently, a series of reactivity tests was conducted to establish whether these building blocks would be suitable for the synthesis of multicyclic peptides. From these results, a series of test peptides, varying in size, amino acid composition, and location of the functional residues was synthesized. With these peptides, the applicability of the CLiPS and oxime ligation cyclization sequence was investigated.

2.1 Scaffold Synthesis

2.1.1 Synthesis of Bis(2,2-diethoxyethyl)amine

Central to all scaffolds is an amine as a versatile nucleophilic handle containing two aldehydes for oxime ligation. For this, bis(2,2-diethoxyethyl)amine was chosen, of which the synthesis is shown in Scheme 2.1. Benzylamine was coupled twice with bromoacetaldehyde diethylacetal. Benzylamine was chosen as the starting amine to prevent over-alkylation, whereby the benzyl-group functioned as a protective group. In the next step, the benzyl group was removed in near-quantitative yield by Pd-catalyzed hydrogenolysis. As expected, bis(2,2-diethoxyethyl)amine proved to be bench-stable.
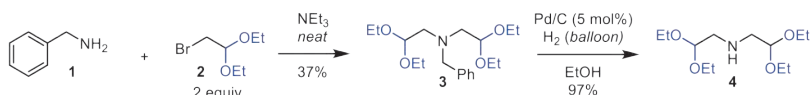
Scheme 2.1: Synthesis of the central amine 4 for the T4-C-scaffolds.

2.1.2 Synthesis of Scaffold T4-C1

To synthesize the first generation T4-C1 scaffold, bis(2,2-diethoxyethyl)amine was coupled to 1,2,4,5-tetrakis(bromomethyl)benzene (Scheme 2.2).[2] This symmetric bromide reacted twice with the same amine in *ortho* fashion, yielding scaffold T4-C1 in a single step. The conditions were chosen such that di-substitution was prevented. For this, a threefold excess of the bromide was present at high dilution, while the amine was added slowly to this solution. The final product was obtained after purification by column chromatography as a white foam. Scaffold T4-C1 contains a quaternary ammonium moiety with a permanent positive charge. The assumed bromide counter-ion was not detectable in high-resolution mass analysis.
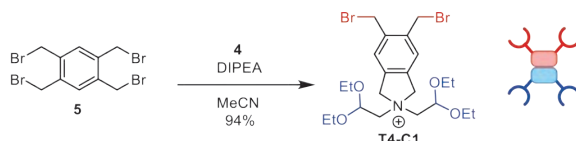
Scheme 2.2: Synthesis of scaffold T4-C1.

This scaffold proved unstable upon prolonged storage. After prolonged storage under N_2 atmosphere (over 4 months) in the fridge, the once white powder had become a sticky black wax. This was most likely due to the hygroscopic nature of the ammonium ion. As a result, a fresh batch of scaffold was prepared for each experiment to ensure a good quality of the scaffold, because the synthesis of scaffold T4-C1 requires a single step. In the UPLC-chromatogram (see Figure 2.2) freshly prepared T4-C1 is visible as a sharp peak at t_R 1.97 min, while the small peak at t_R 1.94 min emerges from a partially hydrolyzed acetal (loss of ethanol). It is most likely that this partial hydrolysis emerges from the slightly acidic aqueous conditions during the LCMS analysis.
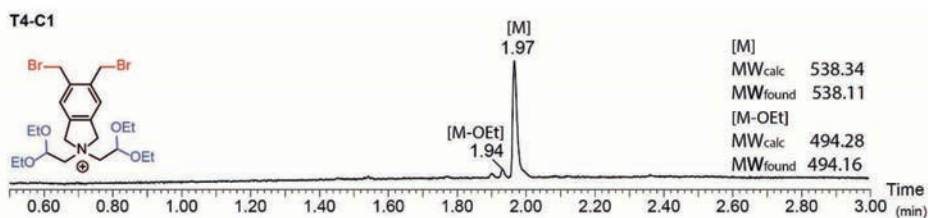
Figure 2.2: UPLC chromatogram of a solution of T4-C1.

The scaffold acetals showed good stability in aqueous solution at neutral pH. Instead, the bromides seemed more susceptible towards hydrolysis. About ~1% hydrolysis of the bromides was observed after 24 hours in aqueous solution, while acetal hydrolysis remained absent. Remarkably, extensive hydrolysis of the bromides was observed when liberating the aldehydes using 15% TFA , showing that oxime ligation cannot be performed prior to the CLiPS reaction.

2.1.3 Synthesis of Scaffolds T4-C2 and T4-C3

Both scaffolds T4-C2 and T4-C3 contain the flexible, rotatable amide linker between the CLiPS and oxime reactive parts and differ in the composition of the CLiPS reactive groups only. The syntheses of the structurally similar scaffolds T4-C2 and T4-C3 commenced from 3,5-dimethylbenzoic acid as the common starting material (Scheme 2.3).
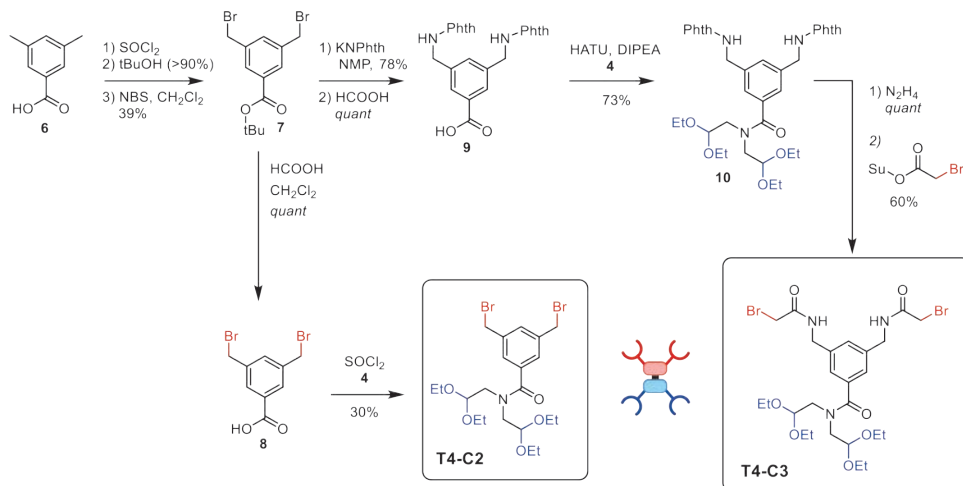
*Scheme 2.3: The synthesis of scaffolds T4-C2 and T4-C3, from the common starting material 3,5-dimethyl benzoic acid (**6**). Phth = phthalimide.*

The first step in the functionalization was protection of the acid as its *tert*-butyl ester. The methyl groups were brominated via radical bromination, using NBS as the bromide source.[5] The reaction was performed photochemically using a 500W halogen construction lamp, and the reaction was stopped after an hour. Because this reaction did not occur selectively, it was stopped when an optimum was found between residual starting material, conversion to desired product and formation of over-brominated products. The reaction was followed using ^{1}H NMR spectroscopy, as these compounds were difficult to separate using TLC analysis. With great difficulty we isolated the desired product by column chromatography. Fortunately, the desired dibrominated product was obtained as a crystalline solid, which was used as seed crystal for subsequent crystallizations from hexanes. As a result, crystallization was the purification method of choice, further obviating tedious column chromatography.

In order to obtain scaffold T4-C2, the *tert*-butyl ester **7** was cleaved by treatment with formic acid in CH_2Cl_2. The resulting acid was activated as an acid chloride, allowing selective coupling of amine **4** at this position only. The presence of the benzylic bromides forced us to use the highly reactive acid chloride, giving a kinetic advantage of amide bond formation over unwanted benzylic bromide substitution. Work-up required special care to prevent acetal hydrolysis arising from (long) exposure to acidic conditions to give scaffold T4-C2 in 30% isolated yield.

Unfortunately, halogen scrambling occurred when using this method, whereby a scaffold mixture was obtained contaminated with approximately 30% of chloride. This gave three compounds with different halogen compositions: dibromide, monochloride-monobromide, and dichloride containing scaffolds. As a consequence, characterization of the scaffold was more complicated. The product ratios were determined via ^{1}H NMR and ^{13}C NMR spectroscopy, while LC-MS measurements also revealed the halogen scrambling. Shown in Figure 2.3a is the UPLC chromatogram of scaffold T4-C2 obtained via the described procedure, showing the specific halogen composition of the scaffold mixture. All three different halogen products yielded distinct peaks (Table 2.1). The corresponding MS-spectrum of each compound is shown in Figure 2.4, along with the calculated spectra. The composition of the scaffold mixture did not change during acetal hydrolysis with a 15% TFA solution. Hydrolysis of the bromides and/or chlorides was not observed, instead the resulting mixture of aldehydes became more polar and eluted faster.
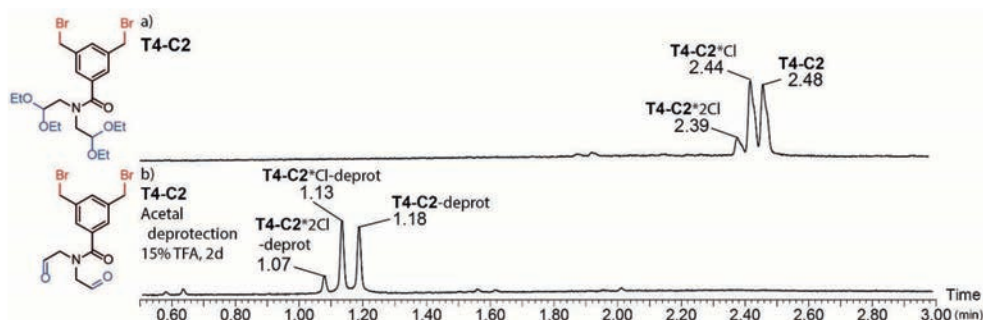
Figure 2.3: UPLC chromatograms of a) the T4-C2 scaffold, with the three peaks belonging to the Cl and Br mixtures. b) deprotected T4-C2 after 18h at rt with 15% TFA, again showing the bromide-chloride mixtures.

Table 2.1: Peak assignment for the UPLC chromatogram of the T4-C2 scaffold.

#	t_R (min)	Halides	m/z found	m/z calc.	Ionized species*	Fraction (%)
1	2.39	2x Cl	404.23	404.14	[M-OEt+H]$^+$	9.9
2	2.44	Cl+Br	450.14	450.09	[M-OEt+H]$^+$	44.4
3	2.48	2x Br	494.09	494.04	[M-OEt+H]$^+$	45.7

*This species forms in the mass spectrometer. The scaffold itself was obtained with the acetals intact.

Measured with UPLC
[T4-C2 - OEt + H]$^+$
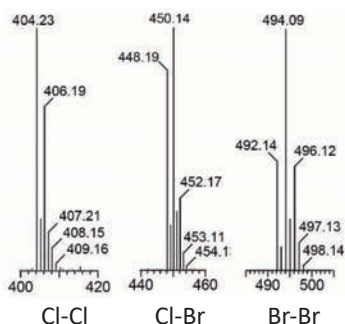
Predicted via MestReNova
[T4-C2 - OEt + H]$^+$
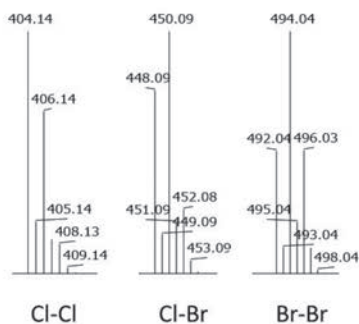
Figure 2.4: Experimental and theoretical mass spectra for the Cl-Cl, Cl-Br, Br-Br derivatives of the T4-C2 scaffold.

While analysis of T4-C2 was hampered by halogen scrambling, it could possibly also have consequences for the CLiPS reaction. The reactivity of chloride-bearing scaffolds is generally lower than the bromide equivalent, and therefore the mixture of halogens could have an effect on the CLiPS reactions. This will be further investigated during the test reactions as described in section 5.

Finally, scaffold T4-C3 was prepared from the common intermediate **7** (Scheme 2.3). This scaffold features a short linker to the bromacetamide functionalities, which was obtained after modification of the benzylic bromides. The first step was to substitute the benzylic bromides via a Gabriel synthesis using the potassium salt of phthalimide. With these phthalimide-protected amines in place, the acid was liberated from its *tert*-butyl

ester with formic acid. Next, the free benzoic acid was coupled with bis(2,2-diethoxyethyl)amine **4**.

As there were no other functional groups that needed consideration, a direct HATU mediated coupling was performed. The benzoic amide **10** was obtained in good yield (73%) and purity, without any sign of acetal hydrolysis. The benzylic amines were liberated by treatment with hydrazine, yielding the crude di-amine quantitatively, which was used without further purification. The bromides were introduced by reaction of the benzylic amines with bromoacetic acid N-hydroxysuccinimide ester.[6] Initially, bromoacetyl bromide was tested, but inferior results were obtained. The mild OSu reagent posed no risk of acetal deprotection, and the by-products were easily removed by extraction with water. Flash column chromatography yielded the T4-C3 scaffold as a white powder in 60% yield.

Even though the route towards T4-C3 was longer, the individual reaction steps were more robust, and purification of the intermediate compounds was facile. Therefore, scaffold T4-C3 was easier to obtain as compared to the T4-C2 analogue. The stability of T4-C3 in aqueous solution was very high, and hydrolysis of neither the bromides nor the acetals was found during prolonged aqueous solvation in neutral conditions (Figure 2.5a). Contrary to the other scaffolds, scaffold T4-C3 was completely stable upon storage over time. Similar to the T4-C2 scaffold, there was no problem in liberating the aldehydes in T4-C3. A solution of the scaffold was treated with 15% TFA, and within 18 hours, the acetals were hydrolyzed cleanly without affecting the bromides (Figure 2.5b).
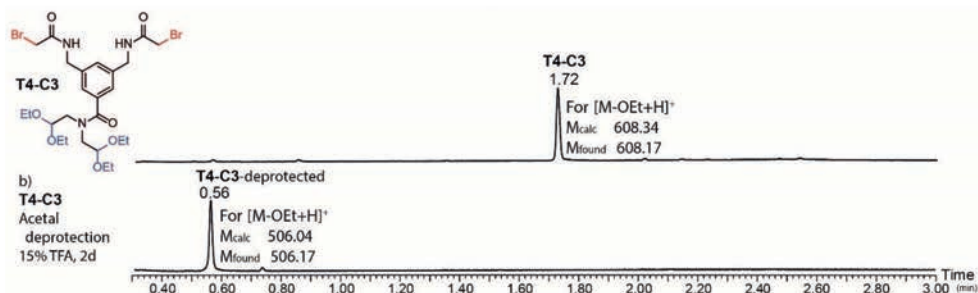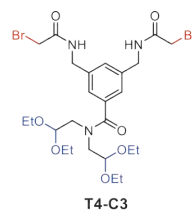
Figure 2.5: UPLC chromatograms of a) the T4-C3 scaffold, as a single peak at t_R 1.72 min. b) UPLC-chromatogram after acetal deprotection of T4-C3 with 15% TFA, yielding a single product at t_R 0.56 min.

2.2   Synthesis of Aminooxy-Functionalized Amino Acids K(Aoa) and hS(ONH₂)

As mentioned in the introduction, we selected an aminooxy-substituted lysine derivative (K(Aoa)) and *homo*-serine derivative (hS(ONH$_2$)) as the aminooxy moiety containing amino acids. During SPPS, the aminooxy side-chain was Boc-protected, as this group is easily introduced and shows a higher stability than other, bulkier, and commonly used aminooxy protective groups. After SPPS, the protective groups were cleaved during the resin/cleavage and global deprotection of the peptide, yielding peptides with the liberated and intact aminooxy group.

Bis-Boc protected Fmoc-K(Aoa)-OH is commercially available, even though quite expensive.[7] The lysine contains a longer side-chain than the usual amino acids, which may have an effect on the outcome of the oxime-type cyclization reactions.
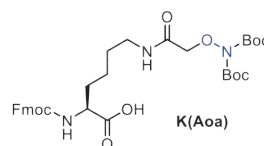
The second amino acid used was *homo*-serine derived Fmoc-hS(ONHBoc)-OH. For this, Fmoc-hS had to be synthesized first. Starting from Fmoc-D(OtBu)-OH, some protective group interchanging steps were performed to arrive at Fmoc-D(OH)-OBn (Scheme 2.4). Then, the *homo*-serine derivative was made by borane-mediated reduction of the side-chain carboxylic acid, yielding Fmoc-hS(OH)-OBn in quantitative yield. For installation of the aminooxy moiety to arrive at **14**, the Mitsunobu reaction was performed using *bis*-Boc hydroxylamine. As a precaution, one Boc-group was subsequently removed, as the second Boc-group is quite loosely attached and can be transferred easily to another nucleophile. This is relevant as during Fmoc-cleavage, a free amine is created in close proximity and hence can be subject to a Boc-transfer. The final step was hydrogenolysis to cleave the benzylic ester, yielding the free carboxylic acid, ready for SPPS.
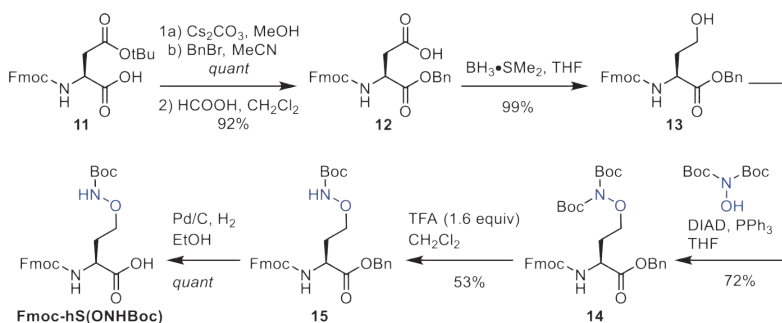
Scheme 2.4: Synthesis of Fmoc-hS(ONHBoc).

2.3   Peptide Synthesis

With the aminooxy-containing Fmoc-protected amino acids in hand, a set of peptides was prepared to study the scope of the cyclization reactions. The peptides were varied in length, amino acid composition, and type of aminooxy amino acid (see Table 2.2). To facilitate ionization in the mass spectrometer, all peptides were designed to contain at least one lysine residue. In addition, one phenylalanine residue was installed to ensure good UV-absorption for spectroscopic detection. Moreover, polarity-wise all peptides were fairly balanced with a very polar residue counterbalanced by a non-polar residue. Structure-inducing residues, such as proline, were used only for the longest peptides in the series. Methionine was omitted from this screening, as it can be disruptive in the CLiPS reaction. Cysteine and the aminooxy amino acids were regarded as functional amino acids and were only included with the purpose of reacting with the scaffolds. They were placed at the termini, or in the middle of the peptide. All peptide 'loops', *i.e.* the space between functional residues, were equally sized, resulting in 3, 4 or 5 amino acids per loop.

Since the peptide sequences are quite complex and contain a lot of information, we devised an appropriate and logical nomenclature and coding strategy. In this way, the characteristic features of the peptides can be read from the name. The code starts with a unique number (see Table 2.2). Next, the type of aminooxy amino acid is specified (either hS(ONH$_2$) or K(Aoa)) and, in superscript, its position within the sequence is defined ([ter] denotes 'terminal', [int] denotes 'internal'. Finally, the peptide loop size (n=3,4, or 5) is added as [n3], [n4] or [n5]. Using this coding logic, the most vital features of the peptide are denoted, making referral easier without having to look up the sequence. Some examples are given in Figure 2.6. The nomenclature code will further be expanded when peptide cyclization reactions are discussed (paragraph 2.5).

Table 2.2: Peptides prepared under strategy 1, containing aminooxy amino acids hS(ONH$_2$) and K(Aoa).

Code	Sequence
1-hS(ONH$_2$)^{int,n3}	Ac-**CEQF**{**hS(ONH$_2$)**}**AKF**{**hS(ONH$_2$)**}**LKNC**-NH$_2$
2-hS(ONH$_2$)^{int,n3}	Ac-**CEWF**{**hS(ONH$_2$)**}SIK{**hS(ONH$_2$)**}LKG**C**-NH$_2$
3-hS(ONH$_2$)^{int,n3}	Ac-<u>A</u>**CEWF**{**hS(ONH$_2$)**}SIK{**hS(ONH$_2$)**}LKGC<u>A</u>-NH$_2$
4-hS(ONH$_2$)^{ter,n3} *****	Ac-{**hS(ONH$_2$)**}EWFCSIKCLKG{**hS(ONH$_2$)**}-NH$_2$
5-hS(ONH$_2$)^{ter,n3}	Ac-<u>A</u>{**hS(ONH$_2$)**}EWFCSIKCLKG{**hS(ONH$_2$)**}<u>A</u>-NH$_2$
6-hS(ONH$_2$)^{int,n4}	Ac-**CERKF**{**hS(ONH$_2$)**}SGAV{**hS(ONH$_2$)**}KLYS**C**-NH$_2$
7-hS(ONH$_2$)^{int,n4}	Ac-<u>A</u>**CERKF**{**hS(ONH$_2$)**}SGAV{**hS(ONH$_2$)**}KLYS**C**<u>A</u>-NH$_2$
8-hS(ONH$_2$)^{ter,n4} *****	Ac-{**hS(ONH$_2$)**}ERKFCSGAVCKLYS{**hS(ONH$_2$)**}-NH$_2$
9-hS(ONH$_2$)^{ter,n4}	Ac-<u>A</u>{**hS(ONH$_2$)**}ERKFCSGAVCKLYS{**hS(ONH$_2$)**}<u>A</u>-NH$_2$
10-hS(ONH$_2$)^{int,n5}	Ac-**CEQFRK**{**hS(ONH$_2$)**}TPVKI{**hS(ONH$_2$)**}SRAYG**C**-NH$_2$
11-hS(ONH$_2$)^{ter,n5}	Ac-{**hS(ONH$_2$)**}EQFRK**C**TPVKI**C**SRAYG{**hS(ONH$_2$)**}-NH$_2$
12-K(Aoa)^{int,n3}	Ac-**CEQS**{**K(Aoa)**}**AKF**{**K(Aoa)**}YKN**C**-NH$_2$
13-K(Aoa)^{ter,n3}	Ac-{**K(Aoa)**}EQF**C**AKF**C**LKN{**K(Aoa)**}-NH$_2$
14-K(Aoa)^{int,n4}	Ac-**CERKF**{**K(Aoa)**}SGAV{**K(Aoa)**}KLYS**C**-NH$_2$
15-K(Aoa)^{ter,n4}	Ac-{**K(Aoa)**}ERKF**C**SGAV**C**KLYS{**K(Aoa)**}-NH$_2$
16-K(Aoa)^{int,n5}	Ac-**CEQFRK**{**K(Aoa)**}TPVKI{**K(Aoa)**}SRAYG**C**-NH$_2$
17-K(Aoa)^{ter,n5}	Ac-{**K(Aoa)**}EQFRK**C**TPVKI**C**SRAYG{**K(Aoa)**}-NH$_2$

* synthesis of this peptide was not successful due to deletions of hS(ONH$_2$).

2-hS(ONH$_2$)^{int,n3} **11**-hS(ONH$_2$)^{ter,n5} **12**-K(Aoa)^{int,n3} **15**-K(Aoa)^{ter,n4}
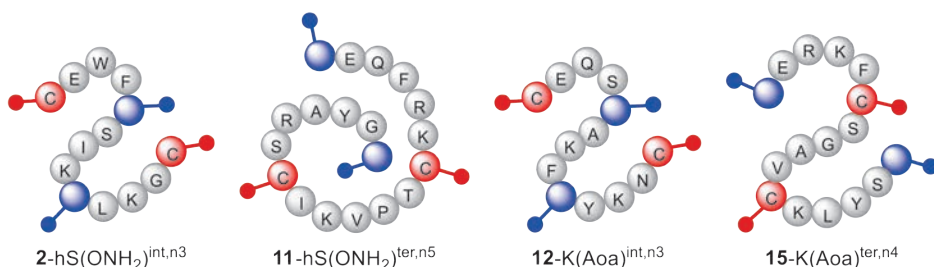
Figure 2.6: Examples of synthesized peptides and their codes.

The synthesis of the peptides was performed by automated SPPS using a Tentagel Rink-amide resin and standard HATU-mediated coupling conditions (see Experimental Section). The most common observation was that for all peptides the yields after purification were rather low (Table 2.3). This could be attributed to the often-poor quality of the crude peptides. The aminooxy moiety was not fully inert during synthesis and gave side reactions. As a consequence, most peptides needed multiple purifications to obtain purities of >90%.

Generally, the crude peptides were present in complex mixtures. In some cases, the desired peptide content was only 10%. LCMS analysis indicated loss of the aminooxy (-ONH$_2$) moiety. Cleavage of the O-N bond and deletions of the aminooxy amino acid were found as the most common side-reactions. Deletions of hS(ONH$_2$) at the termini were quite common, and two peptides (**4**-hS(ONH$_2$)^{ter,n3} and **8**-hS(ONH$_2$)^{ter,n4}) could therefore not be obtained. Addition of an alanine residue at the termini alleviated this problem, and peptides **6**-hS(ONH$_2$)^{ter,n3} and **9**-hS(ONH$_2$)^{ter,n4} were obtained successfully.

The aforementioned difficulties were less prevalent when the side chain extended K(Aoa) residue was incorporated. Deletions of K(Aoa) at the termini were not detected. Additionally, it was believed that the double Boc-protection on the aminooxy moiety protects better against side-reactions.

Table 2.3: Properties of Strategy-1 peptides, including retention times, MWs and yields.

Code	t_R (min)*	MW found	MW calc	Yield
1-hS(ONH$_2$)$^{\text{int,n3}}$	0.89	1604.21	1604.18	L$^{\#}$
2-hS(ONH$_2$)$^{\text{int,n3}}$	1.14	1588.52	1588.18	L$^{\#}$
3-hS(ONH$_2$)$^{\text{int,n3}}$	1.16	1729.28	1729.36	M$^{\#}$
4-hS(ONH$_2$)$^{\text{ter,n3}}$	-	-	1587.18	- ^
5-hS(ONH$_2$)$^{\text{ter,n3}}$	1.07	1729.17	1729.36	L$^{\#}$
6-hS(ONH$_2$)$^{\text{int,n4}}$	0.77	1864.42	1864.50	L$^{\#}$
7-hS(ONH$_2$)$^{\text{int,n4}}$	0.81	2006.82	2006.68	L$^{\#}$
8-hS(ONH$_2$)$^{\text{ter,n4}}$	-	-	1864.50	- ^
9-hS(ONH$_2$)$^{\text{ter,n4}}$	0.84	2006.62	2006.68	L$^{\#}$
10-hS(ONH$_2$)$^{\text{int,n5}}$	0.71	2260.01	2259.99	H$^{\#}$
11-hS(ONH$_2$)$^{\text{ter,n5}}$	0.76	2260.11	2259.99	L$^{\#}$
12-K(Aoa)$^{\text{int,n3}}$	0.66	1774.64	1774.38	L$^{\#}$
13-K(Aoa)$^{\text{ter,n3}}$	0.95	1764.53	1764.29	M
14-K(Aoa)$^{\text{int,n4}}$	0.88	2034.13	2034.70	L$^{\#}$
15-K(Aoa)$^{\text{ter,n4}}$	0.86	2034.59	2034.70	L$^{\#}$
16-K(Aoa)$^{\text{int,n5}}$	0.79	2430.46	2430.19	M
17-K(Aoa)$^{\text{ter,n5}}$	0.78	2430.41	2430.19	M

*t_R as measured on UPLC. Peptides were synthesized on Tentagel Rink amide resin. Yield after purification: Low (L), 1-5%, Moderate (M), 5-20%, Good (G), 20-35%, High (H), 35-50%. $^{\#}$The peptide required 2 purifications. ^Synthesis of the peptide was not successful due to deletions of hS(ONH$_2$).

A further side-reaction with the free aminooxy groups that readily occurred was oxime formation with acetone. This isopropylidene adduct formation was often inevitable during lyophilizing due to the presence of trace amounts of acetone. It is therefore advisable to abstain from cleaning glassware with acetone, in favor of ethanol. However, technical grade ethanol also contains traces of acetone, so caution is advised. For the same reason, the use of pseudoprolines that release acetone upon hydrolysis should be avoided in the sequence. Even another lyophilizer flask on the same vacuum pump, that contains traces of acetone, may give extensive isopropylidine formation.

In principle, the formation of the acetone adduct is reversible. However, after extensive investigation into such trans-oximation reactions with, for example, methoxyamine to liberate the aminooxy moiety, complex mixtures were obtained. Obviously, by avoiding every possibility for acetone adduct formation, the best results were obtained.

2.4 Model Studies

In this section, the initial reactivity tests of the scaffolds are described. These experiments included the reactivity of cysteine derived sulfhydryl nucleophiles in CLiPS reactions. Additionally, the feasibility for oxime ligation was tested. This started with removal of the acetal protective groups and reaction of the liberated aldehydes with aminooxy groups. Both the un-CLiPSed and CLiPSed scaffolds were tested, to ensure full compatibility to the cyclization systems.

For the consecutive CLiPS and oxime ligation reactions, the naming code was expanded. Once a peptide is CLiPSed with a scaffold, it is now a construct of a peptide *onto* a scaffold, denoted **peptide** ∩ *scaffold*. Whether it is CLiPSed or oximed, can be found in superscript of the scaffold as T4$^{\text{C}}$ for CLiPSed or T4$^{\text{C/O}}$ for CLiPSed *and* oximed. For the test reactions, intermolecular oxime ligations were tested with methoxyamine. The aminooxy group are therefore specified in the name, for example T4$^{\text{C/O (MeONH}_2\text{)}}$.

2.4.1 Test-reactions with Scaffold T4-C1

The CLiPS reactivity of T4-C1 towards thiol species was tested using the natural tripeptide glutathione (GSH). This tripeptide consists of the amino acid residues glutamate, cysteine and glycine linked by an isopeptide bond of the glutamate side chain to the cysteine amine and a natural peptide linkage to glycine. As observed for thiols in general, GSH is readily oxidized to the disulfide. Because CLiPS reactions have been described thoroughly in literature, the optimal conditions were used.[1–3] These typically consist of using an 0.5 mM solution of peptide in a 1:1 MeCN/MilliQ-H_2O solvent mixture, after which the pH is adjusted to 8 by addition of a 1M NH_4HCO_3 solution.

It was expected that by using 2 equiv of GSH with respect to scaffold T4-C1, the CLiPS reaction would be forced to completion. However, this was not the case. Instead, the mono-substituted product was observed as the main product.[8] It turned out that the thioether reacted with the remaining bromide to form a cyclic 5-membered sulfonium ion as the major side-product. This unwanted intramolecular reaction could only be suppressed by addition of a large excess of GSH (>10 equiv, usually 20). The intermolecular reactions could also be forced to completion by application of higher concentrations.

Figure 2.7 shows the outcome of the reaction of T4-C1 with 20 equiv of GSH, where the CLiPSed product GSH∩T4-C1^C was observed at a t_R of 0.93 min. When fewer equivalents of GSH were added, the sulfonium ion containing mono-CLiPSed side product was obtained as well (**16**). As the native T4-C1 scaffold suffered from hydrolysis of the bromides before acetal hydrolysis, it was tested whether the acetals could be hydrolyzed after the CLiPS reactions. Therefore, an aqueous 15% TFA-solution was added to GSH∩T4-C1^C, and the reaction was monitored by LC-MS analysis. Remarkably, acetal-to-aldehyde conversion was not observed, not even upon standing for a week. Most likely, the presence of the electron-withdrawing positively charged ammonium species inhibits

*GSH-sulfonium ion **16***

formation of the cationic intermediate that is needed for hydrolysis of the acetal. This indicates that this scaffold, although suitable for CLiPS reactions, is not suitable for oxime ligation.

Figure 2.7: UPLC chromatogram after completion of the CLiPS reaction between T4-C1 and GSH.

2.4.2 Test-reactions with Scaffold T4-C2

In contrast to scaffold T4-C1, the diethyl acetals in scaffold T4-C2 are in a non-charged environment. This facilitates hydrolysis of the acetals, as was shown in Figure 2.3 in the synthesis section. Scaffold T4-C2 was obtained as a mixture of halides and this could affect the outcome of the CLiPS reaction, because of the lower reactivity of chlorides compared to bromides. At first, the reactivity of T4-C2 with glutathione was tested. Even when using 20 equiv of GSH, the CLiPS reaction did not reach full conversion, and nearly 30% of the mono-CLiPSed product was obtained as well (Figure 2.8). Indeed, the chloride proved to be less reactive, as seen by the presence of T4-C2 di-chloride analogue after 30 min of

reaction time (t_R 2.42 min). The mono-CLiPS product reacted slowly to the double CLiPS product. Even after 3 days, still about 25% of the methylene chlorides were left.
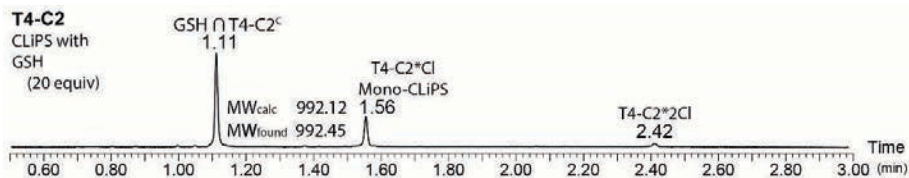

Figure 2.8: UPLC chromatogram of the CLiPS reaction between T4-C2 and GSH, with peaks assigned.

The lower reactivity of the chloride could potentially be of concern for peptide cyclization via CLiPS reactions. If the intramolecular reaction with the chloride is slower than the intermolecular reaction with another bromide, undesired oligomerization might occur. Therefore, CLiPS cyclization was tested with peptide **m1** (Ac-CEFAFKC-NH$_2$) which does not contain any oxime handle. First of all, it was shown that the CLiPS reaction occurred readily, without any trace of oligomerization or incomplete reaction (Figure 2.9a). **m1**∩T4-C2^c was found at t_R 1.64 min, although there was a trace of the linear peptide and its disulfide (at t_R 1.10 and 1.05 min, respectively). This reaction proved that the intramolecular nature of the CLiPS reaction in our system was not impaired by the mixed halogen content of the scaffold. Therefore, issues with further CLiPS cyclizations were not expected.

Next, the acetals were hydrolyzed, yielding **m1**∩T4-C2$^{C\text{-deprotect}}$ at t_R 1.02 min (Figure 2.9b). During this reaction, the majority of the remaining excess of peptide **m1** was converted to the disulfide. Upon addition of MeONH$_2$, the di-aldehyde reacted smoothly, yielding **m1**∩T4-C2$^{C/O\,(MeONH_2)}$ as a single product eluting at t_R 1.35 min (Figure 2.9c). This reaction sequence proved that the T4-C2 scaffold is compatible with the conditions that are required for a one-pot CLiPS/oxime reaction.
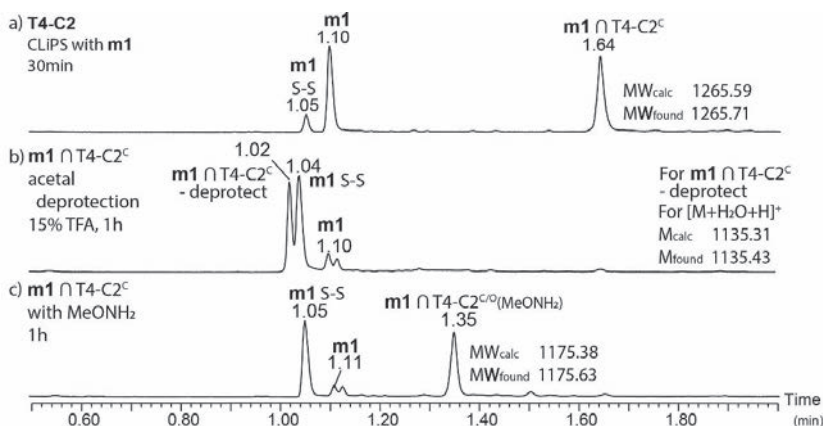

*Figure 2.9: UPLC chromatograms of the CLiPS/deprotection/oxime reaction sequence between T4-C2 and **m1** with a) showing the CLiPS reaction, b) the acetal deprotection, yielding the dialdehyde, and c) the oxime ligation with MeONH$_2$.*

This concludes the reactivity tests with scaffold T4-C2. While the halogen mixture with different reactivities was unfavorable in the intermolecular CLiPS reaction with the mono-cysteine source GSH, cyclization of a peptide containing two cysteines (**m1**) proceeded smoothly. Hydrolysis of the diethyl acetals occurred cleanly under mildly acidic conditions.

Oxime ligation occurred instantaneously after the addition of methoxyamine, which proved the scaffold displays the desired reactivity towards both the CLiPS and oxime ligation reactions.

2.4.3 Test-reactions with Scaffold T4-C3

To test its reactivity in the CLiPS reaction, scaffold T4-C3 was also reacted with GSH. In contrast to the other two scaffolds, T4-C3 reacted cleanly when using only a slight excess (2.1 equiv) of GSH, to obtain GSH∩T4-C3^C quantitatively (Figure 2.10a).
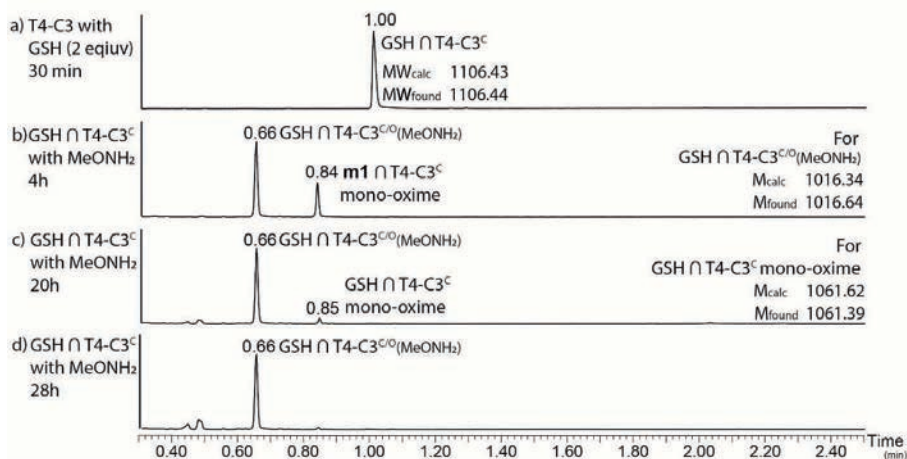

Figure 2.10: UPLC chromatograms of the reaction between a) T4-C3 and GSH, and the subsequent reaction between GSH∩T4-C3^C with MeONH₂ under acidic conditions at b) 4h, c) 20h and d) 28h.

After reaction with GSH, a one-pot consecutive aldehyde liberation/oxime ligation was attempted with methoxyamine·HCl (Figure 2.10b-d). Therefore, a 5M solution of MeONH₂·HCl was added, which coincidentally lowered the pH to 4, whereby no additional pH adjustment for acetal hydrolysis and oxime ligation was required. The mono-oxime, with the other acetal still intact, elutes at t_R 0.84 min. Over time, this peak disappeared, yielding the double oxime at t_R 0.66 min. This one-pot reaction sequence proceeded cleanly and at a reasonable reaction rate, proving the compatibility of acetal hydrolysis coinciding with oxime ligation.

   With the CLiPS/oxime reaction sequence shown intermolecularly, this was repeated with model peptide **m1** (Ac-CEFAFKC-NH₂). As expected, a single product **m1∩T4-C3^C** was obtained (Figure 2.11a). A trace of disulfide was present at t_R 1.05 min. Hereafter, the aldehydes were liberated by treatment with a 15% TFA solution, after which **m1∩T4-C3$^{C\text{-deprotect}}$** showed the expected increase in polarity, shifting to t_R 0.93 min (Figure 2.11b). The peak appeared as a 'shouldered peak', as the dialdehyde was also present in its mono-hydrate form. A very small trace of mono-aldehyde was present at t_R 1.19 min. After methoxyamine was added, **m1∩T4-C3$^{C/O(\text{MeONH}_2)}$** was formed immediately as the sole product (Figure 2.11c).

   To conclude, the T4-C3 scaffold showed good reactivity in the CLiPS test reactions, as well as in the subsequent liberation of the aldehydes and oxime ligation with methoxyamine. With all three scaffolds tested, T4-C1 was dismissed for further reactions as the aldehyde cannot be liberated. Therefore, peptide cyclization reactions were continued with scaffolds T4-C2 and T4-C3.
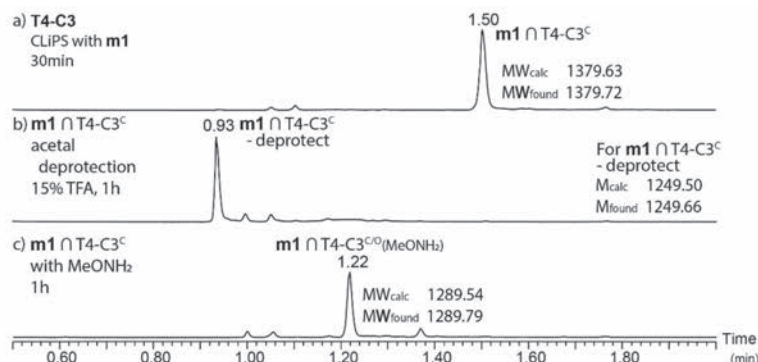
*Figure 2.11: UPLC chromatogram of the CLiPS/oxime reaction sequence for the T4-C3 scaffold with model peptide **m1**, with a) the CLiPS reaction, b) the liberation of scaffold aldehydes and c) the reaction with MeONH₂.*

2.5 Peptide Cyclizations

After *i*) the scaffold synthesis, *ii*) aminooxy-functionalized amino acid synthesis, *iii*) peptide synthesis, and *iv*) testing all individual reaction steps, the scene was set for the cyclizations towards the tricyclic peptidic architectures. In Scheme 2.5, the example is given for the cyclization reaction for **2**-hS(ONH₂)^{int,n3} with scaffold T4-C3, yielding **2**-hS(ONH₂)^{int,n3}∩T4-C3$^{C/O}$.
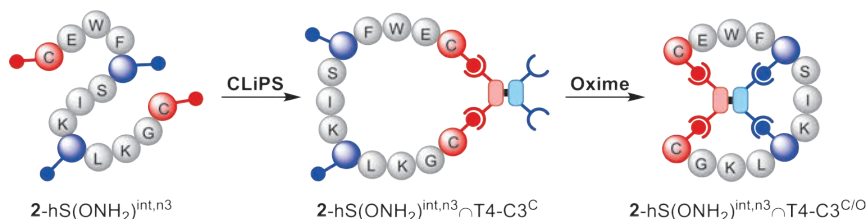
*Scheme 2.5: The schematic synthesis of the tricyclic peptide from **2**-hS(ONH₂)^{int,n3} and T4-C3.*

Because in previous research the optimal conditions for the initial CLiPS reaction had been established, this was not further investigated.[1–3] At first, optimization of the cyclization conditions will be discussed, followed by the cyclization reactions with hS(ONH₂)-containing peptides. Next, our investigations with K(Aoa) peptides are described, to illustrate the effect of amino acid size on the cyclization results.

2.5.1 Optimization of the One-pot Acetal Hydrolysis and Oxime Ligation Conditions

During the test-reactions with the T4-C scaffolds as described above, the liberation of the aldehydes was studied, using quite harsh conditions with TFA solutions. The conditions were not fully optimized in that stage, as these reactions were merely proof-of-principle. Therefore, the liberation conditions were tested for peptide **12**-K(Aoa)^{int,n3} with scaffold T4-C3. After liberation of the aldehydes, oxime ligation should follow, yielding the tricyclic peptide construct. As catalysts for acetal hydrolysis, several acids were tested, which are presented in Table 2.4. In this study, we only focused on aldehyde liberation and whether these conditions were suitable also for the subsequent oxime ligations. Although commonly used in oxime ligation,[9] the use of additives and additional catalysts was not tested for these reactions.

Acetate buffers are commonly used for oxime ligation.[10–12] For our system, however, the acetals were completely stable upon standing in acetate buffers (pH 4) using MeCN/MilliQ-H_2O (1:1) as the solvent. Even upon treatment with up to 1.0 M HOAc (entries 1 and 2), the acetals remained intact for 5 days. Also with formic acid, which has a lower pK_a than HOAc, deprotection was not observed, not even after 5 days. The same was true for citric acid, which is another commonly used buffer component in oxime ligation reactions. Compared to TFA, HCl is not commonly used in peptide chemistry. However, when using 1M of HCl, conversion to **12**-K(Aoa)^{int,n3}∩T4-C3$^{C/O}$ reached completion within a day. When lowering the concentration to 0.1M, the reaction slowed down, yielding only the mono-oxime after a day. Finally, TFA was tested at different concentrations. After addition of a 2.5% TFA solution to the CLiPS mixture, deprotection did not occur. When using a 5% TFA solution, traces of the mono-oxime were still observed after 2 days. By using a 10% solution of TFA, complete conversion to **12**-K(Aoa)^{int,n3}∩T4-C3$^{C/O}$ was observed after standing overnight. In order to reach full conversion within a day, a 15% solution of TFA proved to be optimal. It was therefore decided to use TFA as the acid in further reactions.

*Table 2.4: Screening of different acids to liberate the aldehyde function in **12**-K(Aoa)^{int,n3}∩T4-C3^C for oxime ligation.*

#	Acid	pKa	Conc.*	Time (d)	Result #
1	HOAc	4.75	0.2 M	5	n.r.
2	HOAc	4.75	1.0 M	5	n.r.
3	Formic acid	3.75	1.0 M	5	n.r.
4	Citric acid	3.08	1.0 M	5	n.r.
5	HCl	< 1	1.0 M	1	Full conversion
6	HCl	< 1	0.1 M	4	Full conversion to mono-oxime
7	TFA	0.23	2.5%	2	n.r.
8	TFA	0.23	5%	2	Trace of mono oxime
9	TFA	0.23	10%	1	80% conversion
10	TFA	0.23	15%	1	Full conversion

*In glass vial (5 mL), peptide (0.2 mg) was dissolved in MeCN/MilliQ-H_2O (1:1, 0.5 mM). Scaffold (1.0 equiv) was added mixture was adjusted to pH 8 with a 1M NH_4HCO_3 solution. After completion, acid solution (50µL) was added to mixture. Analysis was stopped after 5d of reaction.
#Conversion to tricyclic **12**-K(Aoa)^{int,n3}∩T4-C3$^{C/O}$ was noted, unless other species are specified.

With the optimal acid in hand, several solvent mixtures were tested to further optimize the cyclization conditions. Peptide **12**-K(Aoa)^{int,n3} was again used as the test-peptide in reaction with T4-C3, and several aqueous solvent mixtures were screened, with MeCN, DMF and DMSO as the organic component. The CLiPS reaction yielded no discernable difference for the tested solvent mixtures, all yielding **12**-K(Aoa)^{int,n3}∩T4-C3^C cleanly in full conversion. In contrast, the oxime ligation reaction gave very different results (see Table 2. 5). In the previous experiments, although the 'standard' solvent mixture of MeCN/MilliQ-H_2O (1:1) gave full conversion to the oximes, signs of oligomerization were observed in the UPLC chromatogram (entry 1). The other tested solvent mixtures using DMSO and DMF as the organic co-solvent, were chosen for their ability to disrupt hydrogen bonding (chaotropic), enforcing better solvation of the peptide. DMF mixtures of both a 1:1 and 2:1 ratio with water (entries 2 and 3) did not yield full conversion towards the oximes in the considered timeframe. A higher ratio of organic solvent had a detrimental effect on the oxime ligation. Adding urea, a well-known anti-aggregation salt, as the aqueous component stopped the oxime ligation reaction completely, regardless of the use of co-solvent (entries 4 and 7). DMSO provided the best results, but only if it was used in a 1:1 ratio. Higher ratios of DMSO were detrimental to the oxime ligation reaction. Therefore, all other cyclization reactions that were performed used aqueous DMSO (in 1:1 ratio), as the solvent and 15% TFA solution as the acid catalyst unless specified otherwise.

Table 2. 5: Aqueous solvent mixtures tested for the oxime ligation to yield 12-K(Aoa)^{int,n3}∩T4-C3$^{C/O}$.

#	Composition			Ratio	Conv (%)*	Comments
1	MeCN	:	H_2O	1:1	100	Trace of oligomerization
2	DMF	:	H_2O	1:1	90	
3	DMF	:	H_2O	2:1	50	
4	DMF	:	8M Urea	1:1	0	No reaction
5	DMSO	:	H_2O	1:1	100	Best
6	DMSO	:	H_2O	2:1	80	
7	MeCN	:	8M Urea	1:1	0	No reaction

* *The reaction mixture was analyzed 16h after adding 15% TFA solution, initiating oxime ligation.*

2.5.2 hS(ONH₂) Cyclizations

With the optimized conditions in hand, the nine successfully prepared hS(ONH$_2$)-containing peptides **1-3**, **5-7** and **9-11** were transformed to the corresponding tricycles using scaffolds T4-C2 and T4-C3. For all peptide and scaffold combinations, the monocyclic CLiPSed intermediate product was obtained as a single peak in the UPLC trace. The first results of the subsequent oxime ligation cyclizations of the hS(ONH$_2$) n=3 peptides are shown in Figure 2.12. For peptide **1**-hS(ONH$_2$)^{int,n3}, only the cyclization with scaffold T4-C3 was performed. Two products were obtained with a mass corresponding to the tricyclic peptide construct (calc. 1911.50, found 1911.31 and 1911.47) (Figure 2.12a). UPLC-MS analysis of the cyclization of peptide **2**-hS(ONH$_2$)^{int,n3} onto scaffold T4-C3 also showed the formation of two products with the same mass (Figure 2.12c). When the more apolar scaffold T4-C2 was used (Figure 2.12b) to constrain peptide **2**-hS(ONH$_2$)^{int,n3}, the products eluted closer together, appearing as a shouldered peak. Peptide **3**-hS(ONH$_2$)^{int,n3} contains an additional alanine at both termini, next to the terminal cysteines. After cyclization of **3**-hS(ONH$_2$)^{int,n3} with scaffold T4-C3, again two product peaks were found in the UPLC-MS chromatogram (Figure 2.12e). For **3**-hS(ONH$_2$)^{int,n3}∩T4-C2$^{C/O}$ a single peak was obtained in the UPLC-chromatogram, without the extra shoulder (Figure 2.12d).
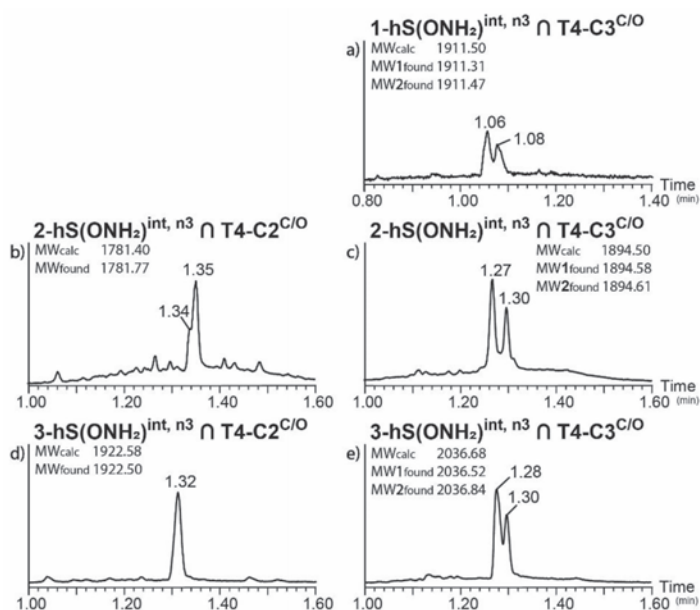

Figure 2.12: UPLC chromatograms of tricyclic peptides of hS(ONH$_2$) with loopsize n=3, for both T4-C2 and T4-C3 scaffolds. Product MW's are denoted in chronological order of encounter.

At this point, we wanted to take a closer look at the origin of the multiple tricyclic peptide products. Our assumption was that these products are rotameric in origin. Because aldehydes were used as the starting carbonyl moieties, *E/Z* isomerism of the resulting oxime linkage is unlikely. By separating and isolating the individual products, additional information about the origin of these multiple products was obtained. For this, the synthesis of **2**-hS(ONH$_2$)^{int,n3}∩T4-C3$^{C/O}$ was repeated on a preparative scale. Starting from peptide **2**-hS(ONH$_2$)^{int,n3} (Figure 2.13a), the CLiPS reaction afforded macrocycle **2**-hS(ONH$_2$)^{int,n3}∩T4-C3^C (Figure 2.13b). Then, a 15% TFA solution was added to liberate the scaffold aldehydes, followed by instantaneous oxime ligation to yield two tricyclic peptide products **2**-hS(ONH$_2$)^{int,n3}∩T4-C3$^{C/O}$ (Figure 2.13c) at t_R 1.27 and t_R 1.30 min in roughly a 3:2 ratio.
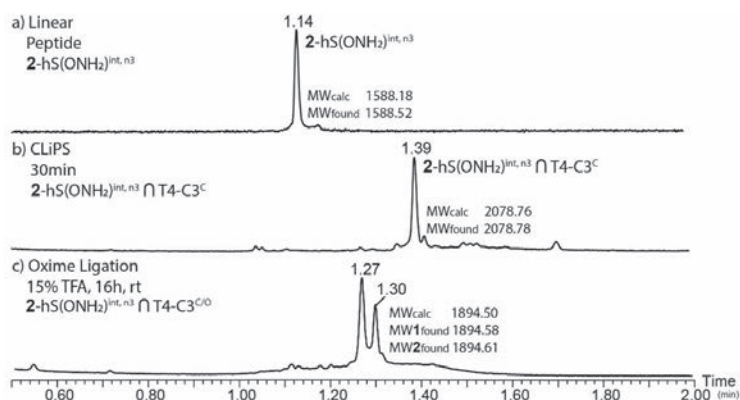
Figure 2.13: UPLC chromatograms of the CLiPS and oxime reactions with peptide
***2**-hS(ONH$_2$)^{int,n3} and scaffold T4-C3, where a) shows the linear peptide **2**-hS(ONH$_2$)^{int,n3}, b)*
*CLiPSed **2**-hS(ONH$_2$)^{int,n3}∩T4-C3^C and c) tricycles for **2**-hS(ONH$_2$)^{int,n3}∩T4-C3$^{C/O}$.*

These tricyclic oxime products were separated by preparative reversed-phase HPLC. However, UPLC-MS analysis of the collected fractions again showed the presence of the two products in the same ratio as before the separation (see Experimental Section). Most likely, the two compounds result from hindered rotation within the rigid multicyclic architecture, giving rotamers. Apparently, these rotamers can be successfully separated on the HPLC timescale (several minutes), but interconvert again on a longer timescale (i.e. hours).

After the successful cyclization of the peptides bearing two cysteines at the termini and two aminooxy residues internally (**1-3**), the inverted peptide **5**-hS(ONH$_2$)^{ter,n3} was tested (Figure 2.14a,b). For **5**-hS(ONH$_2$)^{ter,n3}∩T4-C2$^{C/O}$, remarkably, four products were obtained, all corresponding with the correct mass of the tricyclic peptide. The two main peaks stand equal, while they are flanked by smaller peaks in a 3:1 ratio. While the terminal hS(ONH$_2$) would be expected to yield fewer isomers due to the flexibility of the intermediate CLiPSed product, the presence of the alanines at the peptide termini may increase the rotational barrier, to give multiple stable rotameric products of the tricyclic peptide that elute with different t_R's on UPLC. For **5**-hS(ONH$_2$)^{ter,n3}∩T4-C3$^{C/O}$, the increased flexibility of the scaffold may alleviate this rotational barrier somewhat, yielding only two peaks.
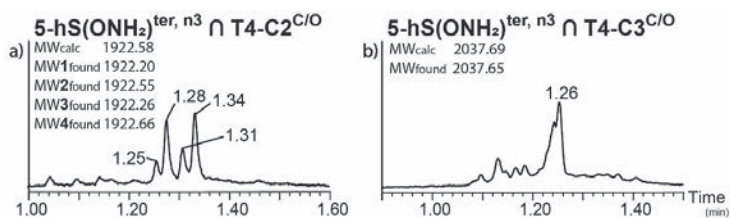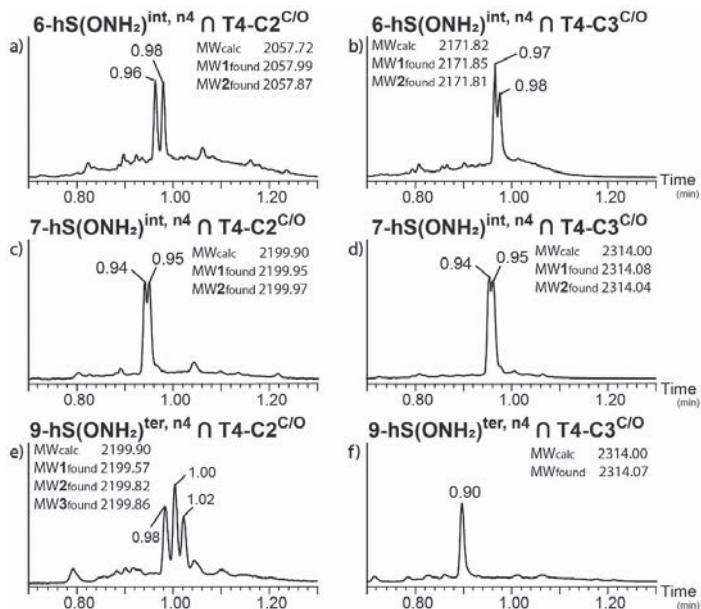
Figure 2.14: UPLC chromatograms of tricyclic peptides of 5-hS(ONH₂)^{ter,n3} for both T4-C2 and T4-C3 scaffolds. Product MW's are denoted in chronological order of encounter.

Next, the scaffold-mediated cyclization of peptides with an additional amino acid in between the reactive amino acid residues was studied. Because the hS(ONH₂) n=4 peptides are more flexible, we expected the formation of less stable rotamers that could possibly also interconvert and therefore give only a single peak in UPLC. The results of the consecutive CLiPS/oxime ligation reactions are shown in Figure 2.15. However, similar results to those with the shorter peptides were obtained, and peptides **6-**hS(ONH₂)^{int,n4} and **7-**hS(ONH₂)^{int,n4} both yielded two tricycle products after cyclization with scaffolds T4-C2 and T4-C3 (Figure 2.15a,b and c,d respectively).

For the inverted-sequence peptide **9-**hS(ONH₂)^{ter,n4} with terminal hS(ONH₂) residues, the increased loop length and associated flexibility worked favorably with scaffold T4-C3 and **9-**hS(ONH₂)^{ter,n4}∩T4-C3$^{C/O}$ was obtained as a single product. Meanwhile **9-**hS(ONH₂)^{ter,n4}∩T4-C2$^{C/O}$, where T4-C2 contains the shorter CLiPS linker, a more rigid tricyclic structure is possibly formed, whereby three rotameric products were obtained.

Figure 2.15: UPLC chromatograms of tricyclic peptides of hS(ONH₂) with loopsize n=4, for both T4-C2 and T4-C3 scaffolds. Product MW's are denoted in chronological order of encounter.

Finally, the n=5 peptides **10-**hS(ONH₂)^{int,n5} and **11-**hS(ONH₂)^{ter,n5} were studied. These peptides were the longest and therefore expected to be the most flexible in this series. The results are presented in Figure 2.16. By using scaffold T4-C3, both the peptides with the

internally and externally positioned aminooxy moieties gave a single major product. For peptide **10**-hS(ONH$_2$)^{int,n5}, the combination with scaffold T4-C2 yielded a single major tricycle product, accompanied by small amount of a second and third rotamer (Figure 2.16a). In contrast, the combination of scaffold T4-C2 and **11**-hS(ONH$_2$)^{ter,n5} only gave a complex mixture (Figure 2.16c).
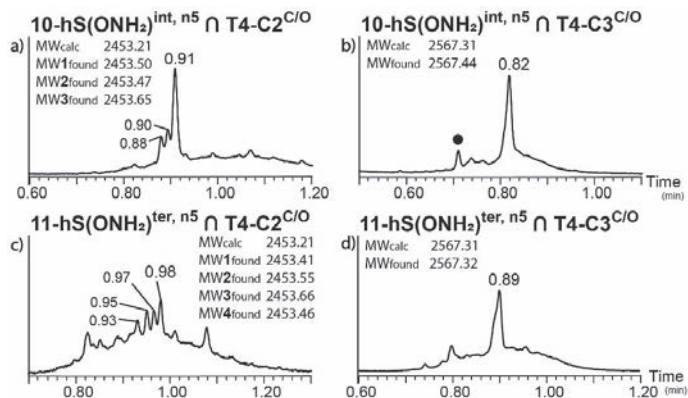

Figure 2.16: UPLC chromatograms of tricyclic peptides of hS(ONH$_2$) with loop sizes n=5, for both T4-C2 and T4-C3 scaffolds. • denotes disulfide of the starting material peptide, which was unreacted in the CLiPS reaction.

From these experiments with amino acid hS(ONH$_2$)-containing peptides, it can be concluded that there is a relation between peptide length, amino acid position and scaffold type, and the formation of multiple tricyclic products. We postulate that the appearance of multiple tricyclic peptide products was the result of rotamer formation. For the larger peptides, combined with the more flexible T4-C3 scaffold, fewer rotamers were obtained. For the T4-C2 scaffold, peptides whereby the hS(ONH$_2$) residues were positioned internally gave the best results, as complex mixtures were obtained when the two hS(ONH$_2$) residues were positioned at the termini.

2.5.3 K(Aoa) Peptides

We then turned our interest to peptides bearing K(Aoa) as the residue for oxime ligation. It is important to realize that the key aminooxy moiety in hS(ONH$_2$) is installed with a 2-atom tether to the α-C, whereas in amino acid K(Aoa) this tether length is increased to 7 atoms, thereby introducing conformational flexibility. We noted in section 2.6.2 that peptide flexibility has a tremendous influence on the extent of rotamer formation in the cyclization reactions.

The smallest peptide in the series, **12**-K(Aoa)^{int,n3} gave quite identical results compared to the hS(ONH$_2$)^{n4} peptides. Two products were obtained with both scaffolds T4-C2 and T4-C3, and these products eluted close together (Figure 2.17a,b). When the K(Aoa) amino acids were positioned at the termini, as in peptide **13**-K(Aoa)^{ter,n3}, a single shouldered product was obtained with scaffold T4-C3, while two rotameric products were obtained using T4-C2.
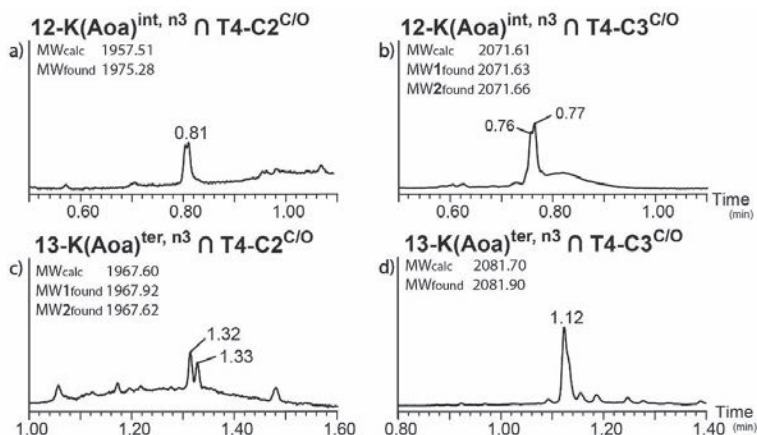
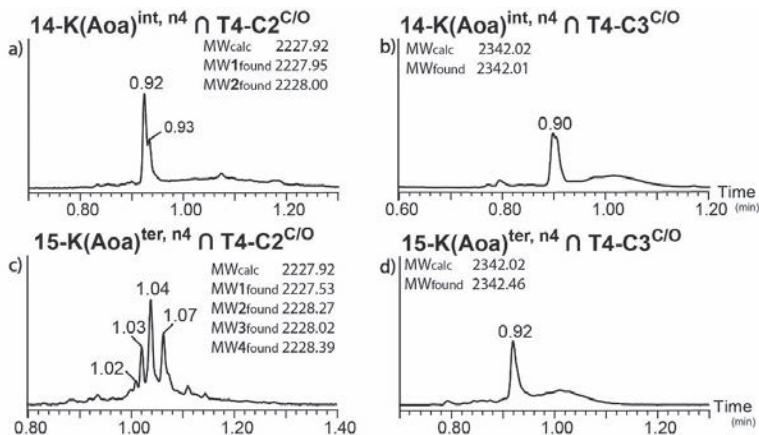*Figure 2.17: UPLC chromatograms of tricyclic peptides of K(Aoa) with loopsize n=3, for both T4-C2 and T4-C3 scaffolds. Product MW's are denoted in chronological order of encounter.*

For the K(Aoa)^{n4} peptides **14** and **15**, similar results were obtained as described above for the hS(ONH$_2$)^{n5} peptides (Figure 2.18). Also here, clean conversion was observed with peptide **14**-K(Aoa)^{int,n4} for both scaffolds (T4-C2 and T4-C3). Peptide **15**-(KAoa)^{ter,n4} yielded quite different results. **15**-(KAoa)^{ter,n4}∩T4-C3$^{C/O}$ was obtained as a single product (Figure 2.18d), while four products were obtained with the T4-C2 scaffold (Figure 2.18c). This is quite similar to what was observed for peptide **11**-hS(ONH$_2$)^{ter,n5} with the T4-C2 scaffold.

Figure 2.18: UPLC chromatograms of tricyclic peptides of K(Aoa) with loopsize n=4, for both T4-C2 and T4-C3 scaffolds. Product MW's are denoted in chronological order of encounter.

For the n=5 peptides **16**-(KAoa)^{int,n5} and **17**-(KAoa)^{ter,n5}, nearly all scaffold combinations yielded the tricyclic peptides as a single peak in the UPLC chromatograms (Figure 2.19). Only the tricycle peptide **17**-(KAoa)^{ter,n5}∩T4-C2$^{C/O}$ was obtained as a mixture of at least 3 different rotamers (Figure 2.19c), similar as observed for all other combinations of peptides having terminal aminooxy residues with scaffold T4-C2.
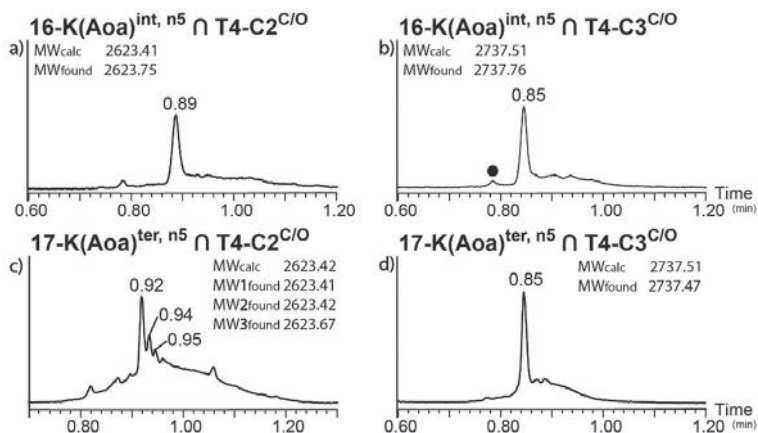
48

Figure 2.19: UPLC chromatograms of tricyclic peptides of K(Aoa) with loopsize n=5, for both T4-C2 and T4-C3 scaffolds. • denotes disulfide of the starting material peptide, which was unreacted in the CLiPS reaction. Product MW's are denoted in chronological order of encounter.

To conclude, we have observed that the combination of scaffold T4-C3 and terminal oxime-residue peptides gave the desired tricycles as single peaks for nearly all tested peptides. In general, scaffold T4-C2 in combination with peptides with terminal aminooxy residues gave complex mixtures of rotamers.

2.6 Conclusions

In this chapter, we intended to establish a robust route towards the synthesis of tricyclic peptides using a combination of CLiPS and oxime ligation cyclization reactions according to strategy 1. This strategy is characterized by a separation of all nucleophiles within the peptide, and all electrophiles at the scaffold. The scaffolds were equipped with acetal protected aldehydes, required for oxime ligation. For this study, three different scaffolds (T4-C1, T4-C2 and T4-C3), two amino acids containing aminooxy groups (hS(ONH$_2$) and K(Aoa)) and 17 peptides were synthesized. The syntheses of all peptides generally suffered from side-reactions, difficult purifications and low yields. For all peptides, the CLiPS reaction proceeded successfully, yielding the monocyclic peptide quantitatively as a single product. For the oxime ligation, the best reaction conditions were found to be utilizing aqueous DMSO solutions. Liberation of the aldehydes was best performed when using a 15% TFA solution to the mixture. Oxime ligation occurred under the same conditions and was finished within 16 hours. The tricyclic product was obtained in all cases, but often as a mixture of different conformational isomers. Generally, larger peptides were more flexible, yielding fewer rotameric products. The peptides containing the longer K(Aoa) residues therefore more often yielded the tricyclic peptide as a single product in the cyclization reactions, compared to the peptides incorporating the shorter hS(ONH$_2$). Finally, the position of the reactive amino acids (cysteines and aminooxy bearing residues, either internal or terminal) was also an important variable, as the peptides with terminal aminooxy residues afforded cleaner products than those with terminal cysteines. The scaffold T4-C3 yielded superior results compared to T4-C2, with most peptides, especially in combination with terminal aminooxy peptides.

2.7 Future Prospects

While we have investigated the basic requirements for the synthesis of tricyclic peptides using CLiPS and oxime ligation reactions under strategy 1, our data set was limited to a

single peptide of each length and composition. Even though all natural *L*-amino acids were shown to be compatible with the cyclization conditions used, the diversity in peptide sequences was very limited. Therefore, testing a broader diversity of different peptide sequences would be expected to establish a more defined set of requirements for successful synthesis of single isomer tricyclic peptide products.

As mentioned, synthesis of the linear peptides needs to be optimized further, because current yields and purities are still (too) low, due to unknown side reactions emerging from the aminooxy moiety containing side chains. For example, we did observe that for K(Aoa) side reactions were much less pronounced, which is most likely the result of double Boc-protection of the aminooxy group. Therefore, investigation of other protecting groups for the aminooxy group in SPPS, for example 4-methyltrityl (Mtt), should be investigated.

In our efforts to discover new bioactive peptides, the next step would be to extend this novel technology to the preparation of low-, medium-, and also high-throughput libraries of tricyclic peptides. Only if the crude quality of the peptides is improved, such library synthesis would be feasible. In general, peptides in which the oxime amino acid is installed at the termini, are recommended for library synthesis, preferably in combination with scaffold T4-C3.

2.8 Experimental Section

2.8.1 Scaffold Synthesis

N-benzyl-*N*-(2,2-diethoxyethyl)-2,2-diethoxyethan-1-amine (**3**)
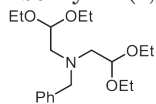
To a flame-dried flask, under N_2 flow, benzylamine (**1**) (5.0 mL, 45.8 mmol, 1.0 equiv) was added, followed by bromoacetaldehyde diethyl acetal (**2**) (16 mL, 106.4 mmol, 2.3 equiv) and triethylamine (18.0 mL, 129.1 mmol, 2.8 equiv). The yellowish mixture was stirred at 100 °C for 18h, resulting in a thick slurry. The solids were filtered off and washed with EtOAc, which was subsequently washed with water, a saturated solution of NaHCO$_3$ and brine, and dried over Na$_2$SO$_4$. The volatiles were removed under reduced pressure to yield an orange oil. The oil was immobilized on silica, and the desired compound was purified via flash column chromatography (20:1 – P.E.:EtOAc) yielding the benzyl-protected amine **3** as a pale yellow oil in 37% yield (5.72 g, 16.83 mmol). **1H NMR** (300 MHz, CDCl$_3$) δ 7.30 (ddt, *J* = 21.7, 13.9, 7.0 Hz, 5H), 4.58 (t, *J* = 5.2 Hz, 2H), 3.81 (s, 2H), 3.65 (dq, *J* = 9.2, 7.1 Hz, 4H), 3.51 (dq, *J* = 9.3, 7.0 Hz, 4H), 2.76 (d, *J* = 5.2 Hz, 4H), 1.20 (t, *J* = 7.1 Hz, 12H). **13C NMR** (101 MHz, CDCl$_3$) δ 139.75, 128.68, 127.86, 126.59, 102.25, 61.75, 59.97, 57.21, 15.17. **IR** (cm^{-1}) 3027, 2973, 2928, 2876, 1602, 1494, 1452, 1372, 1345, 1267, 1114, 1056, 1023, 916, 849, 816, 739, 698. **HRMS** (FD) 339.23924, (calc. 339.23828).

Bis(2,2-diethoxyethyl)amine (**4**)
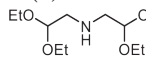
The benzyl-protected amine **3** (5.71 g, 16.8 mmol, 1.0 equiv) was dissolved in 160 mL of EtOH, and the solution was degassed and flushed with N$_2$. Pd/C (10% loading, 267 mg) was added and hydrogen pressure was applied (H$_2$ filled balloon) after evacuation/saturation (3x). The mixture was stirred for 4h at rt, after which TLC indicated that the reaction had finished. The solution was filtered over a Na$_2$SO$_4$/Celite pad and eluted with EtOH. The volatiles were removed under reduced pressure, yielding amine **4** as a pale-yellow oil (4.1 g, 16.2 mmol, 97%). **1H NMR** (400 MHz, CDCl$_3$) δ 4.44 (t, *J* = 5.6 Hz, 2H), 3.60 – 3.50 (m, 4H), 3.44 – 3.34 (m, 4H), 2.59 (d, *J* = 5.6 Hz, 4H), 1.06 (t, *J* = 7.1 Hz, 12H). **13C NMR** (101 MHz, CDCl$_3$) δ 101.70, 61.98, 51.62, 14.99. **IR** (cm^{-1}) 2974, 2876, 1455, 1372, 1346, 1282, 1223, 1118, 1056, 1021, 944, 854, 813, 603, 504. **HRMS** (FD) 249.19077 (calc. 249.19401).

5,6-Bis(bromomethyl)-2,2-bis(2,2-diethoxyethyl)isoindolin-2-ium (**T4-C1**)
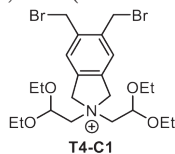
In a flame-dried flask, under N$_2$ flow, 1,2,4,5 tetrakis (bromomethyl)benzene **5** (1.5 g, 3.0 mmol, 3.0 equiv) was dissolved in 110 mL of freshly distilled MeCN, and DIPEA (209 µL, 1.2 mmol, 1.2 equiv) was added. The secondary amine **4** (250 mg, 1.0 mmol, 1.0 equiv) was dissolved in 2.0 mL MeCN, and added dropwise to the solution of **5**. After stirring for 1h, the reaction mixture was concentrated, and immobilized on silica, after which the scaffold was ob-

tained via flash column chromatography (EtOAc to EtOAc:EtOH - 4:1), as a slight orange foam (510 mg, 0.94 mmol, 94%).**¹H NMR** (500 MHz CD₃CN) δ 7.50 (s, 2H), 5.05 (s, 4H), 4.86 (t, *J* = 5.0 Hz, 3H), 4.76 (s, 4H), 3.72 (d, *J* = 4.9 Hz, 4H), 3.71 – 3.63 (m, 4H), 3.46 (dq, *J* = 9.3, 7.0 Hz, 4H), 1.17 (t, *J* = 7.1 Hz, 12H). **¹³C NMR (**126 MHz, CD₃CN) δ 138.63, 134.90, 126.08, 97.95, 70.33, 65.05, 64.27, 30.13, 15.09. **IR** (cm⁻¹) 2973, 2929, 2886, 1443, 1374, 1349, 1219, 1121, 1046, 998, 958, 893, 832, 789. **HRMS** (LC-ESI) for $C_{22}H_{36}Br_2NO_4^+$ calc. 536.1011, found 536.1033. **mp** 32 °C.

### *tert*-Butyl 3,5-dimethylbenzoate (**7a**)
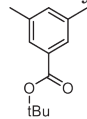
In a flame-dried flask, under N₂ flow, 3,5-dimethyl benzoic acid (**6**) (2.0 g, 13.3 mmol, 1.0 equiv) was suspended in 1.6 mL of toluene. Thionyl chloride (2.0 mL, 27.6 mmol, 2.05 equiv) was added and the mixture was warmed to a gentle reflux and stirred for 4h. The volatiles were removed under reduced pressure, after which the oily residue was diluted with 4 mL of freshly distilled CH₂Cl₂. *t*-BuOH (2.1 mL, 21.3 mmol, 1.6 equiv) was added, followed by pyridine (1.1 mL, 14.0 mmol, 1.05 equiv). The mixture was stirred for 12h, after which the solids were removed by filtration and washed with CH₂Cl₂. The organic phase was washed with 4M HCl, water, 2M NaOH and water. After drying over K₂CO₃, the volatiles were removed, yielding **7a** as a colorless oil (2.5 g, 12.1 mmol, 90%). **¹H NMR** (400 MHz, CDCl₃) δ 7.63 (s, 2H), 7.17 (s, 1H), 2.38 (s, 6H), 1.62 (s, 9H). **¹³C NMR** (101 MHz, CDCl₃) δ 166.12, 137.75, 133.99, 127.09, 80.70, 28.18, 21.13. Analytical data are in concurrence to those found in literature.[13]
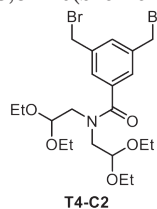
tert-Butyl 3,5-bis(bromomethyl)benzoate (**7b**)
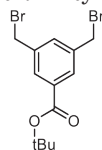
In a flame-dried flask, under N₂ flow, tBu-ester **7a** (14.0 g, 67.6 mol, 1.0 equiv) was dissolved in freshly distilled CH₂Cl₂ (250mL). N-Bromosuccinimide (NBS) (25.3 g, 142.0 mmol, 2.1 equiv) was added and the mixture was degassed and flushed with N₂. The flask was irradiated with a commercially available halogen construction lamp (500W), heating the mixture to a gentle reflux. The mixture was stirred for 1.5h, after which ¹H NMR showed the reaction had reached completion*. The mixture was diluted with CH₂Cl₂ and washed with water. After drying over Na₂SO₄, the volatiles were removed under reduced pressure, yielding a colorless oil. The mixture was crystallized from hexane, providing the desired product **7b** as a white solid (7.6 g, 20.8 mmol, 31%). A second crystallization yielded another 1.7 g (4.7 mmol, 7%). ***The mixture contained both mono- and tribrominated starting material, whereby for the latter a single methyl group was brominated twice.* ¹H NMR** (400 MHz, CDCl₃) δ 7.94 (s, 2H), 7.60 (s, 1H), 4.51 (s, 4H), 1.61 (s, 9H). **¹³C NMR** (101 MHz, CDCl₃) δ 164.31, 138.54, 133.28, 133.10, 129.69, 81.56, 31.94, 28.01. **IR** (cm⁻¹) 3013, 2982, 2969, 2932, 1790, 1714, 1604, 1472, 1449, 1390, 1369, 1319, 1236, 1213, 1154, 1110, 1060, 999, 973, 953, 918, 893, 846, 794, 771, 753, 734, 692. **mp** 52 °C. **HRMS** FD [M+] calcd. for $C_{13}H_{16}Br_2O_2$: 361.951, found 361.950.

3,5-Bis(bromomethyl)benzoic acid (**8**)
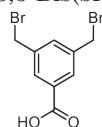
Dibromide **7b** (5.0 g, 13.7 mmol, 1.0 equiv) was dissolved in freshly distilled CH₂Cl₂ (50 mL). HCOOH was added and the solution was stirred overnight at rt, after which ¹H NMR showed completion of the reaction. The volatiles were removed under reduced pressure and co-evaporation with CH₂Cl₂ (3x) yielded **8** as a white solid (4.0 g, 12.9 mmol, 94%) which was used without further purification. **¹H NMR** (400 MHz, CDCl₃) δ 8.10 (s, 2H), 7.71 (s, 1H), 4.55 (s, 4H). **¹³C NMR** (101 MHz, CDCl₃) δ 170.03, 139.08, 134.64, 130.45, 130.31, 31.53. **IR** (cm⁻¹) 2971, 2821, 2710, 2604, 2539, 1686, 1603, 1460, 1437, 1420, 1308, 1278, 1248, 1211, 1162, 1111, 1056, 998, 938, 927, 904, 855, 771, 728, 691, 662. **mp** 123 °C (sublimates), 142 °C (melts). **HRMS** (FD) for $C_9H_8Br_2O_2$ calc. 307.8886, found 307.8891.

### 3,5-Bis(bromomethyl)-*N,N*-[bis(2,2-diethoxyethyl)]-benzamide (**T4-C2**)

In a flame-dried flask, under N₂ flow, acid **8** (1.05 g, 3.4 mmol) was dissolved in 5 mL of CH₂Cl₂. SOCl₂ (5.0 mL, excess) was added and the mixture was heated to 75 °C, and stirred for 5h. The mixture was cooled to rt and the volatiles were removed under reduced pressure. The remaining oil was dissolved in 18 mL of anhydrous CH₂Cl₂. NaHCO₃ (solid, 2.6 g, 30.9 mmol 9.1 equiv), NEt₃ (1.0 mL, 7.2 mmol, 2.1 equiv) and DMAP (25.0 mg, 0.2 mmol, 6 mol%) were added. Amine **4** (676.0 mg, 2.7 mmol, 0.8 equiv) was added dropwise, and the mixture was stirred overnight. After extraction with CH₂Cl₂, the organic phase was washed with water (2x) and brine, and subsequently dried over Na₂SO₄. Filtration and

evaporation yielded the crude product, which was purified via flash column chromatography (3:1 to 2:1 P.E:EtOAc) and **T4-C2** was obtained as an off-white waxy solid (414 mg, 0.8 mmol, 23%). **¹H NMR** (500 MHz, CDCl₃) δ 7.43 (s, 1H), 7.40 (s, 2H), 4.84 (s, 1H), 4.49 (t, J = 4.6 Hz, 1H), 4.46 (s, 4H), 3.81 (p, J = 7.1 Hz, 2H) 3.71 (d, J = 5.0 Hz, 1H), 3.61 (dt, J = 16.3, 8.4 Hz, 4H), 3.50 (d, J = 4.8 Hz, 2H), 3.40 (p, J = 7.0 Hz, 2H), 1.29 (t, J = 6.9 Hz, 6H), 1.17 (t, J = 4.6 Hz, 6H). **¹³C NMR** (126 MHz, CDCl3) δ *171.41*, 171.33, 138.66, *138.60*, 137.79, *137.75*, 130.23, *129.75*, 127.71, *127.19*, 101.20, 100.90, 63.39, 52.73, 49.01, 45.22, 32.13, 32.08, 15.45, 15.33. (italic are rotamers). **IR** (cm⁻¹) 2974, 2929, 2877, 2349, 1735, 1634, 1600, 1468, 1441, 1417, 1374, 1345, 1306, 1236, 1215, 1162, 1116, 1055, 932, 896, 837, 757, 704. **HRMS** (FD) calcd. for C₂₁H₃₃Br₂NO₅: 537.0725, found 537.0702 **mp** 27 °C. *It was estimated, based on ¹H NMR, that the scaffold contained a mixture of Br and Cl substituents with about 38% Cl incorporated. There is 9.9% Cl-Cl present, 44.4% of the Cl-Br, and 45.7% of the Br-Br, as determined via LC-MS.*

tert-Butyl 3,5-bis((phthalimido)methyl)benzoate (**9**)
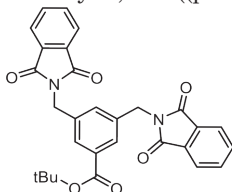
In a flame-dried flask, under N₂ flow, bromide **7b** (500 mg, 1.4 mmol, 1.0 equiv) was dissolved in 27 mL anhydrous DMF. KPhth (1.0 g, 5.5 mmol, 4 equiv) was added next, and the mixture was heated to 125 °C and stirred overnight. The suspension was cooled to rt and the mixture was evaporated to dryness. The mixture was dissolved in CH₂Cl₂ and washed with water, 1M KHSO₄, saturated aqueous NaHCO₃ and water. After drying over Na₂SO₄ the volatiles were removed under reduced pressure. The phthalimide remnants were removed via flash column chromatography (3:1-P.E:EtOAc to remove first spot, then increased to 4:1 EtOAc:P.E.), yielding **9** as a white solid (533 mg, 1.1 mmol, 78%). **¹H NMR** (300 MHz, CDCl₃) δ 7.90 (d, J = 1.4 Hz, 2H), 7.85 (dd, J = 5.4, 3.1 Hz, 4H), 7.72 (dd, J = 5.4, 3.1 Hz, 4H), 7.64 (s, 1H), 4.87 (s, 4H), 1.56 (s, 9H). **¹³C NMR** (75 MHz, CDCl₃) δ 167.88, 164.97, 137.03, 134.06, 133.01, 132.31, 132.02, 128.57, 123.46, 81.35, 41.10, 28.11. **IR** (cm⁻¹) 2975, 2938, 1769, 1706, 1607, 1554, 1536, 1466, 1427, 1391, 1367, 1342, 1310, 1257, 1231, 1155, 1122, 1099, 1086, 973, 957, 918, 896, 845, 794, 774, 726, 710, 695. **HRMS** (FD) calcd. for C₂₉H₂₄N₂O₆: 496.1634, found 496.1634. **mp** 212 °C.

3,5-Bis((phthalimido)methyl)benzoic acid (**10a**)
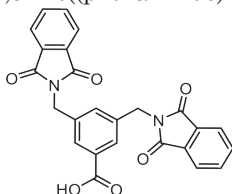
In a flask, phthalimide ester **9** (468 mg, 0.9 mmol) was dissolved in CH₂Cl₂ (5.0 mL), after which HCOOH (10.0 mL) was added. A precipitate started to form, and the mixture was stirred overnight. The solids were filtered off, and washed with CH₂Cl₂. The product was confirmed by ¹H NMR. The off-white solid **10a** was dried under high vacuum, yielding 303 mg (0.7 mmol, 73%). No further purification was necessary for subsequent reactions. **¹H NMR** (400 MHz, DMSO-d_6) δ 13.10 (s, 1H), 7.88 (q, J = 4.4 Hz, 8H), 7.76 (s, 2H), 7.53 (s, 1H), 4.82 (s, 4H). **¹³C NMR**, (126 MHz, CDCl₃) δ 167.61, 166.70, 137.65, 134.61, 131.43, 130.93, 127.27, 123.26, 40.44. **IR** (cm⁻¹) 3064, 1771, 1704, 1604, 1466, 1428, 1393, 1359, 13431311, 1261, 1240, 1190, 1170, 1112, 1102, 1086, 1071, 980, 960, 914, 885, 834, 792, 773, 746, 725, 710. **mp** 228 °C (sublimates), 351 °C melts. **HRMS** (FD) calcd. for C₂₅H₁₆N₂O₆: 440.1008, found 440.1004.

N,N-[Bis(2,2-diethoxyethyl)]-3,5-bis((phthalimido)methyl)benzamide (**10b**)
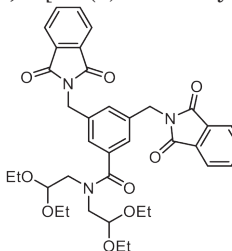
In a flame-dried flask, under N₂ flow, acid **10a** (1.0 g, 2.3 mmol), was suspended in 15.0 mL of anhydrous DMF. HATU (949 mg, 2.5 mmol, 1.1 equiv) and DIPEA (1.0 mL, 5.7 mmol, 2.5 equiv) were added, yielding a clear solution. The mixture was stirred for 30 min, after which the amine **18** (594 mg, 2.4 mmol, 1.05 equiv) was added. The mixture was stirred overnight, after which it was diluted with EtOAc and washed with H₂O and brine. After drying over Na₂SO₄, filtration and evaporation of the volatiles, **10b** was obtained as a pale brown solid, which was used without further purification (1540 mg, 2.3 mmol, *quant*). **¹H NMR** (500 MHz, CDCl₃) δ 7.82 (dd, J = 5.3, 3.1 Hz, 4H), 7.70 (dd, J = 5.4, 3.0 Hz, 4H), 7.54 (s, 1H), 7.33 (s, 2H), 4.82 (s, 4H), 4.77 (t, J = 4.8 Hz, 1H), 4.33 (t, J = 4.7 Hz, 1H), 3.80 – 3.68 (m, 2H), 3.63 (d, J = 4.9 Hz, 2H), 3.57 (dt, J = 15.5, 6.7 Hz, 3H), 3.44 (dt, J = 14.8, 7.0 Hz, 3H), 3.38 (d, J = 4.8 Hz, 2H), 3.25 (p, J = 7.1 Hz, 2H), 1.20 (t, J = 6.6 Hz, 8H), 1.02 (t, J = 6.8 Hz, 6H). **¹³C NMR** (126 MHz, CDCl₃) δ 171.76, 167.76, 137.71, 137.21, 134.03, 132.05, 129.72, 126.25, 123.39, 101.49, 100.98, 63.56, 63.26, 52.70, 49.26, 41.12, 15.42, 15.20. **IR** (cm⁻¹) 2974, 2929, 2877, 1765, 1702, 1635, 1605, 1468, 1445, 1421,

1394, 1348, 1329, 1313, 1260, 1233, 1173, 1119, 1103, 1054, 1016, 958, 960, 938, 914, 886, 846, 799, 733, 712. **HRMS** (FD) calcd. for $C_{37}H_{41}N_3O_9$: 671.2843, found 671.2842 **mp** 161-164 °C.

3,5-Bis(aminomethyl)-*N,N*-[bis(2,2-diethoxyethyl)]-benzamide (**10c**)
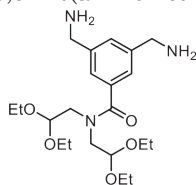
Bisphthalimide **10b** (1.53g, 2.3 mmol) was suspended in 20 mL of toluene/EtOH (1:2). Hydrazine hydrate (51% solution in water, 1.4 mL, 22.8 mmol, 10 equiv) was added and the mixture was stirred at reflux for 2h, during which a thick precipitate was formed. The mixture was cooled to rt after which the solids were filtered off, and washed with CH_2Cl_2. The volatiles were removed under reduced pressure, yielding the crude diamine **10c** in quantitative yield, which was used without further purification. **¹H NMR** (400 MHz, DMSO-d*6*) δ 7.33 (s, 1H), 7.14 (s, 2H), 5.76 (s, 2H), 4.73 (s, 1H), 4.54 (s, 1H),3.73 (s, 4H), 3.71 – 3.63 (m, 2H), 3.62 – 3.55 (m, 3H), 3.55 – 3.40 (m, 5H),3.35 (d, J = 12.5 Hz, 4H), 1.16 (t, J = 6.3 Hz, 8H), 1.08 – 0.95 (m, 6H).

### *N,N*-(bis(2,2-diethoxyethyl)]-3,5-bis(2-bromoacetamidomethyl)-benzamide (**T4-C3**)
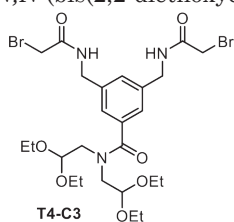
Crude diamine **10c** (containing residual water, 1.2 g, ~2.3 mmol) was dissolved in 55 mL of CH_2Cl_2 and 5.0 mL of EtOH was added. Then, $NaHCO_3$ (1.3 g, 15.9 mmol, 7.0 equiv) and bromoacetic acid *N*-hydroxysuccinimide ester (1.8g, 7.5 mmol, 3.3 equiv) were added and the mixture was stirred for 1h, after which TLC-analysis showed full conversion. The reaction mixture was diluted with water and extracted with CH_2Cl_2. The organic phase was subsequently washed with water, brine and a *sat.* solution of $NaHCO_3$. After drying over Na_2SO_4, filtration and evaporation of the volatiles under reduced pressure, the crude product was obtained, which was purified by flash column chromatography (7:1–EtOAc:P.E.), yielding scaffold **T4-C3** as a fluffy white solid (950 mg, 1.5 mmol, 64% overall).**¹H NMR** (500 MHz, CDCl₃) δ 7.20 (t, *J* = 5.9 Hz, 2H), 7.18 (s, 2H), 7.13 (s, 1H), 4.79 (t, *J* = 4.9 Hz, 1H), 4.46 (t, *J* = 4.8 Hz, 1H), 4.36 (d, *J* = 5.9 Hz, 4H), 3.88 (s, 4H), 3.75 (p, *J* = 7.2 Hz, 2H), 3.66 (d, *J* = 4.9 Hz, 2H), 3.58 (dq, *J* = 14.1, 6.9 Hz, 5H), 3.43 (d, *J* = 4.8 Hz, 2H), 3.37 (dt, *J* = 15.5, 7.2 Hz, 2H), 1.22 (t, *J* = 6.9 Hz, 6H), 1.13 (t, *J* = 6.9 Hz, 6H). **¹³C NMR** (126 MHz, CDCl₃) δ 172.11, 165.89, 138.56, 137.35, 127.32, 125.09, 101.14, 100.80, 63.33, 52.68, 48.78, 43.40, 28.86, 15.28. **IR** (cm⁻¹) 3262, 3067, 2971, 2873, 1678, 1665, 1599, 1480, 1424, 1373, 1341, 1297, 1266, 1248, 1227, 1209, 1177, 1120, 1063, 1027, 933, 905, 858, 830, 799, 763, 723, 708. **HRMS** (FD) calcd. for $C_{25}H_{39}Br_2N_3O_7$: 651.1155, found 651.1136. **mp** 74°C.

2.8.2 Amino Acid Synthesis

Fmoc-D(OtBu)-OBn (**12a**)
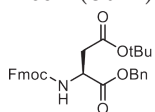
In a flame-dried flask, under Ar-pressure, Fmoc-D(OtBu)-OH (**11**) (43.1 g, 106.1 mmol, 1.0 equiv) was suspended in 400 mL of anhydrous MeOH. Cs_2CO_3 (17.3 g, 53.1 mmol, 0.5 equiv) was added and the mixture immediately became a colorless solution, which was subsequently stirred for 45 min. The volatiles were removed under reduced pressure, yielding a while solid. The residue was dissolved in 500 mL anhydrous MeCN and benzyl bromide (37.9 mL, 318.4 mmol, 3.0 equiv) was added. The mixture was stirred for 3h at rt during which a white precipitate formed. The volatiles were removed and the remaining solid was washed with water and EtOH twice, yielding the desired product as a white solid, in quantitative yield. **¹H NMR** (400 MHz, CDCl₃) δ 7.78 (d, *J* = 7.5 Hz, 2H), 7.62 (d, *J* = 6.9 Hz, 2H), 7.42 (t, *J* = 7.4 Hz, 2H), 7.33 (dd, *J* = 15.3, 7.5 Hz, 7H), 5.93 (d, *J* = 8.5 Hz, 1H), 5.33 – 5.14 (m, 2H), 4.70 (dt, *J* = 8.4, 4.1 Hz, 1H), 4.50 – 4.40 (m, 1H), 4.40 – 4.30 (m, 1H), 4.26 (t, *J* = 7.1 Hz, 1H), 3.01 (dd, *J* = 17.0, 4.5 Hz, 1H), 2.83 (dd, *J* = 16.9, 4.2 Hz, 1H), 1.45 (s, 9H). **¹³C NMR** (101 MHz, CDCl₃) δ 170.70, 169.85, 155.89, 143.81, 143.59, 141.17, 135.15, 128.47, 128.31, 128.13, 127.60, 126.97, 125.08, 125.03, 119.87, 81.74, 67.34, 67.17, 50.55, 46.98, 37.62, 27.89. Analytical data are in accordance with those reported in literature.[14]
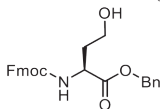
Fmoc-D(OH)-OBn (**12b**)
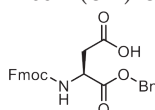
Fmoc-D(OtBu)-OBn **12a** (1.6 g, 3.2 mmol) was dissolved in 15 mL of freshly distilled CH_2Cl_2. 15 mL HCOOH is added to the solution and the mixture is stirred overnight at rt, after which TLC showed full conversion of the starting material. The volatiles were removed under reduced pressure and the remnants of HCOOH were removed by co-evaporation with CH_2Cl_2, yielding

Fmoc-D(OH)-OBn as a white solid (1.3 g, 2.9 mmol, 92%).**¹H NMR** (400 MHz, CDCl₃) δ 11.15 (s, 1H), 7.80 (d, *J* = 7.5 Hz, 2H), 7.66 (d, *J* = 7.4 Hz, 2H), 7.44 (t, *J* = 7.4 Hz, 2H), 7.36 (d, *J* = 7.4 Hz, 7H), 6.16 (d, *J* = 8.5 Hz, 1H), 5.26 (s, 2H), 4.83 (dt, *J* = 8.6, 4.4 Hz, 1H), 4.50 (dd, *J* = 10.4, 7.4 Hz, 1H), 4.46 – 4.38 (m, 1H), 4.26 (t, *J* = 7.1 Hz, 1H), 3.18 (dd, *J* = 17.4, 4.6 Hz, 1H), 3.01 (dd, *J* = 17.4, 4.2 Hz, 1H**). ¹³C NMR** (101 MHz, CDCl₃) δ 175.36, 170.34, 156.04, 143.53, 143.39, 141.02, 134.84, 128.34, 128.20, 127.94, 127.51, 126.87, 124.90, 119.76, 67.44, 67.21, 50.18, 46.79, 36.12. Analytical data are in accordance with those reported in literature.[15]
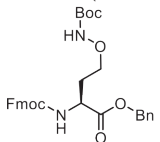
Fmoc-hS-OBn (13)

In a flame-dried flask, under N₂ flow, Fmoc-D(OH)-OBn (**12b**) (11.1 g, 25.0 mmol) was dissolved in 175 mL of freshly distilled THF. The reaction mixture was cooled to 0 °C, after which BH₃·SMe₂ (11.9 mL, 125.0 mmol, 5.0 equiv) was added dropwise over 1h. The mixture was stirred on ice for 2h, and subsequently warmed to rt and stirred overnight, after which TLC showed full consumption of the starting material. The mixture was carefully quenched with sat. NH₄Cl solution and extracted with EtOAc (3x). The organic phase was washed with 1M KHSO₄, brine and dried over Na₂SO₄. The volatiles were removed under reduced pressure, after which Fmoc-hS-OBn **13** crystallized as a white solid (10.7 g, 24.9 mmol, 99%). **¹H NMR** (500 MHz, CDCl₃) δ 7.81 – 7.73 (m, 2H), 7.61 (d, J = 6.6 Hz, 2H), 7.41 (t, J = 7.4 Hz, 2H), 7.33 (dd, J = 15.3, 7.4 Hz, 8H), 5.93 – 5.81 (m, 1H), 5.26 – 5.09 (m, 2H), 4.64 – 4.54 (m, 1H), 4.44 (p, J = 10.5 Hz, 1H), 4.22 (t, J = 6.6 Hz, 1H), 3.74 – 3.65 (m, 1H), 3.65 – 3.52 (m, 1H), 3.16 (s, 1H), 2.18 (td, J = 9.3, 4.6 Hz, 1H), 1.77 (td, J = 9.6, 4.7 Hz, 1H). **¹³C NMR** (126 MHz, CDCl₃) δ 172.28, 156.64, 143.68, 143.57, 143.52, 143.47, 141.17, 135.03, 128.50, 128.38, 128.13, 127.62, 126.97, 124.93, 124.90, 119.88, 119.86, 67.25, 67.04, 58.20, 51.29, 47.03, 35.23, 29.97. Analytical data are in accordance with those reported in literature.[5]

Fmoc-hS(ON-Boc₂)-OBn (14)
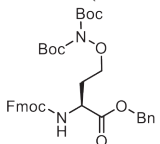
In a flame-dried flask, under N₂, Fmoc-hS-OBn (**13**) (7.01 g, 16.21 mmol) was dissolved in 125 mL of anhydrous THF. Subsequently Boc₂NOH (prepared according to Jacobson *et al.*[16]) (3.97 g, 17.02 mmol, 1.05 equiv) and PPh₃ (4.46 g, 17.02 mmol, 1.05 equiv) were added, and the flask was cooled on an ice bath. DIAD (4.29 mL, 17.02 mmol, 1.05 equiv) was added dropwise via a syringe pump (4.4 mL/h). The mixture was warmed to rt, and stirred overnight. The volatiles were removed under reduced pressure, after which the mixture was immobilized on silica. Flash column chromatography (6:2:1 – P.E.: CH₂Cl₂:EtOAc) provided the product Fmoc-hS(ON-Boc₂)-OBn **14** as a white solid (7.51 g, 11.60 mmol, 72%). **¹H NMR** (500 MHz, CDCl₃) δ 7.77 (d, *J* = 7.5 Hz, 2H), 7.67 (d, *J* = 7.3 Hz, 2H), 7.40 (t, *J* = 7.4 Hz, 2H), 7.37 – 7.33 (m, 2H), 7.33 – 7.24 (m, 5H), 6.63 (d, *J* = 8.6 Hz, 1H), 5.20 (s, 2H), 4.65 (dt, *J* = 10.3, 5.5 Hz, 1H), 4.42 (dd, *J* = 10.2, 7.5 Hz, 1H), 4.38 – 4.29 (m, 1H), 4.24 (t, *J* = 7.2 Hz, 1H), 4.16 – 4.07 (m, 1H), 4.03 – 3.93 (m, 1H), 2.29 (q, *J* = 10.2, 6.0 Hz, 2H), 2.23 (dd, *J* = 12.8, 8.1 Hz, 1H), 1.55 (s, 18H).**¹³C NMR** (126 MHz, CDCl₃) δ 171.63, 156.42, 150.34, 144.08, 143.95, 141.28, 135.52, 128.54, 128.31, 128.17, 127.66, 127.65, 127.07, 127.06, 125.32, 125.31, 119.92, 84.41, 72.54, 67.18, 67.14, 52.04, 47.21, 29.64, 28.10. **IR** (cm⁻¹) 3349, 2979, 2044, 1969, 1953, 1789, 1746, 1715, 1608, 1524, 1477, 1540, 1392, 1368, 1345, 1270, 1246, 1145, 1110, 1001, 911, 846, 793, 755, 736. **HRMS** (FD) calcd. for C₃₆H₄₂N₂O₉: 646.2890, found 646.2866. **mp** 31-34 °C**.

Fmoc-hS(ONHBoc)-OBn (15)

Fmoc-hS(ON-Boc₂)-OBn **14** (11.32 g, 17.51 mmol) was dissolved in 150 mL of CH₂Cl₂. TFA (2.14 mL, 27.94 mmol, 1.60 equiv). It was stirred overnight, after which NMR showed incomplete conversion. 0.90 mL (11.75 mmol, 0.67 equiv) of TFA was added and the reaction mixture was again stirred overnight. The volatiles were removed, after which the mono-Boc compound was purified via flash column chromatography (6:4:1 – P.E.: CH₂Cl₂:EtOAc) yielding Fmoc-hS(ONHBoc)-OBn **15** as a white solid (5.17 g, 9.22 mmol, 53%). **¹H NMR** (500 MHz, CDCl₃) δ 7.79 (d, *J* = 7.6 Hz, 2H), 7.69 (d, *J* = 7.5 Hz, 2H), 7.42 (t, *J* = 7.5 Hz, 3H), 7.40 – 7.27 (m, 9H), 6.57 (s, 1H), 5.22 (s, 2H), 4.64 (q, *J* = 6.5 Hz, 1H), 4.42 (tt, *J* = 17.9, 8.9 Hz, 2H), 4.26 (t, *J* = 7.4 Hz, 1H), 4.01 (ddd, *J* = 11.4, 7.4, 4.3 Hz, 1H), 3.93 (dt, *J* = 10.5, 5.3 Hz, 1H), 2.20 (tq, *J* = 15.4, 9.8, 9.2 Hz, 2H), 1.52 (s, 9H). **¹³C NMR** (126 MHz, CDCl₃) δ 171.96, 157.13, 156.32, 143.98, 143.79, 141.21, 135.33, 128.49, 128.30, 128.19, 127.59, 127.00, 125.21, 119.85, 82.05, 72.89, 67.16, 67.05, 51.81, 47.11, 29.92, 28.14. **IR** (cm⁻¹) 3285, 3065, 2977, 2933, 1702, 1529, 1477, 1449, 1391, 1367, 1337, 1248, 1214, 1159, 1104, 1080, 1057, 1003, 909, 853, 757, 737. **HRMS** (FD) calcd. for C₃₁H₃₄N₂O₇: 546.2336, found 546.2366. **mp** 43 °C.

Fmoc-hS(ONHBoc)-OH
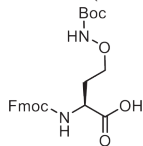
In a flame-dried flask, benzyl-ester Fmoc-*h*S(ONHBoc)-OBn **15** (5.17 g, 9.22 mmol) was dissolved in 200 mL EtOH. The flask was degassed and Pd/C (10 wt% loading, 256 mg) was added. The flask was evacuated and purged with H_2 three times and the reaction mixture was stirred under H_2 pressure (balloon) for 4h at rt. TLC showed full conversion of the starting material and the reaction flask was purged with N_2. The mixture was filtered over Celite and eluted with EtOH. The volatiles were evaporated under reduced pressure, yielding the product Fmoc-hS(ONHBoc)-OH as a white solid (4.20 g, 9.21 mmol, 99%). **^{1}H NMR** (500 MHz, CDCl$_3$) δ 7.91 (s, 1H), 7.75 (d, *J* = 7.2 Hz, 2H), 7.65 (t, *J* = 6.1 Hz, 2H), 7.38 (t, *J* = 7.0 Hz, 3H), 7.29 (t, *J* = 7.3 Hz, 3H), 6.68 (s, 1H), 4.58 (q, *J* = 6.1 Hz, 1H), 4.38 (d, *J* = 6.8 Hz, 2H), 4.23 (t, *J* = 6.7 Hz, 1H), 4.07 – 3.91 (m, 2H), 2.18 (d, *J* = 3.7 Hz, 2H), 1.49 (s, 9H**). ^{13}C NMR** (126 MHz, CDCl$_3$) δ 175.70, 157.66, 156.61, 143.82, 143.65, 141.11, 127.55, 126.97, 125.18, 119.78, 82.32, 72.93, 67.15, 51.61, 46.95, 29.67, 28.07. **IR** (cm^{-1}) 3272, 3065, 2977, 1695, 1524, 1477, 1448, 1393, 1368, 1336, 1249, 1158, 1105, 1080, 1051, 940, 907, 850, 758, 733. **HRMS** (FD) calcd. for $C_{24}H_{28}N_2O7$: 456.1897 found 456.1896. **mp** 46.2 °C

2.8.3 Peptide Synthesis

Amino acids are indicated by single-letter codes; peptides are acetylated at the N-terminus and amidated at the C-terminus. Special amino acids: *homo*-Serine aminooxy derivative hS(ONH$_2$) and Lysine-aminooxy acetic-acid K(Aoa).

2.8.3.1 General Procedure for Fmoc-synthesis of Peptides:

Peptides were synthesized on solid-phase using a Tentagel Rink Amide Resin. Peptide synthesis was performed on a Prelude (Protein Technologies Incl., USA) or Symfony (Protein Technologies Inc., USA). All Fmoc-amino acids were purchased from Biosolve (Netherlands), Bachem GmbH (Germany) and Iris Biotech GMBH (Germany) with appropriate side-chain functionalities protected as N-t-Boc (KW), O-t-Bu (DESTY), N-Trt (HNQ), S-Trt (C) or N-Pbf (R) groups. All solvents used in peptide synthesis (piperidine, trifluoroacetic acid, NMP and DMF) were purchased from Biosolve (Netherlands) in peptide grade quality. Amino acids were dissolved in DMF (200 mM) and used as such. Piperidine was used as a 20% stock solution in NMP, HATU as a 0.4M stock solution in DMF, and DIPEA as a 2M stock solution in NMP. Standard amino acids were coupled via a single-coupling protocol (5-fold excess of HATU/amino acid (1:1) and 10-fold excess of DIPEA) with a reaction time of 15 min. Special amino acids are coupled with a double-coupling protocol (2.5-fold excess of HATU/amino (1:1) acid and 5-fold excess of DIPEA) with a reaction time of 30 min. In case of difficult amino acid couplings, e.g. R, K and C, the double-coupling protocol (10-fold excess of HATU/amino acid (1:1) and 20-fold excess of DIPEA) with a reaction time of 2 x 15 min was used. Acetylation (Ac) of the N-terminus of the peptide was performed by reacting the resin with NMP/Ac$_2$O/DIPEA (10:1:0.1) for 30min. at rt. Acetylated peptides were cleaved from the resin by reaction with a cocktail of TFA/MilliQ-H$_2$O/thioanisole/DODT/TIS (85:5:2.5:5:2.5), or TFA/MilliQ/thioanisole/TIS/Phenol (80:2.5:5:2.5:2.5:7.5) for 2h at rt.

Precipitation of peptides with Et$_2$O/pentane (1:1) followed by lyophilization of the precipitated peptide afforded the crude peptides. Purification of crude peptides was performed by reversed-phase HPLC (mobile phase consists of gradient mixture of eluent-A (MilliQ-H$_2$O containing 0.05% TFA) and eluent-B (MeCN containing 0.05% TFA).

2.8.4 UPLC Analysis and Sample Preparation

2.8.4.1 Peptides

Approximately 0.2 mg of peptide was dissolved in 100μL of 1:1 MeCN: MilliQ-H$_2$O. 10 μL of this solution was diluted with 50 μL of MilliQ-H$_2$O. For analysis, 6 μL was injected onto the UPLC column (C18). Gradient 5-55% MeCN in MilliQ-H$_2$O, 2 min gradient.

2.8.4.2 Reaction Mixtures in MeCN: MilliQ-H$_2$O Solvent Mixtures

20 μL of sample was diluted with 40 μL MilliQ-H$_2$O, and filtered over a pipet-tip frit filter. For analysis, 6 μL was injected onto the UPLC column. Gradient 5-55% MeCN in MilliQ-H$_2$O, 2 min gradient.

2.8.4.3 Reaction Mixtures in DMSO: MilliQ-H$_2$O Solvent Mixtures

30 µL of sample was diluted with 30 µL MilliQ-H$_2$O and filtered over a pipet-tip frit filter. For analysis, 8 µL was injected onto the UPLC column. Gradient 5-55% MeCN in MilliQ-H$_2$O, 2 min gradient.

2.8.5 General CLiPS - Oxime Ligation Cyclization Procedure

In a glass vial (5 mL), the peptide (0.2 mg) was dissolved in DMSO/MilliQ-H$_2$O (1:1) at a concentration of 0.50 mM. The scaffold (1-2 mg/100µL) was added with roughly one molar equivalent relative to the peptide, whereby the peptide weight was taken uncorrected for any TFA-salts present in the lyophilized material (T4-C2 at 0.95 equiv, T4-C3 at 1.05 equiv). A solution of 1M NH$_4$HCO$_3$ was added to reach pH > 8 (30 µL). The reaction mixture was analyzed after 20 min. Upon completion, the reaction mixture was acidified with a 15% TFA solution in MilliQ-H$_2$O (volume of base + 20%, generally 40 µL), to liberate the aldehydes. Oxime ligation occurred simultaneously. The reaction mixture was analyzed at certain time intervals, until the reaction had completed.

2.8.6 Isolated Tricycle 2-hS(ONH$_2$)$^{ter,\ n3}$∩T4-C3$^{C/O}$

In a glass vial (50 mL), peptide **2**-hS(ONH$_2$)$^{ter,\ n3}$ (5.34 mg, 3.36 µmol) was dissolved in 6.70 mL DMSO/MilliQ-H$_2$O (1:1) at a concentration of 0.50 mM. The scaffold T4-C3 (0.85 equiv, 86.51 µL of a 2.16 mg in 100 µL solution) was added. 150 µL of 1M NH$_4$HCO$_3$ solution was added to reach pH >8. The reaction mixture was analyzed after 30 min, showing complete formation of **2**-hS(ONH$_2$)^{ter,n3}∩T4-C3^C. The reaction mixture was acidified with a 15% TFA solution (200 µL), to liberate the aldehydes. The reaction mixture showed complete formation of **2**-hS(ONH$_2$)^{ter,n3}∩T4-C3$^{C/O}$ within 16h. Two products were obtained, with the same mass at t_R 1.27 and 1.30 min. (MW$_{calc}$ 1894.50, M1$_{found}$ 1894.58, M2$_{found}$ 1894.61)

Preparative HPLC purification of the two products was performed on a Supelco column (C5-C10), flow 8 mL/min, with phase A: MilliQ-H$_2$O + 0.05% TFA, and phase B: MeCN + 0.05% TFA. Purification was performed at rt (not the standard 50 °C).

The reaction mixture was diluted with MilliQ-H$_2$O to a final volume of 85 mL (4% DMSO). The peptide was loaded onto the column via a dilution method, where the reaction solution is taken as the mobile phase (2 mL/min). Once the loading peak of DMSO was completely off the column, the gradient was started (8 mL/min, 7 to 37% MeCN, over 35 min). Products started to elute after approximately 19 min. The fractions (~2 mL) were collected in 10 mL glass vials, analyzed by UPLC and lyophilized. Two products were isolated, with fractions 9 and 13 deemed the most representative of the two peaks (Figure 2. 20). All fractions were subsequently analyzed by UPLC. As can be seen in Figure 2. 21, all isolated fractions consisted of a 3:2 mixture of the two products. This phenomenon shows that the isolated products are able to interconvert, while the constituent products can still be separated on HPLC timescale. The amount of product was not measured, as separating them by UPLC was the objective.
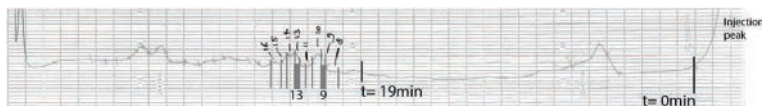

*Figure 2.20: Preparative HPLC chromatogram of the purification of **2**-hS(ONH$_2$)$^{ter,\ n3}$∩T4-C3$^{C/O}$*
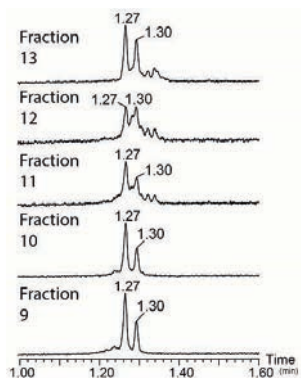
Figure 2.21: UPLC chromatograms of the fractions after separation of the two peaks of
2-*hS(ONH₂)*^{int,n3}∩**T4-C3**$^{C/O}$ *on preparative HPLC.*

2.9 References

(1)   Timmerman, P.; Beld, J.; Puijk, W. C.; Meloen, R. H. *ChemBioChem* **2005**, *6* (5), 821.

(2)   Smeenk, L. E. J.; Dailly, N.; Hiemstra, H.; Van Maarseveen, J. H.; Timmerman, P. *Org. Lett.* **2012**, *14* (5), 1194.

(3)   Chen, S.; Bertoldo, D.; Angelini, A.; Pojer, F.; Heinis, C. *Angew. Chemie - Int. Ed.* **2014**, *53* (6), 1602.

(4)   Haney, C. M.; Horne, W. S. *J. Pept. Sci.* **2014**, *20* (2), 108.

(5)   Jamieson, A. G.; Boutard, N.; Beauregard, K.; Bodas, M. S.; Ong, H.; Quiniou, C.; Chemtob, S.; Lubell, W. D. *J. Am. Chem. Soc.* **2009**, *131* (22), 7917.

(6)   Bernatowicz, M. S.; Matsueda, G. R. *Anal. Biochem.* **1986**, *155* (1), 95.

(7)   Fmoc-L-Lys(Boc2-Aoa)-OH from Iris Biotech GMBH catalogue https://www.iris-biotech.de/en/faa1955 (accessed Jan 18, 2019).

(8)   Chalker, J. M.; Gunnoo, S. B.; Boutureira, O.; Gerstberger, S. C.; Fernández-González, M.; Bernardes, G. J. L.; Griffin, L.; Hailu, H.; Schofield, C. J.; Davis, B. G. *Chem. Sci.* **2011**, *2* (9), 1666.

(9)   Dirksen, A.; Hackeng, T. M.; Dawson, P. E. *Angew. Chemie - Int. Ed.* **2006**, *45* (45), 7581.

(10)   Dirksen, A.; Dawson, P. E. *Bioconjug. Chem.* **2008**, *19* (12), 2543.

(11)   Agten, S. M.; Dawson, P. E.; Hackeng, T. M. *J. Pept. Sci.* **2016**, *22* (5), 271.

(12)   Smeenk, L. E. J.; Timmers-Parohi, D.; Benschop, J. J.; Puijk, W. C.; Hiemstra, H.; Van Maarseveen, J. H.; Timmerman, P. *ChemBioChem* **2015**, *16* (1), 91.

(13)   Pan, Y.; Ford, W. T. *J. Polym. Sci. Part A Polym. Chem.* **2000**, *38* (9), 1533.

(14)   Larroque, A. L.; Dubois, J.; Thoret, S.; Aubert, G.; Chiaroni, A.; Guéritte, F.; Guénard, D. *Bioorganic Med. Chem.* **2007**, *15* (1), 563.

(15)   Thieme, K.; Schnell, I. *J. Am. Chem. Soc.* **2003**, *125* (40), 12100.

(16)   Jayasekara, P. S.; Jacobson, K. A. *Synth. Commun.* **2014**, *44* (16), 2344.

Chapter 3:

Synthesis of Tricyclic Peptides via Strategy 2:

Aminooxy Group Functionalized Scaffolds and Ketone-Containing Peptides

3   Introduction

In this chapter, the results of scaffold-assisted synthesis of tricyclic peptides via the CLiPS reaction and oxime ligation will be discussed. As opposed to Chapter 2, the final oxime ligation reactions will be carried out using aminooxy group functionalized scaffolds and peptides bearing ketones in the side chains (Strategy 2). In other words, the key difference is the reversed orientation of the oxime ligation partners. The functionalities for the CLiPS reaction remain the same, meaning that the scaffold will bear electrophilic bromides and the peptide will be equipped with the nucleophilic cysteine thiolates. This means that *both* the scaffolds and peptides contain a combination of electrophilic as well as nucleophilic sites. As a consequence, protective groups will play a vital role in ensuring that the reactions proceed in an orderly fashion. This does, however, add additional steps to the reaction procedures.

3.1   Scaffold Design

In order to obtain tricyclic peptides via scaffold-assisted CLiPS and oxime ligation/cyclization reactions, the scaffolds should be equipped with the appropriate functionalities. For the CLiPS reactions, benzylic bromides or those derived from bromoacetamide were chosen. For oxime ligation, the scaffold was equipped with two identical aminooxy moieties. As a precaution, the aminooxy groups were protected by N-Boc groups to avoid reactions with the electrophilic bromides present in the same scaffold. Boc-protected derivatives of hydroxylamine have been developed and used in the Mitsunobu reaction to introduce aminooxy groups into compounds in a facile manner. The major drawback of using Boc-protection is the harsh, acidic conditions needed for removal. These conditions are, unfortunately, not compatible with a one-pot type procedure that we used in the previous consecutive CLiPS and oxime ligation reactions.

The scaffolds designed for Strategy 2 are complimentary to those used for Strategy 1, with the Boc-protected aminooxy groups replacing the acetal-protected aldehydes. The scaffolds are modular in nature, whereby the top of the scaffold is functionalized for the CLiPS reaction, while the bottom of the scaffold is functionalized for oxime ligation (Figure 3.1). The top and bottom parts are connected through a central amino function, at which the aminooxy functionalities are installed. The manner in which they are connected differs per scaffold. The first scaffold, T4-N1, is the most rigid of the three. This scaffold was inspired by the work of my predecessor, Linde Smeenk.[1,2] The scaffold comprises two benzylic bromides in *ortho* orientation for the CLiPS reaction. The amino group is connected to the phenyl ring via a pyrrolidine ring, thus forming a quaternary ammonium species. The aminooxy moieties are therefore perpendicular to the plane of the phenyl ring, thus making the scaffold prochiral. As a consequence, configurational isomers may be obtained upon reaction with a peptide.

Scaffolds T4-N2 and T4-N3 both feature an amide bond as the central connection between the CLiPS reactive part and the central amine. This rotatable bond introduces flexibility in the form of free rotation, thus avoiding isomer formation. The difference between these two scaffolds are the CLiPS reactive groups. Scaffold T4-N2 bears two benzylic bromides, in *meta* orientation, while scaffold T4-N3 contains the more flexible bromoacetamide moieties. While the bromoacetamides have a presumed lower reactivity compared to the benzylic bromides, the small tethers add flexibility to the system. Moreover, the amides might participate in hydrogen bonding with the peptide, which may further stabilize the conformation of the final multicyclic peptide constructs.[3] In summary, the three scaffolds exhibit different topologies, flexibility and reactivity.
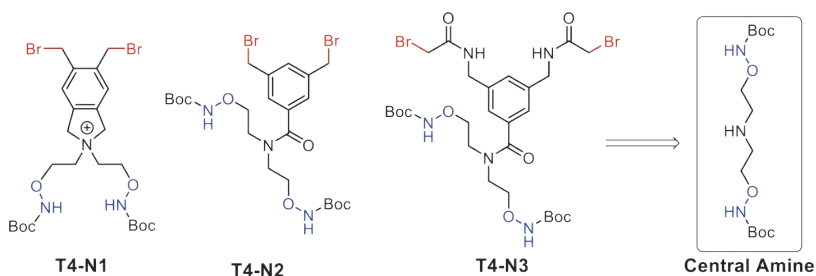
Figure 3.1: The scaffolds designed for Strategy 2 ligation-cyclizations, and the central amine on which all scaffolds are based.

3.2   Carbonyl-Functionalized Amino Acids

3.2.1   Aldehyde Amino Acids

The peptide must contain the complementary orthogonal reactive groups for oxime ligation, i.e. an aldehyde or ketone. For the CLiPS reaction, the peptide must bear two cysteines. Because aldehydes most likely will not result in the formation of *E/Z* isomers, in contrast to ketones, these were considered first. Peptide aldehydes have been explored extensively in the field of protein engineering and are usually used for labelling studies. For this, the aldehyde is incorporated in a masked form, and will become available after revealing the latent functionality by a reaction. The method most frequently used in protein chemistry is the sodium periodate (NaIO$_4$) mediated oxidation of vicinal 1,2-aminoalcohol moieties, originating from an N-terminal serine residue. The major drawback of this approach is the oxidative conditions under which the reaction takes place, especially for sensitive residues such as tryptophan, tyrosine or methionine.[4–6] Another method to introduce an aldehyde-containing amino acid is based on the oxidation of furan-containing peptides by singlet oxygen, pioneered by the group of Madder.[7–9] This process yields a 4-oxo-enal moiety, ready for oxime ligation. However, the oxidation of furan is often incompatible with free thiols of cysteine. The thioether motif, central in CLiPS chemistry, is also susceptible to oxidation, making oxidative methods incompatible with the CLiPS ligation method. Moreover, it is known that the shelf-life of aldehyde-bearing peptides is rather short,[10] requiring cumbersome (repeated) purification and limiting the applicability of these types of peptides.

3.2.2   Ketone amino acids

Because of the various difficulties associated with the synthesis of aldehyde-bearing peptides using our CLiPS/oxime approach, we turned our attention to amino acids bearing a ketone functionality. Multiple ketone-functionalized amino acids have been described in literature, indicating that there are fewer stability issues than for aldehyde amino acids. While there are more suitable options for ketone amino acids, their use has one major drawback compared to the aldehyde amino acids. Ketones are substituted at both sides, which can give rise to the formation of *E/Z* isomers of the formed oxime linkage.

Protein engineering, instead of conventional SPPS synthesis, has been the field where most ketone-bearing amino acids have been described. Pioneered by Schulz and coworkers, the ketone amino acid *para* acetyl phenylalanine (pAcF) was incorporated into a peptide using amber codon suppression.[11,12] Additionally, ketone-containing peptides have mostly been described in labelling studies, where they undergo oxime or hydrazone ligation to introduce a label.[13,14] The most important factor in labelling reactions is the efficiency of said ligation reaction. The configuration of the linkage, whether *E* or *Z*, is of no importance, and therefore often not detailed in publications. For the chemical synthesis

of peptides containing multiple ketone-bearing amino acids, several procedures have been described in literature. However, detailed syntheses of amino acids are not always described, while the cost of commercially available amino acids is generally very high. For this project, we were interested in an amino acid that could easily be synthesized on large scale, which was the case for pAcF (Figure 3.2).[11,12,15,16] Even though the *meta* analogue was described by Gao *et al.*, its synthesis was not high yielding and therefore not of interest for this project.[17] The acetyl-derived methyl group is expected to give *E/Z* mixtures when incorporated into an oxime bond. In order to prevent this, we also made an amino acid featuring the very bulky *tert*-butyl ketone, which are known to exclusively yield the *E*-isomer. Therefore, an aspartic acid derivative featuring a *tert*-butyl ketone, D(Ket) was developed for this project.
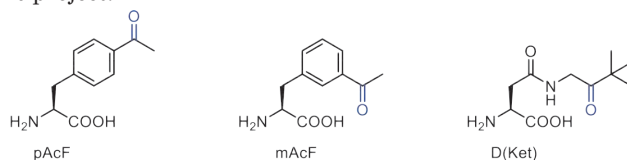

Figure 3.2: Proposed ketone-bearing amino acids (from left to right): para-acetylphenylalanine (pAcF), meta-acetylphenylalanine (mAcF), and tert-butylcarbonylmethylasparagine [D(Ket)].

To summarize, the synthesis of tricyclic peptides via CLiPS and oxime ligation reactions using Strategy 2 will be investigated in this chapter (Figure 3.3). First, the synthesis of the scaffolds and follow up reactivity studies are presented, followed by the synthesis of amino acids and peptides. Finally, the scaffolds are reacted with the peptides, ending this chapter with the synthesis of tricyclic peptides.
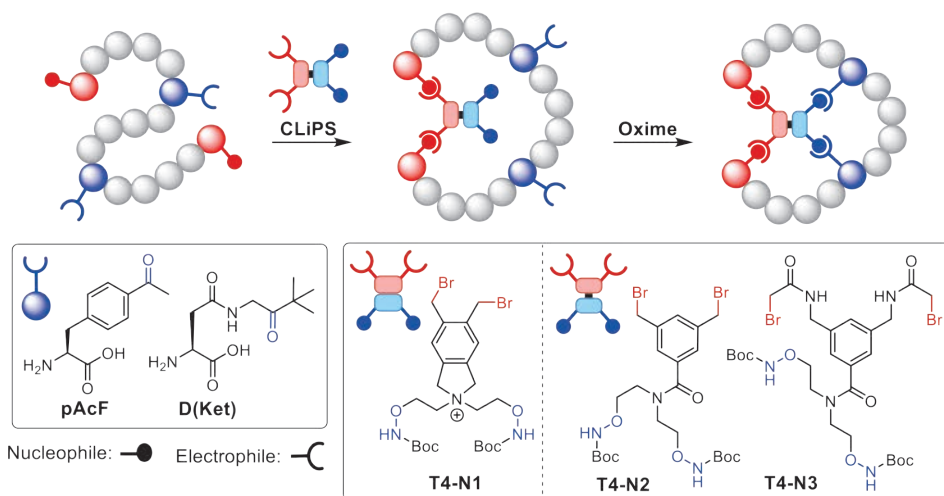

Figure 3.3: The proposed scaffolds and ketone amino acids for the synthesis of tricyclic peptides using Strategy 2.

3.3 Scaffold Synthesis

3.3.1 Synthesis of the Aminooxy-bearing Amine

The synthesis of the bis-aminooxy amine started from commercially available diethanolamine, where the central amine was first Cbz-protected by reaction with Cbz-Cl to obtain **2** in 68% yield (Scheme 3.1). The aminooxy moiety was introduced via a Mitsunobu reaction with *N,N*-di-Boc-hydroxylamine. Installation of the alkoxyamines was

performed by treating benzyl bis(2-hydroxyethyl)carbamate and Boc$_2$N-OH with PPh$_3$/DIAD to give benzyl bis(2-(bis(*tert*-butoxycarbonyl)aminoethyl)carbamate **3** in 61% isolated yield after purification. The second Boc-group on each aminooxy-group is only loosely bound and could therefore be removed by mild acidolysis using 4 equiv of TFA. Because of their reactivity towards nucleophiles, it was paramount that this 'second' Boc-group was removed *before* the amine was liberated via hydrogenolysis of the Cbz-group, as the loosely attached 'second' Boc group is easily transferred to the newly liberated amine. Removal of the Cbz group occurred uneventfully via Pd/C-catalyzed hydrogenolysis, yielding **4**. The O-N bond of the aminooxy has been described as being labile towards reductive cleavage, e.g. hydrogenolysis.[18] However, in our hands, O-N bond cleavage was never observed, nor any other instance of hydrogenolysis in presence of the aminooxy groups.
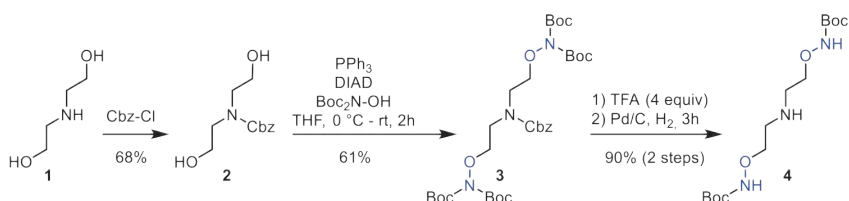
Scheme 3.1: Synthesis of the di-aminooxy-substituted amine for the T4-N-scaffolds.

3.3.2 Synthesis of Scaffold T4-N1

The aminooxy-bearing amine **4** was subsequently used to synthesize scaffold T4-N1. Similar to the synthesis of T4-C1, a double substitution reaction of amine **4** onto 1,2,4,5-tetrakis(bromomethyl)benzene **5** yielded the quaternary ammonium-based scaffold T4-N1 (Scheme 3.2). The reaction was carried out under high dilution, with an excess of **5** to ensure that only mono-substitution occurred. The excess was removed by column chromatography to give the pure scaffold in 64% isolated yield (Figure 3.4). The scaffold was obtained as a white foam, which was very hygroscopic. Additionally, the bromides were rather susceptible to hydrolysis. This unfortunate combination caused deterioration of the scaffold after prolonged storage in the freezer. It is therefore advisable to use this scaffold shortly after preparation.
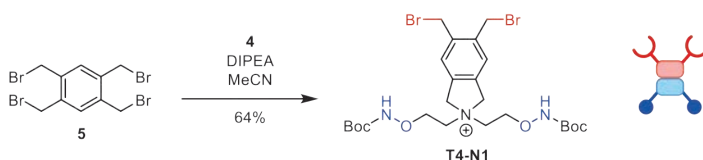
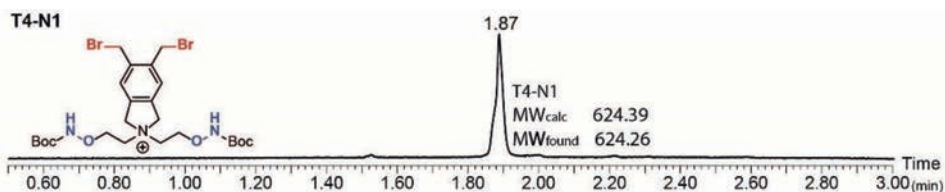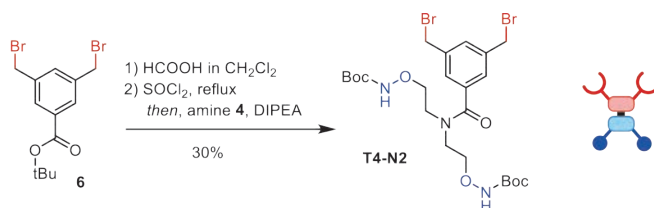*Scheme 3.2: Synthesis of scaffold T4-N1.*

Figure 3.4: UPLC chromatogram of scaffold T4-N1, eluting at t$_R$ 1.87 min.

3.3.3 Synthesis of Scaffold T4-N2

Synthesis of the two remaining scaffolds, containing the central linking amide, proceeded using the common intermediate *tert*-butyl 3,5-bis(bromomethyl)benzoate **6**, of which the synthesis has been discussed in Chapter 2. Scaffold T4-N2 was synthesized from this intermediate in two steps (Scheme 3.3). Liberation of the acid by acidolytic cleavage of the tBu-ester with formic acid was followed by activation and subsequent amide coupling. The method for activation was thoroughly investigated here, as activation with $SOCl_2$, used in Chapter 2, was found to cause halogen scrambling. Several alternatives for activation were tested (HATU, $SOBr_2$, oxalyl chloride and the OSu-ester), but, despite its drawbacks, $SOCl_2$ was the best activating method for this reaction. Scaffold T4-N2 was synthesized with an overall 30% yield starting from *tert*-butyl 3,5-bis(bromo-methyl)benzoate.

Scheme 3.3: Synthesis of the T4-N2 scaffold from the common intermediate tert-butyl 3,5-bis(bromomethyl)benzoate.

During the final amide coupling, halogen scrambling occurred. The extent of halide scrambling was determined via UPLC, where three products were observed (Figure 3.5). Table 3.1 shows the peak assignments, and the calculated fraction of each product. The batch chloride content was calculated at 13%. This determination was supported by ^{13}C NMR measurements, where the C-Br and C-Cl have very different chemical shifts. By using a long delay time between pulses, the signals could be reliably integrated.
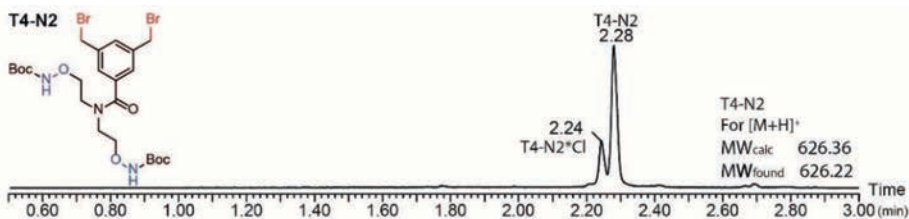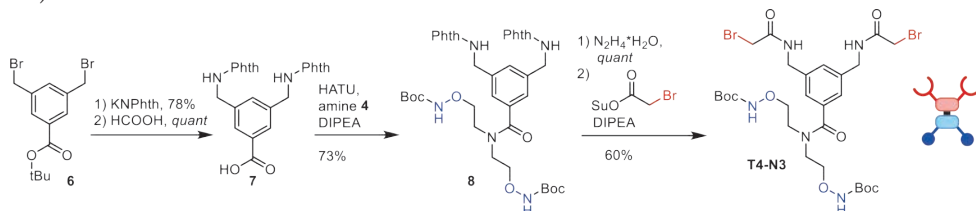

Figure 3.5: UPLC-MS chromatogram of T4-N2.

Table 3.1: Peak assignment of the T4-N2 scaffold, with the determination of chloride content.

Entry	t_R (min)	Halides	m/z found	m/z calc.	Ionized species	Fraction (%)
1	2.21	Cl-Cl	536.43	536.19	$[M+H]^+$	1.1
2	2.24	Cl-Br	580.31	580.14	$[M+H]^+$	23.3
3	2.28	Br-Br	626.22	626.36	$[M+H]^+$	75.5

3.3.4 Synthesis of Scaffold T4-N3

Synthesis of the final scaffold T4-N3 started from *tert*-butyl 3,5-bis(bromomethyl)benzoate (Scheme 3.4), utilizing a procedure similar to that for T4-C3 (Chapter 2). First, the bromides were transformed into phthalimide-protected amines using the Gabriel reaction in 78% yield. The benzoic acid was liberated and the aminooxy groups were introduced by HATU-mediated amide coupling with the central amine **4** in 73% yield over two steps.

Liberation of the amines proceeded quantitatively by hydrazinolysis followed by introduction of the bromoacetamide groups via reaction with bromoacetic acid-OSu ester, yielding the scaffold as a white powder. While synthesis of scaffold T4-N3 comprised the largest number of steps, every reaction in this sequence was robust and could be carried out on large scale. The scaffold was obtained in high purity and is bench-stable (Figure 3.6).

Scheme 3.4: The synthesis of T4-N3 from the common intermediate tert-butyl 3,5-bis(bromomethyl)benzoate. Phth = phthalimide.
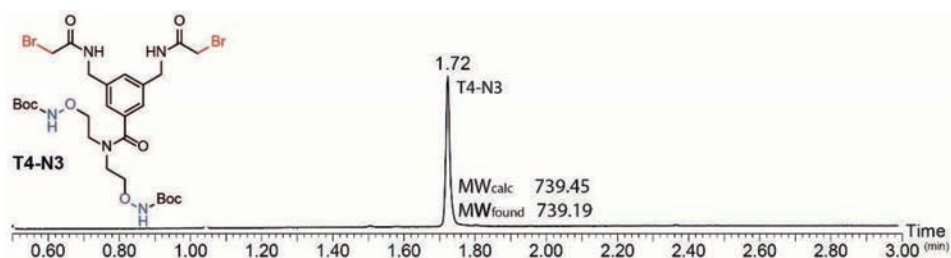

Figure 3.6: UPLC-MS chromatogram of the T4-N3 scaffold.

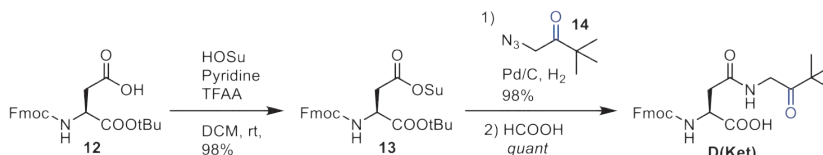## 3.4 Synthesis of Ketone-Bearing Amino Acids

3.4.1 pAcF

As outlined in the introduction, we decided to use ketone-bearing amino acids only as the oxime-partner for Strategy 2. However, the use of ketones could give rise to *E/Z* isomer formation. On the other hand, ketone-bearing amino acids are well described in literature, as is the case for the first amino acid, *para*-acetyl phenylalanine (pAcF). Following the procedure of Tasaku and coworkers, phenylalanine (H-F-OH) was protected at the C- and N-terminus, giving Ac-F-OEt (Scheme 3.5).[15] This starting material was easily prepared via acylation followed by esterification in 82% overall yield. Next, a Friedel-Crafts acylation was used to introduce the acetyl group selectively in a *para* fashion respective to the amino acid backbone on the phenyl-ring in high yield (**11**, 85%). Removal of all protecting groups under acidic conditions yielded the amino acid pAcF. In order to be useful for SPPS, the N-terminus was protected with the Fmoc group, which was performed as the final step in an almost quantitative yield over two steps. In addition to the high yields, only extractions and/or crystallizations were needed as purification methods, making this synthesis efficient and easy to perform. Moreover, this cheap and facile process was easily scaled up, starting with 50 grams of phenylalanine.
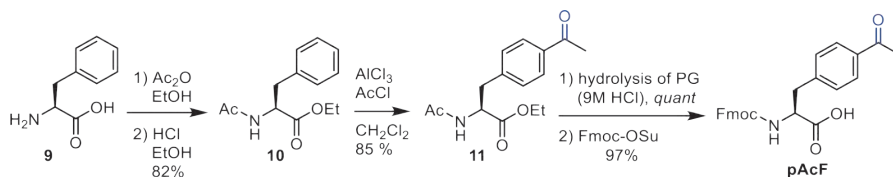
Scheme 3.5: Synthesis of pAcF from phenylalanine.

3.4.2   D(Ket)

The second amino acid, D(Ket), bearing a *tert*-butyl ketone designed to yield exclusively the E-configured oxime, was newly developed for this project. Its structure is based on aspartic acid, where the *tert*-butyl ketone was introduced at the side-chain (Scheme 3.6). Starting from Fmoc-D(OH)-O*t*Bu, the C-terminus remained protected during synthesis. First, the free side-chain carboxylic acid was activated as OSu-ester via the mixed anhydride method. The *tert*-butyl ketone bearing group was synthesized as the azide **14** using a literature procedure.[19] Subsequently, the azide was reduced *in situ* to the amine using Pd/C and H₂, and coupled with the activated ester in a one-pot procedure, thus yielding the amide. The amino acid was completed for incorporation via SPPS by liberating the C-terminus to the free acid, yielding D(Ket) in virtually quantitative yield over two steps. Synthesis of this new amino acid was facile, high yielding and did not require further chromatographic purification. The only downside to this route was the rather high cost of the starting *tert*-butyl ester. Efforts to use a different C-terminal ester were unsuccessful.

Scheme 3.6: Synthesis of Fmoc-D(tBu-ketone)-OH (D(Ket)) starting from aspartic acid.

3.5   Solid Phase Peptide Synthesis Using Ketone-Bearing Amino Acids

3.5.1   Test-syntheses with Peptides Containing pAcF and D(Ket)

The synthesis of peptides containing the amino acids pAcF or D(Ket) was performed next. However, very little is known in literature about incorporating these amino acids using SPPS. Publications referring to the incorporation of pAcF in peptides generally focus on genetic encoding experiments. One paper by Gao and co-workers described the incorporation of mAcF, the *meta* analogue of pAcF, using SPPS. Unfortunately, only 'general coupling procedures' were referenced without giving further details. Therefore, we decided to synthesize peptides using the Fmoc-based synthesis protocol, using HATU/DIPEA as the coupling reagent and piperidine as the reagent for the intermediate Fmoc-deprotection steps. A series of tripeptides was synthesized via manual SPPS using the aforementioned conditions (Table 3.2). These sequences were specifically chosen to test compatibility of the ketone amino acids with several different (nucleophilic) amino acids, bearing different protective groups.

The simple peptide **t1** was synthesized using manual SPPS, using standardized conditions mentioned before. All peptides synthesized were end-capped by N-terminal acylation and contained a C-terminal amide stemming from the Rink Amide resin. The final step in peptide synthesis was resin cleavage and global deprotection, which required strong acidic conditions. Many cocktails have been developed for this purpose, mostly based on TFA, and can contain different additives to scavenge remnants of protecting

groups and reduce side reactions. For **t1**, a resin cleavage cocktail was used containing TFA, H_2O, TIS, DODT and thioanisole, which was developed in house at Pepscan.

Table 3.2: Sequences of test-tripeptides containing pAcF and D(Ket).

#	Sequence	Reason for synthesis
t1	Ac-A-F-F-NH$_2$	Benchmark peptide
t2	Ac-A-pAcF-F-NH$_2$	pAcF reactivity
t3	Ac-C-pAcF-A-NH$_2$	C-Trt cleavage and side reactions
t4	Ac-C-C-pAcF-NH$_2$	C-related side reactions
t5	Ac-K-pAcF-A-NH$_2$	K(Boc) cleavage and side reactions
t6	Ac-E-pAcF-A-NH$_2$	E(OtBu) cleavage and side reactions
t7	Ac-A-D(Ket)-F-NH$_2$	Reactivity of D(Ket) amino acid

Peptide **t2** was synthesized using the same peptide coupling conditions. However, pAcF coupling nearly always gave a positive Kaiser test, meaning that free amines were still present on the resin. Even after four coupling cycles, the Kaiser test remained positive. The synthesis was continued, based on the general notion that four coupling cycles should be sufficient for full coupling. Subsequent coupling of alanine and acylation also yielded positive Kaiser tests, which led us to believe the Kaiser test was not reliable when pAcF was used in the peptide. The final step in peptide synthesis was the resin cleavage. In the Gao paper, the resin cleavage cocktail was described using TFA, H_2O, thioanisole, EDT and phenol. This cocktail was also used for the tripeptide **t2**. The cleaved peptide was lyophilized and the resulting white powder was analyzed via LC-MS. The UV-trace was rather clean, showing a major peak at t_R 6.59 min (Figure 3.7) with a corresponding MW$_{found}$ at m/z 543.1. Unfortunately, the calculated mass for Ac-A-pAcF-F-NH$_2$, is 467.5 ([M+H]$^+$). The MW$_{found}$ was 75.6 Da higher than the MW$_{calc}$, which corresponded to the addition of [EDT-H$_2$O]. The product was determined to be the thio-ketal of peptide **t2**, whereby EDT had reacted with the pAcF ketone functionality in the chain (Figure 3.8).
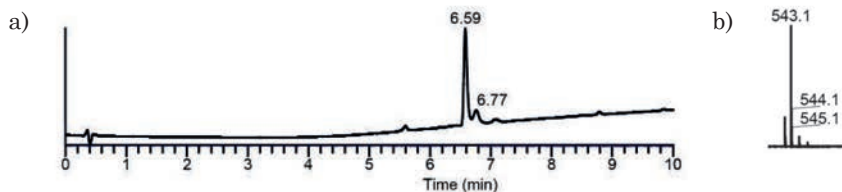

*Figure 3.7: a) LC-MS chromatogram of peptide **t2** after resin cleavage using the Gao cocktail, b) the corresponding mass spectrum.*

Chemical Formula: $C_{25}H_{30}N_4O_5$
Molecular Weight: 466.5380

Chemical Formula: $C_{27}H_{34}N_4O_4S_2$
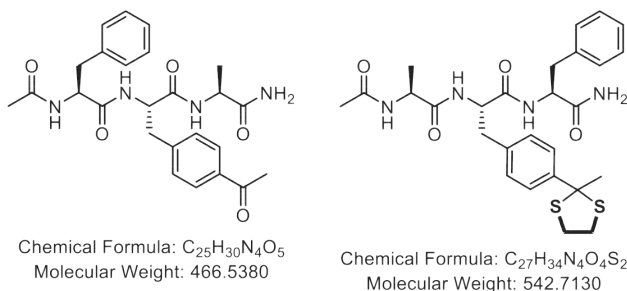Molecular Weight: 542.7130

*Figure 3.8: Structures of the peptide **t2** and the thio-ketal analogue of **t2** after reaction with EDT.*

Further confirmation of this structure was provided by ^{1}H NMR (see Figure 3.9). The spectrum showed only well-defined peaks and virtually no impurities. Nearly all peaks were annotated to the peptide, whereby the α- and β-protons of both F and pAcF overlap. The peaks denoted with ★ could not be ascribed to the peptide. The peak pattern and integral correspond to a -CH_2-CH_2- motif, originating from the thioketal ethylene. The upfield shift of the pAcF methyl group indicated that indeed the ketone had reacted. Due to the confirmed presence of the thioketal, we therefore turned to investigating thiol-free cleavage cocktails.
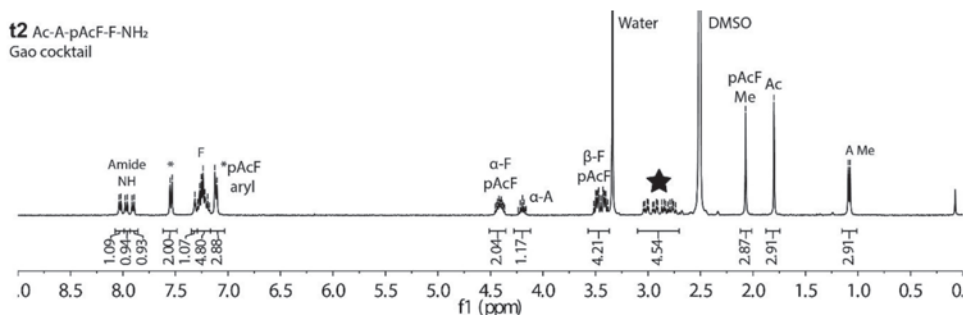

*Figure 3.9: ^{1}H NMR spectrum of **t2** in DMSO-d₆, after resin cleavage with the Gao cocktail. Annotations are provided in the spectrum.*

In literature, quite a large variety of peptide cleavage cocktails are described, depending on which amino acids are present in the peptide.[17,20] In Table 3.3, three additional cleavage cocktails and their components are presented, together with the Gao cocktail already tested.[20] The 'general' cocktail is often used for either very sensitive peptides or peptides that do not contain cysteines or special protecting groups that need scavenging. For the Gao group, the omission of TIS may be due to sensitivity of the pAcF ketone towards reduction. Resin cleavage cocktails devised for sensitive amino acids such as tryptophan, tyrosine and arginine often make use of thioanisole and a thiol-based scavenger.

Table 3.3: The different resin cleavage cocktails and their components (v/v).

Component	General	Gao	EDT-free Gao	Our Mix
TFA	95	80	82.5	80
MilliQ-H_2O	2.5	5	5	5
Thioanisole		5	5	5
TIS	2.5			2.5
EDT		2.5		
Phenol		7.5	7.5	7.5

Because the **t2** peptide reacted with EDT during the Gao cleavage conditions, several other cocktails were screened. First, the general cleavage mixture was tested. As can be seen in Figure 3.10, a more polar peptide was obtained compared to using the Gao cleavage cocktail (t_R 5.47 compared to t_R 6.59). Fortunately, the m/z value of 467.1 belonging to the major peak matched the desired product. A few additional peaks were found, but these could not be correlated to side reactions occurring on the pAcF functionality. Additionally, ^{1}H NMR analysis showed the presence of few impurities (not pictured).
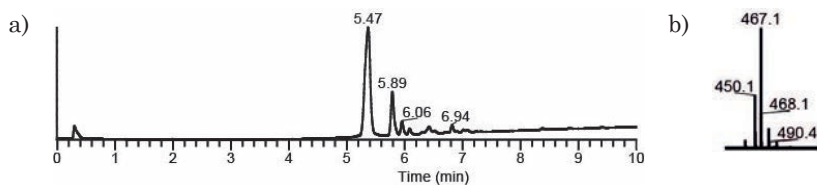
*Figure 3.10: a) LC-MS chromatogram of peptide **t2** after cleavage with the general cleavage cocktail. b) Mass spectrum of the main peak at t_R 5.47 min.*

Comparing the general mix and the Goa cocktail, the presence of phenol and thioanisole in the Gao mix yielded peptides of higher purity. Indeed, when the EDT-free Gao cocktail was used, a single product was obtained with a MW_{found} matching the MW_{calc} (Figure 3.11) without further impurities being present, which demonstrates that phenol or thioanisole significantly suppresses the formation of side products. Moreover, the ^{1}H NMR spectrum (Figure 3.12) corresponds to peptide **t2** and all expected proton resonances were observed. Clearly, the ketone functionality was intact given the apparent signal for the pAcF methyl peak at 2.52 ppm. Additionally, the β-protons of both the phenylalanine and pAcF were shifted upfield to around 2.9 ppm. The aryl protons from pAcF had both shifted downfield and were no longer flanking the F-aryl protons.
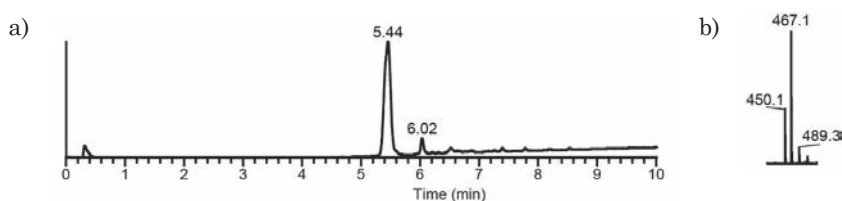

*Figure 3.11: a) LC-MS chromatogram of peptide **t2** after cleavage with EDT-free Gao cocktail. b) corresponding mass spectrum of the main peak at t_R 5.44 min.*
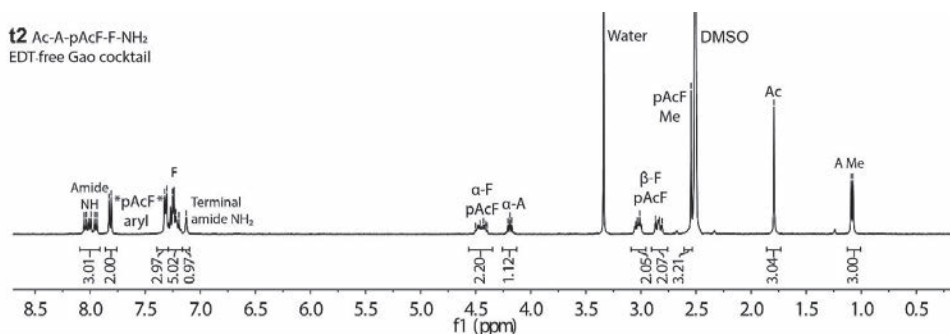

*Figure 3.12: ^{1}H NMR spectrum of **t2** in DMSO-d_6 after resin cleavage with the modified EDT-free Gao cocktail. Annotations are provided in the spectrum.*

Next, peptide **t3** (Ac-C-pAcF-A-NH₂), containing a cysteine residue requiring special treatment as it is S-Trt protected during solid-phase peptide synthesis, was prepared. During deprotection, the trityl cation requires a scavenger, usually in the form of a thiol-based molecule such as EDT, which is incompatible with pAcF. Therefore, resin cleavage was tested with the EDT-free Gao cocktail first. In the UV trace a clear major peak was observed at t_R 7.12 min (see Figure 3.13). However, this product shows very little ionization, with only a weak signal at m/z 687.4, corresponding to the [M+trityl+Na]⁺

cation. This shows that the trityl cation was not sufficiently scavenged and remained attached to the peptide. This was confirmed also by ^{1}H NMR by the appearance of a large multiplet peak in the aromatic region with integral of 17H, of which 15H belonged to the trityl group and 2H to pAcF (Figure 3.14, top).
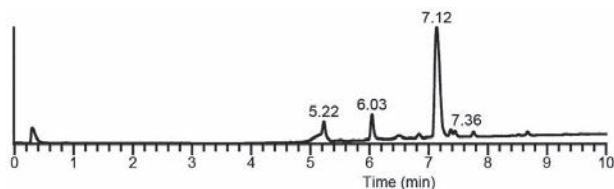

*Figure 3.13: LC-MS chromatogram of peptide **t3** Ac-C-pAcF-A-NH₂ after cleavage with the modified EDT-free Gao cleavage cocktail.*
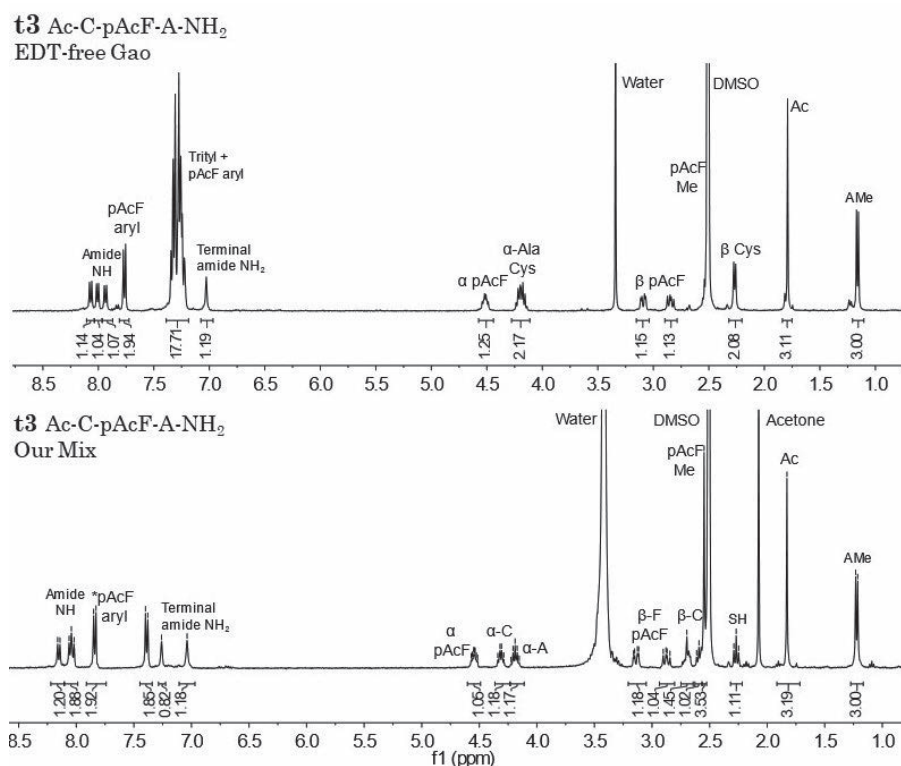
*Figure 3.14: ^{1}H NMR spectrum (in DMSO-d₆) of **t3** (Ac-Cys-pAcF-Ala-NH₂) after resin cleavage with (top) EDT-free Gao cocktail and (bottom) Our Mix with TIS. Peak annotations are given in the spectrum.*

It was evident that an adequate scavenger for the trityl cation was missing from the EDT-free Gao cocktail. While the general cocktail with TIS alone did not yield satisfactory results in previous tests, TIS was therefore added to the EDT-free Gao mixture, which contained phenol as a scavenger. The new cocktail was tested (see Table 3.3 for composition) and fortunately, LC-MS analysis showed that peptide **t3** was obtained as a single product with the correct mass, and the ^{1}H NMR spectrum also matched with formation of this product (Figure 3.14, bottom). The β-protons of cysteine were clearly

visible at 2.6 – 2.7 ppm (partly obscured by water). The cysteine SH was also visible as a triplet at 2.3 ppm. With the globally deprotected peptide in hands obtained in pure form, we also concluded that pAcF and cysteine are well compatible as side-reactions did not occur between the two functionalities. At this stage, it became apparent that the Kaiser test was incompatible with the presence of pAcF, yielding positive results for all subsequent couplings. The reason for this is unclear.

While the cysteine trityl protecting group is usually the most difficult to scavenge adequately, other commonly used amino acids and protecting groups were investigated as well. Primarily, it was determined whether the protecting groups could be removed using our new resin cleavage cocktail. Additionally, compatibility with pAcF and other (nucleophilic) residues was investigated. Peptide **t4**, containing two cysteines, showed similar purity compared to the single-cysteine peptide. The cysteine did not react with pAcF, which proved that the previously observed reaction between pAcF and thiols was due to the resin cleavage cocktail. The ketone of pAcF also did not undergo a side-reaction with the free amine of K, as could be concluded after the successful synthesis of peptide **t5**. Furthermore, full cleavage of the sidechain N-Boc group of K was achieved. The E-containing peptide **t6** abided by the same rules, as the tBu-group on the acid side-chain was removed and the peptide was obtained in good purity. Since most Fmoc-protected amino acids are side chain protected by either OtBu, tBu, Trt and Boc, this short study provided sufficient proof for peptide compatibility. Arginine which is commonly protected by a Pbf group, was not included in our study.

Finally, peptide **t7** (Ac-A-D(Ket)-F-NH₂) containing D(Ket) was synthesized. Once more, the Kaiser test yielded positive results in various stages of the synthesis, underlining reliability issues with this analysis technique for our system. After synthesis, resin cleavage was performed with our new mix. Figure 3.15 shows the ^{1}H NMR spectrum of peptide **t7** after lyophilizing, showing the characteristic tBu signal at 1.1 ppm. The signal for the CH₂ protons next to the ketone overlapped with the α-H proton signal of A. As proton exchange rates are higher in D₂O, the amide NH protons did not show up, except for the terminal NH₂ protons, which resonate at 7.6 and 7.9 ppm. This result confirmed that the selected peptide synthesis conditions, as well as resin cleavage conditions, are suitable for this amino acid too.
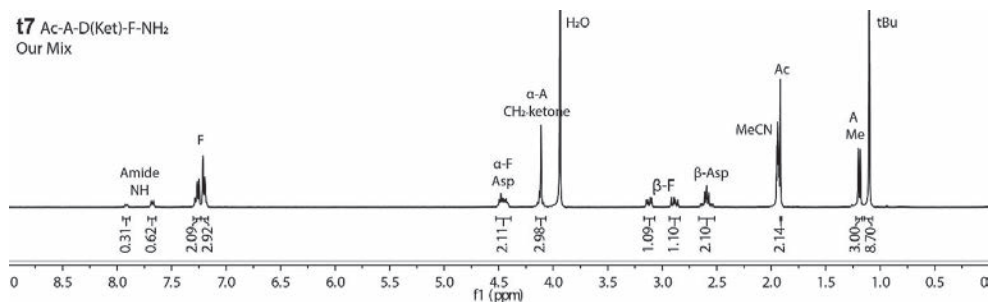
*Figure 3.15: ^{1}H NMR spectrum in CD₃CN:D₂O of **t7** (Ac-A-D(Ket)-F-NH₂) after resin cleavage with our new mix. Peak annotations are given in the spectrum.*

3.5.2 SPPS of Larger Peptides for CLiPS and Oxime Ligation

For the synthesis of tricyclic peptides, linear precursor peptides had to be prepared which contain two cysteines, as well as two ketone-bearing amino acids: pAcF or D(Ket). In Table 3.4, the sequences are presented, with analytical data in Table 3.5. The distance between these functional residues in the loops was varied from 3 to 5 amino acids.

Similar to the peptides for Strategy 1, the sequences of the peptides were not designed with specific biological targets in mind. Instead, residues were included with specific physical properties. Phenylalanine was chosen for UV-activity, lysine for optimal ionization in the mass spectrometer, while acidic residues such as glutamic and aspartic acid were chosen to increase polarity and solubility. Proline, as a turn-inducing amino acid, was introduced in the larger peptides only (loop size 5), because it is expected that in these cases the resulting conformational disturbance will have a smaller effect on the outcome of the cyclization reaction. Methionine was omitted from this screening, as it is known to be disruptive in the CLiPS reaction. Ketone-functionalized amino acid residues and cysteine were placed either at the termini or in the middle of the peptide. All peptide loops were equally sized, resulting in loop sizes of 3x3x3, 4x4x4 or 5x5x5 residues.

The peptides are named in such a way that the key properties of the peptide are explained. The peptide number is followed by the key functional amino acid, either pAcF or D(Ket). The suffix describes the location of the functional amino acid in the peptide sequence (*int*ernal or *ter*minal) and the loopsize (n=1,2,3,4,5) of the peptide. In this manner, the key characteristics of the peptide are denoted, aiding comparison in the later discussions.

Table 3.4: Peptides synthesized for Strategy 2, denoted by their code and sequence.

Code	Sequence
1-pAcF^{int,n1}	Ac-C**E{pAcF}**A**{pAcF}**KC-NH$_2$
2-pAcF^{int,n2}	Ac-C**EK{pAcF}**AS**{pAcF}**KDC-NH$_2$
3-pAcF^{ter,n3}	Ac-**{pAcF}**EWF**C**SIK**C**LKG**{pAcF}**-NH$_2$
4-pAcF^{int,n4}	Ac-**C**NRKF**{pAcF}**TDAV**{pAcF}**KLHS**C**-NH$_2$
5-pAcF^{int,n4}	Ac-**C**ERKF**{pAcF}**SGAV**{pAcF}**KLYS**C**-NH$_2$
6-pAcF^{ter,n4}	Ac-**{pAcF}**ERKF**C**SGAV**C**KLYS**{pAcF}**-NH$_2$
7-pAcF^{int,n5}	Ac-**C**EQFRK**{pAcF}**TPVKI**{pAcF}**SRAYG**C**-NH$_2$
8-pAcF^{ter,n5}	Ac-**{pAcF}**EQFRK**C**TPVKI**C**SRAYG**{pAcF}**-NH$_2$
9-pAcF^{alt,n5}	Ac-**C**EQFRK**{pAcF}**TPVKI**C**SRAYG**{pAcF}**-NH$_2$
10-D(Ket)^{int,n3}	Ac-**C**EWF**{D(Ket)}**SIK**D(Ket)**LKG**C**-NH$_2$
11-D(Ket)^{ter,n3} *	Ac-**{D(Ket)}**EWF**C**SIK**C**LKG**{D(Ket)}**-NH$_2$
12-D(Ket)^{int,n4}	Ac-**C**ERKF**{D(Ket)}**SGAV**{D(Ket)}**KLYS**C**-NH$_2$
13-D(Ket)^{ter,n4}	Ac-**{D(Ket)}**ERKF**C**TDAV**C**KLHS**{D(Ket)}**-NH$_2$
14-D(Ket)^{ter,n4}	Ac-**{D(Ket)}**ERKF**C**SGAV**C**KLYS**{D(Ket)}**-NH$_2$
15-D(Ket)^{int,n5}	Ac-**C**EQFRK**{D(Ket)}**TPVKI**{D(Ket)}**SRAYG**C**-NH$_2$
16-D(Ket)^{ter,n5}	Ac-**{D(Ket)}**EQFRK**C**TPVKI**C**SRAYG**{D(Ket)}**-NH$_2$

* The peptide suffered a deletion of D(ket). Synthesis was not repeated.

Instead of manual synthesis, the larger peptides were synthesized using automated SPPS. The conditions for peptide synthesis, especially resin cleavage and global deprotection, were thoroughly investigated using small peptides. These conditions were applied without alteration. Generally, the crude peptides for both pAcF and D(Ket) were already of acceptable quality. However, since the goal of this project is to meticulously monitor the reactions, all peptides were purified using preparative HPLC, thereby sacrificing the isolated yield. Unfortunately, peptide **11**-D(Ket)^{ter,n3} was not obtained as expected and suffered from deletion of one D(Ket). Although deletions of this amino acid were not observed for the other synthesized peptides, its relative bulkiness may explain this. Because the deletion was supposed to be sequence-dependent, it was decided to not attempt resynthesis of this peptide. Obviously, this peptide was not subjected to the CLiPS and oxime ligation cyclization reactions.

Table 3.5: The ketone-containing peptides synthesized for strategy 2, with retention times and mass data recorded on UPLC-MS, and their isolated yield

Code	t_R (min)	MW calc (Da)	MW found (Da)	Isolated Yield
1-pAcF[int,n2]	nd	972.34	972.14	H
2-pAcF[int,n2]	nd	1258.47	1258.45	H
3-pAcF[ter,n3]	1.08	1733.36	1733.64	M
4-pAcF[int,n4]	1.01	2041.70	2041.78	G
5-pAcF[int,n4]	1.15	2010.68	2010.67	M
6-pAcF[ter,n4]	1.15	2010.68	2010.80	L
7-pAcF[int,n5]	1.07	2406.17	2406.39	G
8-pAcF[int,n5]	1.06	2406.17	2406.58	G
9-pAcF[alt,n4]	1.08	2406.17	2406.76	M
10-D(Ket)[int,n3]	1.54	1779.49	1779.26	H
11-D(Ket)[ter,n3] #	1.48	1567.15	1567.50	G
12-D(Ket)[int,n4]	1.20	2056.74	2056.80	M
13-D(Ket)[ter,n4]	1.08	2102.77	2102.92	G
14-D(Ket)[ter,n4]	1.17	2056.74	2056.71	H
15-D(Ket)[int,n5]	1.08	2452.23	2452.70	M
16-D(Ket)[ter,n5]	1.12	2452.23	2452.78	G

Peptides were synthesized on Tentagel Rink-amide resin. Isolated yield after purification: Low (L), 1-5%, Moderate (M), 5-20%, Good (G), 20-35%, High (H), 35-50%. Retention time and mass were determined via UPLC-MS. #The peptide suffered a deletion of D(ket). Synthesis was not repeated.

3.6   Model Reactions

3.6.1   Test-reactions with T4-N1

To test the first CLiPS reactions, scaffold T4-N1 was reacted with glutathione (GSH), a tripeptide containing cysteine, providing the thiolate nucleophile. Addition of an excess of GSH was required for the reaction to reach full conversion (Figure 3.16). Moreover, the *ortho*-orientation of the bromomethyl functionalities significantly influenced the course of the reaction, as full conversion to GSH∩T4-N1[C] was impeded by intramolecular nucleophilic attack of the thioether sulfur atom within mono-CLiPSed product at the remaining bromomethyl group on the scaffold.[21] This was observed for the scaffold T4-C1 as well (Chapter 2). The resulting benzo-tetrahydrothiophene product eluted at t_R 1.08 min. Only when using a hundred-fold excess of GSH, the cyclization reaction was adequately suppressed.
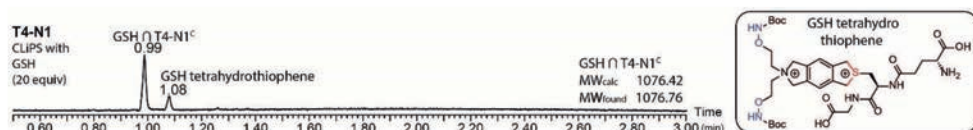

Figure 3.16: UPLC chromatogram of the reaction between GSH and T4-N1, yielding GSH∩T4-N1[C] at 0.99 and the GSH-benzotetrahydrothiophene side product at t_R 1.08 min.

These side-reactions could be overcome by the use of a peptide containing two cysteines. Indeed, when the model peptide **m1** (Ac-CEFAFKC-NH₂) was used in the CLiPS reaction, **m1**∩T4-N1[C] was obtained as the sole product (Figure 3.17a). The peptide was used in slight excess and, as a consequence, some disulfide and a small amount of linear peptide were still present in the reaction mixture at t_R 1.08 and 1.13 min, respectively. The intramolecular nature of this reaction circumvented the formation of side-products as observed for the mono-cysteine peptide GSH. As the model peptide **m1** did not contain any functionalized amino acids for oxime ligation, oxime ligation could only be tested in an intermolecular fashion

Next, the scaffold aminooxy moieties needed to be liberated. For this, after removal of the volatiles by lyophilization, neat TFA was added to the monocyclic peptide, to liberate the aminooxy moieties, resulting in a great polarity shift, to t_R 0.91 min (Figure 3.17b). After removing TFA via evaporation under a stream of nitrogen, the peptide was dissolved in an acetate buffer (pH 5) and acetone was added as a model ketone. The desired product **m1**∩T4-N1$^{C/O}$ (t_R 1.25 min) was formed quantitatively within an hour via reaction of the free aminooxy groups with acetone (Figure 3.17c). The only side-product observed was the peptide disulfide, which originated from the CLiPS reaction. This test reaction clearly proved that the envisioned reaction sequence of successive CLiPS, Boc-removal and oxime ligation, was indeed a feasible method to synthesize scaffolded peptide constructs.
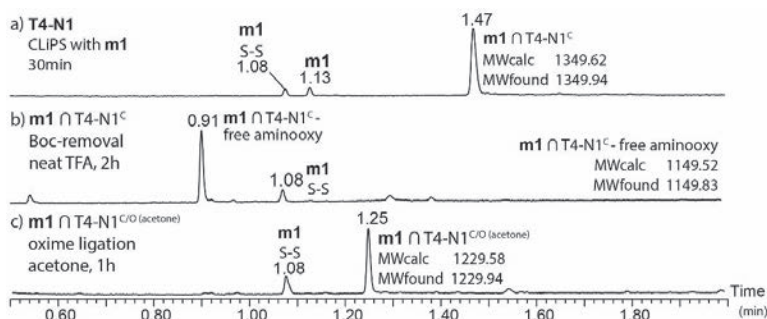

*Figure 3.17: UPLC chromatograms of the CLiPS/oxime reaction between **m1** and T4-N1, with a) CLiPS reaction, b) the subsequent liberation of the aminooxy moieties, and c) the oxime ligation with acetone.*

3.6.2 Test-reactions with T4-N2

The main design features of scaffold T4-N2 are the *meta*-oriented benzylic bromides and the rotatable amide bond connecting the aminooxy moieties to the central core. Scaffold T4-N2 was obtained as a mixture of bromide and chloride halides as a consequence of Br-Cl exchange during scaffold synthesis. The benzylic chloride is known to be less reactive than the benzylic bromide in the CLiPS reaction. The CLiPS reaction was tested using GSH as the thiolate source (Figure 3.18). The reaction went rather smooth, yielding GSH∩T4-N2^c as the main product at t_R 1.14 min. However, mono-CLiPS with the T4-N2*Cl scaffold was observed at t_R 1.51 min. Indeed, the chloride analogue of T4-N2 reacted slower and remained present after long reaction times. Twenty equivalents of GSH were needed to obtain this result, while further increasing the GSH concentration to 100 equivalents ensured that the remainder of the chloride-scaffold also reacted to completion. This supports the observation that benzylic chlorides are less reactive towards free cysteines than bromides.
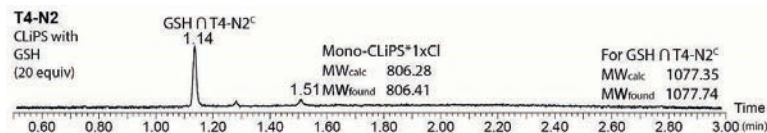

Figure 3.18: UPLC chromatogram of the CLiPS reaction between T4-N2 and GSH.

The lower reactivity of the chloride in the scaffold had resulted in reduced conversion to the fully CLiPSed product for a peptide with a single cysteine residue. However, the final peptides used in the CLiPS-reaction contain two cysteines, where the first reaction occurs *inter*molecularly, while the second reaction is an *intra*molecular cyclization. Indeed, when testing model peptide **m1** (Ac-**C**EFAFK**C**-NH₂), the intramolecular 'driving force' enabled

full conversion to the desired monocyclic peptide **m1**∩T4-N2^C within 30 min. Any oligomerization or side-product formations did not occur, demonstrating that the presence of a benzylic chlorides does not hamper the CLiPS cyclization reaction when performed with a peptide containing two cysteines (Figure 3.19a).

In order to test the CLiPS/oxime ligation sequence on the T4-N2 scaffold, the monocyclic CLiPS construct was subjected to the intermolecular oxime ligation, again using acetone as a symmetric model ketone. To continue with the oxime ligation, the CLiPS mixture was lyophilized and neat TFA was subsequently added to remove the Boc-groups, liberating the aminooxy moieties within two hours (Figure 3.19b). After removing TFA by evaporation, the peptide was dissolved in aqueous DMSO, and excess acetone was added. Oxime ligation occurred rapidly, and within an hour full conversion to the final product was reached (Figure 3.19c), demonstrating the scaffolds' suitability for our purposes in the synthesis of tricyclic peptides using CLiPS and oxime ligation.
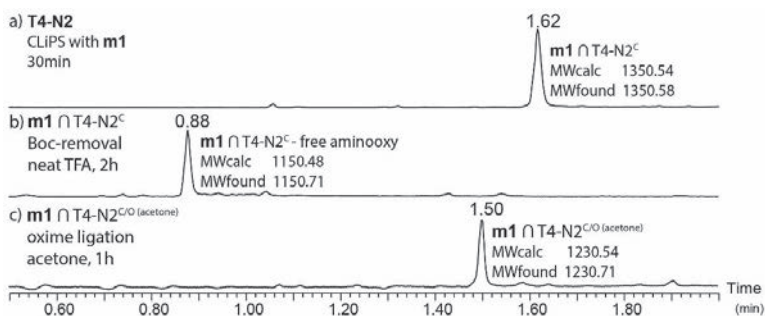

*Figure 3.19: UPLC chromatograms of the CLiPS/oxime reaction sequence between peptide **m1** and scaffold T4-N2, with a) the CLiPS reaction between **m1** and T4-N2, b) the subsequent liberation of the aminooxy moieties, and c) the oxime ligation of **m1**∩T4-N2^C with acetone.*

3.6.3   Test-reactions with T4-N3

Finally, the suitability of scaffold T4-N3, carrying two bromoacetamides, in the CLiPS reaction was investigated using GSH. Contrary to the other scaffolds in this chapter, only two equivalents of GSH were needed to reach full completion of the CLiPS reaction. Clearly, the high reactivity outperforms the other scaffolds (Figure 3.20). This is slightly ironic, as the bromoacetamide has been described by Heinis et al. as having the lower reactivity compared to the benzylic bromide.[3]
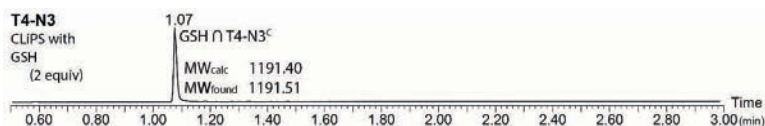

Figure 3.20: UPLC chromatogram of the CLiPS reaction between T4-N3 and GSH.

Finally, the CLiPS/oxime reaction sequence was tested using peptide **m1** (Ac-**C**EFAFK**C**-NH$_2$) as a model for the CLiPS reactions, while oxime ligation was performed with acetone as the ketone in an *inter*molecular fashion. The monocyclic peptide **m1**∩T4-N3^C was obtained in quantitative yield after the CLiPS reaction (Figure 3.21a). A slight excess of peptide was used, whereby some disulfide side-product was also obtained. Next, the reaction mixture was lyophilized and subsequently treated with neat TFA to liberate the scaffold aminooxy moieties, which were obtained quantitatively (Figure 3.21b), while the disulfide remained present. After evaporation of TFA under a stream of nitrogen, the construct was dissolved in aqueous acetonitrile and acetone was added to the reaction mixture. Oxime ligation reached completion after an hour, with the double oxime

product **m1**∩T4-N3$^{C/O(acetone)}$ as the main product (Figure 3.21c). These reactions showed the compatibility of this scaffold with our envisioned CLiPS and oxime ligation reactions to synthesize tricyclic peptides.
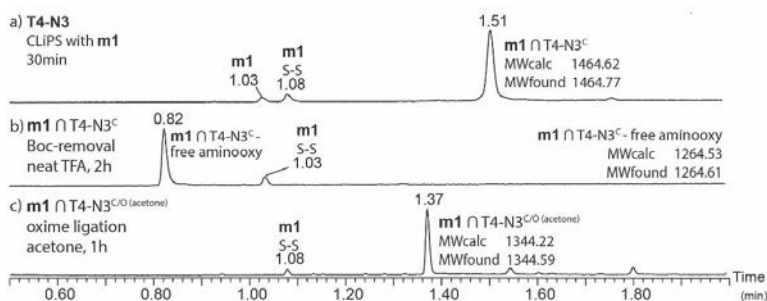

*Figure 3.21: UPLC chromatograms of the CLiPS/oxime reaction sequence for T4-N3 and peptide **m1**, with a) the CLiPS reaction, b) the liberation of the aminooxy moieties and c) the oxime ligation with acetone.*

3.6.4 Test-reactions with Peptides Containing Ketone-bearing Amino Acids - Intermolecular Oxime Ligation

To study the behavior of pAcF and D(Ket) when incorporated into peptides, their reactivity was tested first in an *inter*molecular oxime formation reaction with methoxyamine. This reactivity test was important as it; (1) shows whether the synthesized peptides indeed give oximes after reaction with an aminooxy moiety, and (2) may give insight into oxime bond *E*/*Z* isomer formation. As a result, a peptide with two ketone-bearing amino acid residues may give four *E*/*Z* oxime isomers. Firstly, peptide **7**-pAcF^{int,n5} was dissolved in aqueous MeCN (Figure 3.22a). In the UPLC-chromatogram, the peptide peak is accompanied by two small peaks of the same mass. An excess methoxyamine·HCl solution was added (Figure 3.22b) inducing a pH shift to ~pH 4. Therefore, addition of acidic reagents was not necessary to lower the pH and thus facilitate oxime ligation. After 16h, the oxime-product peak was visible at t_R 1.34 min. The product peak remained rather broad, and the two small accompanying peaks shifted along with the major product. Mass analysis confirmed that the double oxime was formed, with the satellite peaks showing the same mass. Because the product oxime was obtained as a single peak on UPLC, it may be concluded that oxime ligation did not yield any *E*/*Z* mixture. Although we expect the pAcF to have a preference for the *E*-isomer, the existence of the *Z*-isomer cannot be ruled out. Therefore, a mixture of *E*/*Z*-configured oximes may have been formed, which is not separable by UPLC, or which readily interconverts on UPLC timescale.

When benzylhydroxylamine (also as HCl-salt) was used as a bulkier oxime partner, we hoped that eventual *E*/*Z* oxime formation could be detected by UPLC-MS. However, the major observed difference was the much slower reaction rate (Figure 3.22c). After 16h, the reaction with BnONH$_2$ had reached only about 60% conversion to the bis-oxime. For both the mono- and bis-oxime product, the peak shape is similar to the MeONH$_2$ oxime. Moreover, a smaller peak eluting 0.05 min earlier than the major peak was observed for both the mono- and bis-oxime, showing the same mass. As the starting material also contained minor impurities with the same mass, the origin of these small peaks remained unclear as we cannot rule out isomer formation. Therefore, we cannot establish with certainty whether *E*/*Z* isomer formation occurred. We can, however, conclude that oxime ligation with the small nucleophile MeONH$_2$ is faster than with the bulkier nucleophile BnONH$_2$. Despite that, the slower reaction rate could also be a result of the lower nucleophilicity of BnONH$_2$, and not just a result of its size.
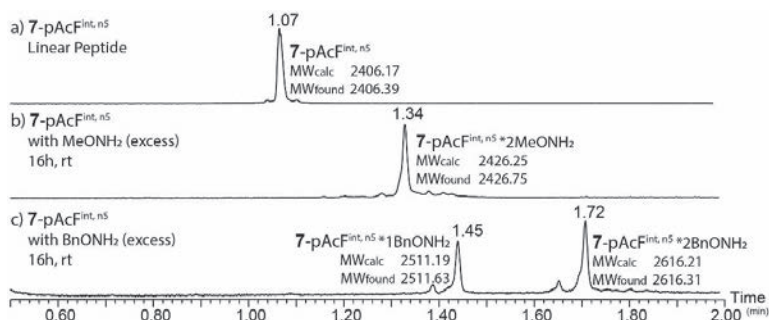
Figure 3.22: The intermolecular oxime ligation of 7-pAcF^{int,n5} (a) with b) methoxyamine and c) benzylhydroxylamine.

The D(Ket)-containing peptide **15**-D(Ket)^{int,n5}, was subjected to the same oxime ligation reactions with MeONH$_2$ and BnONH$_2$. The reaction with MeONH$_2$·HCl did occur, albeit very slowly (Figure 3.23a). The reaction mixture needed to be heated to 40 °C overnight before significant conversion to the mono-oxime was observed (▼, Figure 3.23b). The bis-oxime (★) took longer to form and after 3 days (Figure 3.23c) the conversion to the bis-oxime equaled that of the mono-oxime, albeit still some unreacted starting material was present. Even after 7 days at 40°C there was still starting material left, while only 75% conversion to the bis-oxime had been reached (Figure 3.23d). The peak shapes for the oxime products did not reveal any discernable *E/Z* isomerism of the oxime bond. The reaction was repeated with BnONH$_2$ (not shown), which proved to be extremely slow. Conversion to the bis-oxime had not reached significant levels after two weeks at an elevated temperature of 40°C, leading us to conclude that oxime ligation with D(Ket) was clearly significantly slower than for pAcF. Nevertheless, it should be emphasized that these experiments studied *inter*molecular oxime ligation. In our eventual endeavors to synthesize tricyclic peptides, oxime ligation will be performed in an entropically favored *intra*molecular fashion, where the reaction rate may differ significantly.
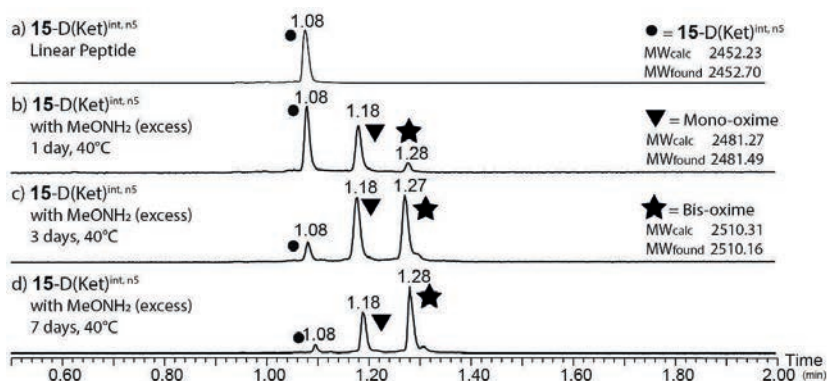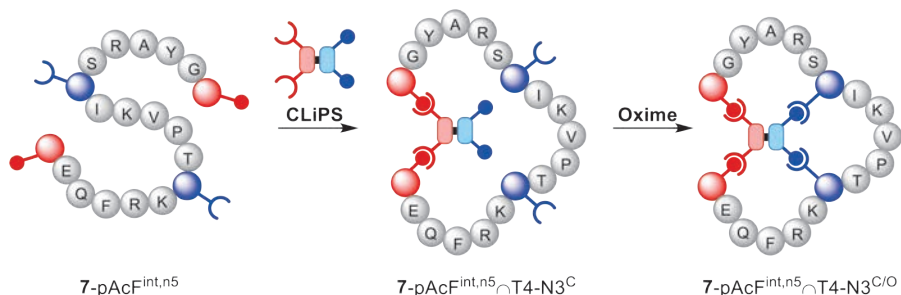

*Figure 3.23: The intermolecular oxime ligation of peptide **15**-D(Ket)^{int,n5} (a) with methoxyamine at 40 °C, after b) 1 day, c) 3 days and d) 7 days, with • being the starting material, ▼ the mono-oxime and ★ the bis-oxime product.*

3.7 Synthesis of Tricyclic Peptides

7-pAcF^{int,n5}   **7-pAcF^{int,n5}∩T4-N3^C**   **7-pAcF^{int,n5}∩T4-N3^{C/O}**

Scheme 3.7: The cartoon representation of the synthesis of the tricyclic peptide **7**-*pAcF^{int, n5}∩T4-N3^{C/O} from peptide* **7**-*pAcF^{int, n5} with scaffold T4-N3.*

In the previous sections, the successful synthesis of aminooxy-bearing T4-scaffolds and the complimentary ketone-bearing peptides were shown. Moreover, test-reactions confirmed the desired reactivity of all scaffold and peptide components. However, the peptide test reactions revealed the lower reactivity of the ketone-bearing amino acids, especially D(Ket), towards *inter*molecular oxime ligation, compared to the aminooxy-containing peptides explored in Strategy 1 (Chapter 2). However, we anticipate that for the synthesis of tricyclic peptides the fact that the double oxime ligation occurs in an *intra*molecular cyclization, will significantly increase the rate of the reaction.

For the synthesis of tricyclic peptides, all peptides were reacted with the three T4 scaffolds. First, they were subjected to the CLiPS reaction, followed by an intramolecular oxime cyclization reaction (see Scheme 3.7 for an example). The CLiPS reactions were carried out in aqueous MeCN (1:1 v/v, 0.5 mM), or in an aqueous DMSO solution if the peptide solubility was low. After addition of the scaffold, the pH was adjusted to pH ≈ 8 by addition of a 1M NH$_4$HCO$_3$ solution. The CLiPS reaction was performed with 1 equivalent of the scaffold with respect to the peptide. The amount of peptide used was not corrected for the presence of any TFA counter-ions, which lowers the actual peptide content, and the scaffold was usually added in a slight excess. Fortunately, the use of scaffold in excess was preferred, as the addition of peptide in excess results in disulfide formation, which forms a persistent product that hampers the analysis of further reactions.

Oxime ligation occurred spontaneously after liberation of the aminooxy moiety via Boc-removal. For this, TFA was removed under a stream of N$_2$, after which the construct was dissolved in aqueous DMSO, allowing oxime ligation to take place. DMSO was chosen as the solvent due to the superior results that were obtained for the peptide cyclizations as described in Chapter 2. Because the reaction mixture was slightly acidic by itself, most likely due to the formation of TFA-salt adducts of the peptide in the previous step, it was not necessary to add any additional buffer to reach the optimum pH for oxime ligation. While this stepwise reaction sequence comprises overall more steps, and could be considered more laborious, the protocol could be highly standardized. Additionally, this procedure enabled more flexibility with solvent choice, as different mixtures could be chosen at each step. For example, aqueous MeCN worked best for lyophiliziation after CLiPS, while DMSO was the solvent of choice for oxime ligation.

3.7.1 The CLiPS Reactions

During the test-reactions, we showed the typical behavior of the scaffolds during the CLiPS reactions. With the ketone-functionalized peptides, the behavior of all scaffolds was the same. Generally, the linear peptides were obtained in high quality, followed by a CLiPS reaction that yielded a single product. Disulfide formation of the starting peptide

and excess scaffold were observed as standard side-products. The oxime ligation was determined to be the most important step, where product distribution and isomer formation occurs.

In the next section, the cyclization reactions towards tricyclic peptides will be discussed per peptide, in reaction with each of the three different scaffolds. Because the CLiPS reaction is well established and performs as expected, we will focus on the oxime ligation step only. It is therefore important to note that the presented results are the culmination of a sequence of reactions, and not just a single reaction. By focusing only on the final reaction, the effects of the position of the amino acid and the peptide loop size can be better distinguished per peptide-scaffold combination.

3.7.2 Synthesis of Tricyclic Peptides using pAcF Peptides

First, peptides containing the non-canonical amino acid pAcF were studied, because this amino acid was described earlier in literature. Furthermore, pAcF contains a (relatively) sterically uncongested ketone moiety, which further promotes its reactivity. The first two peptides that were studied were **1**-pAcF^{int,n1} and **2**-pAcF^{int,n2}, with one and two amino acid loop peptides, respectively. For both peptides, the pAcF residues were installed in the middle of the peptide sequence. For these two peptides, only scaffolds T4-N1 and T4-N3 were tested. The results of the oxime ligation following the initial CLiPS reactions, are shown in Figure 3.24.
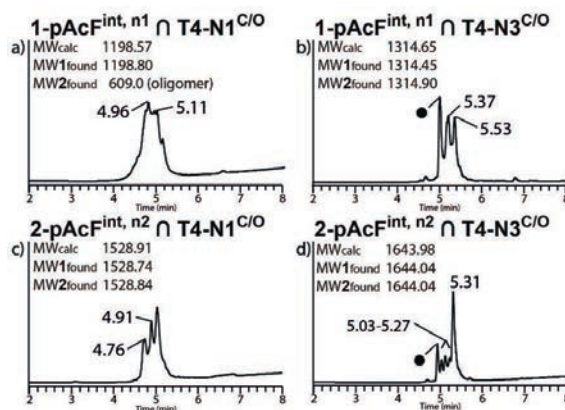

*Figure 3.24: LC chromatograms of peptides **1**-pAcF^{int,n1} (a,b) and **2**-pAcF$^{int\ n2}$ (c,d) in the cyclization with scaffolds T4-N1 and T4-N3. • denotes the disulfide of the starting peptide. Product MW's are denoted in chronological order of encounter.*

For **1**-pAcF^{int,n1}∩T4-N1, the tricyclic product appeared as a big blob, indicative of oligomerization. The mass of the desired product was observed, together with oligomeric species and mono-oxime products (where the second oxime ligation had not (yet) taken place). The rigid T4-N1 contains a quaternary ammonium moiety, which functions as a prochiral center. This, combined with the small peptide size, rendered a very constrained system where the functional residues cannot easily meet. Instead, oligomerization occurred readily, yielding such a broad LC trace.

Unwanted oligomerization was alleviated mostly by using the flexible T4-N3 scaffold. Aside from the disulfide of the starting peptide, two product peaks were obtained, both showing the mass of **1**-pAcF^{int,n1}∩T4-N3$^{C/O}$. From the previous studies of the Strategy 1 peptides, it was concluded that smaller and more constrained peptide loops give rise to increased rotamer formation. Therefore, the appearance of two products in the LC

chromatograms does not necessarily mean that ligation resulted in the formation of E/Z oxime mixtures.

For the slightly larger peptide **2**-pAcF[int,n2], the results were quite different. The reaction with scaffold T4-N1 yielded two noticeable tricycle products, alongside an unidentified product. Contrarily, with scaffold T4-N3 the product distribution became more complicated compared to the smaller peptide. Aside from the disulfide eluting at t_R 4.95 min, a major tricycle product peak was observed at t_R 5.31 min, accompanied by three minor products in the region 5.03-5.27 min. All mass traces corresponded to the expected tricyclic peptide. For this construct, the formation of E/Z oximes most likely contributed to the appearance of four products. However, due to the small peptide size, a contribution from hindered rotation can also not be ruled out.

Thereafter, peptide **3**-pAcF[ter,n3] with loopsize n=3 was investigated. By installing the pAcF amino acid at the more flexible peptide termini, predominant formation of the (thermodynamically) most favored oxime was expected. It has more flexibility and more opportunity to yield a thermodynamic oxime linkage compared to a kinetic 'proximity induced' oxime linkage for the internal ketone. The results of the oxime ligation are presented in Figure 3.25. Flexibility of the scaffold played an important role, and the number of products decreased with increasing flexibility of the scaffold. When the most rigid scaffold T4-N1 was used, three products were observed. The peak eluting at t_R 1.46 min. was rather broad, seemingly consisting of two overlapping products. In contrast, for the more flexible T4-N2 scaffold, tricyclic peptide **3**-pAcF[ter,n3]∩T4-N2[C/O] was obtained as two rather broad product peaks in the UPLC chromatogram. The broadness suggests a possible rotational barrier, whereby multiple rotamers are in a slow equilibrium on UPLC timescale. Finally, the increased flexibility of scaffold T4-N3 yielded a sharp UPLC peak for the major product at t_R 1.55 min, together with a minor product peak of low intensity, at t_R 1.54 min. This minor product could be a rotamer or an E/Z isomer.
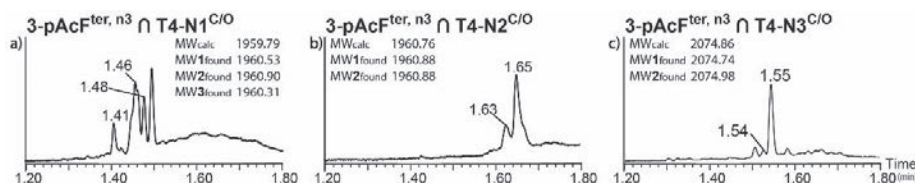

*Figure 3.25: UPLC chromatograms of the tricyclic peptide products from peptide **3**-pAcF[int, n2] with scaffolds T4-N1, -N2 and -N3. Product MW's are denoted in chronological order of encounter.*

Next, the three peptides with loop sizes of four amino acid residues were cyclized by the combined CLiPS/oxime ligation-cyclization. Both peptides **4** and **5** contain pAcF internally, while peptide **6** features pAcF at the termini. The results of the oxime ligation reactions are shown in Figure 3.26. When comparing peptides **4** and **5** (Figure 3.26 rows 1 and 2), it seems that the amino acid composition of the peptide did not significantly influence the cyclization. For example, both peptides yielded four products with the rigid scaffold T4-N1 (Figure 3.26a,d). In combination with scaffold T4-N2, both peptides yielded a clear major product, preceded by a minor product. For scaffold T4-N3, the UPLC chromatogram showed a single product, with a small trace of an isomeric product for **4**-pAcF[int,n4]∩T4-N3[C/O] eluting at t_R 1.03 min.

For peptide **6**-pAcF[ter,n4], where pAcF was installed at the termini, cyclization with the very rigid T4-N1 scaffold yielded a clear major product – which had not been observed previously for this scaffold (Figure 3.26g). In addition, two other small peaks with the same mass were observed, eluting at t_R 1.05 and 1.14 min. respectively. Cyclization of peptide **6**-pAcF[ter,n4] with scaffolds T4-N2 and T4-N3 gave single products in both cases (Figure 3.26h,i). For this set, the position of the amino acid in the peptide influenced

success in the cyclization the most, with terminally installed pAcF giving the best results. Additionally, scaffold flexibility aided the cyclizations, and therefore scaffolds T4-N2 and T4-N3 gave the cleanest reactions.
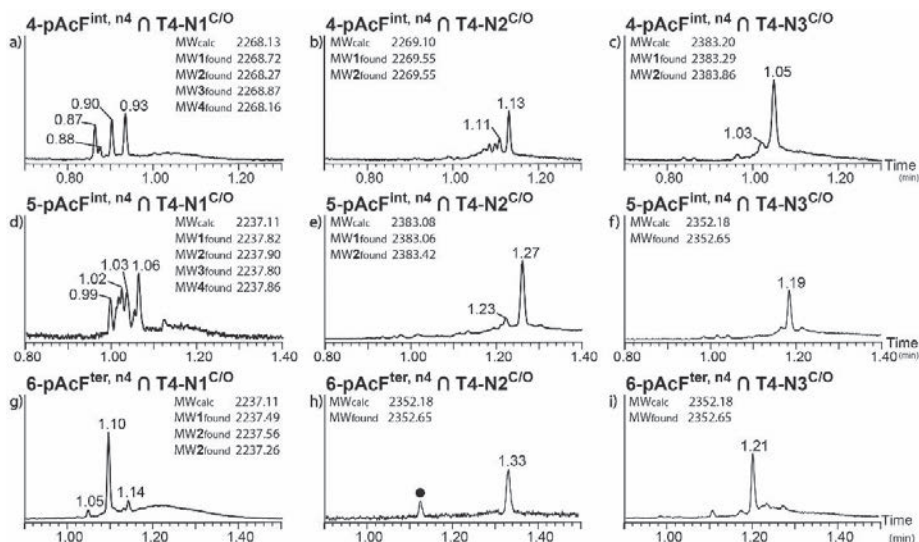

Figure 3.26: UPLC chromatograms of tricyclic peptide products from pAcF n=4 peptides with scaffolds T4-N1 ,-N2 and -N3. • denotes the disulfide of the starting peptide. Product MW's are denoted in chronological order of encounter.

Finally, the longest peptides with loop sizes of five amino acids (n=5) were tested (Figure 3.27). For this series, peptide **9**-pAcF[alt,n5] contained alternating functional residues with the motif C-pAcF-C-pAcF besides the more traditional peptides **7**-pAcF[int,n5] and **8**-pAcF[ter,n5] with internally and terminally installed pAcF amino acids. Tricyclic peptides **7**-pAcF[int,n5]∩T4-N1[C/O] (Figure 3.27a) and **7**-pAcF[int,n5]∩T4-N2[C/O] (Figure 3.27b) showed comparative peak broadening in the UPLC chromatograms. For both scaffolds, the peptide had not fully reacted in the CLiPS reaction, giving rise to a latent disulfide. Tricyclic peptide **7**-pAcF[int,n5]∩T4-N3[C/O] eluted as a main peak flanked by two smaller peaks. For tricycle **8**-pAcF[ter,n5]∩T4-N1[C/O], the four products were more defined, yet the overall elevated baseline bump from t_R 1.04 min and onwards suggests that some oligomerization occurred (Figure 3.27d). Some baseline elevation was noted for peptide **8**-pAcF[ter,n5]∩T4-N2[C/O], where a major and minor product peak were observed in the UPLC chromatogram. The reactions with scaffold T4-N3 yielded **8**-pAcF[ter,n5]∩T4-N3[C/O] as a single tricyclic product.

Lastly, the results for the pAcF/Cys alternating peptide **9**-pAcF[alt,n5] are shown in Figure 3.27g,h,i. The scaffolds' AABB pattern does not match with the peptides' ABAB sequence. Therefore, this peptide/scaffold-combination will test the adaptability of the scaffold and peptide. For the rigid scaffold T4-N1 and the moderately flexible scaffold T4-N2, there was no sign of a favorable adapted conformation, resulting in three or four broad product peaks in UPLC. The low intensity of the peaks was indicative of aggregation and subsequent oligomerization. Surprisingly, the most flexible scaffold T4-N3 yielded a major product for **9**-pAcF[alt,n5]∩T4-N3[C/O], accompanied by traces of isomeric products. Obviously, the mismatched ABAB peptide sequence is not a desirable design element as the cyclization results show mostly oligomerization. However, these results again show the importance of flexibility in the cyclization success, which can be introduced by using peptide precursors with a sufficiently large loop-size.
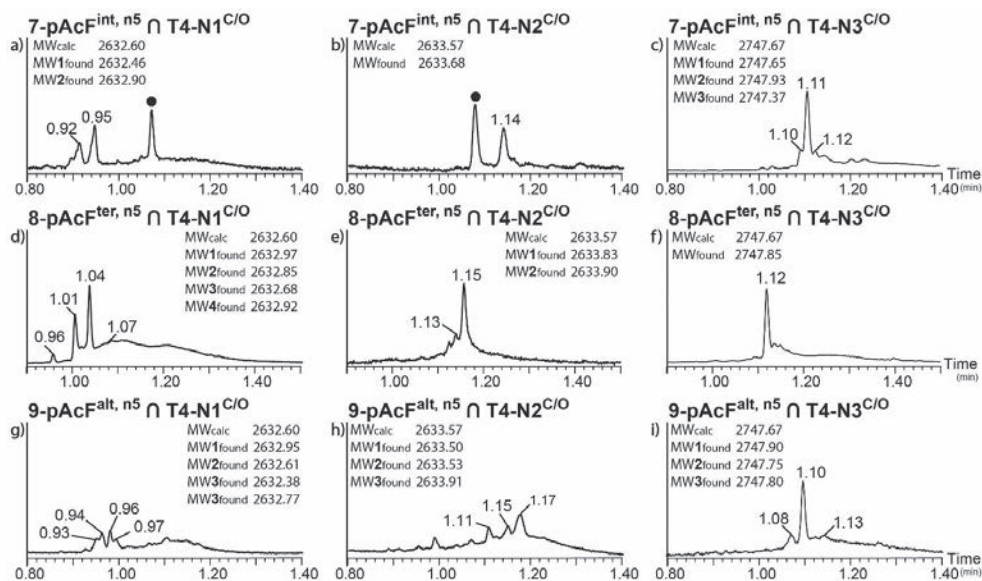
Figure 3.27: UPLC chromatograms of tricyclic peptide products from pAcF n=5 peptides with scaffolds T4-N1, -N2 and -N3. •disulfide of starting peptide. Product MW's are denoted in chronological order of encounter.

With the completed cyclization of all pAcF-containing peptides, it can be concluded that the position of the pAcF amino acids in the peptide has a large effect on the cyclization efficiency. Generally, installing the pAcF residues at the termini yielded fewer isomers, but only if the peptide contained more than two amino acids in the loop. The scaffold flexibility was the second important determinant. For scaffold T4-N3 the best results were obtained, usually providing a major tricyclic product along with small amounts of isomers of the same mass. For the rigid scaffold T4-N1, almost all peptides yielded four isomers. Scaffold T4-N2, showing an in-between flexibility, yielded more favorable results compared to scaffold T4-N1. The cleanest tricyclic peptides were obtained with scaffold T4-N3. Isomer formation most likely originated from hindered rotation, as the relation with the flexibility of the scaffold is rather pronounced. Moreover, the cyclization results, whereby increased peptide length yielded fewer rotamers, are similar as observed for the Strategy 1 peptides, as discussed in the previous chapter. Contrary to Strategy 1, minor products accompanying the major product were found that may be attributed to *E/Z* isomer formation. However, definite proof for the existence of *E/Z* isomerism was not provided, as this could not be determined.

3.7.3 The Synthesis of Tricyclic Peptides using D(Ket) Peptides

Finally, peptides featuring the sterically congested amino acid D(Ket) were investigated in the consecutive CLiPS and oxime ligation cyclization reactions. For this series, only the larger peptides with 3, 4 and 5 amino acids in the loop were synthesized. We expected that the D(Ket) functionalized peptides were less prone to oxime *E/Z* isomer formation, as the *tert*-butyl side-chain is very bulky. Surprisingly, tricyclic peptide **10**-D(Ket)[int,n3]∩T4-N1[C/O], where D(Ket) is internally located, was obtained as a mixture of only two isomers, instead of the four obtained for the pAcF peptide (Figure 3.28). The single peak in the UPLC chromatogram for **10**-D(Ket)[int,n3]∩T4-N2[C/O] was equally unexpected, as cyclizations with T4-N2 have generally yielded more complex mixtures. After these results, the single product obtained with T4-N3 cyclizations was more in line with previous findings.
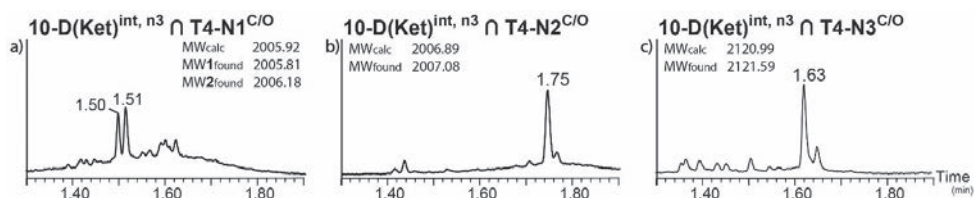
*Figure 3.28: UPLC chromatograms of tricyclic peptide products of **10**-D(Ket)^{int,n3} with scaffolds T4-N1, -N2 and -N3. ★ mono-oxime (bicyclic) product. Product MW's are denoted in chronological order of encounter.*

Previously, the n=4 peptides, which are of intermediate size, also exhibited intermediate results. Often, these peptides showed improved rotational freedom compared to n=3 peptides, but were not yet sufficiently flexible as compared to the more favorable n=5 peptides, and therefore yielded multiple isomers and broad peaks on UPLC. The D(Ket) peptides proved to differ substantially from these previous findings (Figure 3.29). In general, peptide **12**-D(Ket)^{int,n4} gave disulfide formation as a major side-product during the CLiPS reactions, whichever scaffold was used (Figure 3.29a-c). Most probably its conformation favors formation of the disulfide. However, the oxime ligation reactions proceeded nicely yielding single products for all three scaffolds. For the rigid T4-N1 scaffold this was again quite special, as multiple products were expected.

When D(Ket) was installed terminally as for peptides **13**-D(Ket)^{ter,n4} and **14**-D(Ket)^{ter,n4}, remarkable results were obtained. First of all, with scaffold T4-N1, both peptides yielded i) a disulfide byproduct during the CLiPS cyclization and ii) oxime ligation gave two separate products (Figure 3.29d,g). Moreover, for the cyclizations with scaffolds T4-N2 and T4-N3, the tricyclic peptides were obtained as sharp single peaks in the UPLC chromatograms (Figure 3.29e,f,i). Only for **14**-D(Ket)^{ter,n4}∩T4-N2$^{C/O}$ a small amount of an isomeric byproduct was obtained (Figure 3.29h). The cyclization reactions starting from scaffolds T4-N2 and T4-N3 were accompanied by varying amounts of mono-oxime bicyclic byproduct. The mono-oxime species did not react further, even when the reaction was heated to 40 °C over a prolonged period of two weeks. Even after a month, the product composition remained unchanged. We have discovered previously that the intermolecular oxime ligation of D(Ket) with an aminooxy group is a slow reaction. In the intramolecular case, this reaction was significantly faster. In addition, the reaction seemed to be rather selective, whereby only the right conformations were able to cyclize. Most probably, after the first cyclization, the system is unable to equilibrate to a productive conformation, blocking further cyclization from taking place.
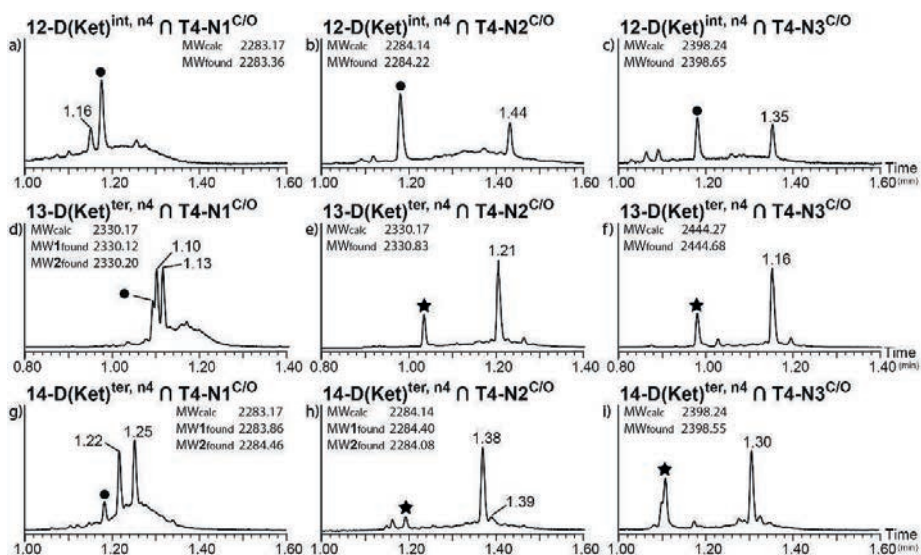
Figure 3.29: UPLC chromatograms of the tricyclic peptide products from D(Ket) n=4 peptides with scaffolds T4-N1, -N2 and -N3. ★ mono-oxime (bicyclic) product. •disulfide of starting peptide. Product MW's are denoted in chronological order of encounter.

For the largest peptides (n=5), we observed results similar to the n=4 peptides, whereby nearly all peptides and scaffold combinations gave the tricyclic peptides as single peaks in UPLC, often accompanied by mono-oxime species (Figure 3.30). For scaffold T4-N1, peptide **15**-D(Ket)[int,n5] yielded a single product, while **16**-D(Ket)[ter,n5]∩T4-N1[C/O] was obtained as two product peaks in UPLC, similar to the n=4/D(Ket) peptides. Moreover, the results for scaffolds T4-N2 and T4-N3 were comparable for peptide **15**-D(Ket)[int,n5] and **16**-D(Ket)[ter,n5]. All tricyclic products were obtained as single products, accompanied by a transient mono-oxime species. For peptide **15**-D(Ket)[int,n5], the mono-oxime was present in larger amounts compared to the cyclizations starting from peptide **16**-D(Ket)[ter,n5]. This is perhaps due to the more constrained nature of the peptide bearing D(Ket) internally. In contrast, peptide **16**-D(Ket)[ter,n5] bears the D(Ket) amino acids on the flexible termini of the peptide, affording more conformational freedom, hence a higher success rate for oxime ligation is achieved.
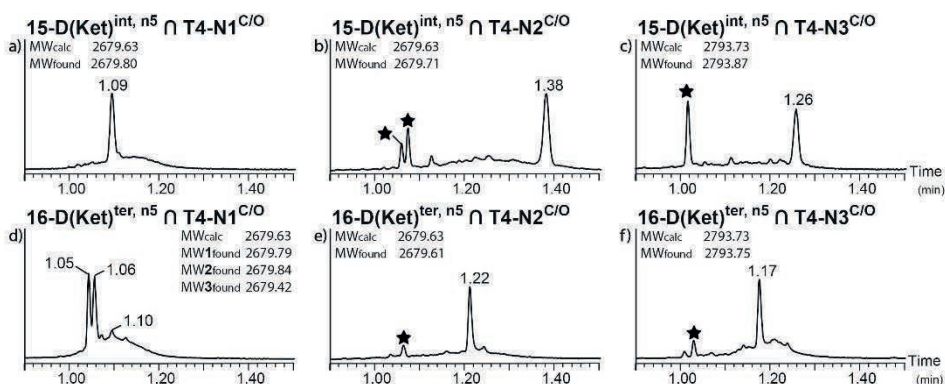

Figure 3.30: UPLC chromatograms of the tricyclic peptide products from D(Ket) n=4 peptides with scaffolds T4-N1, -N2 and -N3. ★ mono-oxime (bicyclic) product. Product MW's are denoted in chronological order of encounter.

For the D(Ket) peptides, it may be concluded that the scaffold seems not to influence the outcome of the cyclization reactions too much, as nearly all investigated peptide/scaffold combinations yielded the tricyclic peptide as a single peak in UPLC. Variation of the peptide length did not give very different results either, in sharp contrast to the pAcF-containing systems, where vast variations in cyclization success were found. In essence, the D(Ket) amino acid itself was the key to the success of tricyclization. Fortunately, the slow reactivity in intermolecular reactions was alleviated by performing the reactions in an intramolecular fashion. However, for many systems relatively large amounts of persistent mono-oxime products were observed. We therefore speculate that oxime ligation can only occur if the peptide is in an energetically favored conformation, otherwise it does not react.

3.8 Conclusion

For the synthesis of tricyclic peptides under Strategy 2 conditions, a scaffold is required bearing the aminooxy group while the peptide is functionalized with the complimentary ketone. The synthesis of the aminooxy-scaffolds T4-N1, T4-N2 and T4-N3 was rather straightforward, exploring the same scaffold core as for Strategy 1. The complementary ketone-derived amino acids were easily synthesized, without the need for purification by column chromatography. While the amino acid pAcF is described in literature, the D(Ket) was designed specifically for this project. During peptide synthesis, protection of the ketones was not required. Resin cleavage and global amino acid side chain deprotection was a crucial step, as the ketone amino acids are not compatible with thiol-based scavengers. A tailor-made cleavage cocktail with other scavengers was devised instead, yielding peptide products of high crude quality after automated SPPS. Peptides were purified by preparative HPLC allowing precise monitoring of the follow-up reactions. For pAcF-functionalized peptides, positioning of this amino acid at the termini, in combination with the most flexible scaffold T4-N3 scaffold showed the best tricyclization results.

Generally, for the less flexible systems, the number of isomeric products formed was much larger. The peptide loop length formed another important factor, as for the more flexible peptides with larger loop sizes fewer isomers were obtained. The isomerism most probably stems from hindered rotation, similar to the Strategy 1 constructs, or from the formation of *E/Z* configured oximes. Structural proof of the *E/Z* oxime formation was not carried out (such as NMR structure determination), but could be of importance for future research. The D(Ket)-functionalized peptides gave different outcomes as compared to the previously studied cyclization reactions. For nearly all cyclizations with the various scaffolds and D(Ket)-containing peptides, a single tricyclic peptide product was obtained, independent of loop length of position of the amino acid. In other words, the D(Ket) amino acid itself was the key factor to success. However, the majority of the cyclizations studied with D(Ket)-functionalized peptides suffered, due to very low reactivity of the sterically congested ketone, from incomplete conversion to the tricyclic peptide – most often a transient mono-oxime persisted.

The results presented in this chapter show which factors were most impactful on the outcome of the consecutive cyclization reactions. However, for nearly all peptide-scaffold combinations, some amount of isomers and by-products such as disulfide or mono-oxime species were present.

3.9 Future Prospects

For drug discovery purposes, peptide library generation is an important investigative tool. Even though this was not attempted for Strategy 2, it certainly is a possibility in the future. Most importantly, the synthesis of the starting peptides containing the ketone-

functionalized amino acids was usually successful. While purifications were carried out for this project, the crude quality of the peptides would allow for library screening.

Unfortunately, the major issue lies with the varying results for the cyclization reactions and the number of products obtained after the CLiPS and oxime ligation. For the D(Ket) peptides, while often single products, the persistent mono-oxime product could be troublesome. However, it would be worthwhile to do a test-screening to see whether these products interact with the screening. For the pAcF peptides, library screening options can be optimistically explored. While we have uncovered the most important variables, there is not yet an ideal peptide-scaffold combination that is guaranteed to yield single product tricycles. However, the T4-N3 scaffold generally yielded the best results. When looking at peptide size, 4 amino acids in the loop gave quite consistent results, albeit with some minor (isomeric) byproducts. Whether these interfere with library screening should be tested by synthesizing a small peptide library, and performing a biological essay. Based on those results, further screening could commence.

3.10 Synthesis of Tricyclic Peptides – A Comparison Between
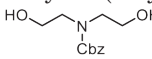
the Strategies 1 and 2

When comparing the Strategy 2 system with Strategy 1, there are three key differences. First, the synthesis of the ketone-bearing amino acids was more straightforward than for the aminooxy amino acids. No column purification was required and their syntheses were more easily scalable. Scaffold synthesis was rather similar, making this not a divisive issue. Peptide synthesis yielded better quality crude peptides for Strategy 2. The only precaution that had to be taken was a special resin cleavage cocktail. The ketones were surprisingly inert and had a better shelf-life than the aminooxy peptides. For the cyclization results, we saw a stronger relation between the scaffold and peptide for strategy 2 systems. For pAcF, the scaffold had the biggest effect, while for the D(Ket) peptides, the amino acid determined the success. This was in sharp contrast with the aminooxy peptides, where loop size was deemed the most important predictor of success. While not strictly complimentary, the systems under Strategy 1 and 2, do each have their own advantages and flaws. The choice for which is best depends on the requirements of the systems. For example, for facile cyclization reactions, Strategy 1 peptides offer an easier one-pot procedure. In contrast, peptide synthesis yielded better results for the pAcF and D(Ket) peptides, as they did not suffer from side reactions. That makes them better suited for potential peptide library generation experiments. However, the more laborious nature of the cyclization procedure is less attractive. Moreover, the cyclizations are more prone to isomer formation, or byproduct formation (for D(Ket)).

What we are left with are two systems where the output matches the intended design: for all systems, tricyclic peptides have been synthesized in a manner which was intended. However, all systems contain a flaw which hinders it from being immediately applicable to peptide library generating tools. The peptide datasets investigated were quite limited so more research is required to find the best parameters with which to continue on library generation. For now, the proof-of-principle has been demonstrated and the intended design for the synthesis of tricyclic peptides has been experimentally confirmed to function as intended.
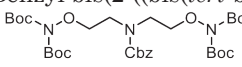
3.11 Experimental Procedures
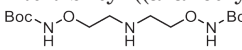
3.11.1 Scaffold Synthesis

Benzyl bis(2-hydroxyethyl)carbamate (**2**)

In a flame-dried flask, under N_2 flow, diethanolamine (**1**) (3.4 mL, 25.0 mmol, 1.0 equiv) was dissolved in 35 mL of freshly distilled MeCN. The solution was cooled to 0 °C, after which solid K_2CO_3 (6.93 g, 50.0 mmol, 2.0 equiv) was added. Then, Cbz-Cl (3.7 mL, 26 mmol, 1.01 equiv) was added to the mixture in a dropwise fashion. The suspension was warmed to rt. and stirred overnight. The volatiles were removed via rotary evaporation. The resulting slurry was redissolved in EtOAc and washed with water and brine. After drying over Na_2SO_4, the volatiles were removed under reduced pressure, yielding a colorless oil. Flash column purification (5% EtOH in EtOAc) provided **2** as a colorless oil (4.097 g, 17.12 mmol, 68%).**^{1}H NMR** (400 MHz, CDCl$_3$) δ 7.38-7.30 (m, 5H), 5.13 (s, 2H), 3.84 (s, 2H), 3.77 (s, 2H), 3.55 − 3.44 (m, 4H), 3.44 − 3.33 (s, 2H). **^{13}C NMR** (100 MHz, CDCl$_3$) δ 156.58, 136.17, 128.33, 127.90, 127.63, 67.16, 61.36, 60.99, 52.33, 51.76. **IR** (cm^{-1}) 3368, 3064, 3032, 3942, 2879, 1671, 1496, 1473, 1455, 1415, 1363, 1262, 1217, 1130, 1046, 989, 906, 858, 768, 734, 696. **HRMS** (FD) calcd. for C$_{12}$H$_{17}$NO$_4$: 239.1158, found 239.1157.
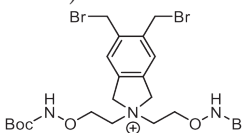
Benzyl bis(2-((bis(*tert*-butoxycarbonyl)amino)oxy)ethyl)carbamate (**3**)

In a flame-dried flask, under N_2 flow, Cbz-protected diethanolamine **2** (10.0 g, 41.9 mmol, 1.0 equiv) was dissolved in 230 mL of freshly distilled THF. PPh$_3$ (23.0 g, 87.8 mmol, 2.1 equiv) and Boc$_2$*N*-OH (20.5 g, 87.8 mmol, 2.1 equiv) were added, and the solution was cooled to 0 °C. DIAD (17.3 mL, 87.8 mmol, 2.1 equiv) was added in dropwise fashion via a syringe pump (5 mL/h). The mixture was warmed to rt and stirred overnight. The volatiles were removed under reduced pressure, providing a yellow oil. Flash column chromatography (3:2:0.5 − P.E.:CH$_2$Cl$_2$:EtOAc) yielded **3** as a colorless oil (21.4 g, 31.9 mmol, 76%). **^{1}H NMR** (400 MHz, CDCl$_3$) δ 7.39 − 7.30 (m, 5H), 5.14 (s, 2H), 4.10 (t, J = 5.0 Hz, 2H), 4.04 (t, J = 5.5 Hz, 2H), 3.67 (q, J = 5.2 Hz, 4H), 1.53 (s, 18H), 1.51 (s, 18H). **^{13}C NMR** (100 MHz, CDCl3) δ 155.73, 149.88, 136.43, 128.49, 128.03, 127.93, 83.72, 83.68, 75.00, 74.90, 67.21, 47.26, 46.68, 28.01. **IR** (cm^{-1}) 2979, 2936, 1792, 1751, 1703, 1475, 1457, 1412, 1393, 1368, 1344, 1271, 1247, 1140, 1109, 1092, 1038, 1004, 912, 890, 848, 794, 768, 751, 735, 697. **HRMS** (FD) calcd. for C$_{32}$H$_{52}$N$_3$O$_{12}$: 670.3551, found 670.6468.

Di-*tert*-butyl ((azanediylbis(ethane-2,1-diyl))bis(oxy))dicarbamate (**4**)

The protected amino-oxy compound **3** (840 mg, 1.2 mmol, 1.0 equiv) was dissolved in 20 mL of CH$_2$Cl$_2$. TFA (368 μL, 4.8 mmol, 4.0 equiv) was added in dropwise fashion, after which the mixture was stirred for 16h at rt. TLC and NMR analysis showed the *mono*-deprotection. The volatiles were removed under reduced pressure. To remove the Cbz-group, the oily residue was redissolved in 25 mL of EtOH. The solution was evacuated, and purged with N_2. Pd/C (10 wt%, 75 mg) was added. H_2 pressure was applied via a balloon. The solution was thrice evacuated and saturated with H_2. The solution was stirred for 3h at rt, after which it was filtered over a Celite pad. After elution with EtOH the volatiles were removed under reduced pressure, yielding an opaque oil. Further purification via flash column chromatography (EtOAc:EtOH − 5:1) yielded the deprotected amine **4** as a very sticky foam (363 mg, 1.1 mmol, 90%) (can also be a solid, as the oil solidifies). **^{1}H NMR** (400 MHz, CDCl$_3$) δ 4.26 − 4.13 (m, 4H), 3.40 − 3.18 (m, 4H), 1.50 (s, 18H). **^{13}C NMR** (125 MHz, CDCl$_3$) δ 158.30, 82.98, 71.54, 45.93, 28.17. **IR** (cm^{-1}) 3198, 2981, 2938, 1672, 1446, 1395, 1369, 1287, 1253, 1201, 1161, 1112, 1051, 1011, 925, 837, 799, 774, 721. **mp** 61-70 °C. **HRMS** (FD) calcd. for C$_{14}$H$_{29}$N$_3$O$_6$: 336.2134, found 336.2192.

5,6-Bis(bromomethyl)-2,2-bis(2-(((*tert*-butoxycarbonyl)amino)oxy)ethyl)isoindolin-2-ium (**T4-N1**)

To a flame-dried flask, under N_2 flow, 1,2,4,5-tetrakis (bromomethyl)benzene **5** (1.35 g, 3.0 mmol, 3.0 equiv) was added and dissolved in 175 mL of freshly distilled MeCN. DIPEA (348 μL, 2.0 mmol, 2.0 equiv) was added and the mixture was stirred until all solids had dissolved. A solution of the deprotected amine **4** (335 mg, 1.0 mmol, 1.0 equiv) in 20 mL of MeCN was added to the solution of

5 in dropwise fashion over the course of an hour, and the mixture was stirred overnight. Full consumption of the starting material was shown via LC-MS analysis. (EtOAc, then 5:1 up to 2:1 EtOAc:EtOH) yielded scaffold **T4-N1** as an off-white foam (400 mg, 0.64 mmol, 64%). **^{1}H NMR** (400 MHz, CH$_3$CN+D$_2$O) δ 7.47 (s, 2H), 5.05 (s, 4H), 4.74 (s, 4H), 4.18 (s, 4H), 3.95 – 3.88 (m, 4H), 1.43 (s, 18H). **^{13}C NMR** (100MHz, CH$_3$CN+D$_2$O) δ 157.78, 138.90, 134.88, 126.62, 82.51, 70.58, 69.38, 60.80, 30.16, 28.10. **IR** (cm^{-1}) 3255, 3236, 3134, 2976, 2934, 2177, 2164, 2157, 2033, 1712, 1453, 1393, 1367, 1273, 1250, 1213, 1159, 1107, 1007, 946, 926, 841, 799, 772. **HRMS** (LC-ESI) for C$_{24}$H$_{38}$Br$_2$N$_3$O$_6^+$ calc 622.1127 found 622.1148. **mp** 101 °C.

Di-*tert*-butyl ((((3,5-bis(bromomethyl)benzoyl)azanediyl)bis(ethane-2,1-diyl))bis(oxy))dicarbamate (**T4-N2**)
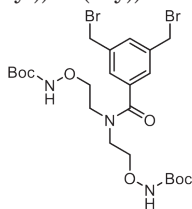
To a flame-dried Schlenk flask, under N$_2$ atmosphere, acid **6** (2.00 g, 6.49 mmol) was added, followed by SOCl$_2$ (9 mL, excess). The mixture was heated to reflux, for 1.5h, after which the remaining SOCl$_2$ was removed *in vacuo*. After co-evaporation with toluene, the acid-chloride was obtained as a pale-yellow solid. CH$_2$Cl$_2$ (50 mL) was added, followed by DMAP (50 mg, 6 mol%), The amine **4** (1.94 g, 5.8 mmol, 0.9 equiv) was dissolved with NEt$_3$ (1.13 mL, 6.5 mmol, 1 equiv) in CH$_2$Cl$_2$ (5 mL). The mixture was stirred for 2h at rt. After extraction with CH$_2$Cl$_2$, the organic phase was washed with 1M KHSO$_4$ (1x) and water (2x), and subsequently dried over Na$_2$SO$_4$. Filtration and evaporation yielded the crude product, which was purified via column chromatography (3:1 to 2:1 P.E:EtOAc) and **T4-N2** was isolated as a colorless oil (763 mg, 1.22 mmol, 21%). *The product was isolated as a single spot on TLC. In LC-MS, the presence of the desired product was shown. Additionally, the presence of partially chlorinated product was shown by mass, and confirmed via the isotope pattern. As the peaks are too close to integrate, the ratio of Cl-substitution was determined via NMR, as in ^{1}H NMR and ^{13}C NMR the -CH$_2$-Cl and the -CH$_2$-Br signals can be distinguished. Using a long delay time, the ratio can be determined by integration of the signals. In ^{1}H NMR, with a delay of 10s, the ratio Br:Cl was determined at 1 : 0.30. In ^{13}C NMR, with a delay of 15s, the ratio of Br:Cl was determined at 1 : 0.29.* **^{1}H NMR** (300 MHz, CDCl$_3$) δ 8.37 (s, 1H), 7.96 (s, 1H), 7.38 (s, 1H), 7.33 (s, 1H), 4.50 (s, 1H, of CH$_2$-Cl, 4.39 (s, 3H, of CH$_2$-Br), 4.01 (s, 2H), 3.87 (s, 2H), 3.79 (s, 2H), 3.49 (s, 2H), 1.47 – 1.33 (m, 18H, overlapping singlet of Boc-groups). **^{13}C NMR** (75 MHz, CDCl$_3$) δ 171.36, 171.30, 156.68, 156.42, 138.61, 138.28, 136.93, 130.16, 129.68, 127.12, 126.60, 81.39, 81.09, 74.01, 73.23, 47.79, 44.80, 43.66, 31.76, 27.93. **IR** (cm^{-1}) 3247, 2977, 2933, 1715, 1620, 1598, 1475, 1444, 1392, 1366, 1270, 1247, 1159, 1109, 1049, 1010, 910, 836, 771, 757, 729, 704. **mp** 38 °C **HRMS** (FD) calcd. for [C$_{23}$H$_{35}$Br$_2$N$_3$O$_7$]$^+$ 624.0920, found, 624.0880. The Boc-group was easily lost during ionization. The mono-chloride mass was also found.

Di-*tert*-butyl ((((3,5-bis((phthalimido)methyl)benzoyl)azanediyl)bis(ethane-2,1-diyl))bis(oxy))dicarbamate (**8a**)
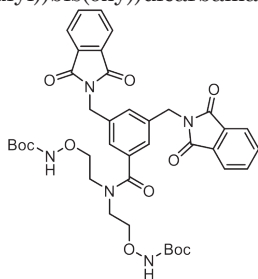
Phthalimide *tert*-butyl ester **6b** (1.82g, 3.7 mmol) was dissolved in 1:2 CH$_2$Cl$_2$:HCOOH (60 mL). The reaction mixture was stirred for 2 days at rt yielding a white suspension. The solids were filtered off, and washed with CH$_2$Cl$_2$, yielding **7** as a very fine white powder (1.8 g, contains water, *quant*). The free acid **7** was suspended in DMF (25 mL). HATU (1.53 g, 4.0 mmol, 1.1 equiv) was added followed by DIPEA (1.28 mL, 7.3 mmol, 2 equiv). This mixture was left for 15 min, during which a yellow solution formed, which later formed a precipitate. The amine **4** (1.32 g, 3.9 mmol, 1.1 equiv) was dissolved in 17 mL DMF, and added dropwise to the HATU solution. The reaction mixture remained yellow but became quite opaque with more precipitate. The reaction was finished after 2h. The reaction mixture was evaporated to yield a very viscous yellow oil. EtOAc was added and the organic phase was washed with H$_2$O, *sat.* NaHCO$_3$ solution, H$_2$O, 1M KHSO$_4$, H$_2$O, brine and was subsequently dried over Na$_2$SO$_4$. The product was purified by column chromatography (1:1 to 1:2 P.E:EtOAc). **8a** was isolated as a white powder (1.87 g, 2.4 mmol, 67%). **^{1}H NMR** (300 MHz, CDCl$_3$) δ 8.42 (s, 1H), 8.08 (s, 1H), 7.68 (dd, *J* = 5.3, 3.1 Hz, 4H), 7.58 (dd, *J* = 5.4, 3.1 Hz, 4H), 7.43 (s, 1H), 7.28 (s, 2H), 4.71 (s, 4H), 3.97 (s, 2H), 3.85 (s, 2H), 3.75 (s, 2H), 3.42 (s, 2H), 1.33 (s, 18H). **^{13}C NMR** (75 MHz, CDCl$_3$) δ 171.87, 167.75, 156.88, 156.63, 137.24, 137.06, 134.10, 131.77, 129.64, 126.22, 123.33, 81.39, 81.07, 74.27, 73.41, 47.96, 43.87, 40.98, 28.17. **IR** (cm^{-1}) 3266, 2976, 2934, 1770, 1707, 1624, 1468, 1426, 1391, 1366, 1344, 1248, 1161, 1108, 1050, 1012, 955, 728, 711. **HRMS** (FD) calcd. for [M+H]$^+$ C$_{39}$H$_{44}$N$_5$O$_{11}^+$: 758.3032 found 758.3005. **mp** 78 °C.

Di-*tert*-butyl ((((3,5-bis(aminomethyl)benzoyl)azanediyl)bis(ethane-2,1-diyl))bis(oxy))dicarbamate (8b)
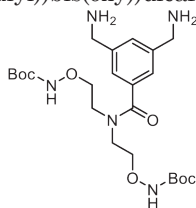
Phthalimide compound **8a** (1.87 g, 2.4 mmol, 1 equiv) was added to a flask, and dissolved in EtOH:Toluene – 2:1 (31 mL). Hydrazine hydrate (50% solution in water, 1.6 mL, 23.6 mmol, 10 equiv) was added and the mixture was heated to reflux, where a solid started to precipitate after 30 min. The mixture was refluxed overnight, after which the yellow suspension was cooled to rt. The solids were filtered off and washed with CH_2Cl_2 (3x). The volatiles were removed under reduced pressure, yielding the desired product **8b** as a white solid (1.1 mg, 2.2 mmol, 92%), which was used in the next reaction step without further purification. **^{1}H NMR** (500 MHz, CDCl$_3$) δ 8.51 (s, 1H), 8.21 (s, 1H), 7.33 (s, 2H), 7.31 (s, 1H), 4.11 (s, 2H), 4.00 (s, 2H), 3.92 (s, 4H), 3.87 (s, 2H), 3.59 (s, 2H), 1.49 (s, 18H). **^{13}C NMR** (125 MHz, CDCl3) δ 173.28, 157.34, 156.60, 143.71, 136.76, 127.11, 124.05, 81.65, 81.48, 74.01, 73.35, 48.03, 45.97, 43.39, 38.62, 28.26.

Di-*tert*-butyl ((((3,5-bis((2-bromoacetamido)methyl)benzoyl)azanediyl)bis(ethane-2,1-diyl))bis(oxy))dicarbamate (T4-N3)
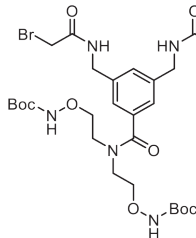

The amine **8b** (688 mg, 1.4 mmol) was dissolved in 36 mL CH_2Cl_2. To fully dissolve the compound, 7 mL of EtOH was added. Solid NaHCO$_3$ (381 mg, 4.5 mmol, 3.3 equiv) was added, followed by bromoacetyl-O-succinimide ester (1.07 g, 4.5 mmol, 3.3 equiv) which was added in one portion. The reaction mixture was stirred at rt for 30 min, after which LC-MS shows the reaction had completed. The volatiles were removed under reduced pressure and the remainder was dissolved in CH_2Cl_2 and washed with 1M KHSO$_4$ (3x) and brine (2x) and dried over Na$_2$SO$_4$. The volatiles were removed under reduced pressure. The product was further purified by column chromatography (7:1-EtOAc:Petroleum

Ether), yielding the finished scaffold **T4-N3** as a white foam (635 mg, 0.9 mmol, 62%). **^{1}H NMR** (500 MHz, CDCl$_3$) δ 8.30 (d, J = 15.0 Hz, 2H), 7.62 (t, J = 5.9 Hz, 2H), 7.21 (s, 2H), 7.16 (s, 1H), 4.32 (d, J = 5.9 Hz, 4H), 4.02 (s, 2H), 3.92 (s, 2H), 3.84 (s, 4H), 3.77 (s, 2H), 3.46 (s, 2H), 1.44 (s, 18H). **^{1}H NMR** *(500 MHz, DMSO-d$_6$, 25 °C)* δ 9.99 (s, 2H), 8.82 (t, J = 5.8 Hz, 2H), 7.23 (s, 1H), 7.17 (s, 2H), 4.32 (d, J = 5.8 Hz, 4H), 3.94 (s, 2H), 3.92 (s, 4H), 3.79 (s, 2H), 3.70 (s, 2H), 3.46 (s, 2H), 1.42 (d, J = 13.8 Hz, 18H). **^{1}H NMR** *(500 MHz, DMSO-d$_6$, 75 °C)* δ 9.75 (s, 2H), 8.61 (s, 2H), 7.25 (s, 1H), 7.19 (s, 2H), 4.34 (d, J = 5.8 Hz, 4H), 3.92 (s, 4H), 3.89 (s, 4H), 3.60 (s, 4H), 1.44 (s, 18H). **^{13}C NMR** *(125 MHz, CDCl$_3$, rt)* δ 172.47, 166.58, 157.14, 156.76, 138.92, 136.62, 128.38, 127.39, 125.56, 124.58, 81.80, 81.66, 73.71, 73.61, 73.20, 72.99, 48.22, 44.09, 43.72, 43.35, 42.97, 29.64, 29.50, 28.86, 28.74, 28.23, 27.85, 26.96. (note: many double peaks due to rotameric effect). **IR** (cm^{-1}) 3257, 3076, 2975, 2928, 1713, 1657, 1619, 1598, 1536, 1476, 1424, 1392, 1366, 1274, 1249, 1160, 1106, 1048, 1026, 899, 836, 792, 761, 688. **HRMS** FD m/z [M-Boc+H$^+$] calcd for C$_{27}$H$_{41}$Br$_2$N$_5$O$_9^+$: 638.0820 found 638.0867. **mp** 60-63 °C.

3.11.2 Amino Acid Synthesis

Ac-F-OEt (**10**)
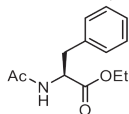
H-F-OH (**9**) (33.07 g, 200.0 mmol, 1.0 equiv) was added to a flask equipped with a with reflux condenser, and suspended in 170 mL EtOH. Ac$_2$O (52 mL, 540.0 mmol, 2.7 equiv) was added and the solution was stirred at reflux overnight. The volatiles (acetic acid remnants) were removed under reduced pressure, yielding a yellowish sticky oil. The mixture was redissolved in 170 mL of EtOH and conc.
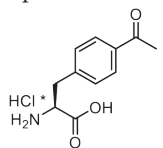
HCl (4 mL, cat) was added. The mixture was heated to reflux and stirred overnight. The volatiles were removed under reduced pressure. The yellow oil was redissolved in EtOAc and washed with a 1M KHSO$_4$ solution, *sat*. NaHCO$_3$ solution and brine, and subsequently dried over Na$_2$SO$_4$. The volatiles were removed under reduced pressure, yielding Ac-F-OEt (**10**) as an off-white solid (38.9 g, 165.3 mmol, 82%). **^{1}H NMR** (500 MHz, CDCl$_3$) δ 7.28 (dt, J = 15.6, 7.0 Hz, 3H), 7.13 (d, J = 6.9 Hz, 2H), 6.16 (d, J = 7.2 Hz, 1H), 4.87 (q, J = 6.0 Hz, 1H), 4.17 (q, J = 7.1 Hz, 2H), 3.12 (tt, J = 13.8, 7.0 Hz, 2H), 1.99 (s, 3H), 1.25 (t, J = 7.1 Hz, 3H). **^{13}C NMR** (125 MHz, CDCl$_3$) δ 171.69, 169.61, 135.95, 129.26, 128.45, 127.00, 61.43, 53.16, 37.90, 23.04, 14.06. **IR** (cm^{-1}) 3312, 3025, 3002, 2973, 2932, 2908, 1946, 1728, 1641, 1530, 1493, 1480, 1444, 1398, 1374, 1345, 1319, 1259, 1220, 1198, 1156, 1129, 1075, 1033, 1021, 966, 929, 909, 867, 824, 813, 764, 745. **mp** 67 °C. *Spectroscopic data are in accordance with those reported in literature.*[22]

Ac-pAcF-OEt (11a)
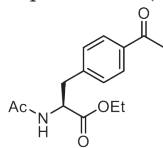
To a flame-dried flask, under N_2 flow and at 0 °C, $AlCl_3$ (12.40 g, 93.0 mmol, 5.5 equiv) was added, followed by the dropwise addition of AcCl (7.2 mL, 101.3 mmol, 6.0 equiv). To the chunky suspension, a solution of Ac-F-OEt (10) (4.00 g, 17.00 mmol, 1 equiv) in 18 mL of CH_2Cl_2 was added dropwise. The dark orange solution was stirred for 30 min on ice, then the mixture was warmed to rt and stirred overnight. The mixture was crashed onto ice, containing 10% 1M HCl solution. The product was extracted with CH_2Cl_2, and the organic phase was washed twice with a *sat*. $NaHCO_3$ solution and water. After drying over Na_2SO_4, the volatiles were removed under reduced pressure to yield a dark brown oil. Flash column chromatography (1:2 – Petroleum Ether:EtOAc) provided the product 11a as a yellowish oil, which crystallized upon standing (4.26 g, 15.36 mmol, 90%). **¹H NMR** (400 MHz, CDCl₃) δ 7.84 (d, J = 8.2 Hz, 2H), 7.19 (d, J = 8.2 Hz, 2H), 6.17 (d, J = 7.5 Hz, 1H), 4.86 (dd, J = 19.7, 7.7 Hz, 1H), 4.14 (q, J = 6.2 Hz, 2H), 3.19 (dd, J = 13.8, 6.1 Hz, 1H), 3.10 (dd, J = 13.8, 5.9 Hz, 1H), 2.54 (s, 3H), 1.95 (s, 3H), 1.21 (t, J = 7.1 Hz, 3H). **¹³C NMR** (100 MHz, CDCl3) δ 197.50, 171.19, 169.48, 141.59, 135.78, 129.39, 128.32, 61.51, 52.79, 37.74, 26.38, 22.90, 13.94. *Spectroscopic data are in accordance with those reported in literature.[15]*

H-pAcF-OEt -HCl salt (11b)

To a flask, equipped with a reflux condenser, 11a (7.00 g, 25.2 mmol, 1.0 equiv) was added. A 9M HCl solution was added (100 mL, excess) and the slight orange mixture was heated to 90°C and stirred for 6h. The mixture was cooled to rt, yielding a precipitate. This precipitate was filtered and washed with acetone and Et_2O to yield the product 11b as fine, slightly brown needles (3.77 g, 15.4 mmol, 61%). The remaining solution was evaporated to dryness, yielding a yellow solid, which was washed with acetone and Et_2O. Filtration yielded the second batch of the product as a pale-yellow solid (2.32 g, 9.47 mmol, 37%). **¹H NMR** (500 MHz, D₂O) δ 7.89 (d, J = 8.1 Hz, 2H), 7.36 (d, J = 8.1 Hz, 2H), 4.28 – 4.20 (m, 1H), 3.26 (ddd, J = 58.6, 14.5, 6.7 Hz, 2H), 2.55 (s, 3H). **¹³C NMR** (125 MHz, D₂O) δ 203.57, 171.59, 140.59, 135.99, 129.81, 129.29, 54.09, 35.75, 26.31. *Spectroscopic data are in accordance with literature.[15]*

Fmoc-pAcF-OH (pAcF)
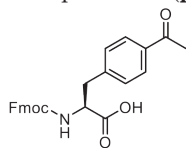
The free H-pAcF-OH (1.00 g, 4.1 mmol, 1 equiv) was dissolved in 11 mL of 1,4-dioxane, after which 15 mL of an aqueous saturated $NaHCO_3$ solution was added, and the solution was subsequently cooled to 0 °C. A solution of Fmoc-OSu (1.45 g, 4.3 mmol, 1.05 equiv) in 10 mL of acetone was added in a dropwise fashion. The flask was warmed to rt, and the solution was stirred overnight. The volatiles were removed under reduced pressure and the remaining solution was diluted with EtOAc. The organic phase was washed with a 1M $KHSO_4$ solution (8 times) followed by brine. After drying over Na_2SO_4, the volatiles were vaporized under reduced pressure, yielding pAcF as an off-white solid (1.72 g, 4.0 mmol, 97%). **¹H NMR** (500 MHz, MeOD) δ 7.89 (d, J = 8.1 Hz, 2H), 7.78 (d, J = 7.5 Hz, 2H), 7.57 (dd, J = 11.1, 7.7 Hz, 2H), 7.38 (t, J = 6.4 Hz, 4H), 7.28 (q, J = 7.0 Hz, 2H), 7.20 (d, J = 7.3 Hz, 1H), 4.50 (dd, J = 9.6, 4.6 Hz, 1H), 4.30 (dd, J = 10.5, 7.2 Hz, 1H), 4.22 (dd, J = 10.4, 7.1 Hz, 1H), 4.12 (t, J = 6.9 Hz, 1H), 3.31 (d, J = 4.5 Hz, 1H), 3.03 (dd, J = 13.7, 9.8 Hz, 1H), 2.52 (s, 3H). **¹³C NMR** (125 MHz, MeOD) δ 198.79, 173.70, 156.85, 143.75, 143.52, 141.09, 135.40, 129.28, 128.16, 127.31, 126.68, 124.83, 124.74, 119.44, 66.49, 55.01, 46.89, 37.15, 25.20. **IR** (cm⁻¹) 3311, 1679, 1606, 1538, 1448, 1267, 1084, 1048, 826, 759. **HRMS** (ESI+), for $C_{26}H_{23}NO_5$ calc 430.1654, found 430.1663. **mp** 155-160 °C.

### Fmoc-D(Osu)-OtBu (13)
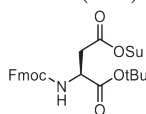
In a flame-dried flask, Fmoc-D(OH)-OtBu (12, purchased from Fluorochem) (10.00 g, 24.3 mmol) was dissolved in 120 mL of anhydrous CH_2Cl_2. HOSu (5.87 g, 51.0 mmol, 2.1 equiv) and pyridine (9.78 mL, 121.5 mmol, 5.0 equiv) were added and the mixture was cooled on ice. TFAA (6.76 mL, 48.6 mmol, 2.0 equiv) was added dropwise. Once addition was finished, the mixture was warmed to rt and stirred overnight. The organic phase was washed 3x with 1M $KHSO_4$ solution, water and brine, and dried over Na_2SO_4. The solvent was removed under reduced pressure, yielding the activated ester 13 as an off-white foam (12.06 g, 23.71 mmol, 98%). **¹H NMR** (300 MHz, CDCl₃) δ 7.76 (d, J = 7.5 Hz, 2H), 7.62 (d, J = 7.4 Hz, 2H), 7.40 (t, J = 7.3 Hz, 2H), 7.31 (t, J = 7.4 Hz, 2H), 5.90 (d, J = 7.8 Hz, 1H), 4.65 (dt, J = 8.4, 4.5 Hz, 1H), 4.38 (dd, J = 7.2, 4.5 Hz, 2H), 4.25 (t, J = 7.3 Hz, 1H), 3.26 (dd, J = 8.7, 4.5 Hz, 2H),

2.84 (s, 4H), 1.49 (s, 9H). **^{13}C NMR** (125 MHz, CDCl$_3$) δ 168.73, 168.37, 166.32, 155.90, 143.81, 141.27, 127.71, 127.12, 125.31, 125.25, 119.95, 83.62, 67.45, 50.56, 47.09, 34.21, 27.77, 25.57. **IR** (cm^{-1}) 3341, 2976, 2944, 1814, 1784, 1735, 1650, 1631, 1612, 1563, 1511, 1477, 1449, 1427, 1394, 1368, 1340, 1292, 1202, 1152, 1062, 1045, 992, 879, 842, 811, 759. **HRMS** (FD) calcd. for C$_{27}$H$_{28}$N$_2$O$_8$: 508.1846, found 508.1845. **mp** 69-72 °C.

1-Azido-3,3-dimethylbutan-2-one (14)
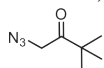
In a flask, 1-bromo-3,3-dimethylbuta-2-one (6.73 mL, 50.0 mmol) was dissolved in 40 mL of acetone, after which NaN$_3$ (4.23 g, 65.0 mmol, 1.3 equiv) was added. The suspension was stirred overnight at rt. The suspension was filtered over a Celite pad and eluted with acetone. The volatiles were removed under rotary evaporation where the flask was kept under 40 °C. The resulting oil was further dried under high vacuum, yielding the desired azide **13** as a yellowish oil (6.95 g, 49.2 mmol, 98%). **^{1}H NMR** 400 MHz, CDCl$_3$) δ 4.10 (s, 2H), 1.20 (s, 9H). *Spectroscopic data are in accordance with those reported in literature.*[19]

Fmoc-D(Ket)-OtBu (15)
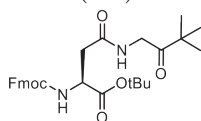
In a flame-dried flask, Fmoc-Asp(OSu)-OtBu (**13**) (11.65 g, 22.9 mmol) was dissolved in 200 mL of freshly distilled THF. Azide **14** (5.18 g, 36.5 mmol, 1.6 equiv) was added, after which the mixture was degassed and purged with N$_2$. Pd/C (10 wt% loading, 3 mol%, 760 mg) was added, and the reaction vessel was evacuated and purged with H$_2$ (repeated trice). The reaction mixture was stirred under H$_2$ pressure (balloon). The reaction was monitored via TLC, and upon consumption of the starting material, the reaction was flushed with N$_2$. The mixture was filtered over a Celite pad, and eluted with CH$_2$Cl$_2$. The volatiles were removed under reduced pressure. The remaining oil was dissolved in EtOAc and the organic phase was washed with 1M KHSO$_4$, water, and brine. After drying over Na$_2$SO$_4$, the volatiles were removed under reduced pressure, yielding **15** as a white fluffy solid (11.67 g, 22.9 mmol, 99%). **^{1}H NMR** (300 MHz, CDCl$_3$) δ 7.75 (d, *J* = 7.4 Hz, 2H), 7.61 (d, *J* = 7.3 Hz, 2H), 7.39 (t, *J* = 7.4 Hz, 2H), 7.30 (t, *J* = 7.4 Hz, 2H), 6.40 (s, 1H), 6.00 (d, *J* = 8.1 Hz, 1H), 4.51 (dt, *J* = 8.3, 4.2 Hz, 1H), 4.44 – 4.31 (m, 2H), 4.27 (d, *J* = 4.2 Hz, 2H), 4.26 – 4.17 (m, 2H), 2.97 (dd, *J* = 15.7, 4.2 Hz, 1H), 2.79 (dd, *J* = 15.6, 4.3 Hz, 1H), 1.47 (s, 9H), 1.18 (s, 9H). **^{13}C NMR** (125 MHz, CDCl$_3$) δ 210.43, 169.93, 156.13, 143.94, 141.27, 127.67, 127.06, 125.24, 119.94, 82.40, 67.17, 51.36, 47.15, 44.77, 43.10, 37.86, 27.91, 26.34. **IR** (cm^{-1}) 3368, 3064, 2976, 2925, 1714, 1671, 1555, 1507, 1476, 1466, 1448, 1395, 1366, 1342, 1287, 1247, 1215, 1167, 1113, 1077, 1049, 1013, 1000, 989, 955, 943, 906, 849, 825, 776, 759, 734. **HRMS** (FD) calcd. for C$_{29}$H$_{36}$N$_2$O$_6$: 508.2573, found 508.2553. **mp** 186 °C

Fmoc-D(Ket)-OH (D(Ket))
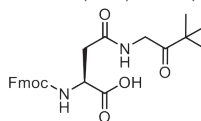
The *tert*-butyl ester **15** (11.66 g, 22.9 mmol) was dissolved in CH$_2$Cl$_2$: HCOOH (1:2, 300 mL). The reaction mixture went from yellowish to red to dark green over 36h, after which TLC shows the deprotection is complete. The volatiles were removed under reduced pressure and the resulting oil was dissolved in EtOAc. The organic phase was washed with 1M KHSO$_4$ solution (3x), water (2x) and brine (2x). The remaining product was very bright yellow. The organic phase was dried over Na$_2$SO$_4$ while stirring for 15 min. To remove the discoloration, some activated carbon powder was added, and stirred for 5 min. After filtration, the volatiles were removed under reduced pressure, yielding the product amino acid **D(Ket)** as a pale-yellow solid (10.40 g, 22.9 mmol, *quant*). The product amino acid **D(Ket)** was used in peptide synthesis without further purification, even though some impurities are noticeable on ^{1}H NMR. *Peptides were of good quality and no detrimental effect of any impurities was recorded.* Column purification was performed for analytical data: EtOAc: CH$_2$Cl$_2$ 1:1, after which first spots were eluted, then 0.05% HOAc was added, to elute the acid **D(Ket)**. **^{1}H NMR** (400 MHz, CDCl$_3$) δ 10.21 (s, 1H), 7.76 (d, J = 7.4 Hz, 2H), 7.62 (d, J = 6.4 Hz, 2H), 7.39 (t, J = 7.3 Hz, 2H), 7.35 – 7.25 (m, 3H), 7.01 (s, 1H), 6.35 (d, J = 7.3 Hz, 1H), 4.70 – 4.59 (m, 1H), 4.37 (d, J = 6.3 Hz, 2H), 4.30 (s, 2H), 4.22 (t, J = 7.2 Hz, 1H), 3.09 (d, J = 13.3 Hz, 1H), 2.92 (dd, J = 15.7, 5.4 Hz, 1H), 1.17 (s, 9H). **^{13}C NMR** (100 MHz, CDCl$_3$) δ 210.32, 173.43, 171.12, 156.20, 143.68, 143.63, 141.14, 127.60, 126.99, 125.12, 119.84, 67.29, 50.51, 46.94, 44.94, 43.02, 37.41, 26.17. **IR** (cm^{-1}) 3325, 3066, 2967, 1709, 1646, 1519, 1477, 1448, 1416, 1367, 1328, 1244, 1155, 1105, 1049, 994, 940, 912, 874, 845, 758, 733. **HR MS** (ESI+) for C$_{25}$H$_{28}$N$_2$O$_6$ calc 453.2026, found 453.2017. **mp** 101 °C.

3.11.3 Peptide Synthesis

3.11.3.1 General Procedure for Fmoc-synthesis of Peptides:

Peptides were synthesized on solid-phase using a Tentagel Rink Amide Resin. Peptide synthesis was performed on a Prelude (Protein Technologies Incl., USA) or Symfony (Protein Technologies Inc., USA). All Fmoc-amino acids were purchased from Biosolve (Netherlands) or Bachem GmbH (Germany) with appropriate side-chain functionalities protected as N-t-Boc (KW), O-t-Bu (DESTY), N-Trt (HNQ), S-Trt (C) or N-Pbf (R) groups. All solvents used in peptide synthesis (piperidine, trifluoroacetic acid, NMP and DMF were bought from Biosolve (Netherlands) in peptide grade quality.

Amino acids were dissolved in DMF (200 mM) and used as such. Piperidine was used as a 20% stock solution in NMP, HATU as a 0.4M stock solution in DMF, and DIPEA as a 2M stock solution in NMP. Standard amino acids were coupled via a single-coupling protocol (5-fold excess of HATU/amino acid (1:1) and 10-fold excess of DIPEA) with a reaction time of 15 min. Special amino acids were coupled with a double-coupling protocol (2.5-fold excess of HATU/amino acid (1:1) and 5-fold excess of DIPEA) with a reaction time of 30min. In case of difficult amino acid couplings, e.g. R, K and C, the double-coupling protocol (10-fold excess of HATU/amino acid (1:1) and 20-fold excess of DIPEA) with a reaction time of 2 x 15 min was used. Acetylation (Ac) of the N-terminus of the peptide was performed by reacting the resin with NMP/Ac_2O/DIPEA (10:1:0.1) for 30 min. at room temperature. The acetylated peptide was cleaved from the resin by reaction with a cocktail of TFA/ MilliQ-H_2O/thioanisole/TIS/Phenol (80:5:5:2.5:7.5) for 2h at room temperature.

Precipitation of peptides with Et_2O/pentane (1:1) followed by lyophilization of the precipitated peptide afforded the crude peptides. Purification of crude peptides was performed by reversed-phase HPLC (mobile phase consists of gradient mixture of eluent-A (MilliQ-H_2O containing 0.05% TFA) and eluent-B (MeCN containing 0.05% TFA).

3.11.4 Peptide Cyclizations

3.11.4.1 CLiPS

In a glass vial (5 mL), the peptide (0.2 mg) was dissolved in MeCN:MilliQ-H_2O (1:1) at a concentration of 0.50 mM. The scaffold (1 to 2 mg/100 µL) was added with a molar equivalent relative to the peptide, whereby the peptide weight was taken uncorrected for any TFA-salts present in the dry material (T4-N1) at 0.95 equiv, T4-N2 at 1.05 equiv and T4-N3 at 0.85 equiv). A solution of 1M NH_4HCO_3 was added to reach pH >8 (30 µL). The reaction mixture was analyzed after 20 min. Upon completion, the reaction mixture was lyophilized to dryness. The reaction can also be performed in DMSO:MilliQ-H_2O mixtures, but DMSO is less suitable for lyophilizing. This has, however, no noticeable effect on the further reactions.

3.11.4.2 Scaffold Deprotection

To remove the Boc-groups on the scaffold aminooxy group, the lyophilized product was treated with excess 2:1 TFA:CH_2Cl_2 (300 µL total). The solution was left for 2h at rt, after which the volatiles were evaporated under a flow of N_2. For larger scale reactions, the material was again dissolved in CH_2Cl_2, and evaporated to dryness, to remove all TFA remnants.

3.11.4.3 Oxime Ligation

The free aminooxy peptide was dissolved in DMSO:MilliQ-H_2O to reach a peptide concentration of 0.50 mM (same as the CLiPS reaction). The pH did not necessarily needed adjustment, and this step was usually omitted. If the pH needed adjustment, the optimum was considered to be pH 4.5, reached by adding a 1M acetate buffer of pH 4.5. The reaction was generally carried out at rt, but some systems (mostly concerning D(Ket) peptides) showed the best results at 40 °C. Therefore, the glass reaction vessel was placed on a heating plate with a temperature set of 40 °C, without stirring bar.

3.12 References

(1) Smeenk, L. E. J.; Dailly, N.; Hiemstra, H.; Van Maarseveen, J. H.; Timmerman, P. *Org. Lett.* **2012**, *14* (5), 1194.

(2) Smeenk, L. E. J.; Timmers-Parohi, D.; Benschop, J. J.; Puijk, W. C.; Hiemstra, H.; Van Maarseveen, J. H.; Timmerman, P. *ChemBioChem* **2015**, *16* (1), 91.

(3) Chen, S.; Bertoldo, D.; Angelini, A.; Pojer, F.; Heinis, C. *Angew. Chemie - Int. Ed.* **2014**, *53* (6), 1602.

(4) Clamp, J. R.; Hough, L. *Biochem. J.* **1965**, *94* (1), 17.

(5) Geoghegan, K. F.; Stroh, J. G. *Bioconjugate Chem.* **1992**, *3* (2), 138.

(6) Yamasaki, R. B.; Osuga, D. T.; Feeney, R. E. *Analytical Biochemistry*. 1982, pp 183–189.

(7) Antonatou, E.; Verleysen, Y.; Madder, A. *Org. Biomol. Chem.* **2017**, *15* (38), 8140.

(8) Carrette, L. L. G.; Gyssels, E.; De Laet, N.; Madder, A. *Chem. Commun.* **2016**, *52* (8), 1539.

(9) Antonatou, E.; Hoogewijs, K.; Kalaitzakis, D.; Baudot, A.; Vassilikogiannakis, G.; Madder, A. *Chem. – A Eur. J.* **2016**, *22* (25), 8457.

(10) Malins, L. R.; Degruyter, J. N.; Robbins, K. J.; Scola, P. M.; Eastgate, M. D.; Ghadiri, M. R.; Baran, P. S. *J. Am. Chem. Soc.* **2017**, *139* (14), 5233.

(11) Tian, F.; Tsao, M. L.; Schultz, P. G. *J. Am. Chem. Soc.* **2004**, *126* (49), 15962.

(12) Chin, J. W.; Cropp, T. A.; Anderson, J. C.; Mukherji, M.; Zhang, Z.; Schultz, P. G. *Science (80-.).* **2003**, *301* (5635), 964.

(13) Lang, K.; Chin, J. W. *ACS Chem. Biol.* **2014**, *9* (1), 16.

(14) Sletten, E. M.; Bertozzi, C. R. *Angew. Chemie Int. Ed.* **2009**, *48* (38), 6974.

(15) Takasu, A.; Kondo, S.; Ito, A.; Furukawa, Y.; Higuchi, M.; Kinoshita, T.; Kwon, I. *Biomacromolecules* **2011**, *12* (10), 3444.

(16) Wang, L.; Zhang, Z.; Brock, A.; Schultz, P. G. *Proc. Natl. Acad. Sci.* **2003**, *100* (1), 56.

(17) Bandyopadhyay, A.; Gao, J. *J. Am. Chem. Soc.* **2016**, *138* (7), 2098.

(18) Liu, F.; Thomas, J.; Burke, T. R.; Liu, Fa, Thomas, Joshua, Burke Jr., T. R. *Synthesis (Stuttg).* **2008**, *2008* (15), 2432.

(19) Banfi, L.; Bagno, A.; Basso, A.; De Santis, C.; Riva, R.; Rastrelli, F. *Eur. J. Org. Chem.* **2013**, *2013* (23), 5064.

(20) AAPPTec. SPPS Cleavage Cocktails https://www.peptide.com/cleavage-cocktails-i-522.html (accessed Feb 22, 2019).

(21) Chalker, J. M.; Gunnoo, S. B.; Boutureira, O.; Gerstberger, S. C.; Fernández-González, M.; Bernardes, G. J. L.; Griffin, L.; Hailu, H.; Schofield, C. J.; Davis, B. G. *Chem. Sci.* **2011**, *2* (9), 1666.

(22) Tobisu, M.; Yamakawa, K.; Shimasaki, T.; Chatani, N. *Chem. Commun.* **2011**, *47* (10), 2946.

Chapter 4:

Synthesis of Tetracyclic Peptides via CEPS, CLiPS and Oxime Ligation

4   From Tricyclic to Tetracyclic Peptides

With the successful completion of the synthesis of tricyclic peptides via CLiPS and oxime ligation as described in the previous chapters, we aimed at further development of this chemistry towards increased complexity by introducing an additional peptide loop, arriving at tetracyclic peptides. However, as the T4-scaffolds have only four reactive positions, the origin of the additional loop cannot stem from additional connections to the scaffold. Instead, modification of the *peptide* can be used to introduce the additional peptide loop. If the starting peptide has already undergone a macrocyclization, follow up CLiPS and oxime ligation reactions with a T4 scaffold will yield a tetracyclic instead of a tricyclic peptide (see Figure 4.1, the additional peptide loop is highlighted in dark grey).
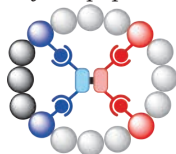

Figure 4.1: Schematic representation of a tetracyclic peptide prepared from a macrocyclic peptide and scaffold T4.

Several cyclization strategies have been explored over time to synthesize macrocyclic peptides.[1–3] For our purposes, head-to-tail cyclization is the method of choice, as this leaves the side-chains available for our further reactions. Even though many methods for head-to-tail peptide cyclization are available, we turned to chemo-enzymatic peptide synthesis (CEPS) for this project, as enzymes exhibit excellent chemo-, regio- and stereoselectivity. Several enzymes, such as omniligase-1, butelase and sortase have been successfully employed for head-to-tail peptide cyclization.[4–9]

Omniligase-1 is especially interesting as it has been shown to be compatible with the use of non-canonical amino acids such as azidohomoalanine (Aha).[10] For cyclization of a peptide to occur, it has to be equipped with a C-terminal carboxyamidomethyl (Cam) ester (Figure 4.2). Peptide Cam-esters are easily prepared by using a pre-functionalized resin, which, upon resin cleavage and global deprotection of the peptide, yields the free peptide Cam-ester ready for head-to-tail cyclization using omniligase-1.[11]

The enzyme recognition pocket for Cam-esters spans six amino acids around the ligation site of the peptide. Two (P1' and P2') are located at the N-terminus, while P4-P1 are located C-terminally (Figure 4.2). Due to the properties of this recognition pocket, the minimal peptide length must exceed 12 amino acid residues to accommodate cyclization, including those residues in the recognition site. The amino acids in this region determine the success of peptide macrocyclization, and not all amino acid residues are well tolerated at all positions. However, omniligase-1 is quite promiscuous and not subject to a specific recognition sequence, as can be the case for other enzymes.[4]
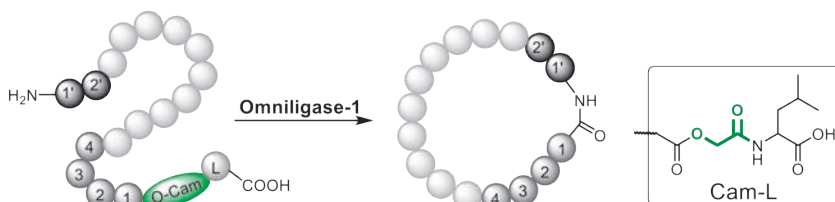

Figure 4.2: Macrocyclization of a peptide using omniligase-1. Positions P1' and P2' are located at the N-terminus (black) and positions P4-P1 are C-terminal (dark grey), adjacent to the Cam-ester (green).

The goal of the research described in this chapter is to determine whether omniligase-1-mediated peptide macrocyclization can be used to fashion monomacrocyclic peptides, which can then be subjected to follow-up templated CLiPS and oxime ligation reactions, to ultimately generate tetracyclic peptides. The CLiPS reaction requires the peptide to be

equipped with two cysteine residues providing the complementary reactivity with the scaffold-centered alkyl bromide electrophiles. For oxime ligation, the peptide can be functionalized with either an aminooxy or a ketone-bearing amino acid. Strategy 1 peptides contain the aminooxy functionalized $hS(ONH_2)$ moiety, while the scaffold is equipped with the complementary aldehydes. Strategy 2 peptides bear ketone-functionalized amino acids (pAcF) and (D(Ket)) and the scaffold the aminooxy moieties.

The proposed reaction scheme is presented in Figure 4.3. First, the linear peptide, equipped with the Cam-ester and bearing the CLiPS/oxime functionalities was synthesized, followed by the omniligase-1-catalyzed macrocyclization reaction. The resulting cyclized peptide was then subjected to CLiPS and oxime ligation reactions with the appropriate scaffolds. Finally, the effects of a) the various different amino acid residues present, b) the peptide length and c) scaffold design, on the outcome of the individual reactions were determined.
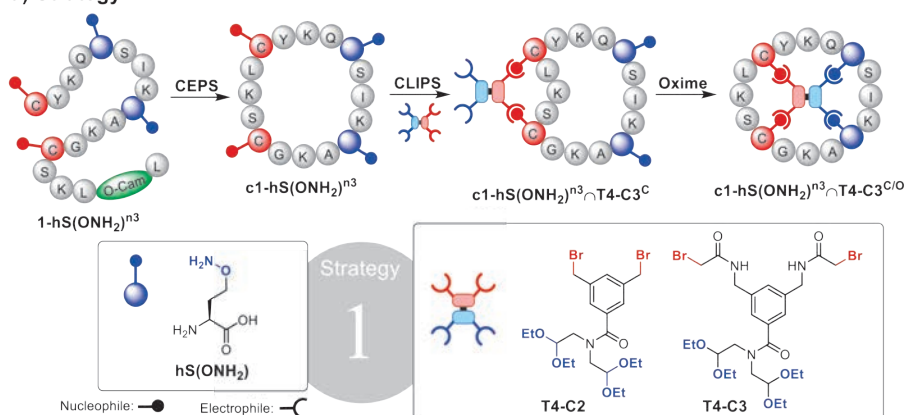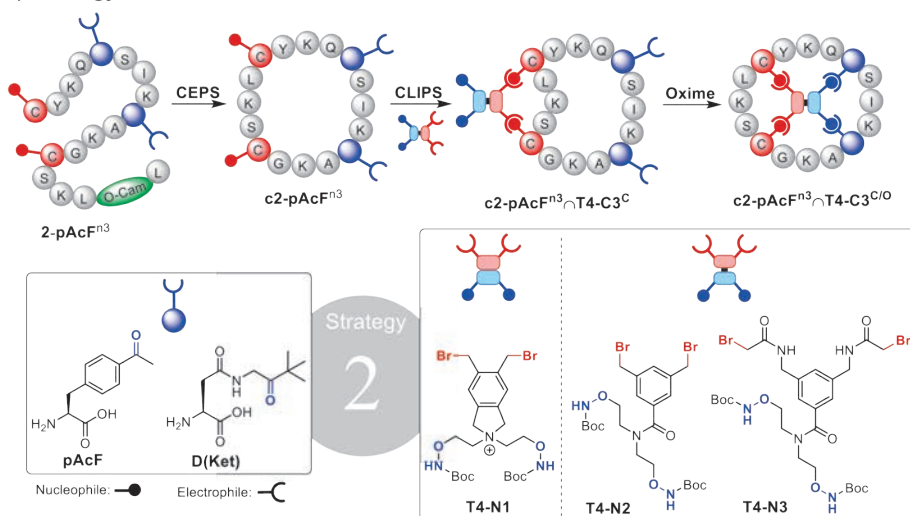

Figure 4.3: Schematic representation of the CEPS/CLiPS/oxime-cyclizations and the different types of scaffolds and amino acids. a) Aminooxy-bearing peptides with scaffolds T4-C2 and T4-C3 (strategy 1). b) Peptides comprising ketone-functionalized amino acids in combination with scaffolds T4-N1, T4-N2, T4-N3 (strategy 2), for the synthesis of tetracyclic peptides.

4.1 Combining CEPS with CLiPS and Oxime Ligation

4.1.1 Peptide Synthesis and Enzymatic Macrocyclization

To investigate whether omniligase-1-mediated CEPS is compatible with the non-canonical amino acids pAcF, D(Ket), and hS(ONH₂) that are required for oxime ligation, a set of linear peptides had to be synthesized, equipped with these amino acids and the Cam-ester. For strategy 1, only hS(ONH₂) was used in peptide synthesis, as this resembles the size of other amino acids. Because K(Aoa) bears an extended side-chain which is somewhat larger than those found in canonical amino acids, it was omitted from this study. For strategy 2 peptides, both pAcF and D(Ket) were tested.

First, feasibility studies were carried out at Enzypep to determine at which positions the unnatural amino acids are accepted in the CEPS macrocyclization reactions. Most important in this case are the residues located at the enzymatic recognition sequence of the peptide (N-terminal residues P1' and P2' and the C-terminal residues P4-P1). It was found that all three amino acids were well tolerated at the majority of positions (pAcF at all pockets, hS(ONH₂) at P3, P2, P1', P2', and D(Ket) at P3, P2). Distinct differences in reaction rate could be compensated for by adding additional enzyme. In general, these results demonstrate the broad applicability and compatibility of CEPS-macrocyclization, even when using non-canonical amino acids.

To test the three consecutive CEPS, CLiPS and oxime ligation cyclization reactions, peptides of various lengths were synthesized with the functional residues at different positions (Table 4.1). These peptides contained either three, four, or five amino acids in each loop, and the positions of the cysteines and amino acids for oxime ligation were varied within the peptide. For the synthesis of tetracyclic peptides, the location for the cysteine and oxime ligation residues are relevant only with respect to the CEPS recognition sites. The sequences were chosen with the main focus on both solubility and polarity with regards to enzyme compatibility. Within a series of peptides of the same length, the sequence remains the same, except for the non-canonical amino acid. In this way, the influence of the individual non-canonical amino acid residues on the CEPS-macrocyclization and of the scaffold on the follow-up CLiPS and oxime reactions was revealed.

Table 4.1: The codes and sequences for the linear peptide Cam-esters prepared for CEPS.

Code	Sequence
1-hS(ONH₂)^{n3}	H-**C**YKQ{**hS(ONH₂)**}SIK{**hS(ONH₂)**}AKG**C**SKL-O-Cam-L-OH
2-pAcF^{n3}	H-**C**YKQ{**pAcF**}SIK{**pAcF**}AKG**C**SKL-O-Cam-L-OH
3-D(Ket)^{n3}	H-**C**YKQ{**D(Ket)**}SIK{**D(Ket)**}AKG**C**SKL-O-Cam-L-OH
4-hS(ONH₂)^{n4}	H-R{**hS(ONH₂)**}FRLPCRQLR**C**FRLP{**hS(ONH₂)**}RQL-O-Cam-L-OH
5-pAcF^{n4}	H-R{**pAcF**}FRLPCRQLR**C**FRLP{**pAcF**}RQL-O-Cam-L-OH
6-hS(ONH₂)^{n5}	H-**C**YKGKQ{**hS(ONH₂)**}SIKAS{**hS(ONH₂)**}AKVRG**C**KFSKL-O-Cam-L-OH
7-pAcF^{n5}	H-**C**YKGKQ{**pAcF**}SIKAS{**pAcF**}AKVRG**C**KFSKL-O-Cam-L-OH
8-D(Ket)^{n5}	H-**C**YKGKQ{**D(Ket)**}SIKAS{**D(Ket)**}AKVRG**C**KFSKL-O-Cam-L-OH

Peptides **4**-hS(ONH₂)^{n4} and **5**-pAcF^{n4} were based on the sequence of a bioactive tetracyclic peptide made previously in our group in a related project.[10] This compound was synthesized via a combination of CEPS/CLiPS/CuAAC reactions instead of CEPS/CLiPS/oxime ligation, as is the topic of this chapter. Moreover, the solution-phase 3D-structure of this tetracyclic peptide was resolved by a combination of different NMR-spectroscopy techniques. Our goal was to compare this CEPS/CLiPS/CuAAC 3D-structure with that of our CEPS/CLiPS/oxime ligation cyclized compound.

As observed earlier in Chapter 2, the synthesis of hS(ONH₂) peptides suffered from both elimination of the aminooxy moiety and occasional isopropylidene capping by traces of acetone of unknown origin, leading to complex mixtures that required multiple

purification steps and thus lowered the yields.[12] For pAcF and D(Ket), the tailored resin cleavage-cocktail without thiol-scavengers was applied, yielding peptides of rather good crude quality. Peptides containing D(Ket) exhibited low solubilities in aqueous solutions, potentially requiring the addition of solubilizing agents (e.g. urea) for efficient enzymatic cyclization. Nevertheless, all linear peptide Cam-esters (n=3,4,5) were successfully cyclized in a head-to-tail fashion using omniligase-1. The resulting macrocyclic peptides, accompanied by their sequence and MS data, are presented in Table 4.2.

Table 4.2: Peptide codes and sequences of the cyclized peptides, including MS data.

Code	Sequence	MW calc.	MW found
c1-hS(ONH$_2$)^{n3}	cyc-**C**YKQ{**hS(ONH$_2$)**}SIK{**hS(ONH$_2$)**}AKG**C**SKL	1771.46	1771.29
c2-pAcF^{n3}	cyc-**C**YKQ{**pAcF**}SIK{**pAcF**}AKG**C**SKL	1917.64	1917.48
c3-D(Ket)^{n3}	cyc-**C**YKQ{**D(Ket)**}SIK{**D(Ket)**}AKG**C**SKL	1964.71	1964.79
c4-hS(ONH$_2$)^{n4}	cyc-R{**hS(ONH$_2$)**}FRLP**C**RQLR**C**FRLP{**hS(ONH$_2$)**}RQL	2574.53	2574.91
c5-pAcF^{n4}	cyc-R{**pAcF**}FRLP**C**RQLR**C**FRLP{**pAcF**}RQL	2720.71	2720.59
c6-hS(ONH$_2$)^{n5}	cyc-**C**YKGKQ{**hS(ONH$_2$)**}SIKAS{**hS(ONH$_2$)**}AKVRG**C**KFSKL	2645.62	2645.59
c7-pAcF^{n5}	cyc-**C**YKGKQ{**pAcF**}SIKAS{**pAcF**}AKVRG**C**KFSKL	2791.80	2791.91
c8-D(Ket)^{n5}	cyc-**C**YKGKQ{**D(Ket)**}SIKAS{**D(Ket)**}AKVRG**C**KFSKL	2837.86	2837.84

4.2   Synthesis of Tetracyclic Peptides by CLiPS and Oxime Ligation

With the monocyclic peptides in hand, the CLiPS and subsequent oxime ligation reactions were carried out. The reaction conditions were optimized previously (see Chapters 2 and 3). For Strategy 1, the CLiPS and oxime ligation were carried out in a one-pot procedure, using aqueous DMSO (1:1, 0.5 mM) as the solvent. After performing the CLiPS reaction under slightly basic conditions (pH 8), the reaction mixture was acidified by the addition of TFA. Under these conditions, both liberation of the aldehyde and subsequent oxime ligation occurred.

For Strategy 2, the reaction sequence had to be performed in three separate steps. After the CLiPS reaction in aqueous MeCN, the volatiles were removed by lyophilization. Dissolving the residue in neat TFA enabled liberation of the aminooxy moieties. After removal of TFA under a stream of N$_2$, the residue was dissolved in aqueous DMSO, after which oxime ligation occurred without the need for additional pH regulating additives.

Because all CLiPS reactions yielded a single product, these will not be discussed further. Therefore, only the results of the following oxime ligation reactions to obtain the final tetracyclic peptides are discussed in the following paragraphs.

4.2.1   Strategy 1 Peptides – hS(ONH$_2$)

The results for the tetracyclic hS(ONH$_2$)-peptides (Figure 4.4) show a similar trend as found for the tricyclic peptide series (Chapter 2). First of all, there is a clear effect of the peptide loop-length. The strain exerted within the small peptide with three residues in each loop of **c1**-hS(ONH$_2$)^{n3} limits the rotational freedom. Therefore, in the UPLC-trace two sharp peaks appeared for both **c1**-hS(ONH$_2$)^{n3}∩T4-C2$^{C/O}$ and **c1**-hS(ONH$_2$)^{n3}∩T4-C3$^{C/O}$. A different behavior was observed for the peptides with four residues in the loops. For peptide **c4**-hS(ONH$_2$)^{n4}, both scaffolds yielded two products, which appeared as broadened peaks. We attribute this peak broadening to slow equilibration between several conformers on the UPLC timescale, *en route* to coalescence, while being comparatively faster than the **c1**-hS(ONH$_2$)^{n3}-tetracycles. The largest peptide, **c6**-hS(ONH$_2$)^{n5}, yielded single products for both the scaffolds, similar to the tricyclic peptides discussed in Chapter 2. From this small set of test-peptides, it may be concluded that by increasing the peptide loop lengths, superior results are obtained, especially in combination with the most flexible scaffold (T4-C3).
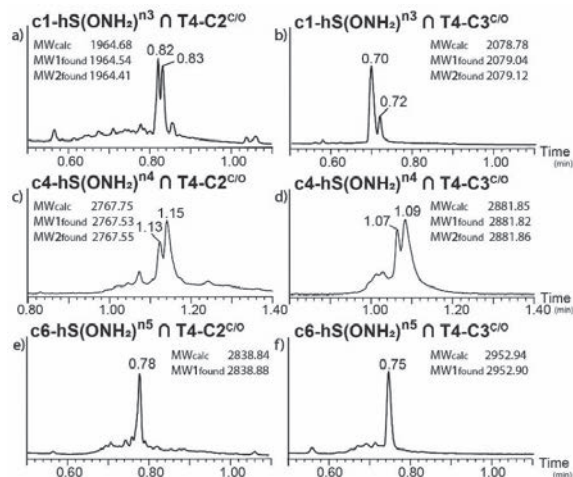
Figure 4.4: UPLC chromatograms of Strategy 1 oxime ligations with hS(ONH₂) containing bicyclic peptides (n=3,4,5) with scaffolds T4-C2 and T4-C3. Product MW's are denoted in chronological order of encounter.

4.2.2 Strategy 2 Peptides – pAcF

For the pAcF peptides, the results are again quite similar to those obtained for the tricyclic peptides (Figure 4.5). Here, the loop size is of less importance, but the scaffold-type that was used *is*. This becomes clear when comparing the results for each different scaffold.

For the rigid scaffold T4-N1 (Figure 4.5a,d,g), four products were obtained for all reactions. These peaks all correspond to the expected tetracyclic product. The loop size is irrelevant, as all three peptides, differing in loop sizes from three to five residues, showed similar UPLC-traces. Interestingly, for **c2**-pAcF^{n3} and **c5**-pAcF^{n4} a distinct major product was obtained, while **c7**-pAcF^{n5} yielded the four tetracycles in a 1:2:2:1 ratio.

Scaffold T4-N2 gave two to three products, visible as broadened peaks in the UPLC traces (Figure 4.5b,e,h). The loop length seemed to have very little effect, and broad product peaks were obtained in all cases. The cyclization of **c5**-pAcF^{n4}∩T4-N2$^{C/O}$ gave two products and their attempted separation via preparative HPLC will be discussed at the end of this paragraph.

The CLiPS/oxime ligation reactions of the macrocyclic peptides with scaffold T4-N3 yielded single products (Figure 4.5c,f,i). However, in the case of **c5**-pAcF^{n4}∩T4-N3$^{C/O}$, it was revealed that actually two products were formed when using a less steep gradient for the UPLC-analysis. By increasing the peptide loop length to five amino acids, **c7**-pAcF^{n5}∩T4-N3$^{C/O}$ was obtained as the single product. For the Strategy 2 pAcF peptides, the most flexible systems yielded the best results. Hence longer peptides, particularly in combination with scaffold T4-N3, performed best.

As outlined above, the amino acid sequence of **c5**-pAcF^{n4}∩T4-N2$^{C/O}$ was identical to a tetracyclic peptide that was prepared previously in our group using the CuAAC reaction as the last cyclization step, instead of oxime ligation.[10] The solution-phase structure of this compound containing 1,4-linked triazoles was elucidated via ^{1}H NMR analysis. To allow ^{1}H NMR analysis for comparison, the two tetracyclic products of **c5**-pAcF^{n4}∩T4-N2$^{C/O}$ were separated.
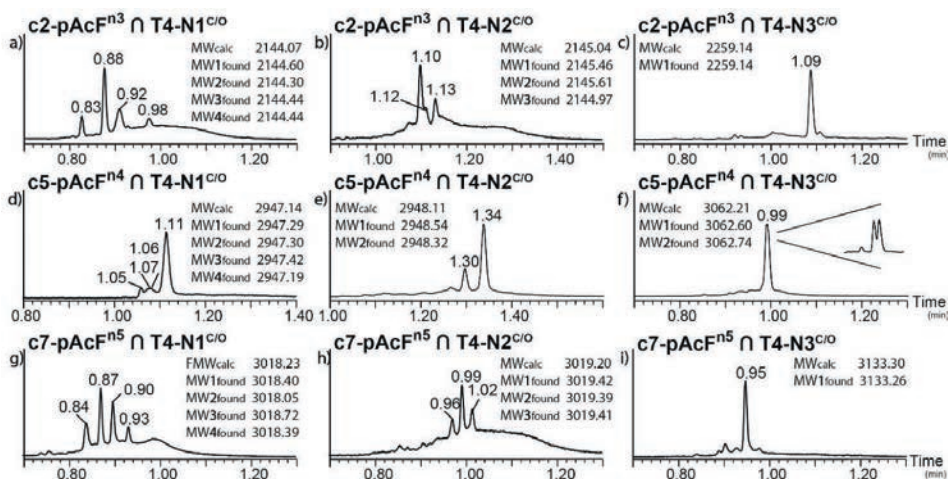
Figure 4.5: UPLC chromatograms of strategy 2 oxime ligations with pAcF peptides and scaffolds T4-N1, T4-N2 and T4-N3, reacted for 16h at 40 °C. Product MW's are denoted in chronological order of encounter.

In Figure 4.6, the entire reaction sequence is presented, from monocyclic peptide (a) to the purified tetracyclic peptide (d). The reaction was carried out starting with 5.4 mg of the CEPS-cyclized peptide. The two products that were obtained in the final oxime ligation reaction were separated by preparative HPLC. The fact that these products could be separated means that no interconversion occurred on the HPLC timescale. Most likely, the two products are configurationally stable isomers originating from oxime *E/Z* linkages instead of rotamers. We hoped that NMR would support this assumption. However, ^{1}H NMR studies revealed that the tetracyclic structure of **c5**-pAcF^{n4}∩T4-N2$^{C/O}$ was present in many different conformations due to hindered rotation around the scaffold's amide bond, and probably as well as a slow equilibrium of the *E/Z* oxime bond during the prolonged NMR data acquisition, preventing a detailed structure determination.
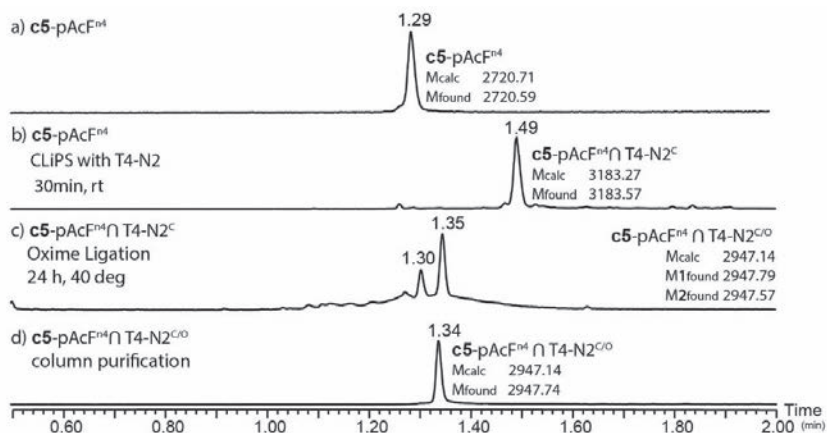

*Figure 4.6: The reaction sequence for peptide **c5**-pAcF^{n4}, showing a) the monocyclic peptide, b) the CLiPS reaction, c) the oxime ligation and d) the results of the peptide purification via preparative HPLC.*

4.2.3 Strategy 2 Peptides – D(Ket) Peptides

The results for the peptides containing the sterically congested D(Ket), of which we expected to obtain E-configured oximes only, are presented in Figure 4.7. Due to the lower acceptance of D(Ket) in the enzyme pocket in the initial CEPS macrolactamization step, only the peptides with the most divisive loop lengths of three and five amino acids were synthesized. For both peptides, the anticipated tetracycle was obtained as a single product for all scaffolds. However, for all reactions with peptide **c3**-D(Ket)^{n3}, its disulfide that had not reacted during the CLiPS reaction, was obtained as a byproduct. Additionally, a mono-oxime was present for all reactions. These byproducts had a transient character and did not change in appearance and intensity over time. These results are in concurrence with those found for the tricyclic peptides as described in Chapter 3.

Formation of the final CLiPS/oxime ligation construct as a single product was quite surprising in the case of the T4-N1 scaffold (Figure 4.7a,d), as this scaffold generally yields multiple isomers due to its rigid structure. However, aside from the anticipated product, this scaffold also yielded at least two mono-oxime products. It seems that for this scaffold, multiple, energetically unfavorable mono-oxime products were formed, that did not react further. Meanwhile, the increased rotational flexibility of the other scaffolds also led to fewer mono-oxime species. This supports the hypothesis that only energetically favorable tetracycles are formed.
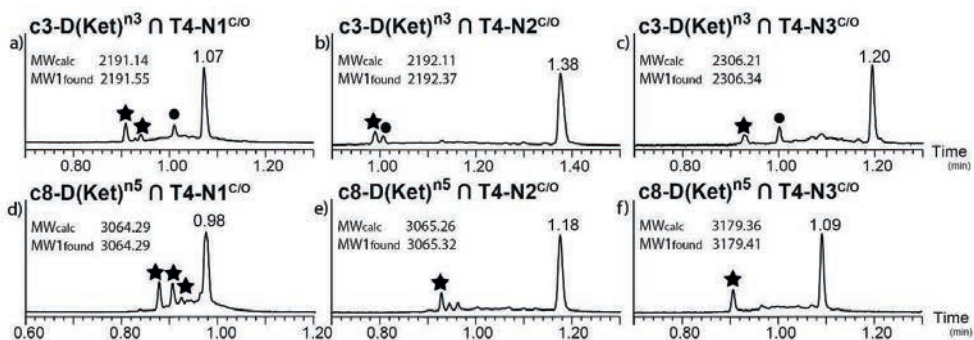

Figure 4.7: UPLC chromatograms of strategy 2 oxime ligations with D(Ket) peptides and scaffolds T4-N1, T4-N2 and T4-N3, reacted for 16h at 40 °C. ★ = mono-oxime; • = disulfide starting material not reacted during CLiPS.

4.3 Conclusion and Future Prospects

In this chapter the results of the successful synthesis of tetracyclic peptides via a combination of CEPS, CLiPS and oxime ligation are described. The omniligase-1 enzyme was used to cyclize the linear Cam-ester peptides, and it was shown that this enzyme is compatible with the presence of non-canonical amino acid residues required for oxime ligation in the binding pocket. The use of head-to-tail cyclized peptides enabled the use of previously described T4-scaffolds for the synthesis of more complex tetracyclic peptides.

The results presented in this chapter, from issues concerning peptide synthesis and the results for the CLiPS and oxime ligations, show numerous similarities with those found for the tricyclic peptides as described in Chapters 2 and 3. Peptide length seems to be the most influential factor when cyclizations with the hS(ONH$_2$)-containing peptides are concerned. For pAcF, the scaffold used in the reactions overpower other variables. For D(Ket), the nature of the bulky *tert*-butyl ketone determines the outcome of the reaction, instead of loop size or scaffold-type. Unfortunately, further structural analysis of

tetracyclic product **c5**-pAcF^{n4}∩T4-N2$^{C/O}$ via ^{1}H NMR was unsuccessful and therefore we were not able to elucidate the configuration of the oxime double bond.

Overall, consecutive peptide cyclizations by CEPS, CLiPS and oxime ligation reactions provide access to the regioselective synthesis of tetracyclic peptides. Further studies should focus on the synthesis of a larger peptide library. Additional screening for biological activity can be added. This may ultimately contribute to the discovery of, for example, new antimicrobially active lead compounds.

4.4   Acknowledgements

4.5   Experimental Section

Syntheses of amino acids, scaffolds, and procedures for the CLiPS and oxime ligations have been described in Chapters 2 and 3.
The enzymatic cyclization of Cam-esterified peptides, as well as feasibility studies regarding the oxime amino acids, are described in the Supporting Information of the Org. Lett. paper which was written about this work.[13] Details about the ^{1}H NMR measurements to elucidate the structure of isolated tetracycle c5-pAcF^{n4}∩T4-N2$^{C/O}$ can be found here as well.

4.5.1   Isolated tetracycle c5-pAcF^{n4}∩T4-N2$^{C/O}$

In a glass vial, peptide **c5**-pAcF^{n4} (5.35 mg, 1.96 µmol) was suspended in 1.95 mL of MeCN, followed by the addition of 1.95 mL of MilliQ-H$_2$O, to fully dissolve the peptide (0.50 mM). 87.75 µL (1.05 equiv, uncorrected) of scaffold T4-N2 solution (1.44 mg in 100 µL) was added to the peptide. 100 µL of a of 1M NH$_4$HCO$_3$ solution was added, with the resulting pH of 8.5. Analysis of the CLiPS mixture showed full conversion to the desired product **c5**-pAcF^{n4}∩T4-N2^C, with some excess of scaffold still being present. The solution was lyophilized, yielding a white powder. To remove the Boc-groups of the scaffold, 4 mL of TFA was added, followed by 2 mL of CH$_2$Cl$_2$. The solution was stirred for 2h at rt, resulting in a slightly yellowish solution. Under a stream of nitrogen, the volatiles were evaporated, yielding a sticky residue. This residue was dissolved in CH$_2$Cl$_2$, and the volatiles were removed once more, yielding a sticky white residue film on the vial. This residue was dissolved in 1 mL of DMSO, followed by the addition of 3 mL of milliQ-H$_2$O. The reaction mixture was stirred at 40 °C over the weekend. The mixture was analyzed, showing 2 products of **c5**-pAcF^{n4}∩T4-N2$^{C/O}$ with identical mass, at t$_R$ 1.30 and 1.34 min.

Preparative HPLC purification of the peptides was carried out on a Supelco column (C5-C10, flow 8 mL/min), with gradient elution from 0-38% B in A; Eluent-A: milliQ-H$_2$O + 0.05% (v/v) TFA, and eluent-B: MeCN + 0.05% (v/v) TFA. Purification was performed at rt. The reaction mixture was diluted with MilliQ-H$_2$O to a final volume of 80 mL (2.5% DMSO). The peptide was loaded onto the column *via* a dilution method, where the reaction solution was taken as the mobile phase (4 ml/min). Once the DMSO-peak had eluted completely, the gradient was started (8 mL/min, 0 to 38% B in A over 35 min). Products started to elute after approximately 27 min. The fractions (~3 mL) were collected in glass vials, analyzed on UPLC and lyophilized.

c5-pAcF^{n4}∩T4-N2$^{C/O}$ **Product 1** (t$_R$ 1.30 min) was present in fr. 10 and 11, but not pure.
HRMS (ESI+), for C$_{139}$H$_{209}$N$_{43}$O$_{25}$S$_2$, MW$_{calc}$ 2945.5924,

[M+2H]$^{2+}$ calc 1473.8015, found 1473.8158.
[M+3H]$^{3+}$ calc 982.8703, found 982.8719.
[M+4H]$^{4+}$ calc 737.4047, found 737.4042.

c5-pAcF^{n4}∩T4-N2$^{C/O}$ **Product 2** (t$_R$ 1.34 min) was present in fraction 12 to 15, in pure form (1.85 mg total).
HRMS: ESI-QTOF for [C$_{139}$H$_{209}$N$_{43}$O$_{25}$S$_2$]$^+$ [M+H]$^+$ calc 2945.5919, found 2945.8657.
HRMS (ESI+), for C$_{139}$H$_{209}$N$_{43}$O$_{25}$S$_2$, MW$_{calc}$ 2945.5924,
[M+2H]$^{2+}$ calc 1473.8015, found 1473.8117.
[M+3H]$^{3+}$ calc 982.8703, found 982.8701.
[M+4H]$^{4+}$ calc 737.4047, found 737.4029.
Product 2 was used for ^{1}H NMR analysis.

4.6 References

(1)   White, C. J.; Yudin, A. K. *Nat. Chem.* **2011**, *3*, 509.
(2)   Rubin, S. J. S.; Qvit, N. *Curr. Top. Med. Chem.* **2018**, *18* (7), 526.
(3)   Thakkar, A.; Trinh, T. B.; Pei, D. *ACS Comb. Sci.* **2013**, *15* (2), 120.
(4)   Schmidt, M.; Toplak, A.; Quaedflieg, P. J. L. M.; Ippel, H.; Richelle, G. J. J.; Hackeng, T. M.; van Maarseveen, J. H.; Nuijens, T. *Adv. Synth. Catal.* **2017**, *359* (12), 2050.
(5)   Nguyen, G. K. T.; Kam, A.; Loo, S.; Jansson, A. E.; Pan, L. X.; Tam, J. P. *J. Am. Chem. Soc.* **2015**, *137* (49), 15398.
(6)   Jia, X.; Kwon, S.; Wang, C.-I. A.; Huang, Y.-H.; Chan, L. Y.; Tan, C. C.; Rosengren, K. J.; Mulvenna, J. P.; Schroeder, C. I.; Craik, D. J. *J. Biol. Chem.* **2014**, *289* (10), 6627.
(7)   Schmidt, M.; Toplak, A.; Quaedflieg, P. J. L. M.; van Maarseveen, J. H.; Nuijens, T. *Drug Discov. Today Technol.* **2017**, *26*, 11.
(8)   Wu, Z.; Guo, X.; Guo, Z. *Chem. Commun.* **2011**, *47* (32), 9218.
(9)   Toplak, A.; Nuijens, T.; Quaedflieg, P. J. L. M.; Wu, B.; Janssen, D. B. *Adv. Synth. Catal.* **2016**, *358* (13), 2140.
(10)   Richelle, G. J. J.; Schmidt, M.; Ippel, H.; Hackeng, T. M.; van Maarseveen, J. H.; Nuijens, T.; Timmerman, P. *ChemBioChem* **2018**, *19* (18), 1934.
(11)   Nuijens, T.; Toplak, A.; van de Meulenreek, M. B. A. C.; Schmidt, M.; Goldbach, M.; Quaedflieg, P. J. L. M. *Tetrahedron Lett.* **2016**, *57* (32), 3635.
(12)   Liu, F.; Thomas, J.; Burke, T. R.; Liu, Fa, Thomas, Joshua, Burke Jr., T. R. *Synthesis (Stuttg)*. **2008**, *2008* (15), 2432.
(13)   Streefkerk, D. E.; Schmidt, M.; Ippel, J. H.; Hackeng, T. M.; Nuijens, T.; Timmerman, P.; van Maarseveen, J. H. *Org. Lett.* **2019**, *21* (7), 2095.

Chapter 5:

Synthesis of Pentacyclic Peptides

5   Introduction

As an extension to the templated CLiPS/oxime synthesis of tri- and tetracyclic peptides as discussed in the previous chapters, we here describe the development of methodology towards pentacyclic peptides. After the synthesis of tetracyclic peptides by using T4-type scaffolds, a further increase in complexity would be desirable. However, with the current set of T4-scaffolds, this cannot be achieved. Instead, a scaffold bearing more reactive sites was needed. By increasing the number of reactive positions in the scaffold from four to six, penta- and hexa-cyclic peptides may be obtainable. The six reactive positions of these T6-type scaffolds should then consist of three CLiPS and three oxime-type reactivities.

  A straightforward topology for the required 'three-by-three' scaffolds for *both* previously described CLiPS/oxime ligation cyclization strategies, can be found in the shape of an all-functionalized phenyl ring. The fact that a phenyl ring is flat and C_6-symmetric, facilitates the synthesis and perhaps even the CLiPS and oxime ligation-cyclization reactions. While this flat molecular scaffold may contain many symmetry axes, there is no rotational freedom within the scaffold, meaning there is no chemical exchange between each position. These scaffolds are therefore structurally most comparable to the rigid T4-1 scaffold (see Chapters 2 and 3).

  A logical approach for the substitution pattern of the hexa-substituted benzene ring is of the ABABAB-type, thus showing alternating reactivities (Figure 5.1). For the tri- and tetracyclic peptides, the scaffold topologies created a distinct difference in cyclization success. Therefore, alternatively, both reactivities may be introduced at each of the 1,3,5-positions. This substitution pattern allows for more rotational flexibility, reminiscent of the T4-2 and T4-3 scaffolds.
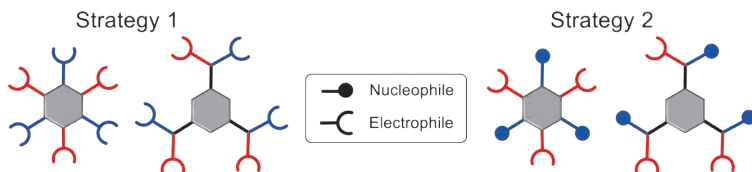

Figure 5.1: Schematic representation of the scaffold design for the synthesis of pentacyclic peptides.

For the CLiPS reaction, the scaffolds can be equipped with either an electrophilic benzylic bromide, or a bromo-acetamide functionality, which have been explored previously for the T4-scaffolds. Oxime ligation can be applied in two different directions. The scaffold either bears the aminooxy moiety, while the peptide bears the carbonyl, or *vice versa*. For Strategy 1, the peptide bears all nucleophilic moieties, being the cysteine sulfhydryl group for the CLiPS reaction and the aminooxy group for the oxime ligation reaction. As a consequence, the scaffold is decorated with two sets of three complimentary activated bromides and aldehydes as the electrophiles. For Strategy 2, the oxime precursors are reversed and consequently the scaffold bears the protected aminooxy part, while the peptide is equipped with the carbonyl-bearing amino acids.

  For Strategy 1 we envisioned three different scaffolds, the structures of which are shown in Figure 5.2. The first, T6-C1, was designed with all reactivities at closest proximity to the aromatic core. This densely-substituted scaffold was not necessarily equipped with protected aldehydes. As described previously in this thesis, scaffold-assisted cyclizations may be facilitated by introducing more flexibility into the system. Therefore, scaffold T6-C2 was designed with a small aliphatic linker between the aromatic core and the acetal-protected aldehyde. The rotationally most flexible scaffold, T6-C3, features a typical 1,3,5-substitution pattern, allowing for rotational freedom reminiscent of the T4-2 and T4-3 scaffold. This is the only scaffold with the bromoacetamide linker.

The reactivity of the scaffolds towards the CLiPS-type reactions was investigated using glutathione (GSH) as a cysteine-containing model peptide. In case of the scaffolds T6-C2 and T6-C3, liberation of the aldehyde was followed by intermolecular oxime ligation with methoxyamine.

For the peptides, which will undergo the cyclization reactions towards pentacyclic peptides, the amino acids hS(ONH$_2$) and K(Aoa) were incorporated, as they are equipped with the complimentary aminooxy moiety. Their synthesis was described in Chapter 2. In total, 4 peptides with loop lengths of 3 and 5 amino acids between the functional residues were prepared. Peptide synthesis was accomplished via regular Fmoc-based automated SPPS under standardized conditions. The cyclization reactions to obtain pentacyclic peptides were investigated using the previously optimized conditions, which are described in detail in Chapter 2.
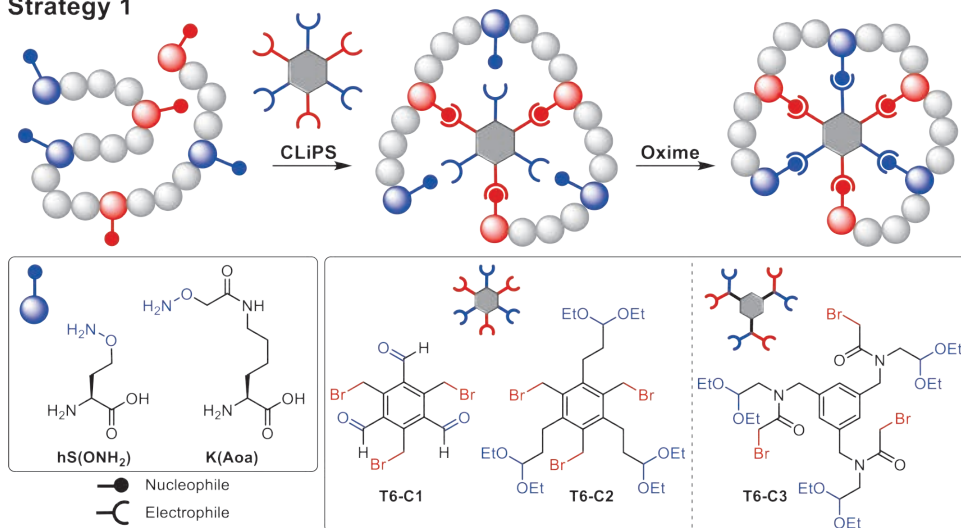
Strategy 1

Figure 5.2: Schematic representation of the reaction sequence, amino acids and scaffolds envisioned for the synthesis of pentacyclic peptides utilizing Strategy 1.

For the scaffolds used in Strategy 2, the aminooxy moiety was protected as a Boc-carbamate. Three different scaffolds were designed (Figure 5.3). Scaffold T6-N1 is similar to T6-C2, with benzylic bromides for the CLiPS reactions and a small spacer connecting the aromatic core with the aminooxy moieties. The second scaffold for this series, T4-N2, is unlike any other scaffold from Strategy 1 as here the bromides are connected via a spacer, instead of the oxime functionalities. The bromoacetamides at the benzylic spacer for the CLiPS reactions are accompanied by the aminooxy moieties at the flanking benzylic positions. The final T6-N3 scaffold shows the same 1,3,5-substitution pattern as scaffold T6-C3 from Strategy 1. The aminooxy group is derived from ethanolamine, while the bromides are introduced as bromoacetamides.

These three scaffolds were subsequently tested in their reactivity towards cysteines in the CLiPS reactions using GSH as a cysteine-containing model substrate. Subsequently, liberation of the aminooxy moieties was followed by oxime ligation with acetone as the model substrate. In total, 4 peptides equipped with the complimentary ketone groups for oxime ligation were synthesized, differing in loop lengths of three to five amino acids between the scaffold-reactive residues. Para-acetyl phenylalanine (pAcF) and the aspartic acid *tert*-butyl ketone derivative (D(Ket)) were used without further side-

chain protections and were fully compatible with standard Fmoc-SPPS. Resin cleavage demanded special attention and a tailored cation-scavenging cleavage cocktail was devised for these amino acids (Chapter 3). Finally, the synthesis of pentacyclic peptides was investigated, whereby the functionalized peptides were reacted with the synthesized scaffolds in the CLiPS and oxime ligation cyclization reaction sequence.
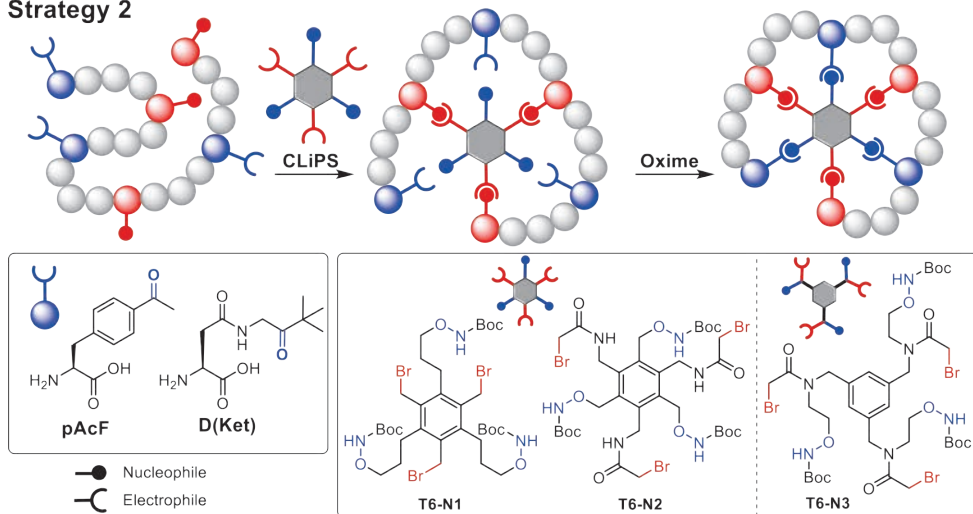

Figure 5.3: Schematic representation of the reaction sequence, amino acids and scaffolds envisioned for the synthesis of pentacyclic peptides utilizing Strategy 2.

5.1 Strategy 1: Combining Electrophilic CLiPS/Oxime Functionalities in the Scaffold

5.1.1 Attempted Synthesis of Scaffold T6-C1

T6-C1 is the sterically most congested scaffold of the envisioned series. In Scheme 5.1, the devised synthetic route is depicted. This route is characterized by introduction of the aldehyde prior to the bromide. Starting from mesitylene, methylbromination using para-formaldehyde in HBr and HOAc yielded 2,4,6-tris(bromomethyl)mesitylene **2** in quantitative yield.[1,2] Subsequent transformation of the bromides into aldehydes was performed using NaH and 2-nitropropane in a modified Hass-reaction.[3,4] The resulting trialdehyde **3** is only a trifold benzylic bromination step away from the final desired T6-C1 scaffold. As discussed below, this transformation could not be accomplished, not even after protection of the aldehydes as the corresponding dimethyl acetals.

In Table 5.1, the conditions that were tested for the final bromination step are shown. For the brominating reaction, NBS was the reagent of choice as it is most commonly used and mild. However, in most cases, NBS reacted at the aldehydes instead of the methyl groups. In the ^{1}H NMR spectrum, the aldehyde proton disappeared, while the methyl peak remained intact. Adding fewer equivalents of NBS (entry 2) or performing the reaction stepwise at rt (entry 3) gave the same outcome, as did alternative methods for initiating the reaction. By replacing NBS for NCS (entries 6 and 7), some conversion to the benzylic chlorides was observed. Unfortunately, also in this case the aldehydes reacted here as well. Radical bromination by using molecular bromine (entry 8) under irradiation also showed unwanted reactivity at the aldehydes.
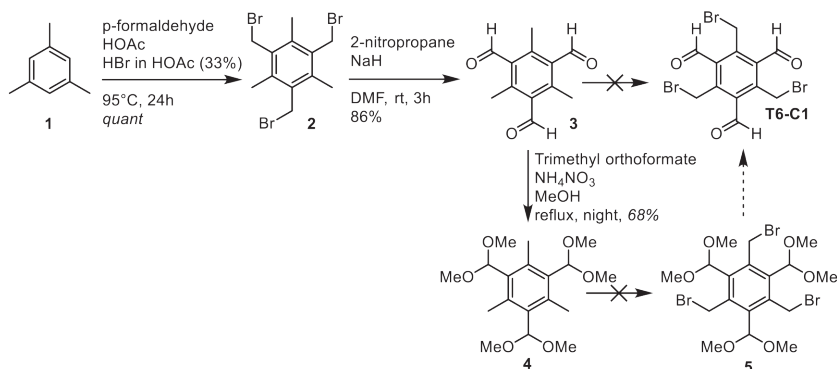
Scheme 5.1: Proposed synthesis route for scaffold T6-C1.

*Table 5.1: Reaction conditions tested for the bromination of **3** to yield T6-C1.*

#	Bromide source	Equiv	Initiator*	Time (h)	T (°C)	Result
1	NBS	5	BPO	2	80	Aldehyde peak lost
2	NBS	3.6	BPO	0.5	70	Aldehyde peak lost
3	NBS˜	3x1	BPO	3x0.5	rt	Slower, but aldehyde is consumed
4	NBS	3.2	Lamp	1	40	Complex mixture
5	NBS	3.5	AIBN	2	80	Complex mixture
6	NCS#	4.5	BPO	18	75	Aldehyde is lost, some Bn-Cl
7	NCS#	4.5	BPO	2	80	Complex Mixture
8	Br$_2$	12	Lamp	2	40	Aldehyde peak is lost

All reactions were carried out in CCl$_4$. * Initiator was added in 0.1 equiv. BPO = benzoyl peroxide, AIBN = azobisisobutyronitrile, lamp = 500 W halogen lamp. ˜ Bromide source was added in three portions. # Instead of a bromide source, a less reactive chloride source was used.

Next, we attempted bromination while the aldehyde functionalities of **3** were acetal-protected, as benzylic bromination has been described in the presence of a 1,3-dioxolane-protected benzylic aldehyde.[5] However, our attempts to transform the three aldehydes of **3** into 1,3-dioxolanes failed, as full conversion could not be reached and isolation of the pure tri-aldehyde from the mixture was unsuccessful. As an alternative, it was decided to proceed with the dimethylacetal-protected aldehyde **4**. The best conditions for this protection were found to involve trimethyl orthoformate as a water-capturing agent, NH$_4$NO$_3$ as the acid-catalyst and methanol as the solvent. However, incomplete conversion was again observed, yielding inseparable mixtures. Fortunately, the desired compound **4** crystallized from the bulk mixture and was used for seed-crystallization in additional preparations, thus facilitating purification of the desired product. Subsequent NBS-mediated bromination of the tri-acetal compound **4** to yield **5**, using several different conditions always yielded very complex mixtures. Finally, molecular bromine in combination with irradiation was attempted, however, no discernable product was observed. These results led us to conclude that radical bromination in presence of the dimethylacetal was not feasible.

Since introduction of a bromide functionality in the presence of a free, or acetal-protected aldehyde was not an option, we changed the order of events. It was attempted to install the benzylic bromides first, followed by introduction of the aldehydes. The devised alternative route to T6-C1, with bromination preceding nitrile-to-aldehyde conversion, is presented in Scheme 5.2. The key reaction is reduction of the carbonitriles to the aldehydes in the presence of the benzylic bromides. This step is known in literature,

but only for one pair of carbonitrile and benzylic bromide.[6] The presumed difficulty here was that the reaction had to be performed thrice instead of once.

First, mesitylene was brominated, yielding **6**,[1] followed by the transformation of the aryl bromides into carbonitriles by the Rosenmund-von Braun reaction, yielding **7**.[7–9] The carbonitrile groups proved to be resistant to radical bromination of the methyl groups and the benzylic bromides of **8** were obtained in good yield. Finally, the carbonitrile group was reduced to the aldehyde to provide scaffold T6-C1. For this reaction, DIBAL was chosen as the reducing agent, as a similar reaction was reported on a disubstituted aryl compound containing a single carbonitrile and benzylic bromide.[6,10,11] Moreover, in our hands this reaction worked nicely on the same model substrate, demonstrating the feasibility for this approach.

The same conditions were then applied to the trisubstituted tricarbonitrile **8**. DIBAL reduction was carried out in a solvent mixture of DCM, THF and toluene at temperatures from -78 °C to rt. Crucial to the success was careful quenching of DIBAL at low temperatures using $KHSO_4$ on ice. While the reaction seemed to work, it was hampered by incomplete conversion, which could not be resolved by adding more equivalents of DIBAL. Additionally, isolation of the desired scaffold product was difficult, as the di- and trialdehyde could not successfully be separated using column chromatography. These issues were particularly tenacious during scale-up, required to make sufficient amounts of the T6-C1 scaffold. At this stage of the project, we chose to halt further attempts to synthesize scaffold T6-C1.
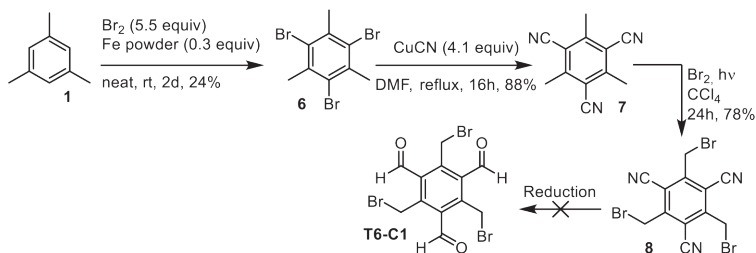
Scheme 5.2: The synthesis of T6-C1 by introduction of the bromide before the aldehyde.
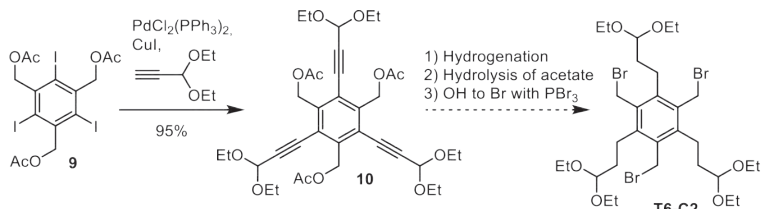
5.1.2 Attempted Synthesis of Scaffold T6-C2

The design of scaffold T6-C2 features a short spacer between the aromatic core and the aldehyde. From our synthetic experience with T6-C1, it was decided that a strategy where the aldehydes are introduced prior to the benzylic bromides, would be most promising. In Scheme 5.3, the devised route for the synthesis of T6-C2 is shown. We chose to introduce the elongated aldehyde via the robust Sonogashira reaction, while the benzylic bromides were to be introduced via a substitution reaction, avoiding radical bromination.

Tri-iodide **9** was readily obtained by iodination of mesitylene, followed by oxidation with $KMnO_4$ in presence of Ac_2O.[12] The reaction was low yielding, similar to literature precedents, but could easily be carried out on large scale, starting from cheap starting materials. Subsequent Sonogashira coupling with commercially available 3,3-diethoxyprop-1-yne gave tri-yne **10** in 95% isolated yield, containing the aldehydes protected as diethyl acetals.

Introduction of the bromides can be achieved after saponification of the acetates followed by direct PBr_3-mediated transformation of the hydroxyl groups into bromides, or by first making the mesylate and subsequent reaction with LiBr. However, as the liberated hydroxyl groups may attack the neighboring alkynes, it was chosen to hydrogenate the alkynes to the inert alkanes prior to saponification of the acetates. Interestingly, when using Pd/C and H_2, the alkene was isolated as the sole product. Moreover, when adding

different batches of Pd/C or by applying an increased hydrogen pressure, alkane formation was still not observed. Instead, a side-product was obtained where the acetate was hydrogenolytically cleaved to give the methyl group. Because this side-reaction seemed inevitable and attempts to circumvent byproduct formation were unsuccessful, we focused on the synthesis of a different type of scaffold.

Scheme 5.3: The attempted synthesis of T6-C2, featuring an elongated acetal moiety.

5.1.3 Synthesis of Scaffold T6-C3

The third scaffold, being the rotationally most flexible T6-C3, was synthesized in only two steps (Scheme 5.4). Starting from benzene 1,3,5-tricarbaldehyde **11**, reductive amination with 2,2-diethoxyethanamine (**12**) yielded amine **13** in quantitative yield. This intermediate was coupled with 2-bromoacetyl bromide (**14**), yielding the desired 1,3,5-substituted scaffold T6-C3 in 67% yield. The presence of tertiary amides gave rise to rotamers, which complicated analysis by ^{1}H NMR spectroscopy.
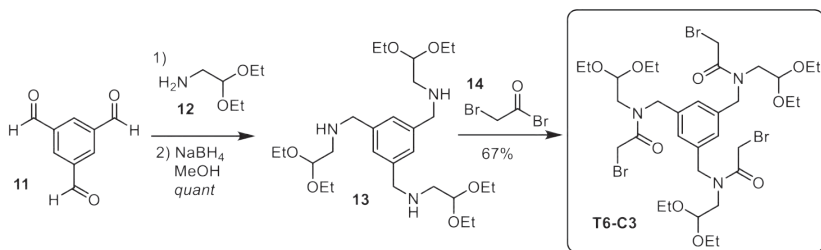
Scheme 5.4: Synthesis of scaffold T6-C3.

Unfortunately, UPLC analysis (after prolonged storage in the freezer) showed that the scaffold had decomposed (Figure 5.4). A mixture of compounds with minimal UV-activity was obtained, alongside some of the scaffold, showing a very faint ionization trace. The small peak at t_R 2.21 min was the T6-C3 scaffold, although showing an m/z-signal corresponding with the loss of ethanol. Test reactions with GSH were performed and the CLiPSed product was successfully obtained. However, we had to abandon Strategy 1 since the quality of scaffold T6-C3 was lower than acceptable.
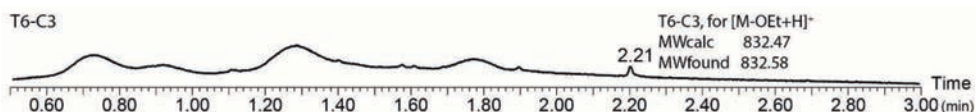

Figure 5.4: UPLC chromatogram of the T6-C3 scaffold after prolonged storage. The annotated peak belongs to the T6-C3 scaffold.

5.1.4 Linear Peptide Synthesis Bearing Aminooxy Amino Acids

The synthesis of in total four different peptides, with both aminooxy group containing amino acids K(Aoa) and hS(ONH2) was attempted, but the crude quality of all four was rather poor (see Table 5. 2 for the sequences). The previously explored side-reactions, such as deletions, were more pronounced, most likely due to the longer peptide sequences featuring an additional aminooxy residue. Material of sufficient purity was to be expected only after multiple purification cycles, which was not desirable in this project. As the scaffolds for this strategy were either not obtained or of insufficient quality, we diverted our efforts to Strategy 2, discussed in the next paragraph.

Table 5. 2: Peptides synthesized for Strategy 1 cyclizations.

#	Sequence	MW_{calc}
1	Ac-{**hS(ONH2)**}EW**F**C**SIK{hS(ONH2)}**LK**G**CAK**G**{**hS(ONH2)**}SVL**C**-NH2	2362.28
2	Ac-{**hS(ONH2)**}EQF**R**K**C**TPVKI{**hS(ONH2)**}SRAYG**C**YKGAQ{**hS(ONH2)**}SIKAS**C**-NH2	3513.64
3	Ac-{**K(Aoa)**}EW**F**C**SIK{K(Aoa)}**LK**G**CAK**G**{**K(Aoa)**}SVL**C**-NH2	2617.58
4	Ac-{**K(Aoa)**}EQF**R**K**C**TPVKI{**K(Aoa)**}SRAYG**C**YKGAQ{**K(Aoa)**}SIKAS**C**-NH2	3768.94

5.2 Strategy 2: Combining Electrophilic CLiPS with Nucleophilic Oxime Functionalities

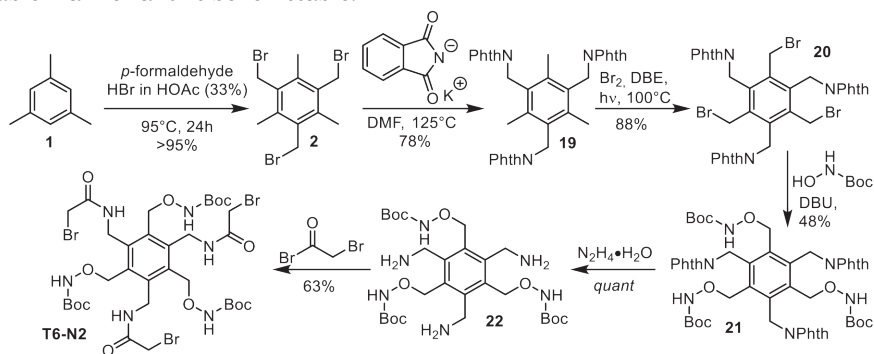### 5.2.1 Synthesis of Scaffold T6-N1

For the synthesis of scaffold T6-N1 (Scheme 5.5), the same Sonogashira approach was explored as described for scaffold T6-C2 (Scheme 5.3). Starting from the same iodide **9**, N-Boc-propargyloxyamine **15** was used here for the Sonogashira reaction, to introduce the aminooxy moiety in **16**.[13] To circumvent side reactions, the alkyne bonds were hydrogenolytically reduced to the saturated alkanes in **18**. As was similarly observed for the T6-C2 scaffold, reduction did not proceed past the alkene stage (**17**) and, in addition to this, the benzylic acetals suffered from hydrogenolysis after prolonged reaction times. Fortunately, it was found that when saponification of the acetates was performed prior to reduction of the alkenes, the sequential reactions proceeded in high yield, with little to no side reactions. Even though the PBr3 -mediated transformation of the hydroxyl groups into bromides seemed quantitative, the isolated yield after column purification was rather low. Scaffold T6-N1 was obtained as a colorless foam which tended to form a gel upon prolonged storage.
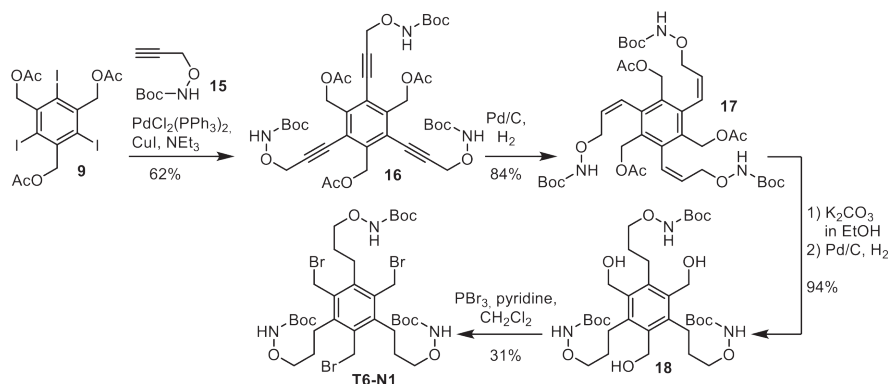
Scheme 5.5: Synthesis of scaffold T6-N1.
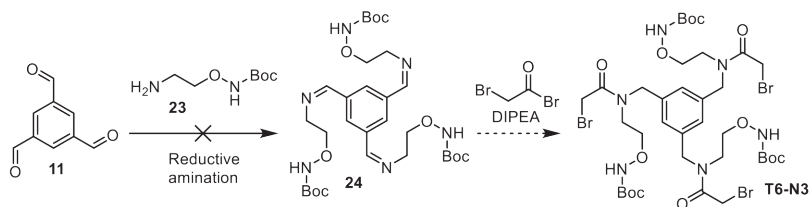
5.2.2 Synthesis of Scaffold T6-N2

Scaffold T6-N2 contains bromoacetamide groups,[14] while the aminooxy residues are closest to the aromatic core (Scheme 5.6). After bromomethylation of mesitylene, the introduced bromines were substituted by phthalimides in a Gabriel synthesis.[15,16] Bromination of this compound proceeded uneventfully with molecular bromine under irradiation with a commercially available 500W construction lamp.[15] The benzylic bromides were substituted by Boc-protected hydroxylamine, thereby introducing the aminooxy moieties. The benzylamine was liberated from the phthalimides by hydrazinolysis. Finally, the bromoacetamides were introduced via a reaction with 2-bromoacetyl bromide, yielding T6-N2 as a white powder in 19% overall yield. The scaffold was obtained in a reliable and scalable manner and is bench-stable.

Scheme 5.6: Synthesis of scaffold T6-N2.

5.2.3 Attempted Synthesis of Scaffold T6-N3

Synthesis of the rotationally most flexible scaffold T6-N3 was attempted following the route as depicted in Scheme 5.7. The devised strategy started similar to that of the successful synthesis of scaffold T6-C3, with a reductive amination at benzene 1,3,5-tricarbaldehyde **11**. Unexpectedly, *tert*-butyl (2-aminoethoxy)carbamate (**23**) proved to be an unsuitable amine for this reductive amination step. After allowing the tris-imine to form, reduction to the corresponding amines was performed using NaBH$_4$. However, for this ethanolamine aminooxy derivative, full conversion to the tris-imine was never obtained and inseparable mixtures were formed instead. Analogs of the amine differing in protective group or spacer lengths between the amine and aminooxy groups were tested, but to no avail. Again, a problem was encountered with the fact that three subsequent reactions needed to reach full completion in the same molecule. Additionally, the dramatic effect of a seemingly unimportant substituent on the outcome of the reaction was demonstrated in this manner. By just changing a diethyl acetal into an aminooxy moiety, the triple imine bond formation reaction no longer reached completion.

Scheme 5.7: The envisioned synthesis of scaffold T6-N3.

5.2.4 Linear Peptide Synthesis Containing Ketone-bearing Amino Acids

The methodology for peptide synthesis and follow up reactions was thoroughly investigated in the previous chapters (see Chapter 3 for experimental details). The purpose of this chapter is mainly a proof-of-principle exploration of the synthesis of pentacyclic peptides. Therefore, the synthesized peptides already bear a complete set of three cysteines and either three pAcF or D(Ket) amino acids. With respect to peptide loop-size, the most divisive as identified in previous chapters, being n=3 or 5, were selected. The sequences of the four synthesized peptides are shown in Table 5.3.

Due to the ABABAB-type substitution pattern of the scaffolds, the peptide naturally follows this orientation. Therefore, the peptide codes do not bear the suffixes [int] or [ter] for the position of the oxime amino acids. Rather, the ketone amino acid is always located at the N-terminus. As a consequence, the C-terminus bears the cysteine. Due to their respective sizes, the peptides were designed to be rather polar, in order to ensure their solubility in aqueous solutions, particularly because the D(Ket) amino acid is rather apolar. The peptide sequences were therefore an amalgamation of the peptide sequences as used in the previous chapters. The peptides' physical properties were confirmed by UPLC-MS measurements (Table 5.4).

Table 5.3: Peptides synthesized for this project, showing the codes and peptide sequences.

Code	Sequence
5-pAcF^{n3}	Ac-{**pAcF**}EWF**C**SIK{**pAcF**}LKG**C**AKG{**pAcF**}SVL**C**-NH$_2$
6-pAcF^{n5}	Ac-{**pAcF**}EQFRK**C**TPVKI{**pAcF**}SRAYG**C**YKGAQ{**pAcF**}SIKAS**C**-NH$_2$
7-D(Ket)^{n3}	Ac-{**D(Ket)**}EWF**C**SIK{**D(Ket)**}LKG**C**AKG{**D(Ket)**}SVL**C**-NH$_2$
8-D(Ket)^{n5}	Ac-{**D(Ket)**}EQFRK**C**TPVKI{**D(Ket)**}SRAYG**C**YKGAQ{**D(Ket)**}SIKAS**C**-NH$_2$

Table 5.4: Retention times and mass data as determined by UPLC/ESI-MS measurements.

Code	t_R (min)*	MWcalc	MWfound
5-pAcF^{n3}	1.60	2581.55	2581.42
6-pAcF^{n5}	1.10	3732.91	3732.74
7-D(Ket)^{n3}	1.64	2650.64	2650.56
8-D(Ket)^{n5}	1.11	3802.00	3802.10

*Measured on a 5-55% MeCN in MilliQ gradient over 2 min.

5.3 Optimization of the CLiPS and Intermolecular Oxime Ligation Reactions with Scaffolds T6-N1 and T6-N2

The synthesized scaffolds T6-N1 and T6-N2 were first subjected to the CLiPS reaction, Boc-removal conditions and the final (intermolecular) oxime ligation, in order to gauge the reactivity and stability of these scaffolds. For the benzylic bromide scaffold T6-N1, its quite apolar character was noticeable and the compound turned out to be insoluble in MeCN. Figure 5.5 shows the corresponding UPLC chromatogram using a 5-80% MeCN gradient in MilliQ-H$_2$O with T6-N1 eluting at a t_R of 2.39 min. Fortunately, its solubility in aqueous DMSO was just sufficient to be able to perform all CLiPS reactions, as usual, in aqueous MeCN (1:1).
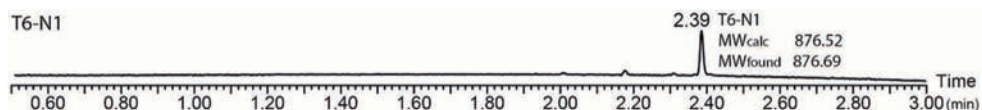

Figure 5.5: UPLC chromatogram of the T6-N1 scaffold.

The required reactivity in the CLiPS reaction was confirmed for T6-N1 using GSH as a model peptide (Figure 5.6). While a 20-fold excess of GSH was necessary for the reaction to reach full conversion, a single product was obtained, eluting at a t_R of 1.10 min. The reaction sequence was then continued by carrying out the oxime ligation reactions. For this, the reaction mixture was lyophilized, after which it was treated with neat TFA to liberate the aminooxy moieties. Although UPLC-MS analysis confirmed the loss of all three Boc protective groups, the retention time of the fully deprotected product remained the same at t_R 1.10 min. This was surprising as the free aminooxy groups generally are more polar than the protected ones. It should be noted that the SS-dimer of GSH appeared as a side product at t_R 1.24 min. Removal of TFA under a stream of N_2 and subsequent addition of acetone yielded the product tri-oxime. This product is inexplicably more polar than its tris-aminooxy precursor (Figure 5.6c), while in previous experiments the isopropylidene adducts were found to be less polar. This sequence of reactions proved that the CLiPS reaction, followed by aminooxy liberation and oxime ligation is a viable option for the T6-N1 scaffold.
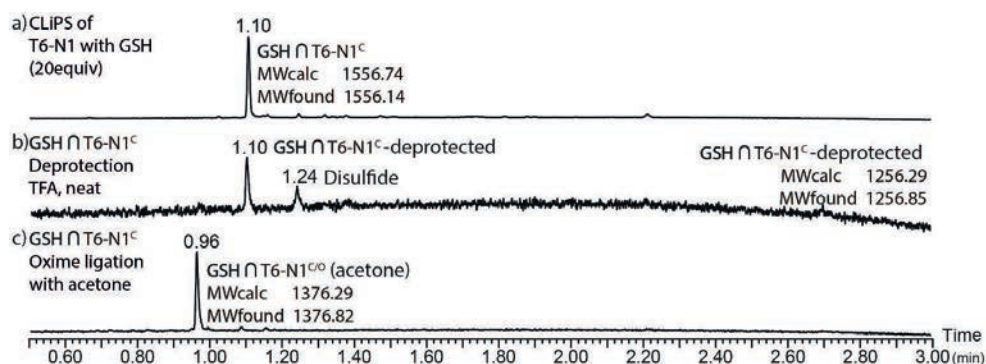

Figure 5.6: UPLC chromatograms of a) the CLiPS reaction between T6-N1 and GSH, followed by b) aminooxy liberation and c) oxime ligation with acetone.

Next, scaffold T6-N2 was subjected to the same sequence of test reactions and conditions. The scaffold itself is somewhat more polar than the T6-N1 scaffold, eluting at a t_R of 2.04 min (Figure 5.7). The increased polarity stems from the bromoacetamide groups.[14]
For the CLiPS reaction, the scaffold was reacted with GSH (Figure 5.7a). The reaction, with 20-fold excess of GSH, yielded a single product. For GSH∩T6-N2^C, the TFA-induced deprotection could not be monitored by UPLC, as the product was not detected in multiple experiments neither by UV nor via its ion-current MS spectrum. Gratifyingly, the anticipated product GSH∩T6-N2$^{C/O\text{-acetone}}$ was indeed observed at a t_R of 0.73 min after oxime ligation with acetone. This product was also more polar than the starting GSH∩T6-N2^C. An unknown side product was also detected at a t_R of 0.57 min. The origin remained unknown, justifying further investigations during the following peptide cyclization reactions.
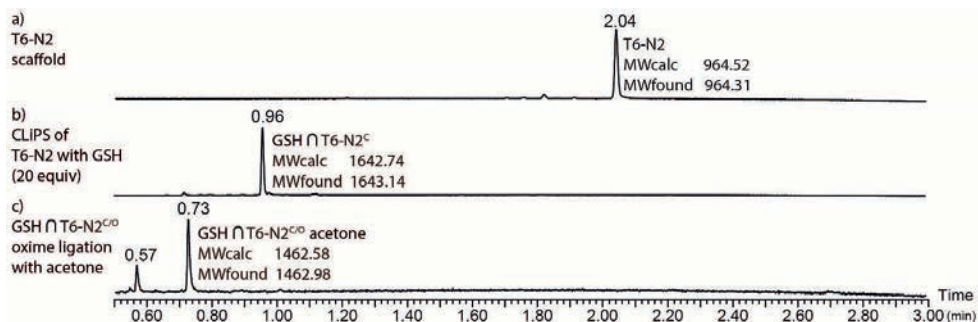
Figure 5.7: UPLC chromatograms of T6-N2: a) neat, b) in the CLiPS reaction with GSH and subsequent Boc-deprotection (not pictured) and c) after oxime ligation with acetone.

5.4 Peptide Cyclizations

5.4.1 pAcF Peptides

With all scaffolds and peptides in hand, the cyclization reactions towards pentacyclic peptides were investigated next. It was assumed that all CLiPS reactions proceed as expected, in quantitative conversion to the desired bicyclic peptide. Therefore, in line with the previous chapters, we put our focus on the results of the final macrocyclizations (i.e. from bicycle to pentacycle) via oxime ligation.

We started with the pAcF-containing peptides **5** and **6**, as they are the least hindered ones. The optimized standard procedures, as described in Chapter 3, were applied in all cases. The CLiPS reaction was carried out in aqueous MeCN (1:1, 0.5 mM) using the peptide in slight excess (1.1 equiv). Following addition of the scaffold, the pH was adjusted to pH >8 by adding a 1M NH_4HCO_3 solution. After completion of the reaction, which was monitored by UPLC, the CLiPS mixture was lyophilized, followed by treatment of the lyophilized peptide construct with $TFA:CH_2Cl_2$ (2:1 v/v) to remove the protecting Boc-groups. Deprotection required two hours, after which the volatiles were evaporated by a stream of N_2. The residue was then dissolved in aqueous DMSO (1:1, 0.5 mM) and oxime ligation occurred without any other additives. Oxime ligation was carried out at 40°C to ensure full conversion in an acceptable timeframe.

For both the T6-N1 and T6-N2 scaffolds, the CLiPS reactions with peptides **5**-pAcF^{n3} and **6**-pAcF^{n5} proceeded as expected, yielding a single peak for all peptide-scaffold combinations (not shown). Interestingly, the CLiPS intermediates in the pentacycle synthesis showed a reduced polarity as compared to the starting materials instead of a more polar construct, as was always observed in case of the CLiPS-oxime tricycles (see Chapters 2 and 3). For example, where the linear peptide **5**-pAcF^{n3} has a t_R of 1.60 min, the CLiPSed products eluted at t_R 1.80 min for both scaffolds. For **6**-pAcF^{n5} this shifted from t_R 1.10 to t_R 1.20-1.30 min. Even though this seems a bit unusual when compared to previous cyclizations, it can be rationalized when taking into account the scaffold design, featuring many more aliphatic bonds around a heavily-substituted aromatic core.

The results for the oxime ligations with the pAcF peptides **5**-pAcF^{n3} and **6**-pAcF^{n5}, are shown in Figure 5.8. For the shorter peptide **5**-pAcF^{n3}, both scaffolds yielded a complex mixture of products, without a clear major product (Figure 5.8a,b). For both reactions, the UPLC-trace was dominated by a big bump spanning 0.4 min, which is indicative of oligomerization. For both scaffolds, about four different product peaks were distinguished. From the ESI-MS spectra we concluded that all peaks show m/z-signals corresponding with the mass of the desired pentacyclic product. However, the sheer number of peaks indicates that the pentacycle has formed in many different isomeric forms. The peak profile did not change over time, suggesting that the outcome of the reaction was kinetically, rather than thermodynamically controlled. It is quite interesting that for

5-pAcF^{n3}∩T6-N1$^{C/O}$, the bump representing oligomerized products lays free from the other peaks, as most often products display very similar polarities. Moreover, the product peaks from t_R 1.90-2.00 min. were more apolar than the starting peptide. This is unusual because the oxime ligation most often increases the polarity of the multicyclic peptide construct that is formed (see Chapters 3 and 4). The shift to a longer retention time is a break from this trend. For **5**-pAcF^{n3}∩T6-N2$^{C/O}$ this was less pronounced, even though the pentacyclic product peaks lay only slightly in front of those of the starting peptide, which elutes at t_R 1.60 min.
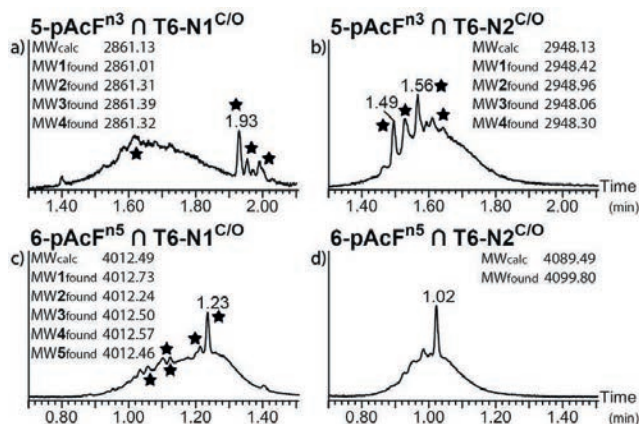

Figure 5.8: UPLC chromatograms of the oxime cyclization reactions of pAcF peptides with scaffolds T6-N1 and T6-N2. ★ denotes an (isomeric) peak of pentacyclic peptide. Product MW's are denoted in chronological order of encounter.

For the larger peptide **6**-pAcF^{n5}, clearly one major product was formed in the oxime ligation cyclization reaction with both scaffolds (Figure 5.8c,d). However, similar to the shorter peptides, both reactions suffered extensively from oligomerization. We believe that this could be attributed to a scrambling of the reactivity pattern, i.e. the oxime linkage was not formed between the 'closest' partners, but between other neighbors, which complicates the mixture. For **6**-pAcF^{n5}∩T6-N1$^{C/O}$, there were a large number of different product peaks hidden in the oligomerization bump, with well-defined m/z-signals corresponding to the correct mass of the pentacyclic peptide product. For pentacycle **6**-pAcF^{n5}∩T6-N2$^{C/O}$, however, this was different. The major product peak very clearly showed m/z-signals corresponding to the pentacyclic product mass, while the oligomerization bump did not. We believe that for these peptides, thermodynamics may have played a bigger role in the cyclization results compared to the smaller tricyclic peptides, because the product composition was found to change significantly over time. Figure 5.9 shows the UPLC chromatograms of the CLiPS/oxime reaction to give **6**-pAcF^{n5}∩T6-N2$^{C/O}$ at various timepoints. The CLiPS reaction yielded a single bicyclic product at t_R 1.26 min. Figure 5.9b shows the reaction composition 6h after starting the oxime ligation reaction. The pentacycle was present at t_R 1.04 min, while incomplete oxime ligation products are denoted by "•". When the reaction mixture was left overnight, most of these incomplete oxime-intermediates had converged into a single product peak at t_R 0.86 min., while also a second pentacycle product peak appeared at t_R 1.00 min. Over the weekend, the oxime ligation reached completion and the pentacycle peak at t_R 1.00 min. had lost intensity, yielding nearly a single product peak at t_R 1.02 min, which shows that the oxime pentacyclization reaction is indeed a dynamic process.
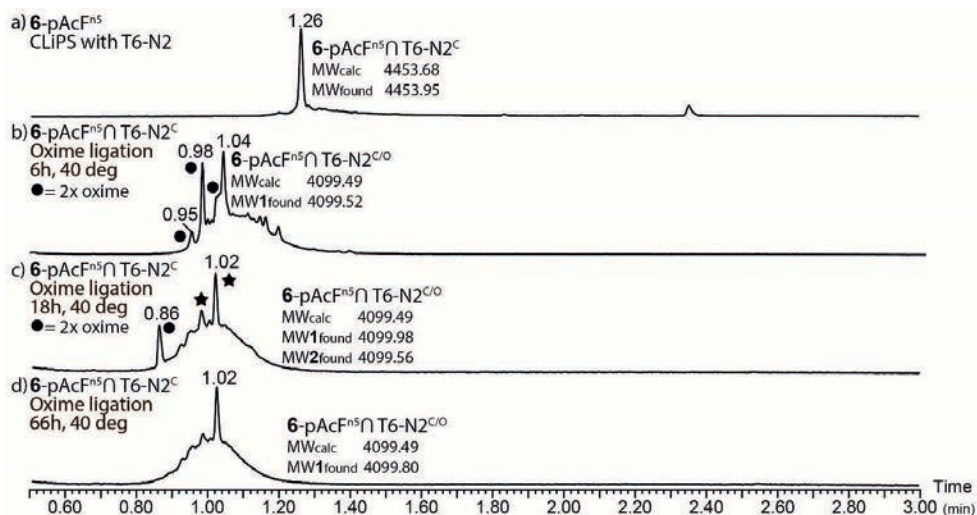
Figure 5.9: UPLC chromatograms of the CLiPS and oxime ligation reaction between 6-pAcF^{n5} and T6-N2, showing a) CLiPSed product, and the oxime ligation after b) 6h, c) 18h and d) 66h. ● denotes incomplete oxime ligation (2x oxime linkages had formed). ★ denotes an (isomeric) peak of the pentacyclic peptide product. Product MW's are denoted in chronological order of encounter.

While this interconversion of products was not observed for **6**-pAcF^{n5}∩T6-N1$^{C/O}$ (data not shown), we can cautiously conclude that the more flexible the system is, the more opportunities it has to yield a thermodynamically favored product. We assume this results in one major product, contrary to the multiple kinetic products obtained for the short peptide **5**-pAcF. We conclude from these results that the CLiPS/oxime ligation reaction sequence *can* be applied to the synthesis of pentacyclic peptides containing pAcF. However, due to extensive oligomerization of the tested peptides, this system is not yet viable for library synthesis and screening methods. The set of peptides tested was rather limited and there is room for further improvement. Primarly, more peptide sequences need to be screened to find out wether the observed oligomerization is common for more peptides. However, proof of principle for the chemistries involved has been provided with the experiments described above.

5.4.2   D(Ket) Peptides

After the encouraging results for the pAcF peptides, the D(Ket) peptides were investigated next. Previously, it was observed in experiments with peptides containing multiple D(Ket) residues, that the corresponding intermolecular oxime ligation reactions required much longer reaction times. Intramolecular reactions using T4-templates gave incomplete conversion, presumably because the peptide was trapped in an unfavorable conformation and could not react further. In addition, equilibration reactions towards a thermodynamic product were assumed not to take place within the normal timeframe as a result of the much lower reactivities of the D(Ket) functionality.

The results of the oxime ligation cyclization reactions between the D(Ket) peptides and scaffolds T6-N1 or T6-N2 are shown in Figure 5.10. The small peptide **7**-D(Ket)^{n3} showed a very different reactivity towards both scaffolds. For T6-N1, a single product was obtained, while for T6-N2 a complex mixture was obtained consisting of incompletely converted products. Upon standing for two weeks, any further conversion into desired pentacyclic product was not observed. Similar to the pAcF pentacycles, the pentacyclic peptide products of the cyclizations were less polar than the starting peptides.
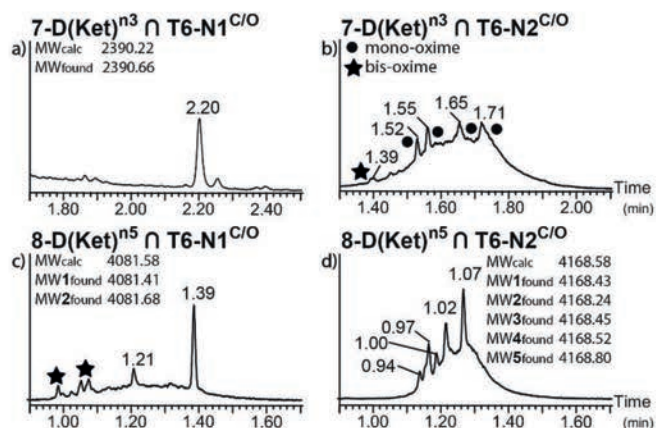
Figure 5.10: UPLC chromatograms of the D(Ket) peptides with scaffolds T6-N1 and T6-N2. Product MW's are denoted in chronological order of encounter.

Formation of **7**-D(Ket)^{n3}∩T6-N1$^{C/O}$ was the first case providing a single pentacyclic product, although this happened only after a prolonged reaction time (see Figure 5.11 and Figure 5.12). After the first CLiPS reaction yielding a single bicyclic intermediate, the volatiles were removed by lyophilization, followed by deprotection of the scaffold aminooxy groups to initiate the oxime ligation reaction. After 4 hours (Figure 5.12c), a plethora of different products was found, amongst which were the fully liberated construct (━) where no oxime ligation had taken place yet, together with the mono- and bis-oxime products (● and ★, respectively). After 20 hours, the desired pentacyclic product was present as the main product, together with some leftover of the intermediate bis-oxime intermediate. After 42 hours, the pentacycle was virtually the only remaining product present, showing the remarkable selectivity of this gradual but selective oxime ligation. It is to be expected that a similar process *could* have happened for the T6-N2 construct. However, it seems that the intermediates are sort of "trapped" in an unfavorable conformation, thus hampering further reaction towards the complete pentacyclic peptide product (Figure 5.10b).
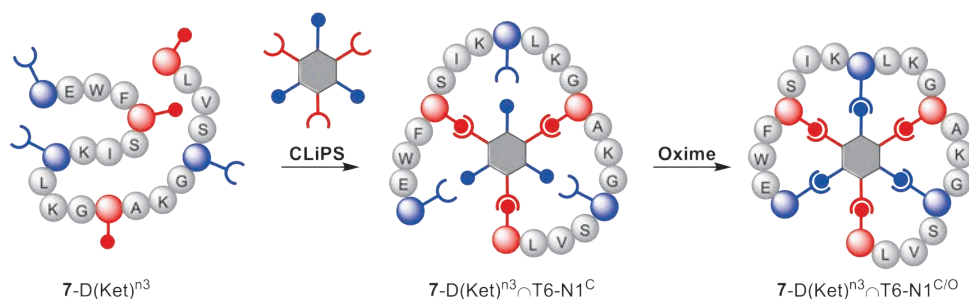

*Figure 5.11: Schematic representation of the synthesis of pentacyclic peptide **7**-D(Ket)^{n3}∩T6-N1$^{C/O}$.*
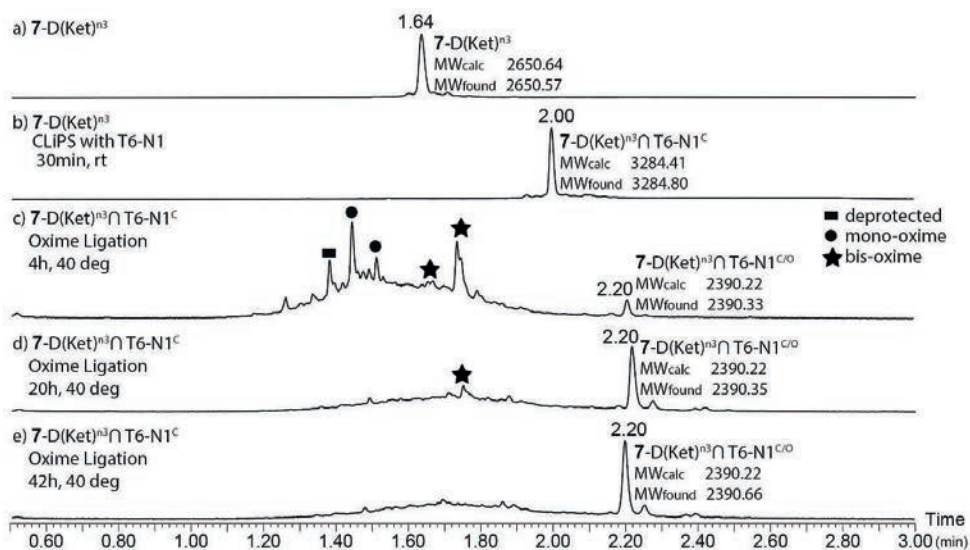
Figure 5.12: Time-resolved UPLC chromatograms of the CLiPS/oxime ligation for peptide 7-D(Ket)^{n3} with scaffold T6-N1, where a) the linear peptide, b) the CLiPS reaction mixture and the oxime ligation after c) 4h, d) 20h and e) 42h.

The larger peptide **8**-D(Ket)^{n5} provided very similar results as observed with peptide **7**-D(Ket)^{n3}, indicating that the peptide loop lengths are not essential. For the T6-N1 scaffold (Figure 5.10), again one major isomer of the pentacyclic product was obtained, besides a second isomer in minute amounts together with some minor intermediates. After allowing the reaction mixture to stand for 48 hours, any further change in the composition of the mixture was not observed. Although the CLiPS/oxime reactions for peptide **8**-D(ket)^{n5} with scaffold T6-N2 went to completion, the pentacyclic peptide was obtained as a mixture of isomers. Five isomeric products were formed within a few days, but the mixture did not equilibrate further to give a single thermodynamically favoured isomer. It seems that the low reactivity of the D(Ket) amino acid also impeded the reversibility of the oxime ligation.

The reason why there is such a difference in reaction outcome between the T6-N1 and the T6-N2 scaffold is most likely related to the very different flexibility of both scaffolds. For T6-N1, the aminooxy moieties are placed at the end of a small tether, increasing the flexibility of the system. Additionally, the peptide is more tightly locked after the initial CLiPS reactions positioning the peptide in closer proximity to the aromatic core. Therefore, the peptide ketone might be better aligned with the scaffold aminooxy moieties, leaving enough space for the oxime groups to align. For T6-N2, the CLiPSed product may be too flexible, since the distance to the aromatic core is much longer. Therefore, the most favorable alignments of the oxime moieties may not necessarily position the remaining ketones and aminooxy groups in productive orientations. Also scrambling of the intended pattern, whereby the oxime is not formed with the (on paper) nearest ketone but with its neighbor, could yield conformations with free oxime moieties that can no longer react, resulting in incomplete conversion products.

5.5 Conclusion

This work shows the proof-of-principle for the synthesis of pentacyclic peptides using a combination of CLiPS and oxime ligation. Due to the inaccessibility of suitable T6-scaffolds for strategy 1, only the applicability of Strategy 2 towards pentacyclic peptides was

investigated. We described the synthesis of two new scaffolds, T6-N1 and T6-N2, which were reacted with in total four different peptides (**5-8**). While only scaffold T6-N1 gave rise to the formation of a single isomerically pure product, we can generally attest that we provided the first proof-of-principle for peptide cyclizations at hexavalent scaffolds.

Both the pAcF and D(Ket) peptides gave pentacyclic peptides upon reaction with either the T6-N1 or T6-N2 scaffold. Success in the reactions was dependent on several factors, where scaffold T6-N1 performed better in nearly all reactions. For the pAcF peptides, the peptide length was the most influential parameter for a successful reaction, with an increased loop length giving the cleanest results. For D(Ket) peptides, the very low reactivity of the sterically hindered ketone in oxime ligation reactions remains an issue. However, in combination with scaffold T6-N1, isomerically pure pentacyclic products were obtained for both peptides that we investigated. The occurrence of intermediate products, relating to incomplete oxime-cyclization reactions, remains an issue, especially with the T6-N2 scaffold. However, the obtained results are sufficiently encouraging to render further research worthwhile.

5.6   Future Prospects

Currently, we have only provided proof-of-principle results for the synthesis of pentacyclic peptides via CLiPS/oxime ligation-cyclization reactions. As we have seen in our endeavors to synthesize tri- and tetracyclic peptides, the results of these cyclization reactions vary substantially for the different strategies investigated. Therefore, it would definitely be worthwhile to further explore successful synthesis of suitable scaffolds for the Strategy 1 route towards pentacyclic peptides.

For Strategy 2, only a small set of peptides was investigated. The most logical means to expand this work is by investigating in more detail the effect of peptide loop length in a more systematic manner. That would involve the screening of a much larger set of peptides, differing both in loopsize and in amino acid composition.

Another option to expand this chemistry is to start from monocyclic, back-bone cyclized peptides to yield hexacyclic peptides, in the spirit of the tetracycle-syntheses as described in Chapter 4. Similar experiments from our lab have established a favorable link between the monocyclic starting material and cyclization success for a CLiPS/CuAAC system. While there are quite a few parallels between the tricycles and tetracycles, investigation is necessary to establish the same link between the penta- and hexacycles. The combination of data sets would gain valuable insights into the cyclization process.

5.7   Experimental Section

1,3,5-Tris(bromomethyl)-2,4,6-trimethylbenzene (**2**)
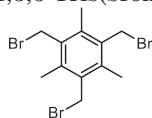
To a flame-dried flask, under N_2, mesitylene **1** (0.7 mL, 5.0 mmol, 1.0 equiv) was added, followed by acetic acid (2.6 mL) and HBr in AcOH (33% wt solution) (3.5 mL). Then *para*-formaldehyde (570 mg, 18.8 mmol, 3.7 equiv) was added and the solution was stirred at 95 °C. After 3h, a solid material started to develop. The mixture was stirred for another 9h, after which the mixture was cooled to rt. After crashing the mixture onto ice, the solids were filtered and dried. The solid was recrystallized from CH_2Cl_2:P.E. to yield the desired product **2** as a crystaline material (colorless needles) (1.99 g, 5 mmol, 99%). **^{1}H NMR** (500 MHz, CDCl$_3$) δ 4.61 (s, 6H), 2.50 (s, 9H). **^{13}C NMR** (126 MHz, CDCl$_3$) δ 137.84, 133.18, 29.93, 15.38. *Spectroscopic data are in accordance with those reported in literature.*[1,2]

2,4,6-Trimethylbenzene-1,3,5-tricarbaldehyde (**3**)
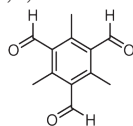
In a flame-dried flask, under N_2 flow, NaH (60% suspension in mineral oil, 180 mg, 4.5 mmol, 4.5 equiv) was dissolved in 6 mL of anhydrous DMF, and cooled on ice. 2-Nitropropane (540 μL, 6.0 mmol, 6.0 equiv) was added dropwise to the solution, and the mixture was stirred for 15 min. 2,4,6-tris(bromomethyl) mesitylene (400 mg, 1.0 mmol, 1.0 equiv) was dissolved in 9 mL of anhydrous

DMF and this solution was added to the reaction mixture. After 3h, TLC indicated that the reaction had reached completion and was subsequently quenched with water. After extraction with CH_2Cl_2, the organic phase was washed with brine and dried over Na_2SO_4. Subsequent filtration and removal of the volatiles under reduced pressure yielded the crude product as a yellow solid. Further purification via flash column chromatography (3:1 – P.E.-EtOAc) yielded the product as an off-white solid (185 mg, 0.91 mmol, 91%). **^{1}H NMR** (500 MHz, CDCl$_3$) δ 10.62 (s, 3H), 2.65 (s, 9H). **^{13}C NMR** (126 MHz, CDCl$_3$) δ 194.20, 143.08, 134.85, 16.15. *Spectroscopic data are in accordance with those reported in literature.* [3]

### 1,3,5-Tribromo-2,4,6-trimethylbenzene (6)
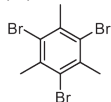
A 3-necked flask was equipped with a gas trap to safely remove the HBr that is released during the reaction. The flask was charged with iron powder (481 mg, 8.7 mmol, 0.3 equiv) and bromine (4 mL, 188.0 mmol, 5.5 equiv) was added. Mesitylene (**1**) (3 mL, 28.9 mmol, 1.0 equiv) was added dropwise via a slow addition pump over the course of an hour. The mixture was kept overnight at rt, after which water was added. The solid was filtered and the sludge was dissolved in CH_2Cl_2 after which the product was crystallized from P.E. The reddish solid was carefully washed with acetone, until a fine white crystalline solid was obtained (2.44 g, 6.84 mmol, 24%). **^{1}H NMR** (500 MHz, CDCl$_3$) δ 2.68 (s, 9H). **^{13}C NMR** (126 MHz, CDCl$_3$) δ 136.96, 124.94, 26.28. *Spectroscopic data are in accordance with those reported in literature.* [17]

### 2,4,6-Trimethylbenzene-1,3,5-tricarbonitrile (7)
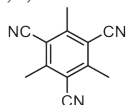
To a flame-dried flask, under N_2 flow, trisbromomesitylene (**6**) (6.00 g, 16.8 mmol, 1.0 equiv) was added and dissolved in 60 mL of NMP. CuCN (6.18 g, 69.0 mmol, 4.1 equiv) was added and the mixture was stirred for 8h at 180 °C. It was subsequently cooled to rt, and the mixture was diluted with EtOAc. Remnants of the Cu-salts were removed by washing with water and water/ethylenediamine (9:1) until the aqueous phase remained colorless. After washing with brine, the organic phase was dried over Na_2SO_4 and the solvent was removed under reduced pressure, to yield a brown solid. Column chromatography (7:1 – P.E.:EtOAc) yielded product **7** as a white solid (3.00 g, 14.8 mmol, 88%). **^{1}H NMR** (500 MHz, CDCl$_3$) δ 2.84 (s, 9H). **^{13}C NMR** (126 MHz, CDCl$_3$) δ 149.90, 129.45, 114.32, 20.78. **IR** (cm^{-1}) 2926, 2228, 1566, 1438, 1380, 1214, 1061, 1020, 978, 732, 508, 465. **mp** 172°C *Spectroscopic data are in accordance with those reported in literature.* [8]

2,4,6-Tris(bromomethyl)benzene-1,3,5-tricarbonitrile (8)
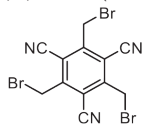
To a flame-dried flask, argon flushed, tricarbonitrile **7** (1.01 g, 5.1 mmol, 1.0 equiv) was added and suspended in 50 mL CCl$_4$. Bromine was then added (2 mL, 76.4 mmol, 15.0 equiv) and the reaction mixture was irradiated with a commercial 500W halogen lamp and the mixture was thus stirred for 24h, after which the reaction micture was diluted with CH_2Cl_2 and extracted with a 0.5M solution of $Na_2S_8O_3$. The collected organic phases were dried over Na_2SO_4 and the volatiles were removed under reduced pressure. Flash column chromatography (9:1 – P.E.:EtOAc) yielded the desired product **8** as a white solid (695 mg, 4.0 mmol, 78%). **^{1}H NMR** (500 MHz, CDCl$_3$) δ 4.84 (s, 6H). **^{13}C NMR** (126 MHz, CDCl$_3$) δ 149.90, 115.37, 111.83, 25.44. *Note: While CCl$_4$ is preferably avoided, the reaction only worked in CCl$_4$, whereby higher dilution provided the best results. CH_2Cl_2, CHCl$_3$, DCE were not suitable solvents for this reaction. Spectroscopic data are in accordance with those reported in literature.* [8]

1,3,5-Triiodo-2,4,6-trimethylbenzene 9a
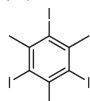
In a flame-dried flask, under N_2 flow, iodine (102.0 g, 40.0 mmol, 6.0 equiv) was dissolved in 120 mL of CCl$_4$. Mesitylene **1** was added, followed by (diacetoxyiodo)benzene (50 g, 116.3 mmol, 1.7 equiv). The bright purple solution was stirred overnight during which an off-white cake was formed on the side of the flask. The solids were filtered off, resulting in a yellowish solid, containing I_2 crystals. The cake was washed with acetone until the cake no longer gave off an orange color. The product **9a** was isolated as an off-white solid (25.7 g, 51.7 mmol, 76%). **^{1}H NMR** (400 MHz, CDCl$_3$) δ 3.01 (s, 9H). *Spectroscopic data are in accordance with those reported in literature.* [12]

(2,4,6-Triiodobenzene-1,3,5-triyl)tris(methylene) triacetate (9)
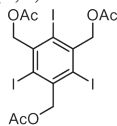
Ac$_2$O (470 mL), AcOH (235 mL) and H$_2$SO$_4$ (47 mL) were pre-mixed in a flask and **9a** (25 g, 50.2 mmol, 1.0 equiv) was added to this solution, yielding a milky pink suspension. KMnO$_4$ (31.82 g, 301.3 mmol, 4.1 equiv) was added in small portions over 3h, due to the heat evolution after every step. The yellow suspension was stirred over two days. The solution was concentrated, after which water was added. The aqueous phase was extracted with CH$_2$Cl$_2$ (6x), and the collected organic phases were washed with brine, and dried over Na$_2$SO$_4$. After concentration, the product was precipitated from acetone. The precipitate was filtered, washed with acetone and dried under reduced pressure, yielding **9** as a fine, off-white powder (14.78 g, 22.0 mmol, 44%). **¹H NMR** (400 MHz, CDCl$_3$) δ 5.72 (s, 6H), 2.13 (s, 9H). *Spectroscopic data are in accordance with those reported in literature.*[12]
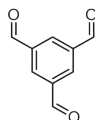
(2,4,6-Tris(3,3-diethoxyprop-1-yn-1-yl)benzene-1,3,5-triyl)tris(methylene) triacetate (10)
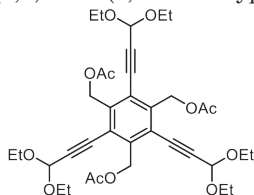
To a flame-dried high pressure tube under Ar, **9** (90 mg, 0.14 mmol, 1.0 equiv), 1.0 mL of NEt$_3$, Pd(PPh$_3$)$_2$Cl$_2$ (5.6 mg, 8.1 μmol, 6.0 mol%) and CuI (1.2 mg, 6.07 μmol, 4.5 mol%) were added. Finally, 3,3-diethoxyprop-1-yne (70 μL, 0.49 mmol, 3.6 equiv) was added and the tube was sealed. The orange mixture was heated to 50 °C and stirred for 2 days. After filtration over a Celite pad and subsequent elution with CH$_2$Cl$_2$, the volatiles were removed under reduced pressure, yielding the crude mixture as a brown oil. Flash column chromatography (3:1 – P.E.:EtOAc)provided product **10** as a brownish crystalline solid (83 mg, 0.12 mmol, 91%). **¹H NMR** (500 MHz, CDCl$_3$) δ 5.48 (s, 3H), 5.40 (s, 6H), 3.79 – 3.69 (m, 6H), 3.69 – 3.57 (m, 6H), 2.07 (s, 9H), 1.24 (t, J = 7.1 Hz, 19H). **¹³C NMR** (126 MHz, CDCl$_3$) δ 170.61, 140.15, 125.80, 95.33, 91.59, 78.66, 63.44, 61.18, 20.56, 15.05. **IR** (cm^{-1}) 2974, 2930, 2897, 2231, 1738, 1560, 1479, 1159, 1393, 1356, 1326, 1225, 1151, 1109, 1088, 1047, 1026, 1007, 969, 919, 836, 806, 730, 700. **HRMS (FD)** for C$_{36}$H$_{48}$O$_{12}$ calc. 672.3146 found 672.3316. For C$_{34}$H$_{43}$O$_{11}$$^+$ (-OEt) calc 627.2800, found 627.2745. **mp** 74°C.
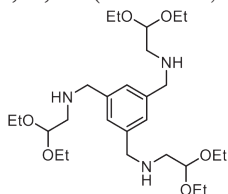
Benzene-1,3,5-tricarbaldehyde (11)

Benzene-1,3,5-triyltrimethanol (400 mg, 2.38 mmol, 1.0 equiv) was suspended in 8 mL of *t*BuOH, and IBX (4.00 g, 14.27 mmol, 6.0 equiv) was added. The mixture was heated to reflux and stirred for 5h. The suspension was cooled to rt and the solids were filtered off and subsequently washed with CH$_2$Cl$_2$. The clear filtrate was evaporated to dryness, yielding **11** as a white powder (385 mg, 2.38 mmol, *quant*). **¹H NMR** (500 MHz, CDCl$_3$) δ 10.21 (s, 3H), 8.64 (s, 3H). **¹³C NMR** (126 MHz, CDCl$_3$) δ 189.78, 137.80, 134.76. Spectroscopic data are in accordance with those reported in literature.[18]
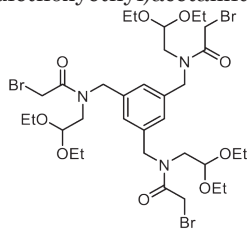
N,N′,N″-(benzene-1,3,5-triyltris(methylene))tris(2,2-diethoxyethan-1-amine) (13)

In a flame-dried flask under N$_2$, tri-aldehyde **11** (162 mg, 1.0 mmol, 1.0 equiv) was dissolved in 6 mL of 1:1 CHCl$_3$:MeOH. Then 2,2-diethoxyethanamine (**12**) (653 μL, 4.5 mmol, 4.5 equiv) was added dropwise and the mixture was stirred for 1h at rt, after which the volatiles were removed under reduced pressure to yield the imine as an orange oil (499 mg, 1.0 mmol, 98%). The residue (458 mg, 0.9 mmol, 1.0 equiv) was dissolved in 4 mL of MeOH and cooled to 0 °C. NaBH$_4$ (204 mg, 5.4 mmol, 6.0 equiv) was added and the mixture was stirred for 1h, after which TLC showed full consumption of the starting material. The reaction mixture was quenched with a *sat*. NH$_4$Cl solution and extracted with CH$_2$Cl$_2$. The combined organic phases were washed with a *sat*. NaHCO$_3$ solution and brine, and subsequently dried over Na$_2$SO$_4$. The volatiles were removed under reduced pressure to yield the tri-amine **13** as a pale-yellow oil (457 mg, 0.9 mmol, 98%), which was used without further purification. **¹H NMR** (500 MHz, CDCl$_3$) δ 7.12 (s, 3H), 4.58 (t, *J* = 5.5 Hz, 3H), 3.74 (s, 6H), 3.63 (dt, *J* = 14.2, 7.0 Hz, 6H), 3.53 – 3.42 (m, 6H), 2.70 (d, *J* = 5.5 Hz, 6H), 1.15 (t, *J* = 7.1 Hz, 15H). **¹³C NMR** (126 MHz, CDCl$_3$) δ 140.22, 126.42, 101.91, 62.10, 53.58, 51.46, 15.18.

N,N′,N′′-(benzene-1,3,5-triyltris(methylene))tris(2-bromo-*N*-(2,2-diethoxyethyl)acetamide) (**T6-C3**)

The crude tri-amine (**13**) (457 mg, 0.89 mmol, 1.0 equiv) was dissolved in 7.5 mL of CH_2Cl_2, after which 13 mL of a *sat.* $NaHCO_3$ solution was added. The mixture was cooled to 0°C and a solution of bromoacetyl bromide (227 µL, 2.70 mmol, 4.5 equiv) in 6 mL of CH_2Cl_2 was added dropwise. The biphasic solution was warmed to rt and stirred for 2h, after which TLC showed full conversion. The product w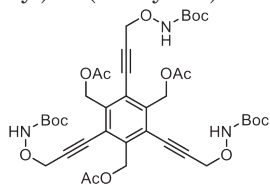as extracted with CH_2Cl_2 and the organic phase was washed with a *sat.* $NaHCO_3$ solution and dried over Na_2SO_4. The volatiles were removed under reduced pressure, yielding an orange oil. Purification by flash column chromatography (1:1 – P.E.:EtOAc) provided the desired product as a pale orange oil (318 mg, 0.36 mmol, 41%).**^{1}H NMR** (500 MHz, CDCl₃) δ 7.06 – 6.81 (m, 3H), 4.69 (d, J = 6.3 Hz, 3H), 4.60 (d, J = 8.2 Hz, 4H), 4.44 (dt, J = 18.1, 4.5 Hz, 2H), 4.07 (t, J = 11.0 Hz, 4H), 3.78 (s, 2H), 3.75 – 3.62 (m, 6H), 3.59 – 3.48 (m, 2H), 3.44 (dt, J = 15.3, 7.4 Hz, 4H), 3.36 (s, 6H), 1.20 – 1.12 (m, 18H). **^{13}C NMR** (126 MHz, CDCl₃) δ 168.38, 168.29, 168.20, 167.41, 167.38, 138.89, 138.42, 138.31, 138.05, 137.89, 137.56, 126.16, 126.01, 124.34, 123.57, 100.83, 100.79, 100.73, 64.11, 64.03, 63.85, 63.81, 53.12, 53.09, 51.01, 50.96, 49.74, 49.65, 49.55, 49.38, 49.31, 49.21, 27.03, 26.74, 26.46, 26.30, 26.14, 25.92, 15.34, 15.25. **IR** (cm^{-1}) 3363, 2973, 2927, 1730, 1632, 1448, 1420, 1374, 1344, 1290, 1206, 1166, 1106, 1049, 960, 878, 720. **HRMS** for $C_{31}H_{51}Br_3N_3O_8$, [M-OEt+H]$^+$ calc 831.1221, found 830.1365.

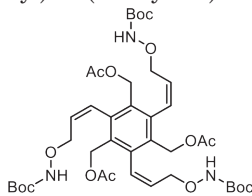*Tert*-butyl (prop-2-yn-1-yloxy)carbamate (**15**)

In a flame-dried flask, under N_2 flow, propargyl bromide (80% wt. solution in toluene, 10 mL, 89.76 mmol, 1.0 equiv), was dissolved in 266 mL of freshly distilled MeCN and the solution was cooled to 0 °C. *Tert-* butyl hydroxycarbamate (13.75 g, 116.7 mmol, 1.15 equiv) was added, followed by DBU (17.45 mL, 116.7 mmol, 1.3 equiv). The mixture was stirred for 30 min at 0 °C, after which the mixture was warmed to rt and stirred for 1h. The volatiles were removed under reduced pressure and the residue was suspended in CH_2Cl_2. A saturated solution of $NaHCO_3$ was added and the organic phase was washed twice, followed by washing with brine. After drying over Na_2SO_4, the residue was concentrated. Flash column purification (10:1-P.E.:EtOAc) yielded **15** as a colorless oil (1.28 g, 59.65 mmol, 66%). **^{1}H NMR** (400 MHz, CDCl₃) δ 7.36 (s, 1H), 4.50 (d, J = 2.3 Hz, 2H), 2.52 (t, J = 2.3 Hz, 1H), 1.51 (s, 9H). *Spectroscopic data are in accordance with those reported in literature.*[13]

(2,4,6-Tris(3-(((*tert*-butoxycarbonyl)amino)oxy)prop-1-yn-1-yl)benzene-1,3,5-triyl)tris(methylene) triacetate (**16**)

To a flame-dried high-pressure tube under a flow of argon, iodide **9** (100 mg, 0.15 mmol, 1.0 equiv), $PdCl_2(PPh_3)_2$ (7.0 mg, 8.9 µmol, 6.0 mol%), and CuI (1.3 mg, 6.6 µmol, 4.5 mol%) were added and suspended in 1.2 mL of NEt_3. To the resulting yellow suspension aminooxy-alkyne **15** (112 mg, 0.54 mmol, 3.6 equiv) was added. The tube was sealed and heated to 50°C and the mixture was stirred overnight. The resulting brown suspension was filtered over Celite and eluted with CH_2Cl_2. The volatiles were removed under reduced pressure. Flash column purification (2:1 to 1:1 – P.E.:EtOAc) yielded **16** as a yellowish foam (75 mg, 0.094 mmol, 62%). **^{1}H NMR** (500 MHz, CDCl₃) δ 7.99 (s, 3H), 5.50 (s, 6H), 4.74 (s, 6H), 2.12 (s, 9H), 1.51 (s, 27H). **^{13}C NMR** (126 MHz, CDCl₃) δ 171.25, 156.43, 139.06, 126.23, 95.14, 81.95, 80.92, 64.14, 63.18, 28.15, 20.76.

(2,4,6-Tris((Z)-3-(((*tert*-butoxycarbonyl)amino)oxy)prop-1-en-1-yl)benzene-1,3,5-triyl)tris(methylene) triacetate (**17**)

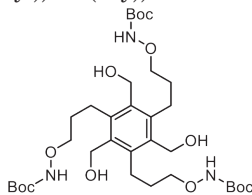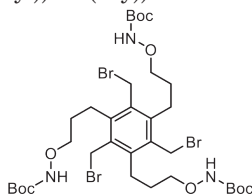In a flame-dried flask under N$_2$ flow, trialkyne **16** (2.19 g, 2.73 mmol, 1.0 equiv) was dissolved in 100 mL EtOH. The solution was degassed and purged with N$_2$. NEt$_3$ was added (5% v/v, 5.2 mL) and the solution was again degassed and purged with N$_2$. Pd/C (10% wt. loading, 500 mg, 20 mol%) was added and the solution was degassed. H$_2$ pressure was applied (balloon) and the reaction vessel was again degassed and purged with H$_2$ (3x) to saturate the flask with H$_2$. The mixture was stirred overnight under H$_2$ pressure, after which TLC analysis and ^{1}H NMR showed full consumption of the starting material. The reaction mixture was filtered over Celite and eluted with CH$_2$Cl$_2$. The volatiles were removed under reduced pressure. Flash column chromatography (2:1 to 1:1 - P.E.:EtOAc) yielded **17** as a yellow foam (1.86 g, 2.298 mmol, 84%). ^{1}**H NMR** (400 MHz, CDCl$_3$) δ 7.76 (d, *J* = 13.0 Hz, 3H), 6.59 (dt, *J* = 33.3, 14.4 Hz, 3H), 6.05 (dt, *J* = 11.8, 6.6 Hz, 3H), 4.90 (d, *J* = 56.2 Hz, 6H), 4.02 (s, 6H), 1.93 (s, 9H), 1.35 (s, 27H). ^{13}**C NMR** (101 MHz, CDCl$_3$) δ 170.34, 156.65, 139.58, 139.49 (broad peak), 131.16, 130.79, 129.59, 129.38, 81.34, 72.54, 62.19, 27.94, 20.50.

Tri-*tert*-butyl(((2,4,6-tris(hydroxymethyl)benzene-1,3,5-triyl)tris(propane-3,1-diyl))tris(oxy))tricarbamate (**18**)
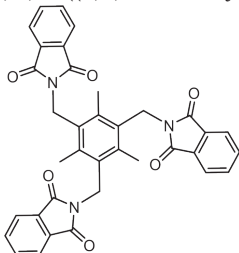
Trialkene **17** (163 mg, 0.201 mmol) was dissolved in 9 mL of EtOH. K$_2$CO$_3$ (5 mg, cat.) was added and the opaque solution was stirred overnight. The volatiles were removed under reduced pressure and the residue was dissolved in CH$_2$Cl$_2$ and washed with brine. The aqueous phase was twice more extracted with CH$_2$Cl$_2$ and the organic phase was dried over Na$_2$SO$_4$. The volatiles were removed under reduced pressure, yielding the alcohol as a pale-yellow foam. The alkene alcohol residue was dissolved in 7 mL of EtOH and degassed and purged with N$_2$. Pd/C (10 wt% loading, 32 mg, 10 mol%) was added and the solution was again degassed. H$_2$ pressure was applied (balloon) and the reaction vessel was degassed and purged with H$_2$ (3x) to saturate the flask with H$_2$. The mixture was stirred overnight under H$_2$ pressure, after which TLC analysis and ^{1}H NMR showed full conversion of the starting material. The mixture was filtered over Celite and eluted with EtOH. The volatiles were removed under reduced pressure, yielding the desired product as a colorless foam (131 mg, 0.190 mmol, 94% over 2 steps). **Alkene alcohol:** ^{1}**H NMR** (300 MHz, CDCl$_3$) δ 7.71 (s, 2H), 7.03 – 6.86 (m, 3H), 6.30 – 6.08 (m, 3H), 4.54 (s, 6H), 4.25 (d, *J* = 8.4 Hz, 6H), 2.80 (t, *J* = 6.5 Hz, 2H), 1.45 (s, 27H). **Alkane alcohol:** ^{1}**H NMR** (500 MHz, CDCl$_3$) δ 8.14 (s, 3H), 4.65 (s, 6H), 3.92 (s, 6H), 3.49 (br s, 3H), 3.02 – 2.85 (m, 6H), 1.82 (s, 6H), 1.50 (s, 27H). ^{13}**C NMR** (126 MHz, CDCl$_3$) δ 157.23, 141.79, 135.33, 81.51, 76.29, 58.40, 30.76, 28.29, 26.08. **IR** (cm^{-1}) 3433 (br), 3263 (br), 2973, 2926, 1710, 1477, 1455, 1392, 1366, 1276, 1250, 1162, 1110, 1003, 754. **HRMS** (FD) for C$_{33}$H$_{57}$N$_3$O$_{12}$ calc. 688.4020, found 688.4028 **mp** 68 °C.

Tri-*tert*-butyl(((2,4,6-tris(bromomethyl)benzene-1,3,5-triyl)tris(propane-3,1-diyl))tris(oxy))tricarbamate (**T6-N1**)

In a flame-dried flask under a flow of Ar, tri-ol **18** (50 mg, 72.6 µmol, 1.0 equiv) was dissolved in 2.5 mL freshly distilled CH$_2$Cl$_2$ and cooled to 0 °C. Pyridine (26 µl, 0.3 mmol, 4.5 equiv) was added, followed by dropwise addition of PBr$_3$ (24 µL, 0.25 mmol, 3.5 equiv). After 1h on ice, the solution was warmed to rt and became opaque. LC-MS analysis showed full conversion to the desired product. The reaction mixture was diluted with EtOAc and quenched with *sat.* NaHCO$_3$ solution. After neutralization with KHSO$_4$ (pH 7), the product was extracted with EtOAc (3x). The collected organic phases were washed with brine and dried over Na$_2$SO$_4$. After filtration, the volatiles were removed under reduced pressure, yielding **T6-N1** as a colorless foam (20 mg, 22.8 µmol, 31%). ^{1}**H NMR** (500 MHz, CDCl$_3$) δ 7.22 (s, 3H), 4.60 (s, 6H), 4.03 (t, J = 5.8 Hz, 6H), 3.01 (t, J = 9.5, 8.2 Hz, 9H), 1.99 (d, J = 12.9 Hz, 6H), 1.51 (s, 27H). ^{13}**C NMR** (126 MHz, CDCl$_3$) δ 157.08, 142.83, 133.61, 81.90, 76.26, 29.60, 28.75, 28.25, 26.48. **IR** (cm^{-1}) 3275, 2925, 2854, 1712, 1476, 1454, 1366, 1248, 1161, 1107, 773, 517. **HRMS** (ESI+) for C$_{28}$H$_{47}$Br$_3$N$_3$O$_7$, calc 774.0964, found 774.0975. **mp** 56-57°C.

2,2',2''-((2,4,6-trimethylbenzene-1,3,5-triyl)tris(methylene))tris(isoindoline-1,3-dione) (19)

In a flame dried flask, under N_2, 2,4,6-tris (bromomethyl)mesitylene **2** (5.01 g, 12.5 mmol, 1.0 equiv) was suspended in 200 mL of anhydrous DMF. Potassium phthalimide (KPhth, 14.00 g, 75.6 mmol, 6.0 equiv) was added and the slurry was vigorously stirred for 18h at 125 °C. The white solid was filtered off and washed twice with DMF, water and acetone. The white amorphous solid was dried under high vacuum, yielding **19** in 78% (5.85 g, 9.8 mmol). **1H NMR** (400 MHz, CDCl$_3$) δ 7.80 (dd, J = 5.4, 3.0 Hz, 6H), 7.70 (dd, J = 5.4, 3.1 Hz, 6H), 4.97 (s, 6H), 2.52 (s, 9H). *Spectroscopic data are in accordance with those reported in literature.*[15]

2,2',2''-((2,4,6-Tris(bromomethyl)benzene-1,3,5-triyl)tris(methylene))tris(isoindoline-1,3-dione) (20)

In a flame-dried flask, under N_2 flow, tris(phthalimide) **19** (2.50 g, 4.18 mmol, 1.0 equiv) was suspended in 30 mL of DBE. Br$_2$ (711 µL, 13.80 mmol, 33 equiv) was added and the mixture was heated to reflux, while irradiated with a commercially available 500W construction lamp. After 2h, the solution had become light orange, after which 1H NMR spectroscopy showed the reaction had not reached full conversion. A second portion of Br$_2$ (400 µL, 7.76 mmol, 1.86 equiv) was added and reflux and irradiation was continued for another 2h, after which 1H NMR spectroscopy showed full conversion. The reaction mixture was quenched with a 0.5M Na$_2$S$_2$O$_3$ solution, and

extracted with CH$_2$Cl$_2$. A sticky yellow solid was obtained after removal of the volatiles under reduced pressure. Flash column chromatography (3:1 to 1:1 – P.E.:EtOAc) provided the product **20** as a white solid (3.09 g, 3.71 mmol, 88%). *Spectroscopic data are in accordance with those reported in literature.*[15]

Tri-*tert*-butyl(((2,4,6-tris((1,3-dioxoisoindolin-2-yl)methyl)benzene-1,3,5-triyl)tris (methylene))tris(oxy))tricarbamate (21)

In a flame-dried flask, under N_2 flow, tris(phthalimide) **20** (2.50 g, 3.0 mmol, 1.0 equiv), was suspended in 42 mL of freshly distilled MeCN and the mixture was cooled to 0 °C. *N*-Boc hydroxylamine (1.80 g, 13.5 mmol, 4.5 equiv), was added after which DBU (1.80 mL, 12 mmol, 4 equiv) was added in dropwise fashion. The suspension turned into a clear yellowish solution after 10 min. The mixture was warmed to rt and stirred overnight. The volatiles were removed under reduced pressure. The residue was dissolved in CH$_2$Cl$_2$ and washed with a *sat.* NaHCO$_3$ solution and brine, followed by drying over Na$_2$SO$_4$. After filtration and removal of the

volatiles under reduced pressure, the crude product was obtained as a bright yellow foam. Flash column purification (2.5:1 – P.E.:EtOAc) yielded **21** as a bright yellow solid (1.43 g, 1.4 mmol, 48%). **1H NMR** (500 MHz, CDCl$_3$) δ 7.80 (dd, J = 5.4, 3.0 Hz, 6H), 7.70 (dd, J = 5.4, 3.1 Hz, 6H), 7.26 (s, 3H), 5.45 (s, 6H), 5.39 (s, 6H), 1.42 (s, 27H). **13C NMR** (126 MHz, CDCl$_3$) δ 168.25, 156.16, 139.09, 135.69, 133.95, 131.95, 123.20, 81.60, 72.47, 36.81, 28.15. **IR** (cm^{-1}) 3289, 2977, 2930, 2331, 2246, 1771, 1704, 1612, 1466, 1393, 1367, 1329, 1243, 1159, 1107, 1088, 1003, 963, 940, 913, 861, 838, 824, 792, 772, 714. **HRMS** (ESI) C$_{46}$H$_{47}$N$_6$O$_{13}$$^+$ for [M-Boc+H]$^+$, calc. 891.3196 found 891.31891. **mp** 106-115 °C.

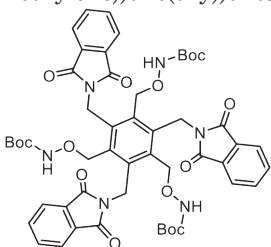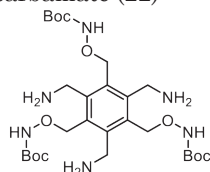## Tri-*tert*-butyl(((2,4,6-tris(aminomethyl)benzene-1,3,5-triyl)tris(methylene))tris(oxy))tricarbamate (22)

Tris(phthalimide) **21** (200 mg, 0.20 mmol, 1.0 equiv) was suspended in 3.5 mL of EtOH:toluene (2:1), after which hydrazine-hydrate (50% sol. in water, 110 µL, 1,61 mmol, 8.0 equiv) was added. The suspension was heated to reflux. When the mixture had reached 70°C, it became colorless. After stirring for 20 min. at reflux, a white solid started to precipitate. Reflux was continued for 12h, after which the solids were filtered off and the residue was evaporated to dryness, yielding **22** as an off-white solid (118 mg, 0.20 mmol, 98%), which was used without further purification in the next step. **^{1}H NMR** (500 MHz, CDCl$_3$) δ 5.16 (s, 6H), 4.12 (s, 6H), 1.53 (s, 27H). **^{13}C NMR** (126 MHz, CDCl$_3$) δ 157.25, 145.71, 131.96, 81.51, 72.04, 39.78, 28.33. **IR** (cm^{-1}) 3289, 2977, 2930, 2331, 2246, 1771, 1704, 1612, 1466, 1393, 1367, 1329, 1243, 1159 ,1107, 1088, 1003, 963, 940, 913, 861, 838, 824, 792, 772, 714.

Tri-*tert*-butyl(((2,4,6-tris((2-bromoacetamido)methyl)benzene-1,3,5-triyl)tris(methylene)) tris(oxy))tricarbamate (T6-N2)
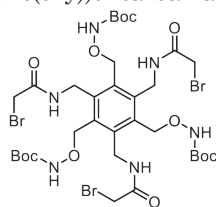
The triamine **22** (118 mg, 0.20 mmol, 1.0 equiv) was suspended in 7.0 mL CHCl$_3$ and the suspension was cooled to 0 °C. Subsequently, 7.0 mL of a *sat.* NaHCO$_3$ solution was added. Bromoacetyl bromide (70 µL, 0.79 mmol, 4.0 equiv) was added dropwise and the solution was warmed to rt and stirred for 3h. LC-MS confirmed the absence of starting material and the product was extracted with CH$_2$Cl$_2$. Subsequently, the organic phase was washed with brine and dried over Na$_2$SO$_4$ and the volatiles were removed under reduced pressure. The product was purified via flash column chromatography (1:1 – P.E.:EtOAc), yielding **T6-N2** as a colorless solid (120 mg, 0.13 mmol, 63%). **^{1}H NMR** (500 MHz, CDCl$_3$) δ 8.81 (s, 3H), 8.13 (s, 3H), 5.31 (s, 6H), 4.79 (d, J = 6.2 Hz, 6H), 3.85 (s,6H), 1.47 (s, 27H). **^{13}C NMR** (126 MHz, CDCl3) δ 166.73, 157.56, 141.69, 133.99, 82.53, 71.98, 37.72, 28.98, 28.24. **IR** (cm^{-1}) 3270, 3085, 2975, 2929, 1714, 1655, 1541, 1476, 1432, 1392, 1367, 1277, 1251, 1207, 1159, 1101, 1008, 845, 772, 655. **HRMS** (FD+(eiFi)) C$_{33}$H$_{51}$Br$_3$N$_6$O$_{12}$, calc 962.1094, found 962.1114. **mp** 102-107 °C.

Benzyl (2-hydroxyethyl)carbamate (23a)

In a flame-dried flask, under N$_2$ flow, ethanolamine (2 mL, 33.13 mmol, 1.0 equiv) was dissolved in 65 mL of distilled CH$_2$Cl$_2$. NEt$_3$ (5.5 mL, 39.76 mmol, 1.2 equiv) was added and the mixture was cooled to 0 °C. Cbz-Cl (6 mL, 41.74 mmol, 1.25 equiv) was added in dropwise fashion, after which the mixture was warmed to rt and stirred overnight. A 1M KHSO$_4$ solution was added and the product was extracted with CH$_2$Cl$_2$. The organic phase was washed with brine and dried over Na$_2$SO$_4$. The volatiles were removed under reduced pressure, to yield a colorless oil. The oil was redissolved in a 1:1 mixture of P.E.:EtOAc, upon which white crystals formed. The crystals of **23a** were subsequently filtered and dried (3.41 g, 17.45 mmol, 53%). **^{1}H NMR** (400 MHz, CDCl$_3$) δ 7.43 – 7.29 (m, 5H), 5.21 (s, 1H), 5.13 (s, 2H), 3.75 (d, J = 4.6 Hz, 2H), 3.38 (q, J = 5.2 Hz, 2H), 2.25 (s, 1H). **^{13}C NMR** (126 MHz, CDCl3) δ 157.12, 136.33, 128.51, 128.14, 128.09, 66.87, 62.20, 43.46. **IR** (cm^{-1}) 3318, 3061, 3035, 2940, 2882, 1691, 1538, 1452, 1322, 1212, 1148, 1114, 1079, 1058, 1031, 988, 907, 839, 779, 744, 694. **mp** 57°C.

Tert-butyl (2-(((benzyloxy)carbonyl)amino)ethoxy)(*tert*-butoxycarbonyl)carbamate (23b)

In a flame-dried flask, under N$_2$ flow, Cbz-protected ethanolamine **23a** (1.32 g, 6.75 mmol, 1.0 equiv) was dissolved in 33 mL of freshly distilled THF. Boc$_2$NOH (1.73 g, 7.42 mmol, 1.1 equiv) and PPh$_3$ (1.95 g, 7.42 mmol, 1.1 equiv) were added and the solution was cooled to 0 °C. DIAD (1.46 mL, 7.42 mmol, 1.1 equiv) was added to the solution in a dropwise fashion and the mixture was stirred overnight. Subsequently, the yellow solution was immobilized on silica and subsequent flash column chromatography (10:4:1 – P.E.:CH$_2$Cl$_2$:EtOAc) provided the product **23b** as a colorless oil (2050 mg, 4.99 mmol, 74%). *Note: A second portion of the product (contaminated with Boc$_2$NOH) was also isolated (328 mg, 0.80 mmol, 11%).* **^{1}H NMR** 1H NMR (500 MHz, CDCl$_3$) δ 7.33 (dd, J = 20.2, 6.6 Hz, 5H), 5.74 (s, 1H), 5.11 (s, 2H), 4.01 (t, J = 4.7 Hz, 2H), 3.49 – 3.39 (m, 2H), 1.53 (s, 18H). **^{13}C NMR** (126 MHz, CDCl$_3$) δ 156.28, 150.14, 136.46, 128.28, 127.84, 84.17, 75.43, 66.46, 39.28, 27.88. **IR** (cm^{-1}) 3365, 2979, 2936, 1791, 1751, 1716, 1587, 1513, 1477, 1455, 1394, 1368, 1347, 1269, 1246, 1144, 1110, 1035, 1026, 911, 899, 847, 794, 774, 750, 736, 696.

Tert-butyl (2-aminoethoxy)carbamate (**23**)
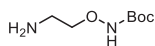
To remove one Boc protecting group, protected amine **23b** (1.96 g, 4.8 mmol, 1.0 equiv) was dissolved in 50 mL of freshly distilled CH_2Cl_2. TFA (730 µL, 9.6 mmol, 2.0 equiv) was added dropwise and the solution was stirred overnight at rt. ^1H NMR spectroscopy showed full conversion to the *mono*-Boc derivative, after which the volatiles were removed under reduced pressure. In order to remove the Cbz-group[19] the oily residue was dissolved in 47 mL of EtOH. The solution was evacuated and the flask was refilled with N_2 (repeated trice). Then, 330 mg of Pd/C (10% loading) was added H_2 pressure was applied via a balloon, and the flask was evacuated and refilled with H_2 trice. The mixture was stirred for 2.5h, after which TLC analysis showed full conversion to the fully liberated amine. The reaction mixture was subsequently filtered over a Celite pad and eluted with EtOH. The volatiles were removed under reduced pressure to yield **23** as a colorless oil (819 mg, 4.7 mmol, 97%). **^1H NMR** (400 MHz, CDCl₃) δ 8.67 (br. s, 1H), 4.05 (s, 2H), 3.20 (s, 2H), 1.43 (s, 9H). **^{13}C NMR** (101 MHz, CDCl₃) δ 158.80, 82.83, 71.93, 37.70, 27.92. **IR** (cm⁻¹) 2983, 2938, 1670, 1480, 1456, 1390, 1370, 1287, 1256, 1177, 1130, 1056, 1015, 968, 912, 837, 799, 758, 721.

5.8 References

(1)   van der Made, A. W.; van der Made, R. H. *J. Org. Chem.* **1993**, *58* (5), 1262.

(2)   Rosien, J. R.; Seichter, W.; Mazik, M. *Org. Biomol. Chem.* **2013**, *11* (38), 6569.

(3)   Balamurugan, R.; Mohanakrishnan, A. K. *Tetrahedron* **2007**, *63* (45), 11078.

(4)   Hass, H. B.; Bender, M. L. *J. Am. Chem. Soc.* **1949**, *71* (5), 1767.

(5)   Foot, J. S.; Giblin, G. M. P.; Taylor, R. J. K. *Org. Lett.* **2003**, *5* (23), 4441.

(6)   Callebaut, B.; Hullaert, J.; Van Hecke, K.; Winne, J. M. *Org. Lett.* **2019**, *21* (1), 310.

(7)   Rosenmund, K. W.; Struck, E. *Ber. Dtsch. Chem. Ges.* **1919**, *52* (8), 1749.

(8)   Yoon-Heung, T.; Yoon-Soo, H.; Yong-Kwan, K.; Ki-Dong, K.; Sang-Dae, K. Red light emitting compounds for organic electroluminescent devices and organic electroluminescent devices using them. EP1435384, 2004.

(9)   Zanon, J.; Klapars, A.; Buchwald, S. L. *J. Am. Chem. Soc.* **2003**, *125* (10), 2890.

(10)   Zhang, X.-X.; Lippard, S. J. *J. Org. Chem.* **2000**, *65* (17), 5298.

(11)   Zhang, X.-X.; Fuhrmann, P.; Lippard, S. J. *J. Am. Chem. Soc.* **1998**, *120* (39), 10260.

(12)   Almen, T.; Andersson, S.; Wistrand, L.; Golman, K.; Antonsen, O.; Fossheim, R.; Wiggen, U. N.; Wikstrom, H.; Klingstedt, T.; Luenbach, I.; Berg, A.; Dugstad, H. Iodinated x-ray contrast media. U.S. Patent 6310243, 2001.

(13)   Frost, J. R.; Vitali, F.; Jacob, N. T.; Brown, M. D.; Fasan, R. *ChemBioChem* **2013**, *14* (1), 147.

(14)   Chen, S.; Bertoldo, D.; Angelini, A.; Pojer, F.; Heinis, C. *Angew. Chemie - Int. Ed.* **2014**, *53* (6), 1602.

(15)   Roelens, S.; Vacca, A.; Francesconi, O.; Venturi, C. *Chem. Eur. J.* **2009**, *15* (33), 8296.

(16)   Gabriel, S. *Berichte der Dtsch. Chem. Gesellschaft* **1887**, *20* (2), 2224.

(17)   Bruns, D.; Miura, H.; Vollhardt, K. P. C.; Stanger, A. *Org. Lett.* **2003**, *5* (4), 549.

(18)   Van Arman, S. A. *Tetrahedron Lett.* **2009**, *50* (33), 4693.

(19)   Dal Molin, M.; Verolet, Q.; Colom, A.; Letrun, R.; Derivery, E.; Gonzalez-Gaitan, M.; Vauthey, E.; Roux, A.; Sakai, N.; Matile, S. *J. Am. Chem. Soc.* **2015**, *137* (2), 568.

Summary

in English

Synthesis of Multicyclic Peptides via CLiPS and Oxime Ligations

Cyclic and multicyclic peptides are ubiquitous in Nature. They have shown interesting biological activities as for example antibacterial agents. Due to their constrained nature, they show improvements compared to their linear counterparts, such as higher metabolic stabilities, specificities and oral availabilities. This class of compounds has inspired scientists to emulate these topologies. A variety of methods has been developed to synthesize monocyclic peptides. Methods to further constrain peptides to bicyclic peptides have even found application in high-throughput library-based synthesis methods, such as phage display. While these advances have shown the importance of constraining a peptide to increase activity, there is still room for improvement. Adding peptide cycles, yielding tricyclic, or even higher multicycles, is a challenging objective where the current methodologies may fall short.

In this thesis, the scaffold-assisted synthesis of tri-, tetra-, and pentacyclic peptides is described, using the sequential combination of CLiPS and oxime ligation as orthogonal ligation techniques (Figure S.1). The CLiPS reaction is a well-known constraining technology, whereby nucleophilic cysteine thiolates react with scaffold-bound methylene bromide electrophiles. Oxime ligation is a click-type reaction between an electrophilic aldehyde or ketone and a nucleophilic aminooxy group, forming an oxime linkage that can exhibit *E/Z* isomerism. There are two possible strategies to combine CLiPS with oxime ligation. In the first, the scaffold bears all electrophiles, while the peptides bear all nucleophiles. In the second strategy, the oxime groups are reversed, meaning that both the peptides and scaffolds contain both nucleophilic and electrophilic groups. Within this framework, our aim was to develop a one-pot procedure, to access isomerically pure multicyclic peptides.
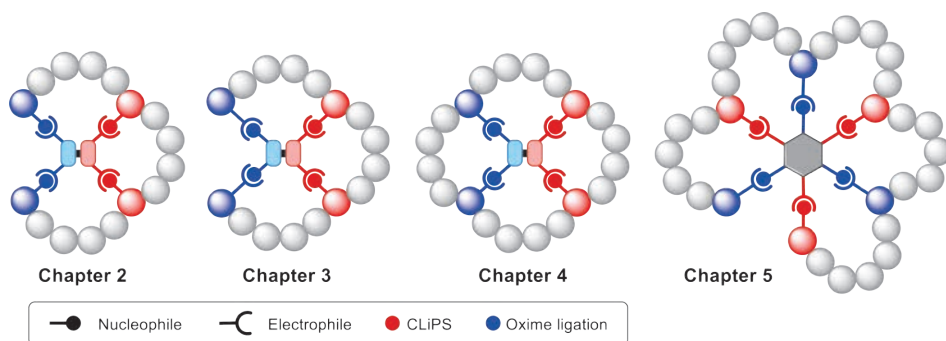
Figure S.1: Overview of the work in this thesis.

Chapter 2 describes the synthesis of tricyclic peptides according to strategy 1. Here, the scaffolds contain all electrophiles (arylmethyl bromides and aldehydes or ketones), while the peptides are equipped with all nucleophiles (thiolates and aminooxy groups). Three scaffolds were synthesized, of which two were suitable for our purposes. Two aminooxy-group bearing amino acids (hS(ONH$_2$) and K(Aoa)) were synthesized and successfully applied in solid phase peptide synthesis. Unfortunately, the aminooxy group, although Boc-protected, was not completely inert during peptide synthesis. Side-reactions and deletions occurred, rendering the crude peptides in poor quality, requiring multiple purification cycles. Of the envisioned 17 peptides, 15 were successfully obtained and subsequently subjected to the CLiPS and oxime ligation cyclization reactions. We have found conditions to perform the CLiPS reaction, scaffold deprotection and subsequent oxime ligation via careful regulation of the pH of the reaction mixture.

For all peptides, the tricyclic peptide product was formed. However, in many cases a mixture of products was obtained. Attempts to separate the components indicated that the product isomers are of rotameric origin, meaning that products interconvert slowly, but are separable on HPLC timescale. The number of rotamers decreased with peptide length, and when 4 or 5 amino acids were spacing the reactive residues, fewer products were found. To make this methodology truly applicable for high-throughput peptide library screening, the peptide synthesis must be optimized, whereby the crude peptides can be obtained in higher purity.

In **Chapter 3**, the synthesis of tricyclic peptides via strategy 2 is explored. This strategy is characterized by the mixing of electrophiles and nucleophiles in both the scaffolds and peptides. Therefore, the scaffolds were equipped with electrophilic arylmethyl bromides and nucleophilic aminooxy groups, while the peptides bear both nucleophilic thiolates and electrophilic aldehydes or ketones. Three novel scaffolds were developed, bearing aminooxy groups that were Boc-protected during scaffold synthesis and the CLiPS reaction. The peptides were equipped with ketone-functionalized amino acids, an unhindered para-acetyl phenylalanine (pAcF) and a sterically congested, aspartic acid-derived *tert*-butyl ketone (D(Ket)). Peptide synthesis was compatible with the unprotected ketone in the amino acid residues. However, peptide resin cleavage and global deprotection required special attention, as the ketones were found to be reactive towards common thiol-scavenging agents. When these were omitted, 15 peptides were obtained with high purity.

The peptides were subsequently subjected to the CLiPS and oxime ligation cyclization reactions. Contrary to 'strategy 1', the reaction sequence could not be performed in a one-pot procedure. After the CLiPS reaction, liberation of the scaffold aminooxy moieties could only be achieved after removal of the solvent and treatment with neat TFA. Evaporation of TFA and dissolution of the residue in aqueous solvent yielded the tricyclic peptides without addition of pH regulating agents. For all peptides, the tricyclic peptide product was obtained, yet for many as a mixture of products. Interestingly, the role of the scaffold was more pronounced, and fewer isomers were obtained when using the scaffold T4-N3. However, there was a significant variation in the cyclization success, and additional research is required to determine which peptide properties are necessary for reliable and reproducible cyclization results. On the contrary, for the majority of the peptides containing D(Ket) as the reactive amino acid, a single product was obtained, albeit accompanied by a persistent mono-oxime by-product that did anyhow not react further. This technology is now ready for application in low- or medium diversity library synthesis and screening.

Chapter 4 involves the synthesis of tetracyclic peptides, whereby the CLiPS and oxime cyclization ligation reactions were preceeded by enzymatic macrolactamization of the peptides using CEPS-cyclization. This builds on the chemistry developed in Chapters 2 and 3 and both strategies 1 and 2 were investigated. Omniligase-1 mediated CEPS-cyclization was successful using hS(ONH$_2$) and ketone-bearing amino acids pAcF and D(Ket). However, the placement of these residues in the recognition zone of the enzyme was precarious, as not all positions were suitable, requiring careful planning of the cyclization site. For the 8 peptides synthesized, the tetracyclic peptide was obtained in all cases, sometimes accompanied by the formation of several different isomers. The variables established for cyclization success in previous chapters were applicable to these syntheses as well. For strategy 1 peptides, loop size – being the space between consecutive functional residues - was the main indicator for success, whereby longer peptides yielded the best results. Peptides bearing pAcF afforded the best results using scaffold T4-N3 while for all D(Ket) peptides a single product was obtained with the persistent mono-oxime

intermediate as a by-product. Efforts to separate isomeric tetracycles with pAcF were successful, and structure elucidation via ^{1}H NMR was attempted. However, in solution, the product existed in too many conformations for the structure to be assigned properly.

      Chapter 5 explored the synthesis of pentacyclic peptides, again via both strategies 1 and 2. Novel phenyl-based scaffolds were developed. For strategy 1, only one scaffold was successfully synthesized, which ultimately turned out to be unstable upon prolonged storage. Pre-existing difficulties in peptide synthesis using aminooxy bearing amino acids resulted in peptides of very poor quality, which would have required many purification cycles. Therefore, our efforts focused only on strategy 2-type cyclizations to prepare pentacyclic peptides. Two scaffolds were developed, and two peptides bearing pAcF and two with D(Ket) were synthesized. One of the major discoveries in this chapter was the dynamic nature of the oxime ligation reaction, which was not observed in previous chapters. The exclusive formation of an isomerically pure pentacyclic product with a pAcF peptide was observed, and its gradual appearance was followed over time, whereby several mono- and di-oxime intermediates were identified. Eventually, for some mixtures, the intermediates converted to a single product. For the D(Ket) peptides, formation of the desired product was slow, but eventually very selective, yielding a single product in combination with scaffold T6-N1. The preliminary results from this very small peptide sample are highly encouraging and render a broader investigation into this method worthwhile.

Samenvatting

in het Nederlands

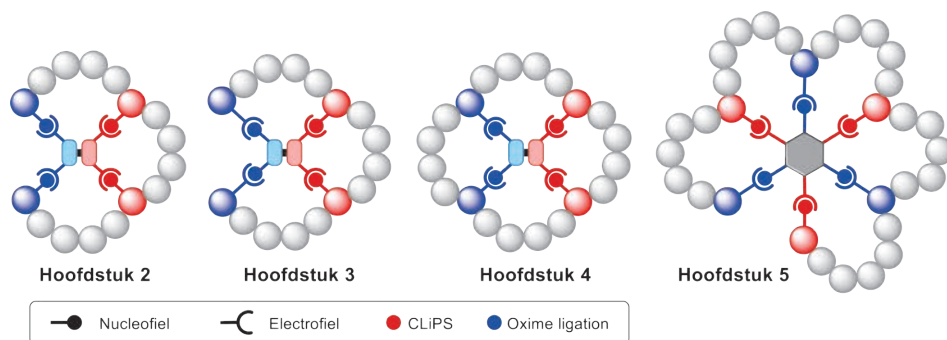# Synthese van Multicyclische Peptiden, via CLiPS en Oxime Ligaties

Cyclische en multi-cyclische peptides zijn overal terug te vinden in de natuur. Ze vervullen verschillende rollen, bijvoorbeeld als antibioticum. Verschillende bacteriën produceren cyclische peptiden als chemisch wapen tegen andere bacteriën, om zo te overleven. Doordat (multi)cyclische peptiden zich in een starre conformatie bevinden, zijn ze in een aantal opzichten beter dan hun lineaire soortgenoten. Ze zijn bijvoorbeeld stabieler tegen metabole afbreking in het lichaam en werken ze specifieker op hun doelwit. Daarnaast zijn ze makkelijker oraal toe te dienen, in plaats van intraveneus. Door deze voordelen zijn ze een interessante klasse verbindingen en is er een rijke geschiedenis voor wat betreft de chemische synthese van topologische variaties.

Aan de basis staat de synthese van monocyclische peptiden, waar in de loop der jaren verschillende methodes voor zijn ontwikkeld. Het aanbrengen van verdere restricties, zoals in een bicyclisch peptide, heeft geleid tot nog specifiekere activiteit en stabiliteit van bioactieve peptiden. Een aantal methoden heeft zelfs toepassing gevonden in bibliotheeksynthese methoden, waar grote hoeveelheden diverse verbindingen op simpele manier gesynthetiseerd én getest kunnen worden op activiteit. Een belangrijke conclusie van veel van deze onderzoeken is dat het aanbrengen van restricties in de structuur, waardoor peptiden multicyclisch worden, vaak gepaard gaat met een verbetering van gunstige eigenschappen. Daarom is met bicyclische peptiden het einde nog niet in zicht. De synthese van tricyclische peptiden, of zelfs nog hogere multicycles, is daardoor een onderzoeksgebied waar veel belangstelling voor is. Echter is er nog geen makkelijk toepasbare methode om op een selectieve manier dit soort verbindingen in elkaar te zetten, ongeacht wat de peptidesequentie is.

In dit proefschrift wordt de ontwikkeling van zo'n breed toepasbare methode voor de synthese van tri-, tetra- en pentacyclische peptides beschreven (Figuur S. 1). Centraal in de synthese is het "scaffold", ofwel het platform of de stijger, waar peptides op vastgezet moeten worden, op de juiste plek en met de juiste manier, om zo de complexere multicyclische structuren te verkrijgen. De methode rust op de combinatie van orthogonale ligatie technieken – reacties die stapsgewijs – na én naast – elkaar plaats kunnen vinden, zonder elkaar te beïnvloeden. De reacties die daarvoor gekozen zijn, zijn CLiPS ligatie en oxime ligatie.

De CLiPS ligatie is een bekende en robuuste methode om peptiden vast te zetten aan een platform. Hierbij wordt het nucleofiele thiol van een cysteine in het peptide aan het platform gebonden, door nucleofiele substitutie van een platform-gebonden methyl-bromide electofiel. Hierbij ontstaat een thio-ether, waarbij het peptide aan het platform gebonden wordt. Oxime ligatie is een zogenoemde click-reactie waarbij een electrofiel aldehyde of keton reageert met een amino-oxy nucleofiel tot een oxime. De oxime binding kan *E/Z* stereoisomerie vertonen.

De CLiPS reactie vindt altijd plaats op dezelfde wijze, waarbij er altijd meerdere cysteines in het peptide aanwezig zijn, om de complementaire bromide-electrofielen te substitueren op het platform molecuul. Er zijn twee manieren waarop de CLiPS met oxime ligatie gecombineerd kan worden. In de eerste, genaamd strategie 1, bevat het platform molecuul de electrofiele groepen, terwijl de peptiden de nucleofielen bevatten. In strategie 2 zijn de reactieve groepen voor oxime ligatie van plek veranderd, en bevatten het platform molecuul én de peptiden zowel nucleofiele als electrofiele groepen. Op basis van deze strategieën was het doel om een één-pot procedure te ontwikkelen om isomeer-zuivere multicyclische peptiden te synthetiseren.

Figuur S. 1. Overzicht van het werk in dit proefschrift, waarin de synthese van tri-, tetra- en pentacyclische peptiden wordt onderzocht.

In **Hoofdstuk 2** wordt de synthese van tricyclische peptiden volgens strategie 1 beschreven. Hier bevatten de platform moleculen alleen electrofiele groepen (arylmethyl bromides voor CLiPS en aldehydes of ketonen voor oxime ligatie) terwijl de peptiden de nucleofiele groepen bevatten (cysteine thiolaten en amino-oxy groepen). Drie platform moleculen werden gesynthetiseerd, waarvan er twee geschikt werden bevonden voor dit project. Twee aminozuur-derivaten met een amino-oxy groep werden gesynthetiseerd (hS(ONH$_2$) en K(Aoa)) en toegepast in peptide synthese op een vaste drager. Echter bleek de amino-oxy groep, hoewel deze Boc-beschermd was tijdens de synthese, niet volledig inert te zijn in peptide synthese reacties. Bij-reacties en deleties van deze aminozuren kwamen voor, waardoor de peptiden vóór zuivering van slechte kwaliteit waren. Meerdere zuiveringsrondes waren vaak nodig om peptide materiaal van voldoende zuiverheid te verkrijgen. Van de beoogde zeventien peptides werden er vijftien succesvol gesynthetiseerd en gebruikt in de CLiPS en oxime ligatie reacties. Uiteindelijk is er een robuuste procedure ontwikkeld waarbij de CLiPS reactie, het ontschermen van het platform molecuul en de oxime ligatie voltooid werden in één reactievat door het zorgvuldig reguleren van de pH van het reactiemengsel.

Elk peptide waarmee de reactiesequentie werd uitgevoerd resulteerde in de formatie van tricyclisch peptide product. Echter werd in veel gevallen een mengsel van isomeren gevonden. Pogingen om de isomeren van elkaar te scheiden waren niet succesvol, en duiden erop dat de isomeren van rotamerische oorsprong zijn. Deze rotamere producten kunnen langzaam in elkaar over gaan, maar zijn te scheiden op HPLC-tijdschaal. Het aantal rotameren verminderde als functie van de peptidelengte. Wanneer de reactieve aminozuren gescheiden waren door vier tot vijf aminozuurresiduen werden er minder rotameren gevonden. Om deze methodologie werkelijk toepasbaar te maken voor high-throughput peptide library screening, moet de peptidesynthese geoptimaliseerd worden, waarbij er – zonder zuivering – peptiden van hogere zuiverheid verkregen kunnen worden.

In **Hoofdstuk 3** wordt de synthese van tricyclische peptiden via strategie 2 beschreven. Deze strategie wordt gekarakteriseerd door het mixen van nucleofielen en electrofielen op zowel de platform moleculen en de peptiden. De platformen bevatten zowel de electrofiele arylmethyl bromide voor CLiPS als de nucleofiele amino-oxy groepen voor de oxime ligatie. De peptiden bevatten zowel nucleofiele cysteine-thiolen als electrofiele ketonen. Drie nieuwe platform moleculen zijn gesynthetiseerd, waarvan de amino-oxy groepen Boc-beschermd waren tijdens synthese van de platform moleculen en de CLiPS reacties. De peptiden bevatte de onbeschermde keton-gefunctionaliseerde aminozuren para-acetyl phenylalanine (pAcF) of een asparaginezuur derivaat uitgerust met een sterisch gehinderd *tert*-butyl keton (D(Ket)). Deze aminozuren zijn in onbeschermde vorm compatibel met standaard peptidesynthese methoden. Echter, het afsplitsen van het

peptide van de hars vereist een speciale cocktail omdat de ketonen kunnen reageren met veelgebruikte thiol-scavengers. Een speciale afsplitsings-cocktail werd ontwikkeld voor deze peptiden, waardoor er vijftien peptiden in hoge zuiverheid zijn verkregen.

De opvolgende CLiPS, Boc-ontscherming en oxime ligatie reacties konden helaas niet in een werkelijke één-pots-procedure uitgevoerd worden. Daarvoor wijken de condities van de ligatie reacties te veel af van de Boc-ontscherming. Na de CLiPS ligatie werd het reactiemengsel gevriesdroogd. Hierna werd de Boc-ontscherming voltooid in pure TFA, waarna dit onder een stikstofstroom werd verdampt. Hierna werd het peptide wederom opgelost in waterige oplossing, waarna de oxime ligatie zich meteen voltrok, zonder verdere regulering van de pH. Voor alle peptiden werd het tricyclische product verkregen, echter vaak als mengsel. Voor deze strategie was de rol van het platform molecuul groter, waarbij met platform T4-N3 een minder verschillend aantal producten werden gevonden. De resultaten varieerde echter vaak, en er was geen overduidelijk recept voor succes. Er is dus meer onderzoek nodig om reproduceerbaar cyclisatie-succes te bewerkstelligen. Voor peptiden met D(Ket) werd vaak wel een enkel tricyclisch product gevonden, met een mono-oxime als bijproduct wat niet verder reageerde. Deze strategie zou, in huidige vorm, kunnen toegepast worden in initiële medium-diversiteit bibliotheek-synthese en screening.

In **Hoofdstuk 4** wordt de synthese van tetracyclische peptiden beschreven, waarbij gestart wordt met een cyclisch peptide, in plaats van een lineair peptide. Zowel strategie 1 als strategie 2 werden toegepast. De cyclisatie van de peptiden vond plaats met onbeschermde peptiden door middel van een enzymatische macrocyclisatie door omniligase-1. De drie aminozuren hS(ONH$_2$), pAcF en D(Ket) waren allen compatibel met het enzym, echter was de plaatsing van deze aminozuren op de posities in de herkennings-sequentie niet altijd mogelijk. Hierdoor moest de ligatie plek zorgvuldig gekozen worden en dus per peptide aangepast worden. Van alle acht gesynthetiseerde peptiden werd het tetracyclische peptide ook gevormd, echter soms in bijzijn van isomeren. De factoren die cyclisatie succes bepalen zoals gevonden in hoofdstukken 2 en 3 speelde eenzelfde rol voor de tetracyclische peptiden. Voor strategie 1 peptides was de loopgrootte van grootst belang. Voor pAcF peptiden was de combinatie met het platform molecuul T4-N3 het meest gunstig, terwijl er praktisch 1 product werd gevormd voor alle D(Ket) peptides. Voor een pAcF peptide werden er twee isomeren gescheiden via preparatieve HPLC, maar verdere structuuropheldering met ^{1}H NMR was niet succesvol vanwege het grote aantal conformaties waarin het tetracyclische peptide zich in oplossing bevindt.

In **Hoofdstuk 5** wordt de synthese van pentacyclische peptiden besproken, via zowel strategie 1 als 2. Voor dit project werden nieuwe platform moleculen ontworpen op basis van fenylringen. Er werd één platform ontwikkeld voor strategie 1, welke uiteindelijk niet stabiel genoeg bleek over een lange bewaartijd. Peptidesynthese voor deze strategie werd geplaagd door eerdere problemen gerelateerd aan de amino-oxy aminozuren, waardoor de kwaliteit en zuiverheid van de peptiden erg laag was. Hierdoor is voornamelijk strategie 2 onderzocht. Twee platform moleculen, twee pAcF-peptiden en twee D(Ket) peptiden zijn gesynthetiseerd. Één van de belangrijkste ontdekkingen uit dit hoofdstuk is het dynamische karakter van de oxime ligatie, welke niet expliciet naar voren kwam in eerdere hoofdstukken. Voor een pAcF peptide werd de formatie van een isomeer-zuiver pentacyclisch product geobserveerd over de tijd, waarbij verschillende mono- en di-oxime intermediairen onderweg gevormd werden. Voor sommige peptides werd er uiteindelijk één enkel pentacyclisch product gevormd. Voor de D(Ket) peptiden was de cyclisatie erg traag, maar wederom zeer selectief waarbij er in combinatie met het T6-N1 platform molecuul een enkel product werd gevormd. De voorlopige resultaten voor deze zeer beperkte selectie van peptiden zijn zeer bemoedigend voor verder onderzoek.

Dankwoord

Acknowledgements

Ik heb het niet helemaal droog gehouden met het schrijven van dit dankwoord, voornamelijk omdat ik achterin ben begonnen met de mensen die mij het dierbaarst zijn. Ook omdat dit het laatste stuk is dat ik schrijf aan dit proefschrift – een afsluiting van een uitputtend project waar ik al een lange tijd van hoopte dat het eindelijk over zou zijn. Het is een verlossing om nu eindelijk klaar te zijn.

Jan, het eerste college organische chemie was een openbaring. Na maanden natuur- en wiskunde, begon -eindelijk- de studie waar ik dacht aan te zijn begonnen. Het enthousiasme waarmee je lesgeeft draag je over aan alle studenten en dat is een groot talent. Tijdens het promotietraject stond je deur altijd open, iets waar ik veel gebruik van heb gemaakt. Dank voor je steun in (persoonlijk) moeilijke tijden. Je bekijkt vaak dingen uit de positieve kant, en na een gesprek met jou knapte ik vaak op.

Peter, bedankt voor je hulp op jouw manier en dat ik de kans kreeg om promotieonderzoek te doen. Henk, ik ken weinig mensen die zo'n liefde hebben voor de chemie. Zowel in de colleges als bij de werkbesprekingen kon u met veel plezier praten over elegante mechanismes en de complexiteit van bepaalde stappen in syntheses. Met veel plezier kijk ik op deze tijd terug. Geniet van het welverdiende emeritaat.

Nathaniel, many thanks for being part of the user committee for this project. You had many useful suggestions, which several of my students duly tried to execute. You are also a very pleasant person and I wish you all the best in Leiden. Bas, hartelijk dank voor het plaatsnemen in de commissie. Ik heb je leren kennen als bevlogen docent, maar vooral ook als hele aardige man – iets wat mijn broer kan onderschrijven.

Professor Madder, beste Annemieke, ook u wil ik graag bedanken voor het plaatsnemen in de commissie. Na uw mooie lezing bij het Dutch Peptide Symposium (2016) was ik lichtelijk teleurgesteld dat de zeer elegante furan-oxidatie in peptiden helaas niet helemaal compatibel was met mijn chemie, want ik had dit graag toe willen passen in mijn project. Jocelyne, dank dat je deel wilt uitmaken van de commissie. We beoefenen een hele andere tak van sport en ik kijk uit naar jouw vragen tijdens de verdediging.

Tati, when you arrived, the ladies' room became a lot more crowded, as I did not have it all to myself anymore. You also brought a lot of energy, and people, to the group. I enjoyed our talks and wish you all the best with your group and your family. Chris, jouw komst bracht voor ons een lichtelijke inperking van de labruimte, maar ook een verbreding van het onderzoek en een aantal leuke nieuwe collega's. Tijdens een werkbespreking merkte je een keer op 'als je niet een kleine, maar juist een hele grote - bijvoorbeeld een *tert*-butyl groep - naast een keton zet, wordt oxime ligatie ook selectief". Dit heeft geresulteerd in het D(Ket) aminozuur, en het werkte inderdaad. In dit project was het een van de belangrijkste ontdekkingen! Steen, mijn allereerste college aan de UvA werd door jou gegeven, dus ik sluit met jou af. Bedankt voor al je input tijdens werkbesprekingen en hulp bij massa-spectra die mij te complex waren. Ik heb veel van je geleerd.

Voor het (toentertijd) STW-project was ook de gebruikerscommissie een belangrijk onderdeel. In dit kader wil ik graag prof. Jos van Strijp en Pieter-Jan Haas bedanken voor hun input betreft mogelijke toepassing van dit onderzoek in phage-display libraries. Ik vond het heel erg leuk om meer te leren over jullie interessante werk en het is erg jammer dat de grote ambities en het korte tijdbestek niet met elkaar verenigbaar waren.

Een deel van dit project is uitgevoerd bij Pepscan en ik wil de mensen daar bedanken voor de ontvangst, maar ook alle hulp bij het project. Marco and the synthesis team, Richard and the purification team, thank you! Jeroen, Marine and particularly Dana for all peptide-related wisdom. Without the help of all of you I would not have been able to complete all the work and produce such nice UPLC chromatograms.

Marcel Schmidt, our collaboration resulted in the first paper from this work. You are a very focused person, and know exactly what is needed to deliver results. I learned a lot from you and appreciate your approach to get things done. Above all, you are also a very pleasant person to work with and I wish you all the best in your future career.

Zonder het werk van verschillende analisten zal het werk in dit boekje niet mogelijk zijn geweest. Meneer Ed, dank voor het (continue) oplappen van de HPLC en alle massa-metingen. Ik vond het erg gezellig om bij te kletsen tussen de metingen door, bedankt ook voor de carrière-adviezen. Jan-Meine en Andreas, bedankt voor het draaiend houden van de NMR en hulp bij speciale metingen - een dag niet geNMRd is een dag niet geleefd! Dank Dorette, voor de massa-metingen.

Bill en Michiel, zoveel practica heb ik in de laatste jaren niet meer gegeven, maar wanneer het wel zo was, was het een verzorgde reis. Dank voor jullie inzet, het maakt het voor ons allemaal een stuk makkelijker. Met een slechte woordgrap er tussendoor zelfs nog een stuk leuker ook. Ook bedankt voor het ad-hoc klaarzetten van materialen als Jan een demo-proef wilde doen.

Tijdens dit promotietraject heb ik het genoegen gehad om een aantal studenten te begeleiden. I will start with my first student (who I of course cannot say is my favorite, but he knows he is). Dearest Gašper, you were a first-student many people can only dream of. You are hardworking and eager to learn and your work on the T6 scaffolds has ended up in this thesis. Meeting you has been one of the greatest things of the PhD process. While we met over chemistry, we bonded over opera and art and other stuff. I am grateful for your friendship – it is truly a gift. Coming to see you in Slovenia is one of my favorite memories of this time and I cannot wait to see you again in person.
Brecht en Tessa, en Jorick en Celine, dank voor jullie harde werk tijdens hele korte maand-projecten. Anthony en Filip, jullie hebben gewerkt aan projecten die erg lastig waren – de chemie werkte niet mee, maar jullie hebben een belangrijke bijdrage geleverd aan het hele project.

I would like to thank all the colleagues and students in the E-building that I had the pleasure of working with during my time there. Luuk, ik ken denk ik geen betere organisch chemicus dan jij. Dankzij de 'truc van Luuk' ben ik een scaffold en aminozuur rijker en vele frustraties armer. Ik heb veel van je geleerd en je was een ontzettend fijne collega. Veel geluk in de Zaanstreek! Martin, als jij iets uitlegde aan je studenten luisterde ik stiekem mee. Jouw verhuizing naar ons lab was voor mij in ieder geval heel nuttig, zelfs al kwam dit gepaard met Phil Collins. Ik wens je heel veel plezier met je welverdiende pensioen. Hans, het was altijd leuk om je op het lab te zien ik kan jouw humor erg waarderen. Veel plezier met vissen en fietsen en ik hoop dat je nog lang op het lab door hobbyt. Gaston, het was gezellig om een andere klassieke-muziek-fan in de groep te hebben en leuk om je mee te nemen naar de opera. Veel succes in je verdere carrière en misschien tot in het concertgebouw. Roel, Simone, Piotr, Kananat, Wen-Liang, Linda, thank you for the nice working environment. Met de komst van de Slootweg groep, kregen we er een aantal leuke collega's bij. Evi, bedankt voor de leuke gesprekken om de computerschermen heen. Laurian, Flip, Devin, Evi, Marissa, het was erg leuk om jullie te leren kennen. To biocat's Vassilis, Jan, Wesley and Maria, thank you for being kind, lovely and fun. Special thanks to Maria for telling me how to cook proper Italian food – something we enjoy every week.

De onderburen van HomKat en de onder-onderburen van HetKat, wat fijn dat jullie de deur open deden als ik chemicaliën wilde lenen, en wat fijn dat hij open bleef staan voor de gezelligheid. Thierry, je bent een ontzettend lieve jongen, en dankzij jou hebben we ook een 3D-printer thuis. Ontzettend gaaf hoe je voor jouw onderzoek je eigen meetinstrumenten bouwde! Zohar, bedankt voor alle leuke gesprekken bij de NMR. Ik

hoop dat het universum je nog heel veel katten schenkt. Marianne, ik ken weinig mensen zie zo oprecht lief zijn als jij. Ik hoop dat je veel voldoening vindt in je nieuwe carrière. Joeri en Myrthe en Bas en Kyra, de spelletjesmiddagen liggen een beetje stil nu, maar ik kijk erg uit naar de volgende!

Dan nu de belangrijkste mensen, waar de tekst in dit boekje eigenlijk niet genoeg voor is. De mensen die mijn leven hebben gevormd en waar ik innig van houd. Ik ben jullie dankbaar voor de tijd die we samen mogen hebben.

Waar mijn wetenschappelijke vorming voornamelijk plaatsgevonden heeft aan de UvA, heb ik 'de oompjes' te danken voor de culturele. Lieve Dikkiedik, mijn eerste opera, A Dog's Heart, was een openbaring. Het was een fantastische ervaring en ik ben heel blij dat ik nog vele malen met u mee mocht naar zowel de Stopera als het concertgebouw. Uw kennis over kunst maakt elk bezoek een werkelijke privérondleiding. Ik heb hele blije herinneringen aan onze vroege-dinsdagmiddag-diners bij de mensa, voor de colleges kunstgeschiedenis. Het is altijd ontzettend gezellig met u, en de avonden op de Brouwersgracht, of aan de telefoon, koester ik.

Lieve oom Jaap, hoewel u niet altijd letterlijk aanwezig was, bent u altijd een belangrijk lid geweest van ons gezin. De band die u heeft met mam is bijzonder en die bewonder ik enorm. Elk jaar kijk ik uit naar oud-en-nieuw, onze dag. Vroeger vanwege de cadeaus, nu vanwege de tijd samen. Dat we daar nog lang van mogen genieten.

Jelle, lieve grote broer. Met enorme trots liep ik op de UvA toen jij daar ook studeerde. De gesprekken over scheikunde tijdens het avondeten, tot verwarring van de oudjes, waren altijd erg leuk. Ik ben zo blij dat je jouw plek, voor de klas, hebt gevonden. Allerliefste Pap en Mam, jullie stukje is toch wel hetgeen waar woorden echt te kort schieten. Onder woorden brengen wat jullie voor me betekenen, is waar boeken over geschreven kunnen worden. Een warmer nest om in op te groeien had ik me niet kunnen wensen. Een veilig honk, waar ik mezelf mag zijn – niets is meer waard dan dat. En dat hebben jullie me gegeven en daar ben ik eeuwig dankbaar voor.

Liefste Arnout. Jarenlang van afstand bewonderd, nu gelukkige jaren van dichtbij. Jou ontmoeten is zonder twijfel de beste uitkomst van dit promotietraject geweest en zonder jou hadden deze afgelopen jaren er heel anders uit gezien. Je hebt meerdere malen mijn puzzelstukjes bij elkaar gehouden toen ik uit elkaar begon te vallen en gelijmd waar nodig was. Daarvoor ben ik je heel erg dankbaar. Je maakt me ontzettend gelukkig en er is niets fijners dan thuiskomen bij jou.

Amsterdam, december 2020